Understanding Changes in Microbial Metabolism of *Clostridium termitidis* Under Different Growth Conditions Using Continuous, Real-time Monitoring of Fermentation End-products

by

Md. Eftekhar Hossain

A Thesis Submitted to the Faculty of Graduate Studies of

The University of Manitoba

in partial fulfillment of the requirements for the degree of

DOCTOR OF PHILOSOPHY

Department of Biosystems Engineering

University of Manitoba

Winnipeg, Manitoba

Canada

Understanding Changes in Microbial Metabolism for *Clostridium termitidis*

Under different Growth Conditions using

Continuous, Real-time Monitoring of Fermentation End-products

by

Md. Eftekhar Hossain

University of Manitoba, 2019

Supervisory Committee

Professor David B. Levin (Department of Biosystems Engineering, University of Manitoba)
Supervisor

Professor Nazim Cicek (Department of Biosystems Engineering, University of Manitoba)
Departmental Member

Dr. Daniel Gapes (Scion, Rotorua, New Zealand)
Department Member

Professor Richard Sparling (Department of Microbiology, University of Manitoba)
External Member

To Be Determined
External Examiner

Abstract

Metabolic shifts are associated with physico-chemical environment changes during the growth phase of many types of cells. An inability to monitor rapid and/or subtle changes in microbial metabolism may sometimes limit our understanding of microbial physiology. The central focus of this thesis was to better understand changes in microbial metabolism induced by changes in growth conditions (carbon-excess, end-product concentration such as acetate, quick removal of product gases), which may be acquired by continuous monitoring. *Clostridium termitidis* was chosen as the model organism for this work. A mass spectrometry-based Titration and Off-Gas Analysis (TOGA) system was used as an on-line monitoring tool for headspace gases (H_2, CO_2, and ethanol) analysis. In addition, GC, HPLC, and spectrophotometry methods were also used for other metabolites analysis as off-line techniques. Several key metabolic shifts were recognized during the early stationary growth phase under carbon-excess condition, compared to carbon-sufficient and carbon-limited conditions. The H_2 and CO_2 production rates decreased significantly, while the specific rates of ethanol and formate synthesis increased significantly. As a result, the substrate specific yields of H_2 were gradually decreased from exponential phase to late stationary phase, whereas the ethanol yields were increased. Decreased CO_2 synthesis and increased formate synthesis suggested that carbon flux and reducing equivalent shifted from the pyruvate ferredoxin oxidoreductase (PFOR) pathway to the pyruvate formate lyase (PFL) pathway, resulting in a sudden increase of ethanol synthesis. The addition of exogenous acetate during fermentation, resulted in decreased H_2 yields and significantly increased ethanol yields. The substrate specific yields of H_2 and CO_2 also increased significantly in cultures with a high turbulent growth environment, achieved by a high gas sparging rate (HSR) compared to the cultures with a low turbulent growth environment, with a low gas sparging rate (LSR). The growth of *C. termitidis* under LSR favoured higher ethanol yields, via the PFL pathway,

whereas growth of *C. termitidis* under HSR was unfavorable to ethanol synthesis due to re-direction of carbon and reducing equivalents towards the PFOR pathway. An algorithm was developed to create a model to estimate concentrations of non-volatile fermentation end-products using reaction stoichiometry from real-time, on-line, headspace data for H_2, CO_2, and ethanol concentrations obtained with the TOGA system, as well as acid/base balance. The proposed algorithm could not only reliably predict acetate, formate, and lactate concentrations, but also was able to tell qualitatively and quantitatively the metabolic process trends of *C. termitidis*, such as the physiological state (exponential or stationary phase) during which a particular end-product was synthesized, as well as whether the concentration of this end-product decreased or increased as growth conditions changes (metabolic shifts). Thus, real-time, on-line headspace data, together with continuous predicted information were used to detect precise metabolic shifts that resulted in changes in fermentation end-product yields. This integrated process was less cumbersome and offers a number of advantages, such as less labour intensive sampling and minimized contamination threats, which is suitable for industrial scale fermentations.

Acknowledgments

The support and help of many individuals is gratefully acknowledged. With the deepest gratitude, I would like to first thank my advisor, Dr. David Levin for providing me the opportunity to do this research, for his mentorship, optimism and support throughout the duration of my studies. I would also like to sincerely thank my supervisory committee Dr. Richard Sparling, Dr. Nazim Cicek and Dr. Daniel Gapes for their invaluable mentoring advice and support to achieve my goals. I would also like to thank all members of our team, past and present, for their friendship and support. Dr. Rumana Islam, Dr. Thomas Rydzak, Dr. Parveen Sharma, Dr. Valery Agbor, Dr. Sadhana Lal, Dr. Tobin Verbeke, Dr. Marcel Taillefer, Dr. Riffat Munir, Dr. Ryan Sestric, Christopher Dartiailh, Warren Blunt, Alan Froese, Preeti Velayathum and Thinesh Peranantham were all supportive of my studies.

A special thanks to members of the Dr. Sparling's Environmental Microbiology Research Group, and Dr. Cicek's Environmental Engineering Research Group, University of Manitoba for their constant help with respect to various research analyses. I am also grateful of the administrative assistance provided by Evelyn Fehr, Debby Watson, Heather Innis, Mandy Tanner and other staffs in the Biosystems Engineering office.

I am endlessly thankful to my spouse Afroja Yesmin, brothers, sister, and my boys and girl for their profound love, patience, encouragement and understanding throughout my studies. This work would not have been possible without support provided by the University of Manitoba, Department of Biosystems Engineering and by Genome Canada, through the Applied Genomics Research in Bioproducts or Crops (ABC) program, for the grant titled, "Microbial Genomics for Biofuels and Coproducts from Biorefining Processes" and by the Province of Manitoba, through the Science and Technology International Collaboration (STIC) Fund and Natural Sciences and Engineering Research Council (NSERC) of Canada.

Dedication

This work is dedicated to my beloved deceased parents

Md. Bakhtiyar Hossain and Ayesha Akter.

Table of Contents

List of Tables

List of Figures

List of Supplementary Materials

Supplementary Tables

Supplementary Figures

List of Abbreviations

ABC	ATP-binding cassette
ACK	Acetate kinase
ADH	Alcohol dehydrogenase
AdhE	Acetaldehyde/alcohol dehydrogenase
ADP	Adenosine diphosphate
ALD	Acetaldehyde dehydrogenase
ATK	Acetate thiokinase
ATP	Adenosine triphosphate
CAZymes	Carbohydrate active enzymes
CBM	Carbohydrate binding module
CBP	Consolidated bioprocessing
CDW	Cell dry weight
CO_2	Carbon dioxide
CRI	Carbon recovery index
ED	Entner-Doudoroff pathway
EMP	Embden myerhof parnas pathway
EtOH	Ethanol
FC	Faraday cup detector
Fd_o	Ferredoxin oxidase
Fd_r	Ferredoxin reductase
GAO	Glycogen accumulating organisms
GC	Gas chromatography
GHG	Greenhouse gasses
H_2	Hydrogen gas

H2ase	Hydrogenase
HPLC	High pressure liquid chromatography
HSR	High sparging rate
IR	Infrared
LDH	Lactate dehydrogenase
LSR	Low sparging rate
MIMS	Membrane inlet mass spectrometry
MS	Mass spectrometry
NaCl	Sodium chloride
NaOH	Sodium hydroxide
NADH	Nicotinamide adenine dinucleotide
ND	Not detected
NMR	Nuclear magnetic resonance
OD	Optical density
O/R	Oxidation/reduction
OTR	Oxygen transfer rate
PAO	Polyphosphate accumulating organisms
PAT	Process analytical technology
PB	Phosphate buffer
PEP	Phosphoenol pyruvate
PFK	Phosphofructokinase
PFL	Pruvate formate lyase
PFOR	Pyruvate ferredoxin oxidoreductase
Pi	Inorganic phosphate
pi	Post inoculation

PP	Pentose phosphate pathway
PPi	Pyrophosphate
SEM	Scanning electron microscopy
SSF	Simultaneous saccharification and fermentation
TOGA	Titrimetric and off-gas analysis
Torr	Raw mass spectrometry signal in torr
UV	Ultra violet
VIS	Visible

Chapter 1

Introduction and Literature Review

1.1 Background

Global energy demand is continuously rising, but non-renewable fossil fuel energy resources are limited. Reserves of low cost, "sweet crude" are dwindling, and although new reserves of petroleum are being discovered, they are generally in locations that make recovery costly and environmentally dangerous, and/or are of lower quality which requires costly upgrading (Baum et al. 2009; IEA 2013; Husky Energy 2015). Added to this is the issue of the increasing levels of atmospheric carbon dioxide generated by fossil fuel combustion and its contribution to climate change. Thus, our reliance on non-renewable fossil fuels has had a significant impact on global socio-economic and environmental issues. To meet this crisis, researchers are searching for alternative renewable energy sources. Among the renewable energy resources, biomass-derived energy has been suggested to be a significant solution to this problem. Bioethanol and biobutanol have potential to replace fossil fuel derived gasoline (petroleum and diesel) (Pfromm et al 2010; Bankar et al. 2013; Yusoff et al. 2015).

Plant biomass (cellulosic and hemicellulosic) is the most attractive raw material for biofuel production that has been suggested by many researchers (Lynd et al. 2002; Levin et al. 2009; Solomon 2010). Lignocellulosic biomass consists of polymers that contain a variety of six- and five-carbon sugars, along with other aromatic and aliphatic units. These are generally known as cellulose, hemi-cellulose, and lignin. The pentose sugar xylose is the second most abundant sugar after glucose in hemi-cellulosic plant stocks (agricultural residue and wood). Biomass based sugars from agriculture, forestry, municipal, and industrial sources do not compete with food and therefore, present an economic opportunity for biofuel production (Helle and Duff

2004). However, if biomass is to be used as a source of sugars for biofuel production, it must be low cost and abundantly available.

Use of biomass as a feedstock for biofuel production also requires some pre-treatment. The extent of pretreatment depends on the biofuel production process to be used. The current paradigm of using biomass as a source of sugars for fermentation to bioethanol requires size reduction, deconstruction of the lignocellulosic structure by acid or base, or steam explosion, followed by enzymatic digestion to simple sugars and oligomers (Lynd et al. 2002; Galbe and Zacchi 2007). Pre-treatment is essential but involves cost per unit of biofuel production. Alternatively, consolidated biofuel processing (CBP) can be used from minimally treated raw biomass for biofuel synthesis. In this case, suitable organisms are required that can use plant biomass both by saccharification and carbohydrate metabolism (Lynd et al. 2002).

1.2 Carbohydrate metabolism

There are a wide variety of organisms available that can use a broad-spectrum of substrates, but some of them (heterotrophs) can use both pentose and hexose sugars simultaneously. A good number of them cannot metabolize these carbohydrates to biofuels (bioethanol or biobutanol) efficiently. Therefore, due to inefficient carbohydrate metabolism in wild-type strains, the use of recombinant organisms (Katzen and Fowler 1994; Hahn-H et al. 1994; Takahashi et al. 2000; Sonderegger et al. 2004; Shaw et al. 2008) has been proposed to improve the efficiency of biofuel synthesis.

Carbohydrate fermentation involves numerous metabolic reactions to convert sugar into gases, fatty acids, and alcohols. It can be classified according to the main fermentation end-products, such as alcohols, low molecular weight (volatile) fatty acids, methane, and hydrogen. These types of fermentation involve either hexose or pentose sugars as the smallest monomer

unit of carbon and energy sources for the growth of these organisms. Some organisms can also use oligomers of six or five carbon sugars, or intermediate fermentation products as carbon source for their growth. Transport proteins play an important role in transportation of sugar molecule into the cytoplasm. For example, *Clostridium thermocellum* does not grow on xylose, due to the absence of xylose transporters (Stainthorpe and Williams 1988), whereas *C. termitidis* (Ramachandran 2013; Munir 2015) and *Thermoanaerobacter thermohydrosulfuricus* WC1 (Verbeke et al. 2013) possess xylose transporters through which they can uptake xylose for metabolic processes.

For carbohydrate utilization, anaerobic bacteria can use either the Embden-Meyerhof-Parnas (EMP), Pentose Phosphate (PP) or Entner-Doudoroff (ED) pathways. These pathways may change during the growth of the organism, which depends not only on substrate availability (low or high) but also other nutrients (Desvaux 2004; Fuhrer et al. 2005; Liu et al. 2012). Furthermore, not all organisms possess all of the pathways. An organism gains and incorporates metabolic pathways into its genome through an evolutionary process that depends in the surrounding environment. To produce ethanol, *Clostridium thermocellum* (Rydzak et al. 2009) and *Thermoanaerobium brockii*, (Lamed and Zeikus 1980) follow the Embden-Meyerhof-Parnas (EMP) pathway for hexose utilization, where two moles of pyruvate are formed from one mole of glucose. Pyruvate is then converted to acetyl-CoA via pyruvate ferredoxin oxidoreductase (PFOR) and the acetyl-CoA is converted to ethanol by AdhE, a bifunctional acetaldehyde-alcohol dehydrogenase, without forming free acetaldehyde. Since there is no hydrogen acceptor (e.g. oxygen in aerobes), NADH production during pyruvate formation and NADH consumption is balanced. Details of the EMP pathway are explained by several authors elsewhere (Gottschalk 1986; Rydzak et al. 2014; Munir et al. 2015).

In contrast to *Clostridia*, there are some facultative anaerobic bacteria that degrade glucose to pyruvate via the Entner-Doudoroff (ED) pathway (Gottschalk 1986), such as species in the genera *Acetobacter*, *Agrobacterium*, *Rhizobium*, *Serratia*, *Xanthobacter*, *Xanthomona*, *Zymomonas*. Here, 6-phospho-gluconate (6-PG) is produced from glucose-6-phosphate (G-6-P), then enters into pyruvate directly from 2-keto-3-deoxy-6-phospho-gluconate. There is another option to form pyruvate through glyceraldehyde-3-phosphate (G-3-P) and phosphoenolpyruvate (PEP). Normally, this is considered to be the shortest path to form pyruvate compared to the EMP or PP pathways and used by the organisms to conserve energy and to minimize protein costs (Flamholz et al. 2013).

1.3 Substrate utilization

Polymeric substrate degradation and utilization depends on the capacity of the bacteria to carry-out extracellular hydrolysis, as well as the presence of transporter proteins to bring the sugar units into the cell, and the intracellular enzymatic activities of the organism that metabolize the substrate. For example, *C. thermocellum* can hydrolyze plant biomass (cellulose) using cellulosomes attached to its cell wall (Lynd et al. 2002), whereas *C. termitidis* possesses a wide-range of CAZymes, which have the potential capacity to degrade simple to complex carbohydrates (Munir et al. 2016a; Munir et al. 2014). Also, *C. thermocellum* is unable to transport xylose into the cell, due to the absence of a xylose transporter, while *C. termitdis* can transport and metabolize xylose (Munir et al. 2014; Munir et al. 2016b).

Lal and Levin (2016) found a closed relationship between *C. termitidis* and *Clostridium cellobioparam*. They fall under cellulolytic clade-5 and share more than 90% amino-acid sequence identity for enzymes encoded by core metabolism genes. Furthermore, *C. thermocellum, C. termitidis*, and *C. cellobioparam* have been reclassified into the genus

Ruminiclostridium (Yutin and Galperin 2013). Recently, Clostridial cluster III members have been reclassified into four novel genera for which the names *Hungateiclostridium*gen. nov., *Thermoclostridium* gen. nov., *Ruminiclostridium* gen. nov. and *Pseudoclostridium* gen. nov. have been proposed (Zhang et al. 2018). However, while *C. termitidis* is now also known as *Ruminiclostridium termitidis*, this classification is not yet widely used in the literature. Therefore, *C. termitidis* will be used throughout this thesis.

It is well documented that *Clostridium* species follow highly branched fermentative pathways (in both glycolytic and pyruvate nodes) when growing under optimum conditions for nutrients (Fleming and Quinn 1971; Johnson et al. 1981; Islam et al. 2015), pH (Huang et al. 1986; Dabrock et al. 1992; Sridhar and Eiteman 2001), temperature (Farrel and Rose 1967; Karadag and Puhakka 2010), carbon source (Freier et al. 1988; Levin et al. 2006; Ren et al. 2007; Agbor et al. 2014; Munir et al. 2016), and produce both gaseous and soluble fermentation end-products. However, the specific metabolic pathways used by different *Clostridium* species can be very different. For example, while *C. thermocellum* utilizes the glycolytic Embden-Meyerhof-Parnas (EMP) pathway (Rydzak et al. 2009) when growing under carbon-limited to carbon-sufficient conditions, while *C. termitidis* utilizes both the EMP and Pentose Phosphate (PP) pathways (Ramachandran 2013; Munir 2015), *C. butyricum* uses the EMP and Entner-Doudoroff (ED) pathways (Bender et al. 1971), and *Zymomonas mobilis* follows the ED pathway (Conway 1992; Fuhrer et al. 2005). Differences in metabolic pathway utilization in different bacteria reflect differences in the presence or absence of functionally active genes. For example, *Z. mobilis* follows the ED pathway because it does not possess a key enzyme, phosphofructokinase (PFK), required for transferring fructose-6-phosphate (F6P) to fructose-1-6-biphosphate (F1,6BP) (Fuhrer et al. 2005).

Although all of these microorganisms carry-out pyruvate catabolism reactions, their end-product synthesis patterns may vary due to differences in carbon flux through the glycolytic (upstream reactions) and/or pyruvate (downstream) reaction nodes. In addition, deviations from optimum growth conditions may result in metabolic shifts to maintain redox balance. Understanding when and how these changes occur during cell growth can be important for the development of efficient and viable industrial processes for biofuel synthesis. There are a number of ways to understand microbial metabolism, including close observation under various growth conditions (Murray and Khan 1983; Rydzak et al. 2011; Carere et al. 2014), enzymatic analyses (Sridhar et al. 2000; Petitdemange et al. 2001; Rydzak et al. 2009; Veen et al. 2013), isotopic labeling (Gottschalk and Barker 1966; Wiechert et al. 2001; Fischer et al. 2004; Sauer 2006; Liu et al. 2012), and monitoring of metabolites under variable growth environments (Bothun et al. 2004; Carere 2013; Islam 2013; Rydzak et al. 2014). Figure 1.1 provides evaluation of pyruvate catabolic reactions in *C. termitidis* on cellobiose, which is derived with the help of proteomics (Ramachandran 2013; Munir et al. 2015), transcriptomics (Munir et al. 2016), secretomes (Munir et al. 2014), and comparative genomics (Lal and Levin 2016). This figure also shows the major fermentative pathways leading to the synthesis of hydrogen, carbon dioxide, formate, acetate, ethanol, and lactate, which can be grouped into gaseous (H_2 and CO_2), C1 (CO_2 and formate), C2 (acetate and ethanol), and C3 (lactate) products. It is believed that highly branched fermentative pathways limit the efficient production of biofuels to maintain product ratios (C1/C2, H_2/acetate etc.) and redox (O/R) balances. A detailed description of reaction stoichiometry and redox balances are provided in Section 2.1.8 of Chapter 2.

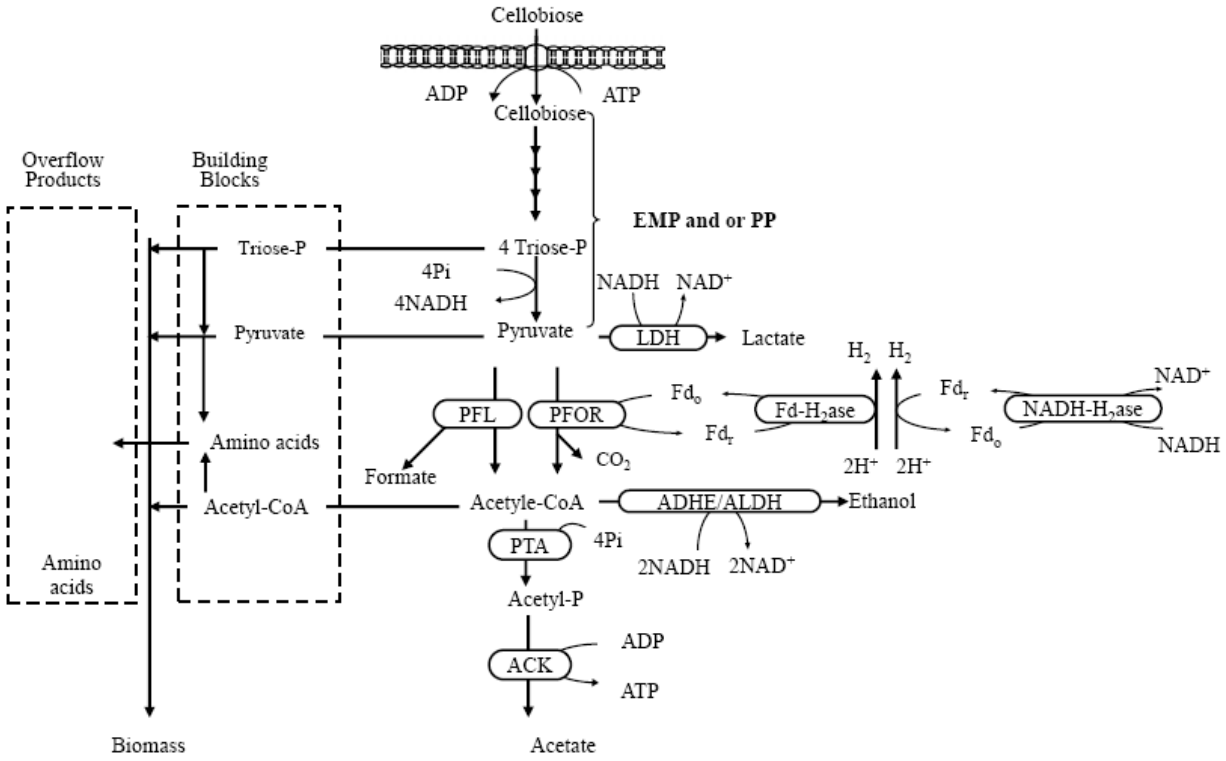

Figure 1.1 Pyruvate catabolic reactions derived from previous studies, including proteomics (Ramachandran 2013; Munir et al. 2015), transcriptomics (Munir et al. 2016), secretomes (Munir et al. 2014), and comparative genomics (Lal and Levin 2016).

1.3.1 Effects of variable substrate loads

Variable substrate loads may affect bacterial cell growth, gas production, and synthesis of other fermentation end-products, such as ethanol, and organic acids by redirecting carbon and electron flow from general pathways. This carbon flux re-distribution is a unique characteristic for an organism (e.g. hyperthermophile, thermophile, or mesophile), while growing from carbon-limited to carbon-excess conditions (Schgnheit and Schafer 1995; Islam et al. 2006; Desvaux 2004). Islam et al. (2006) investigated growth of *C. thermocellum* using soluble substrate (cellobiose), whereas Levin et al. (2006) studied similar quantities of insoluble cellulosic substrates, such as α-cellulose, Whatmann paper, and delignified wood. All of these experiments were performed in closed batch culture systems.

The final cell density of *C. thermocellum* was considerably affected (low) under carbon-limited conditions compared to that under carbon-excess conditions while growth rate remained constant (Islam et al. 2006). Cell specific production rates of hydrogen (H_2), carbon dioxide (CO_2), formate, and ethanol were the lowest at low substrate conditions compared to the rates at medium or high substrate conditions. No significant change of acetate production rate was observed in either low or high cellobiose conditions. It was, however, observed that approximately 90 % of the total carbon flow was directed toward acetate synthesis during the exponential growth phase. Lactate was barely above detection limit at this stage. Medium initial substrate containing cultures directed carbon flow towards predominately acetate (47-58 %) and ethanol (30-44 %). The rest of the carbon was distributed between formate and lactate. In cultures containing high initial cellobiose, carbon flow was directed towards acetate and ethanol (up to 70%) until mid-log phase. Lactate and formate production increased dramatically (lactate

from below 0.20 mmol/L to 5.75 mmol/L and formate from 2.48 mmol/L to 6.64 mmol/L) as the cell growth reached stationary phase.

It has been suggested that under carbon-limited conditions, catabolism was coupled to anabolism resulting in high biomass yields, compared to carbon-excess conditions where high rates of carbon flux were achieved through catabolism (Russell and Cook 1995; Islam et al. 2006). Overflow of metabolism (excretion of metabolic intermediates, such as pyruvate in *C. thermocellum* and *C. cellulolyticum*) was also noticed under carbon-excess conditions, where carbon and electron flow were shifted to less efficient and/or energy spilling pathways (which involves energy conservation by generating ATP). Furthermore, presence of PFL and formate synthesis confirmed that *C. thermocellum* used pyruvate to acetyl-CoA and formate, a branched fermentative pathway, in addition to pyruvate to acetyl-CoA and CO_2 by PFOR (Sparling et al. 2006). Although formate production was reported under both low and high substrate conditions; it was unclear what triggered the higher proportion of formate synthesis in carbon-excess condition. Formate synthesis stoichiometrically competes with H_2 synthesis, which was evident from a sharp drop of specific H_2 synthesis (12.9 mmol/g/L to about 3.0 mmol/g/L) under carbon-excess condition. Levin et al. (2006) reported that by the utilization of cellulosic substrates *C. thermocellum* produced similar to somewhat higher amounts of H_2 and CO_2 than cellobiose in cultures in low to medium substrate. At high substrate concentrations, cellobiose and delignified wood produced similar amounts of H_2 and CO_2, while alpha-cellulose and filter paper produced less gas.

Compared to thermophilic *Clostridia, C. termitidis,* a mesophilic bacterium, has been studied with limited focus on physiological characterization (Hethener et al. 1992) until recent studies emphasized on protein and carbohydrate metabolism (Ramachandran 2013), various

types of substrate hydrolysis, and transcriptomic and proteomic studies (Munir et al. 2015; Munir et al. 2016a) under carbon-sufficient conditions. Other mesophilic *Clostridia*, such as *C. cellulolyticum* has been studied extensively by several authors (Guedon et al. 1999; Payot et al. 1999; Guedon et al. 2000; Desvaux et al. 2001; Desvaux and Petitdemange 2001; Guedon et al. 2002). Although, initial metabolic studies focused on pH-uncontrolled batch experiments, later investigations were concentrated in bioreactors under various growth conditions, including variable substrate loads, which have been reviewed elsewhere (Desvaux et al. 2005; Ramachandran 2013).

Based on phylogenetic analyses, *C. cellobioparum* is the closest anaerobic bacteria to *C. termitidis* (Lal and Levin 2016; Monserrate at al. 2001), as they share more than 90% of core metabolic pathways. Like *C. termitidis*, *C. cellobioparum* also produces significant amount of H_2, CO_2, acetate, and ethanol when cultured on cellobiose and cellulose. In addition, lactate and formate production were also reported, with butyrate and n-propanol observed only for *C. cellobioparum* (Chung 1976; Ren et al. 2007).

1.3.2 Substrate co-utilization

Microorganisms that can ferment a wide variety of sugars derived from plant biomass have economic importance. Specifically, microorganisms that can co-ferment both five-carbon sugars (such as xylose, arabinose, ribose from hemicellulose) and the more common six-carbon sugars (mannose in hemicellulose and glucose in cellulose) in biomass are of great interest. It is a complex task to evaluate preferential or simultaneous substrate utilization by only observing end-product profiles. It is even more complex to obtain kinetic information while co-utilization of substrate occurs. However, understanding these processes can facilitate development of

enhanced strategies for biofuel (hydrogen, ethanol) production by the co-utilization of naturally abundant hexose and pentose sugars.

Taniguchi et al. (1997) conducted a study on substrate co-utilization (glucose and xylose) using *Pichia stipitis* in a 1 L bioreactor. During fermentation of a mixture of glucose and xylose, no xylose was consumed when glucose was present in the broth. Xylose consumption was observed only after nearly all of the glucose was consumed. The ethanol production rate was higher when the cells consumed glucose compared to the rate observed during xylose consumption.

For the production of biofuels, it is necessary to select a suitable organism that can use either cellulose or hemicelluloses as substrate. Fermentation is thought to be more economical for biomass based fuel (ethanol, hydrogen, butanol) production if both pentose and hexose sugars are utilized by microorganisms (Levin et al. 2009). Micro-organisms may be selected based on growth rate, substrate consumption rate, and metabolite production rate. It is to be noted that some pre-treatment (physical and chemical) of lignocellulosic materials is required to have access to cellulose during fermentation. Researchers are trying to avoid chemical pre-treatment by adapting consolidated bioprocessing (CBP) (Carere et al. 2008; Lin et al. 2011), where saccharification and fermentation take place in one system.

There are organisms that have potential for direct utilization of plant-based biomass. *C. thermocellum* (Lynd et al. 2002, Islam 2013), *C. termitidis* (Munir et al. 2016a), *Clostridium stercorarium* (Bronnenmeier et al. 1997), *C. cellulolyticum* (Desvaux et al. 2001), *Clostridium. phytofermentans* (Warnick et al. 2002), and even genetically engineered *Escherichia coli* (Bokinsky et al. 2011) are candidates for CBP, because they can utilize cellulose or hemi-

cellulose, or both. Care must be taken to provide suitable growth conditions, such as pH, temperature, nutrients requirement, aerobic or anaerobic growth environment.

1.4 Nutrient requirements for bacteria

Bacteria require certain nutrients (C, N, S, O, metal ions, vitamins, etc.) for growth. These nutrients are required for the construction of cellular materials with the activity of enzymes and transport systems. During the growth of heterotrophs (exception *Clostridium sticklandii*, which ferments amino acids; Fonknechten et al. 2010), carbon is considered to be the chief source of energy, whereas autotrophs use light, carbon dioxide, other chemicals (Masse et al. 2002). These carbon sources may be simple (glycerol, pentose, hexose) or complex (cellulose, hemicelluloses) forms of sugars. In addition to carbon sources, bacteria need other nutrients, such as vitamins and minerals for their growth. Almost all bacteria possess certain capacity to produce necessary vitamins and biomolecules (such as amino acids) through biosynthetic pathways (e.g. amino acid synthesis pathways) by using available minerals into the growth system. Synthesis of these biomolecules can be energetically expensive (Stouthamer 1973; Gottschalk 1986), which would slow down the growth rate relative to the flux through catabolism (Fleming 1970). For enhanced growth, these vitamins, biomolecules and minerals are sometimes required to be added as a supplement (e.g. in *E. coli*, *C. thermocellum*, *C. termitidis*). It is to be noted that there are a number of bacteria that lack the ability to synthesize all necessary organic compounds (biomolecules) for growth. They depend on one or more growth factors (vitamins, amino acids and purines, and pyrimidines), which have been discussed in detail elsewhere (Johnson et al. 1981; Gottschalk, 1986; Payot et al. 1999; Fowler and Koffas 2010; Islam et al. 2015).

1.4.1 Inorganic nutrients

Nitrogen is one of the main constituents in bacterial cells and is required during the growth of bacteria. Ammonia is the preferred source of nitrogen that bacteria incorporate it into the cell then metabolised to organo-nitrogen through various steps of oxidation (Gottschalk 1986). Other sources of nitrogen are ammonium, nitrate, nitrite, and nitrogen containing organic compounds, such as amino acids. When ammonium is considered as a nitrogen source in anaerobic fermentation process at or near nutral pH (under buffered system), it dissociates to ammonia and hydrogen ion in the following way: $NH_4^+ \leftrightarrow NH_3 + H^+$. Therefore, the action of relevant system needs to be considered where components of acid-base compound are consumed or produced. In a complex system, e.g. fermentation, where bicarbonate, ammonium, organic acids are directly involved in various steps of acid-base buffering and hydrogen ion production. Detail description and model-based approach of this complex system can be obtained elsewhere (Pratt 2003; Stumm and Morgan 1996).

Sulfur is a constituent of cysteine, methionine, thiamine pyrophosphate, co-enzyme-A, biotine, which normally is taken up from various inorganic sources, such as SO_4^{2-}, HS^-, S^{2-}, S^o. In addition to inorganic sources, sulfur can also be obtained from organic compounds. Cysteine is used as an oxygen scavenger in anaerobic fermentation. Furthermore, it also acts as an important biomolecule (chelate) in forming ferredoxins, iron-sulphur proteins that mediate electron transfer in a wide range of metabolic reactions (Orme-Johnson 1973; Roche et al. 2013).

In the annotated genome of *C. termitidis*, a number of ferredoxin genes and their respective proteins have been identified (Munir et al. 2016a; Lal and Levin 2016). These genes are responsible for producing corresponding enzymes that play key roles in carbon and electron distribution by anabolic and catabolic reactions. Among them, pyruvate ferredoxin

oxidoreductase (PFOR), ferredoxin reductase (Fd_r), and ferredoxin oxidase (Fd_o) are important. PFOR plays a role in converting pyruvate to acetyl-CoA, while Fd_r carries electrons to reduce H^+ ion to H_2 gas, and in the process is oxidised to Fd_o, which is further involved in redox reactions. Furthermore, in fermentative bacteria such as *C. thermocellum*, *C. termitidis*, and *Thermotoga marimata*, various kinds of hydrogenases genes, which are responsible for disposing of excess reducing equivalents by producing H_2, have been reported (Rydzak et al. 2014; Munir et al. 2016a; Schut and Adams 2009). A number of Fe-S coupling proteins (ferredoxins and hydrogenases produced from iron and sulphur present in the medium) have been reported in literatures (Schut and Adams 2009; Løvgreen et al. 2011; Blanc et al. 2015), and their presence was detected in the proteome of *C. termitidis* as well (Munir et al. 2016a).

Phosphorous is the constituent of nucleic acids, phospholipids, and nucleotides. It is present into the broth as various forms of inorganic phosphates ($H_2PO_4^-$, HPO_4^{2-}) and creates a phosphate buffering zone. Under this buffering range, they are incorporated into cells to initiate and regulate biochemical reactions. By the addition and removal of phosphate, cells store and release energy as a crucial strategy in the regulation of metabolic process (Gottschalk, 1986). Ferrous (Fe^{2+}) and ferric (Fe^{3+}) ions are the oxidized form of iron (Fe^o). These ions are present in redox carriers, such as cytochrome, ferredoxins and iron-sulfur proteins. They also act as a co-factor of enzymes (e.g. dehydratases). Both sodium and potassium ions are present in the cells, and generally sodium is excreted from the cell to keep its concentration low compared to potassium. These ions are present in the cells at relatively high concentrations compared to other elements (Zn, Mn, Co, Ni, Fe etc.). Sodium ions are occasionally involved in transport processes, such as up taking of hexose in both aerobic and anaerobic bacteria; potassium is not. Potassium is used as a cofactor of some enzymes (e.g. pyruvate kinase) (Gottschalk 1986). Most

transporters for sugars in the *Clostridia* use ATP or protons as the source of energy for transport. Furthermore, excretion of VFA (unionized form of formate, acetate, lactate, and butyrate) is initiated and regulated by passive diffusion during fermentation in bacteria (Herrero et al. 1985a; Herrero et al. 1985b; Gottschalk 1986).

1.4.2 Alternative source of nutrients

When a pure substrate is used, it is essential to provide vitamins and minerals for the growth of organism, resulting in a high product cost. Alternative substrate sources (e.g. pulp and paper industry wastewater) may contain additional nutrients that are essential for growth. Presence of those nutrients in the substrate source, thereby, reduces the production cost.

Pulp and paper industry wastewater contains variable amounts (0.5 - 40 g/L) of carbohydrate polymers that can be used as feedstock for anaerobic fermentation, and the feed stock concentrations are often sufficient for the growth of *Clostridia* and other cellulolytic bacteria for biofuel (hydrogen and ethanol) production. Helle and Duff (2004) showed that presence of sugar in spent liquor (pulp industry effluent) was suitable for low to high substrate loading conditions for the growth of organisms (*Saccharomyces cerevisiae* 259ST). The wastewater also contains almost all necessary major (C, O, H, N, S, P, K, Mg, Ca, Fe, Na, Cl) and minor (Zn, Mn, Mo, Se, Co, Cu, Ni, W) nutrients required for the growth of microorganisms. Presence of those nutrients may reduce the cost of fermentation and ultimately end-product or biofuel cost. It is to be noted that substrate spent liquor requires vitamins, and essential amino acids for the growth of micro-organisms (Gottschalk 1986). Thin stillage, a corn-based ethanol synthesis by-product, had sufficient macro- and micro-nutrients including amino-acids and proteins for initial growth of *C. thermocellum*, but required additional Mg^{2+} to increase ethanol production (Islam 2013).

1.4.3 Growth inhibition

Inhibition is one of the major challenges when converting sugar into biofuels from traditional biomass or waste sources. Inhibition can arise either from the substrate (Palmqvist and Hahn-Hagerdal 2000; Temudo et al. 2009; Verbeke et al. 2017), lignin and lignin derivatives (Kirk et al. 1980), end-products (Herrero and Gomez 1980; Herrero et al. 1985a; Herrero et al. 1985b; Diamantis et al. 2006) or excess inorganic nutrients (Gottschalk 1986; Lynd et al. 2001). Zeikus et al. (1982) described the molecular basis of biodegradation of lignin in anaerobic environments. Effective tracking of fermentation inhibition can provide the opportunity to overcome it.

1.5 Analytical methods used to monitor fermentation

To achieve desirable biofuel production and its manipulation, it is essential to monitor growth of the microorganism. This growth can be monitored either "off-line" or "on-line", depending on the research goals and the availability of appropriate instruments. Figure 1.2 shows typical sampling frequencies over the course of fermentation reaction. Generally, for the monitoring of bacterial growth in a fermentation process, high frequency sampling is avoided because it is time consuming, laborious and tedious. In that case, low frequency of sampling preferred (Figure 1.2A). It may be appropriate for very slowly growing organism. However, by choosing a low sampling frequency, data related to important features of a medium to fast growing organism may be overlooked and lost. For example, when an infrequent sampling method is used, an initial rapid rate of change followed by an almost constant level throughout the course of the fermentation reaction may be observed (Figure 1A). However, using a frequent sampling strategy can reveal important features of the fermentation process that were not detected using the infrequent sampling approach (Figure 1.2B). When both slow and fast

A)

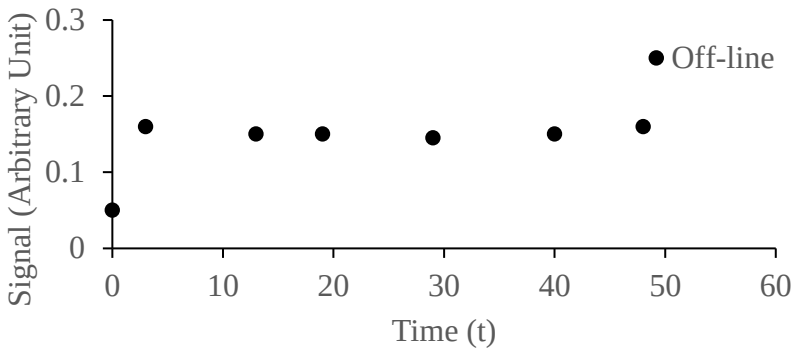

B)

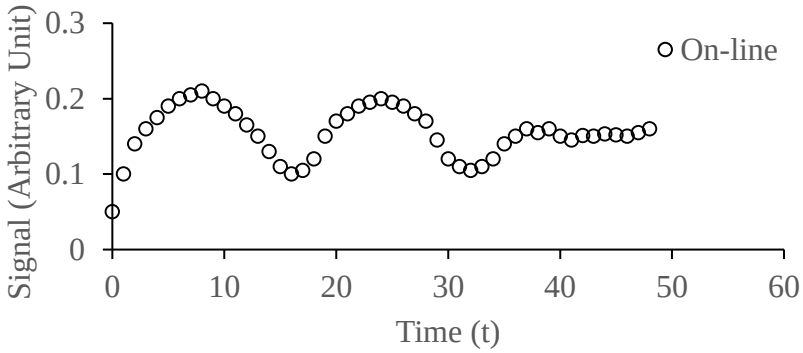

C)

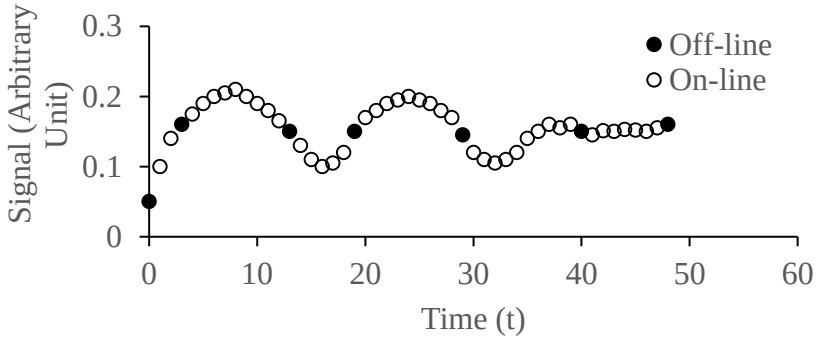

Figure 1.2 Typical sampling frequencies over the course of a fermentation reaction, A) infrequent sampling (off-line); B) frequent sampling (on-line); and C) a combination of both infrequent and frequent sampling, which together may provide a more accurate representation of the response.

sampling frequencies are plotted together, a more representative responses appears (Figure 1.2C), providing more in-depth information regarding the fermentation process (fast or slow, increase or decrease, off or on etc.) (Pratt et al. 2003). Thus, appropriate sampling frequencies and tools must be chosen to achieve effective monitoring

Bacterial fermentation metabolites are present in gas, liquid, and solid phase, which can be detected either via discrete or continuous sampling using a variety of methods, including: 1) ultra-violet (UV), visible (VIS) (Horta et al. 2012), and infrared spectroscopy (IR) (Cavinato et al. 1990; Le Coq et al. 2002; Arnold et al. 2002; Holwerda et al. 2013); 2) chromatographic methods, such as gas chromatography (GC) (Diamantis et al. 2006; Boe 2006), high performance liquid chromatography (HPLC) (Lamed et al. 1980; Rydzak et al. 2009; Islam 2013); 3) mass spectrometry (MS) methods (Boyd et al. 2008; Fisher and Sauer 2003; Heinzle 1992,;Lloyd et al. 1985); and 4) electrochemical sensors based on capacitance (Aathithan et al. 2001; Dutta et al. 2002; Boilot et al 2002; Rudnitskaya and Legin 2008; Giaever and Keese 1993). Conventional on-line sensors, such as oxygen and pH sensors, are also used in bioprocess monitoring (Blunt et al. 2017; Strong et al. 2011). Each method has advantages and disadvantages when compared with each other. For example, in a given fermentation process, information on the cumulative concentrations of H^+ or OH^- ions can be achieved easily from pH data, but this does not provide information about which acidic or basic end-products are responsible for the change in pH, and/or the extent of their contribution to the change., Extensive data processing is required to obtain this information.

On-line monitoring techniques have two important advantages over off-line monitoring methods: 1) on-line monitoring involves high frequency sampling that provides real-time information on biomass growth, volatile product synthesis, and precise pH balance for biological

processes within the shortest possible time, and 2) on-line monitoring is less cumbersome and time consuming. The impact of slight environmental changes (pH, temperature, pressure, substrate or end-product addition) during the growth phase can be visualized with on-line process that may be difficult to observe using off-line measurements. This unique characteristic of on-line methods can provide the opportunity to deal with many unanswered questions in the biofuel production process.

1.5.1 The status of on-line monitoring

On-line monitoring and control of most fermentation processes remains far from flawless. Organisms are usually surrounded by a physical/chemical microenvironment, and even the slightest of changes in this environment can have dramatic impacts on the system as a whole (Scheper et al. 1996). Successful fermentation scale-up requires a good understanding of the physical/chemical environment, and interaction effects between the environment and biological processes (Clementschitsch and Bayer 2006; Pollard et al. 2001). Adequate control strategies can facilitate improvements in efficiency, productivity, reproducibility, quality control, and cost effectiveness (Clementschitsch and Bayer 2006; Landgrebe et al. 2010; Vojinović et al. 2006). Novel fermentation monitoring concepts should either identify significant control variables involved in pathway regulation or improve process knowledge (Clementschitsch and Bayer 2006).

In initial bioprocess development, it is necessary to acquire as many on-line signals (e.g. biomass, off-gas, other solubles) as possible. On-line analysis also measures the environment around the sampling device, which in turn may be impacted by factors such as mass transfer limitations, boundary layer effects, etc. For example, a fermentation with on-line headspace analysis is not directly measureing metabolism, but the net effect of metabolism and mass

transfer operations (mixing, sparging etc.). For well-established fermentation processes in industrial applications, only a few critical parameters may be monitored on-line to enable proper process control and quality assurance (Harms et al. 2002). Establishing quality assurance in an industrial process could enhance conformation with global standards and bring competency in industrial production (Clementschitsch and Bayer 2006). Adopting on-line process monitoring in a typical biological process could save time and resources.

1.5.2 Need for on-line biofuel production monitoring

On-line biofuel production monitoring has been rapidly gaining industrial importance over the past few decades and is expected to play a vital role in the future. Olson et al. (1998) described that on-line analytical monitoring systems were the backbone of bioprocess monitoring both in academia and industry. There are a wide-range of industrial sectors including food and beverage production, pharmaceutical production, energy production, and environmental applications (Vojinović et al. 2006) utilizing on-line process monitoring. These processes are often slow, expensive, and generally complex in nature. Economically viable process control requires extensive attention on resource utilization efficiency in a timely fashion. Process variables such as temperature, pH, substrate and end-product concentration may influence production yields of biofuels. Slight changes in those variables may enhance or decrease end-product distribution by diverting carbon-flux from one-way to another. These variables are essential to track on-line rather than off-line.

Off-line analytical methods involve a number of steps in sampling (frequency, sample filtration or centrifugation), metabolites conversion (digestion, derivatization), sample injection, and separation. These are time-consuming processes and may create risk of possible

contamination while performing these steps. To minimize possible risk of contamination, on-line analytical tool could be a good choice for fermentation monitoring.

Fermentation requires a number of basic process control parameters in place as a part of on-line monitoring techniques. They are temperature, sparging flow rate, internal environment (aerobic or anaerobic), pH, solution potential. Addition of other on-line parameters during fermentation will provide the opportunity to observe effective biofuel production monitoring system. For example, variables related to cell biomass concentration, cell number, cell viability, metabolic stress response, specific quantities of metabolites is of paramount importance. Hence, on-line monitoring methods are required to provide specific knowledge for optimal process operation, e.g. maximal exploitation of the cells synthesis capacity or termination of the cultivation process.

1.5.3 Mass spectrometry (MS)

Due to our research interest of generating continuous data by frequent sampling with a membrane inlet mass spectrometry (MIMS) instrument, I will focus the discussion on mass spectrometry and its application. Mass spectrometry is based on slightly different principles to the other spectroscopic methods, such as UV, IR, or nuclear magnetic resonance (NMR) (Mendham et al. 2006). Quadruple MS technique that utilizes the degree of deflection of charged particles by a magnetic field to find the relative masses of ions and fragments. In an electron impact (EI) mass spectrometer, a high-energy beam of electrons is used to displace an electron from the molecule to form a radical cation known as the "molecular ion". If the molecular ion is unstable then it can fragment to give other smaller ions. Mass analyzers separate the ions according to their mass-to-charge ratio. The principles of mass spectrometry and its

many applications are discussed elsewhere (Gross 2004; Wilkins and Lay 2006; Watrous and Dorrestein 2013).

There are many types of mass analyzers, using either static or dynamic fields, and magnetic or electric fields, but all operate according to the same differential equation. Each analyzer type has its strengths and weaknesses. We shall confine our discussion within MIMS probe mass spectrometry because it can measure analytes of interest (gas, liquid) directly and continuously. This instrument utilizes a membrane to semi-selectively transfer analyte mixtures from a sample to a mass spectrometer. Mass spectrometry can analyze wide variety of chemical species, both qualitatively and quantitatively (Boyd et al. 2008; Heinzle 1992; Lloyd et al. 1985; Hoch and Kok 1963) in very small samples. The samples can be in the form of a gas, a liquid, or a solid. It is to be noted that liquid or solid samples must be vaporized before being sent to the ionization chamber. Therefore, mass spectrometry is used across a wide-range of applications, including clinical, pharmaceutical, environmental, and biotechnological (Yang et al. 2003). It also can provide information on isotopic abundance through which reaction mechanisms, kinetics and biochemical pathways can be predicted (*Gombert et al. 2001;* Sauer 2006).

1.5.4 Mass spectrometry for on-line biological process analysis

The use of low-cost MS instruments in fermentation monitoring was first reported by Ruess et al. (1975). Since then researchers have been trying to incorporate it in on-line fermentation monitoring because it can rapidly measure multiple volatile analytes simultaneously. Response times for the MS instrument are reported to be in the range of a few seconds (Bastidas-Oyanedel et al. 2010; Oeggerli and Hienzle 1994) and detection levels have been reported to be as low as parts per quadrillion (ppq) for organic compounds in aqueous solution (Soni et al. 1995). The response of the instrument is linear over a wide-range of analyte

concentrations. This eliminates the need for complex multivariate procedures to de-convolute the data. However, Heinzle (1992) mentioned that methods such as principal component analysis (PCA) might still be useful for large data sets with many overlapping peaks. Another fascinating advantage of mass spectrometry is the ability to detect isotopes (Heinzle 1987). Isotopic abundance detection permits opportunities for metabolomic studies. Here, isotopic forms of carbon substrates (^{13}C, ^{14}C) and other nutrients (^{15}N, ^{17}O, ^{18}O) are utilized by the organism and the isotopes are tracked down to a particular metabolic intermediate (Sauer 2006) and/or end product (Yang et al. 2003).

There are a number of disadvantages for mass spectrometry as an on-line analytical tool. The major disadvantage is that even with applied soft ionization energy, fragmentation can occur (Hayward et al. 1990; Heinzle 1992; Oeggerli and Heinzle 1994). Fragments of molecules may share non-unique mass to charge ratios, and multiple analytes can end up contributing to a given peak. This complicates the otherwise simple data analysis. For example, the base peak of methanol is m/z 32. Its other major fragments are m/z 31, 29, 15. In a methanol-ethanol mixture, if methanol is measured at m/z 31, then ethanol, which has a base peak of m/z 46, may fragment to contribute to m/z 31 as well (Lloyd et al. 1985). The membrane probes of the instrument can be multiplexed (Heinzle 1992), but this can only be done to a limited degree because reactors must be in near proximity to the mass spectrometer (Oeggerli and Heinzle 1994) to avoid condensation or thermal decomposition of the analytes in the transfer lines.

Another challenge is to ensure the volatility of analytes of interest that may be present during micriobial growth for the detection in the gas phase. For example, the volatility of acetic acid is very low at or near pH 7.2. To make acetic acid volatile, the pH of the sample must be reduced to at least a pH of 2. At or below pH 2, most microorganisms (e.g. *C. termitidis, C.*

thermocellum) are unable to survive (Hethener et al. 1992; Lynd et al. 2002). Therefore, acidification is the only option for acetic acid measurement using off-line method. Furthermore, potential sterility issues are created if the probe is inserted directly in to the fermentation broth. However, the probe can measure headspace gases from the reactor off-gas stream, posing no contamination risk to the system (Oeggerli and Heinzle 1994).

Some gaseous analytes (e.g. water vapor and ethanol) may condense while leaving the reactor headspace. Continuous accumulation of condensates can contribute to high MS signal compared to the actual concentration present in the broth. Therefore, it is required to introduce a heating jacket throughout the off-gas line to avoid condensation of analytes (Chauvatcharin et al. 1995). Alternatively, MIMS probes can be inserted at the top of reactor headspace for representative sampling over the course of fermentation (Blunt 2013).

To monitor the microenvironment surrounding the cells, *in-situ* liquid phase analysis is essential. In that case, MIMS probes need to be inserted into the broth. Membrane probes may or may not be sterilized (Heinzle et al. 1992) because of intrinsic property damage to the membrane. Sterilization can be performed either by steam or chemical treatment (acid/base or ethanol solution). Regardless of the sterilization procedure, calibrations can be performed in-situ and after sterilization without interfering with the biological system. It is uncertain how the mass transfer properties of the probe would be affected after sterilization treatment, particularly for a MIMS. This aspect is beyond the current scope of our study.

1.5.5 Calibration and optimization of MIMS

As the MIMS probe mass spectrometry involves the combination of a few other instruments (mass flow controller, pH controller, mass spectrometry, temperature controller), it is required to calibrate and optimize each instrument individually, so that meaningful MS signals

can be obtained for scientific interpretation. MIMS systems do not provide analyte concentrations directly while calibration is performed. They are a measure of the movement of the molecule of interest across the MIMS membrane. This is correlated to concentration, but is influenced by many other factors. These include probe location, the hydrodynamic environment, the process temperature, presence of cells, presence of chemical species, agitation rate, and aeration rate. All these factors influence permeation rates across the membrane (Heinzle and Laferty, 1980; Chauvatcharin et al. 1995; Yang et al. 2003; Bastidas-Oyanedel et al. 2010).

Therefore, calibration is a major challenge. It should be performed in similar environments that exist around the probe during the fermentation. Unfortunately, the unpredictable nature of fermentation makes replication of the environment difficult. Nearly uniform conditions can be achieved in strictly controlled fermentation processes. The effects of different calibration approaches for MIMS were studied by Bastidas-Oyanedel et al. (2010). They applied two calibration models to acidogenic fermentation of glucose in batch and continuous mode for an anaerobic digestion process. The parameters of interest were ethanol, H_2, and CO_2 in the liquid phase, and H_2 and CO_2 in the gas phase. Two calibration strategies were evaluated: a) standard matrix-free calibration and b) in-process calibration.

A matrix free standard was performed in water using pure components. The in-process calibration was developed from offline analytical methods from samples taken at different times during the course of fermentation. The data from both procedures was fitted with a linear regression. The results showed that for standard calibration procedures, errors ranged from 55-130 % for gas and liquid-phase H_2 and CO_2. Reasonable errors were observed with standard calibration for ethanol, ranging from 11-30 % error compared to offline methods. By comparison, the in-process calibration produced errors between 8-11 % for all species except

dissolved H_2, which showed errors ranging from 21-43 %. All reported errors were within 95 % confidence intervals of comparison with appropriate offline analysis.

Causes of variation may include solubility, hydrogen bonding, salt effects, and mass transfer (Tarkiainen et al. 2005). From this observation, it seems that calibration in the presence of matrix effects produces a much more acceptable level of error, but it was still far from ideal. The study supports the in-process calibration strategy because the errors are within 10 %, while it was about 100 % for standard matrix-free offline analytical method. Overall, careful consideration needs to be exercised when designing MIMS calibration procedures.

1.5.6 Applications of MS for on-line fermentation monitoring

Chauvatcharin et al. (1995) conducted a study on fermentation monitoring using membrane probe and capillary inlet technique. *Saccharomyces cerevisiae* was cultivated in a 15 L reactor equipped with an electronic process control (EPC) (Model MB 1350M, Eyela Co. Ltd., Tokyo) by which the temperature, agitation and airation rates were maintained at 30 ^{o}C, 300 rpm, and 0.5-1.0 vvm, respectively. The pH was monitored by a pH probe (Model HC-82, DKK Co. Ltd., Tokyo) and was also controlled by the EPC at pH 4.5 by feeding 3.0 N NaOH. The medium contained 150 g/L glucose. Initially they used five different kinds of membranes to test suitability and applicability towards gaseous and volatile substances. Dimethylvinylsilicone membrane was selected for its acceptable response and durability. Teflon film was rejected for impermeability to volatiles while three others (Gortex film, poly-1-trimethylsilyl-1-propyne film and silicone membrane) were discarded for fragility. The calibrations were performed for ethanol, acetic acid (pH 3.5) and few other volatiles at 0-80 g/L concentration. To some extent, all analytes showed non-linearity within the range of calibration. It was suggested using non-linear calibration curve fitting where linearity deviated. Acidic pH was used for acetic acid

calibration to make it volatile and it ensured low minimum detection limit (0.5 g/L) compared to that at high pH (10 g/L at pH 6.5).

It was also tested the effects of temperature and pressure on MS signals for ethanol and other volatiles. The signals were compared with GC results. MS signals increased as the temperature rose while signals decreased when pressure of headspace increased. To have comparable results between MS and GC at elevated pressure, a linear model equation was suggested and applied. Good agreements were obtained.

After successful lab-scale fermentation, a demonstration of pilot-scale is essential. For the production of high concentration of ethanol from a reasonably high substrate load, lab-scale (Srinivasan et al. 1995) and pilot-scale (Johnson et al. 1997) studies were conducted using recombinant yeast. An automated on-line analysis of ethanol production was studied in a 2 L fermentor in fed-batch mode, with maximum glucose concentrations of 100 g/L to avoid substrate inhibition. The lab-scale fermentation was carried out at 31 ^{o}C with pH range 4-5. Calibration was performed for ethanol standards ranging from 1-11 %, and a linear response was obtained with $R^2 = 0.984$. Deviations from linearity were found to be minor at high concentration and were thought to be due to a combination of ethanol evaporation from the standards and non-linear effects of the membrane. Ethanol was measured in the liquid phase with a MIMS, and obtained results were compared with those found using offline HPLC analysis.

The MIMS system was adapted to a pilot-scale ethanol production facility by Johnson et al. (1997). The pilot plant facility used a 9000 L reactor with 10% substrate loading. A silicone sheet membrane was used to allow analytes selectively into an ionization chamber of a mass spectrometer. Calibration for ethanol was carried out with matrix-free standard calibration solutions for concentrations ranging between 1-15%, and the data was fitted with a linear

regression up to 10 % concentration. The MS results for ethanol were in good agreement with the parallel results obtained by offline HPLC analysis. The on-line analysis detected small amounts of acetic acid and lactic acid. Presence of these two analytes indicates contamination and its early detection is valuable for smooth process control. The pilot-scale study demonstrated how lab-scale fermentation can be implemented in an industrial scale-up process. This study is also a valuable reference to demonstrate the robustness of the MIMS instrument in an adverse (dusty, shock and vibration) industrial environment. Membrane inlet mass spectrometry has been mostly used in process optimization and quality control, but rarely used in explaining microbial metabolism.

1.6 Titrimetric and off-gas analysis (TOGA)

A titrimetric and off-gas analyzer is a semi-commercial analytical instrument developed in Australia and New Zealand (Gapes 2003; Pratt 2003) that includes a mass spectrometer, a manifold with one or more sampling probes, a bioreactor and a titration system. The key elements of TOGA is the signal integration, facilitated through the hardware interface and control software developed for the instrument. The latest versions of TOGA is capable of delivering an extremely precise quantity of reactants (acid/base) to the reactor. The whole system is connected with a computer through appropriate software (LabBoss V3, Scion, New Zealand) to control the system, with a network of mass flow controllers, recirculation pumps, and solenoid valves. A detailed description of TOGA (early and more recent versions) was discussed elsewhere (Gapes 2003; Pratt 2003; Blunt et al. 2010). Initially, TOGA was designed for the study of biological processes in wastewater treatment systems (Pratt et al. 2003), which was accounted in acid-base buffering (bicarbonates, ammonium, phosphate). A recent version was

specifically designed to be used in biofuel production (Blunt et al. 2014) and other biological product synthesis monitoring (Blunt et al. 2017).

1.6.1 Working principles of TOGA

Since TOGA brings together a number of analytical instruments, a variety of basic principles are involved. But for fermentation purposes, it involves two basic principles-titration and mass spectrometry. The principle of titration is briefly discussed here. Other instruments and their principles were discussed by Gapes (2003) and Pratt (2003). The titration involved here is an acid-base neutralization process, where acid or base can be used as the titrant and analyte is the summation of H^+ ion produced predominantly from fatty acids and CO_2. The production process of H^+ ion is very slow in biological systems compared to chemical process. Therefore, an efficient titration monitoring system is required at the pace of cell growth. The hydrogen ion production rate (HPR) is defined by the rate of base addition required to keep a constant pH. Its unit can be expressed as mol/s.

$$HPR = Q_b M_{OH,\,b} - Q_a M_{H,\,a}$$

where, Q_a , Q_b = flow rate of acid, or base respectively

$M_{OH,\,b}$ = molar concentration of OH^- ion in base

$M_{H,\,a}$ = molar concentration of H^+ ion in acid

TOGA follows a potentiometric titration with a gel pH electrode. pH of the solution is measured and recorded automatically throughout the titration, more accurately than with an indicator. The precision of the pH measurement is 0.02.

In addition to on-line monitoring of the HPR, oxygen transfer rate (OTR), nitrogen transfer rate (NTR), and carbon dioxide transfer rate (CTR) can be measured with this novel analytical tool, under both aerobic and anaerobic conditions. In typical biological and physico-chemical

process, the fluctuation of bio-indicators (such as O_2, N_2, H^+ ion and CO_2) can be monitored by measuring the rate of change of these species. They are defined as, the oxygen uptake rate (OUR), the nitrogen production rate (NPR), the HPR, and the carbon dioxide production rate (CPR), respectively. There are a number of methods available for the monitoring of biological treatment processes and each method has some limitations over others that have been described elsewhere (Gapes and Keller 2001; Pratt et al. 2003). As TOGA involves precise acid/base titration combined with mass spectrometry (MS) of off-gas analysis, it is possible to measure OUR, HPR, CPR etc. precisely under variable environmental conditions (pH, temperature, pressure, aerobic and anaerobic) using mass balancing.

In this work, the mass spectrometer used in the TOGA system is an HPR40 for dissolved species, provided by Hiden Analytical, UK (2010). The Faraday cup detector (FC) and secondary electron multiplier (SEM) detector are used for detecting low to high mass-to-charge ratios. The vacuum manifold consists of four inlets feeding that uses MIMS probes, each being 1.62 mm in diameter. Only one inlet can be open at a given time. The MIMS probes have permeable, replaceable membranes on the tip. The inlet controller module controls the solenoid valves to the inlets on the manifold and has built-in safety features if membrane failure occurs.

The bioreactor is the vessel in which a bacterial culture produces desirable metabolic products under aerobic or anaerobic conditions. Bioreactors can have several features (pH probe, DO probe, redox probe, pressure sensor, temperature probe, condenser, stirring equipment etc.) depending on the design of the experiment and area of research interest. For example, a nitrate or NH_3 probe is essential to determine nitrification/de-nitrification process in wastewater research, but it is less important in fermentation application. The reactor controller can control some of these parameters manually, but the LabBoss software (V3.0) can control all of them.

1.6.2 Factors affecting TOGA performance

There are a number of factors that may affect the overall performance of TOGA. These include calibration of the instrument, high pressure, and leakage in the whole system. Calibration of the whole instrument requires multiple stages of hardware calibration with calibration gases and other analytes of interest. MS detector calibration requires high vacuum/low pressure (10^{-6} torr) inside the detector chamber. The calibration gas should be of high quality with precise composition. Any impurities in the calibration gas (e.g. oil) may jeopardize the detection system. The detection limit for each component of interest need to be established at the very beginning and checked routinely. Insertion of high concentrations of analytes may affect the detector and its performance may drop from linearity (Johnson et al. 1997).

Off-gas analysis involves a number of steps: mass flow calibration, checking of solenoid valve performance within the pressure limit, gas conditioning, dilution of gas concentration etc. Any faulty step can create abnormalities in the TOGA system. For example, high pressure build-up through tubing may reduce performance of solenoid valves. There should be an active "watch dog" system on each component while running the experiment with the TOGA system.

Titration unit calibration involves two phases - gas and liquid. For example, to understand a typical metabolic shift one can dose the fermentation product gas into the headspace and monitor it over the course of fermentation. Liquid phase calibration mostly involves acid/base titration. However, it can be extended to any liquid addition, such as nutrients for growth, inhibition or yield monitoring.

1.6.3 TOGA in wastewater treatment

Biological wastewater treatment requires multiple reactions monitoring over the course of time. Pratt et al. (2003) used mass spectrometry to monitor off-gas from aerobic fermentation.

The raw TOGA sensor response required processing before interpreting the results. The process involved mathematical modeling for the validation of hypothesis, data processing etc. Initially, Gapes and Keller (2001) used an intensity ratio method (Ferreira at al. 1998) for the calculation of gas mass balancing and rate; then compared it with a concentration calibration curve method. It showed that both methods could be used confidently for such calculations with maximum difference of 1.8% for high dissolved oxygen (DO) (3.3 mg/L) and low dissolved oxygen (0.5 mg/L) conditions.

Pratt and his co-authors (Pratt et al. 2003) used nitrification via prokaryotic microorganisms at following conditions: liquor volume 2.9 L, pH 7.5, gas flow rate 525 mL/min (O_2: 23 %, CO_2: 0.12 %, Ar: 1.2 %; make-up He). Sodium acetate was used as a substrate and allyl-thio-urea was used as nitrification inhibitor that ensured acetic acid as only oxygen consuming agent. They used ammonium chloride as nitrogen source for the cell growth.

Off-line analysis was conducted at regular intervals for both volatile fatty acids (VFAs) and ammonium nitrogen concentration measurements. Oxidation of acetic acid was readily observed from the continuous measurement of depleted DO signals. The recovery of DO ensured the completion of oxidation reaction. It was clearly observed the substantial change in DO concentration during the course of reaction. The biological OUR was also determined as a function of both OTR and the rate of change of DO. In a steady state condition, when DO remained constant in a typical biological wastewater treatment system, the contribution of endogenous respiration needs to be considered and it was adapted during this calculation. The rate of HPR was also used as a measure of the aerobic carbon removal process using stoichiometry and mass balancing (Pratt et al. 2003). The comparison was made between the data obtained from TOGA on-line sensor signals with off-line VFA analysis. Good agreements were

obtained with insignificant variations. Similarly, nitrification was also monitored (Gapes and Keller 2001), where OUR was a measure of the overall rate of nitrification. They used nitrifying activated sludge at a slightly basic condition (pH 7.8) and temperature range of 20-25 ^{o}C. During monitoring of ammonia oxidation, the OUR signal was elevated and finally, it dropped down when all ammonia was consumed. The nitrogen speciation was shown during nitrification and it was also compared against off-line analysis. It was observed that the TOGA predicted values were agreed well against off-line data with 95% confidence intervals from the linear regression analysis.

1.6.4 Microbial perturbation, inhibition and nutrient dependency

Perturbations of biological systems are alterations of function (substrate consumption rate, metabolites production rate, gas transfer rate, growth rate, etc.) induced by external or internal mechanisms. Biological systems can be perturbed through a number of means. Examples include environmental stimuli (pH changes, temperature changes, osmotic shock or pressure changes) (Dabrock et al. 1992; Wolfe 2005), small molecules that affect different biological pathways, such as fermentation end-products or toxins (Vallino 1991), and manipulation of gene function, such as gene knockouts (Fong and Palsson 2004; Sauer 2006). Wolfe (2005) reviewed perturbation of *E. coli* strains, whereas other researchers (Sauer 2006; Blank and Kuepfer 2010) reviewed how metabolic regulation and control of flux can be monitored using isotopically labeled substrates. On-line monitoring techniques for off-gases could be used as a robust tool for monitoring microbiological perturbations during biofuel synthesis from plant biomass (cellulose and hemicellulose) including soluble ones (glucose, xylose, cellobiose, etc.).

Inhibition plays an immense role in biofuel production or waste treatment technology (Palmqvist and Hahn-H 2000; Boe 2006). It retards cell growth, changes metabolite production

rates, and diverts carbon-flux through alternative biochemical pathways (Rydzak et al. 2011; Boe et al. 2010). Most common inhibitors are H_2S, CO_2, and furan derivatives from lignin. End-product inhibition is another concern for biofuel researchers (Demain et al. 2005). End-product inhibition control cannot be achieved properly if continuous measurements of the product concentration are not performed.

Growth of wild-type *C. thermocellum* was inhibited by ethanol at concentrations of 4 – 16 g/L (Lynd et al. 2002); however, there were several reports showing that this organism can be adapted to grow in the presence higher ethanol (Herrero and Gomez 1980; and recently Lynd's group in BioEnergy Science Centre, Brown et al. 2011; Tian et al. 2016). Herrero and Gomez compared the ethanol concentration for both the wild type (ATCC 27405) and C9 strains (ethanol tolerant). The inhibited growth rate was an exponential function of the ethanol concentration. They found that C9 strain had higher ethanol tolerance than the ATCC 27405 strain. At an ethanol concentration of 25 g/L, the wild type had a negative growth rate, possibly caused by cell lysis, whereas the resistant strain was able to grow at a rate of 40 % to 50 % greater than the uninhibited strain. High temperature and high fluidity might destabilize cell membranes, which resulted in arresting cell growth by changing membrane protein functionality. On the other hand, Brown et al. (2011) obtained an ethanol tolerant mutant that gradually adapted to exogenous ethanol using a serial transfer approach at 55 ^{o}C. This ethanol tolerant mutant evolved due the changes in bifunctional acetaldehyde-CoA/alcohol dehydrogenase gene (adhE). Using gene deletion and adaptive evolution approach, Tian et al. (2016) obtained a strain with high ethanol tolerance that was produced ethanol at 75 % of the maximum theoretical yield.

Optimization parameters such as stirring, temperature, medium, ionic strength, end-products removal may play a significant role in fermentation processes. Bacteria that degrade

cellulose using cellulosomes require sufficient time to attach themselves to the cellulose (Lamed et al. 1983; Munir et al. 2014). High stirring rate (>100 rpm) may reduce the rate of sysnthesis of end-products. Lack of substrate availability will hamper the growth of cells and, therefore, end product formation. The ability of a microorganism to grow in minimal medium using glucose or other substrates (e.g. pyruvate) indicates that the micro-organism contains the necessary biosynthetic pathways for all macromolecule building blocks (i.e. amino acids synthesize). In contrast, drawing conclusions about biosynthetic pathways of micro-organisms grown with yeast extract is difficult, because the micro-organisms consume necessary amino acids, which are already present in the yeast extract. Therefore, to check biosynthetic pathways defined/minimal media must be used during bacterial growth observations (Fuhrer et al. 2005; Liu et al. 2012). We believe that perturbation, inhibition, and nutriend dependency studies can be achieved efficiently with the help of continuous monitoring of headspace and liquid phase gases.

1.7 Objectives, rationale, and research hypotheses

1.7.1 Research objectives

The central focus of this thesis is to better understand changes in microbial metabolism induced by changes in growth conditions (carbon-excess, end-product concentration such as acetate, quick removal of product gases). Changes in carbon and electron flow during microbial growth (metabolic shifts) result in different patterns (ratios) of end-product synthesis. Differences in end-product concentrations resulting from metabolic shifts are usually detected at the end of the fermentation reaction (stationary phase), or at discrete points within the growth (log) phase, because the number and timing of samples taken for analysis are limited. A deeper understanding of microbial metabolism and the mechanisms responsible for changes in end-product synthesis patterns may be acquired by continuous monitoring. Thus, the primary goal of

the research is to develop and validate analytical tools so that instantaneous changes in metabolism (measured as changes in end-product synthesis patterns) can be achieved under various physico-chemical conditions. TOGA was used as an on-line monitoring tool for headspace gas (H_2, CO_2 and ethanol) analysis. In addition, HPLC and spectrophotometry methods were also used for other metabolites analysis.

Clostridium termitidis was chosen as the model organism for this work because its genome has been sequenced (Lal et al. 2013) and its growth characteristics have been studied (Ramachandran et al. 2008; Munir et al. 2014; 2015; 2016). However, the metabolism of *C. termitidis* and changes in its metabolic behavior has not yet been well studied under different physico-chemical environments. Instantaneous changes in *C. termitidis* metabolism, in response to changes in growth conditions, will be investigated by comparing concentrations and synthesis rates of key metabolites measured at specific time points (discrete sampling) versus real-time (continuous) sampling.

1.7.2 Rationale and research hypotheses

Traditional off-line analytical techniques have been used for understanding microbial physiology in many bioprocesses, such as the microbial synthesis of biofuels (Dabrock et al.1992; Ramachandran et al. 2008; Veen et al. 2013). In such cases, these information (limited discrete sampling) are insufficient in explaining metabolic changes. Perturbation studies using end-product addition are useful in understanding changes in microbial metabolism and reaction mechanisms (Herrero et al. 1985a; Herrero et al. 1985b). The addition of fermentation end-products (acetate, propionate, lactate, butyrate) during the exponential growth phase can induce metabolic shifts that change the ratios of end-products, such as ethanol and H_2 (Zheng and Yu 2005; Rydzak et al. 2011). These shifts occur to maintain redox balance within the cells, but

there are threshold limits beyond which inhibition may result. Some researchers have shown that excess addition of organic acids can induce cell membrane fusion, inhibit amino-acid transport, and uncouple oxidative phosphorylation (Ginsburg et al., 1973; Herrero et al. 1985a).

These studies typically used off-line analytical techniques to measure changes in product synthesis at discrete time intervals. It is time consuming, however, to monitor changes in metabolic pathway perturbations using off-line analytical techniques. Our preliminary studies (Blunt et al. 2014) suggest that continuous monitoring of volatile fermentation end-products using the mass spectrometry-based TOGA system not only can provide real-time information on changes in microbial metabolism, but also help to predict the overall changes in fermentation end-product synthesis patterns induced. Estimation of non-volatile fermentation end-products (formate, acetate, lactate), based on instantaneous measurement of the volatile fermentation products and pH requires the development and validation of a stoichiometric algorithm that can accurately model carbon distribution, product ratios (C1/C2), redox balance (O/R), and carbon recovery.

The main objective/goal underlying this work is that off-line analytical techniques to measure changes in product synthesis at discrete time intervals are insufficient to identify and characterize precise metabolic flux shifts that occur rapidly in response to changing growth conditions. In contrast, continuous, real-time monitoring of fermentation end-products using the mass spectrometry-based TOGA, can provide information on instantaneous changes in microbial metabolism. The changes in growth condition that can induce metabolic shifts of interest include changes in end-product concentrations, carbon loading, pH, and temperature. This thesis will focus on i) changes in carbon-excess condition, ii) changes in end-product concentrations, and

iii) effects of quick removal of dissolved (end-product) gases. These observations lead to the following hypotheses:

Hypothesis 1: Under carbon-excess condition, re-distribution of fermentation end-products will occur through pyruvate catabolic reactions of *C. termitidis* compared to that in carbon-limited condition. To evaluate commercial viability and industrial scale-up, it is required to study the growth of *C. termitidis* under high substrate loading conditions, which has not been studied previously.

Hypothesis 2: Presence of exogenous acetate (one of the fermentation end-products) during the exponential growth phase may divert C-flux towards ethanol production. To adjust the redox balance, *C. termitdis* may synthesize less H_2, and this signature can be found in continuous off-gas measurement.

Hypothesis 3: Fast removal of metabolic dissolved gases (H_2 and CO_2) will increase H_2 production and decrease ethanol production during the growth of *C. termitidis* in a pH controlled bioreactor. The removal of dissolved gas can be done either physically or chemically. The effect of quick removal of gaseous metabolites will be studied here using physical methods.

Hypothesis 4: Continuous measurement of selected, volatile fermentation end-products (H_2, CO_2, and ethanol) and pH, can be used to predict the overall changes in fermentation end-product synthesis patterns induced by surrounding growth environment using stoichiometric end-product algorithm.

Before testing these hypotheses, an experiment (titration of $KHCO_3$ using HCl solution) were designed and performed within a bioreactor environment that produce carbon dioxide from a single source and did not have any interaction with biological systems. The headspace gas was

monitored both off-line (discretely) and on-line (countinuously) so that the detection efficiency could be evaluated against the monitoring systems (“off-line” versus “on-line”).

1.8 Thesis outline

The thesis is developed in seven chapters and their outlines are provided here. In Chapter 1 of this thesis, background information on substrate utilization by various microorganisms, their nutritional requirements, and metabolite identification tools have been presented, and various techniques of on-line fermentation monitoring were reviewed. While there are many methods for detecting and analyzing fermentation metabolites, the review presented in Chapter 1 focused on mass spectrometry (MS) and the use of MS with the titration and off-gas analysis (TOGA) system, examples of how the TOGA system has been used to monitor biological reactions in real-time for process optimization are presented. Four research hypotheses are described here. Chapter 2 presents experimental design and analytical methods to achieve the present research goals. In Chapter 3, the growth and metabolic shifts of *Clostridium termitidis* were monitored under high substrate loading **(**10 g/L cellobiose) using a membrane inlet mass spectrometer (MIMS) and compared those changes with low substrate loading. Several discrete methods were applied to compare and analyze the difference among end-products synthesized during the growth of *Clostridium termitidis*. Chapter 4 presents the results of end-product induced (acetate) metabolic shifts monitoring on the growth of *C. termitidis*. Chapter 5 presents the results of the effects of dissolved gas removal (quick mass transfer process) on ethanol production during the growth of *Clostridium termitidis* under carbon-sufficient conditions. In Chapter 6, formate, acetate and lactate concentrations are predicted under various growth conditions of *C. termitidis* using a stoichiometric end-product algorithm. The predicted data was compared against

discretely obtained data, and described the subtle changes with statistical analysis. In the final Chapter 7, conclusions and future perspectives are discussed.

Chapter 2

Materials and Methods

2.1 Materials and Methods for Chapter 3

2.1.1 Microorganism, substrate and media

Clostridium termitidis CT1112 was obtained from the American Type Culture (ATCC), and was cultured in 1191 medium at 37 ± 1 °C. Filter sterilized, anaerobic cellobiose was used as a carbon source for batch fermentation. Initially, small-scale batch fermentations were carried out in 125 mL serum bottles with a 50 mL working volume. Then culture volume was transferred to a 1 L Corning culture bottle with a 500 mL working-volume, which was considered to be the active culture for the bioreactor inoculation.

Concentrated sterile cellobiose solution was used as a substrate to feed the bioreactor to a final concentration of 10 g/L, 2 g/L and 1 g/L. All chemicals and reagents for media and substrates were obtained either from Fisher Scientific (Ontario, Canada) or Sigma Aldrich (Missouri, USA). Yeast extract was obtained from Becton, Dickinson and Company (New Jersey, USA). To maintain fresh cells, *C. termitidis* was serially sub-cultured by transferring 10 % (v/v) inoculum into 1191 media containing 2 g/L cellobiose. This complex medium contained (per liter of milliQ water): KH_2PO_4, 1.5 g; Na_2HPO_4, 3.35 g; NH_4Cl, 0.5 g; $MgCl_2.6H_2O$, 0.18 g; yeast extract, 2.0 g; resazurin (0.25 mg/mL), 2.0 mL; 10X vitamin solution, 0.50 mL; 10X mineral solution, 1.0 mL. Vitamin supplement and mineral elixir solutions were prepared according to Islam et al. (2006). A filter-sterilized sodium sulfide (Na_2S) stock solution (200 mmol/L) was used as a reducing agent (oxygen scavenger) at a final concentration of 2 mmol/L.

2.1.2 Bioreactor setup

A 7 L round-bottom glass bioreactor (Applikon Biotechnology, Foster City, CA, USA) was used in all experiments. The reactor was equipped with a sterilizable pH gel electrode, liquid sampling port with a 60 mL receiving vessel, gas sampling port, stirring apparatus (flat bed impeller design), an L-shaped sparging apparatus, three baffles, a temperature probe, a heating jacket, and a liquid-cooled condenser. Two custom made micro-bubblers were inserted at the end of the sparging system using silicon rubber tubing. A volume of 2,510 mL of 1191 media was added to the reactor prior to being autoclaved at 121 °C for 60 minutes. The reactor was then sparged overnight at a flow rate of 20 mL/min with an inert carrier gas consisting of 95 % N_2 and 5 % Ar (Praxair, Winnipeg, MB, Canada). The carrier stream was delivered using a two-stage pressure regulator (Swagelok, Winnipeg, MB, Canada) upstream from a thermal mass flow controller (MFC) (Bronkhorst Hi-Tech, El-flow, The Netherlands), and passed through a 0.2 μm filter (Millipore, Billerica, MA, USA) prior to being introduced to the reactor. This setup was left overnight to establish anaerobic conditions. A 200 mmol/L filter sterilized solution of sodium sulfide (Na_2S) was then added through the gas sampling port on the reactor head plate on a 1 % (v/v) basis just prior to inoculation. Similarly, filter sterilized cellobiose was added into the reactor through the gas sampling port to a final concentration of 10 g/L, 2 g/L and 1 g/L. The reactor was then inoculated (10 % v/v) from a 1 L Corning bottle (with a 500 mL working volume) that had been incubated long enough for the culture to reach an OD_{600} of about 0.4.

2.1.3 On-line analytical methods

2.1.3.1 MIMS probe calibration

A membrane inlet mass spectrometer (MIMS, Model HPR-40) equipped with a quadrupole mass analyzer (HAL 201 RC), Faraday Cup (FC) detector and Scanning Electron

Multiplier (SEM) detector (Hiden Analytical, Warrington, UK), was used in conjunction with MasSoft 7® software to measure ethanol, H_2, and CO_2 on-line. For gas-phase calibration, a four-point background-subtracted concentration calibration curve was developed for the MIMS for 0-10 % H_2 and 0-5 % CO_2 (mol/mol) with a linear fit (H_2: slope = 3.228E-9, intercept = 8.575E-10, R^2 = 0.991; CO_2: slope = 5.847E-10, intercept = -1.109E-10, R^2 = 0.996) according to previously described methods (Gapes et al. 2001). Known concentrations of these gasses were prepared in a step-wise fashion by diluting purchased gas mixtures (Praxair, Winnipeg, MB, Canada) into an inert carrier stream using previously calibrated thermal mass flow controllers (Bronkhorst Hi-Tech, El-flow, The Netherlands). The combined calibration gas mixture was then humidified by passing through the bioreactor containing 1191 media at 37 ± 1 ^oC and 100 rpm agitation. The sterile MIMS probe was inserted through rubber sealed gas-sampling port and kept vertically. Then the off-gas was cooled using a condenser (mounted on the reactor head plate) from a room temperature water bath that was circulated with a peristaltic pump. Hydrogen was measured at a mass-to-charge ratio (m/z) of 2 and carbon dioxide was measured at m/z 22. The m/z 44 signal for carbon dioxide was avoided due to interference signal from ethanol at this mass-to-charge ratio.

For ethanol calibration, a standard addition method was used at the end of the fermentation experiment to nullify potential physical or chemical interactions, and then the MIMS-based measurements were compared with the discrete measurements obtained by HPLC analysis. A solution of 10 M ethanol was prepared and added to the reactor vessel to final concentrations of 1, 2, 5, 10, 15, and 50 mmol/L. The MIMS probe was used to measure the ethanol signal at m/z 31 and was allowed sufficiently to equilibrate each concentration step. The

background ion current signal for each metabolite of interest was subtracted, and the remaining value was then fitted to the known concentration using linear regression analysis.

2.1.3.2 Calibration of titration system

The pH control system (Scion, Rotorua, New Zealand) utilized two, high-precision 10 mL injector syringes (Hamilton Syringe Co., Reno, NV, USA) operated by split PID logic administered by a programmable logic controller (PLC, Opto22). The operational details can obtained from Blunt et al. (2014). The rate of base addition was converted to the hydrogen ion production (HP) based on an approach adapted from Pratt et al. (2003), which treats the acid added by the titration system to control pH should it rise above the setpoint. It may be via consumption of acidic materials in the liquid and it will compensate for overshooting:

$$\left[Total\ Hydrogen\ Ion\ Production\ (HP) = \frac{S_b V_b - S_a V_a}{1000}\right]\ (moles) \qquad 2.1$$

Here, S_a and V_a are the strength (mol/L) and volume (mL) of acid being dosed, respectively. Similarly, S_b and V_b are the strength (mol/L) and volume (mL) of base being dosed, respectively. It is to be noted that exact concentration of acid and base was obtained against known concentration of acid/base using potentiometric titration immediately after completion of fermentation. The titration result for the HP was also compared to the theoretical values, based on the obtained end-products profile. It was also assumed that all acids were monoprotic and dissociated completely at pH 7.2.

2.1.3.3 Calibration and optimization of TOGA system

The Titrimetric and Off-Gas Analysis (TOGA) system consists of several instrument components, individual calibration was required for each component. Details of those calibrations were described by Gapes (2002) and Blunt (2011, 2013). Capacitance-based sensor was required against living cell population calibration. In absence of capacitor sensor, OD and

protein assay can be used against on-line (TOGA) measured signals such as CO_2 and H_2 evolved from a typical fermentation run using a monoculture. Cell density was measured using OD measurement in addition to protein assay using Bradford method (Bradford 1976) as off-line technique for comparison.

There are a number of sources that can generate signal noise during on-line monitoring of any fermentation process. These include temperature or pressure fluctuations, flow rate variations, leaks in the vacuum and sampling line, internal and external vibration (Ferrerira et al. 1998). Therefore, it is necessary to observe mass spectral data closely, find the possible sources of noise and perform prompt troubleshooting to obtain reliable data.

Calibration techniques vary according to operating conditions. Therefore, it is essential to optimize under those operating conditions. Table 2.1 summarizes the behaviour of membrane inlet mass spectrometry signals for various gases of interest. There is a trade-off between gas molecules (with and without H-bonding or dipole interactions) and volatile compounds (e.g. ethanol) with water vapour. We have chosen the technique, where the MIMS probe is inserted into the headspace, which provided fairly constant signals for our analytes of interest. By choosing this technique, we were able to effectively quantify ethanol with hydrogen and carbon dioxide.

Table 2.1 Comparison of mass spectrometry (MS) signals for various measurements using MIMS probes.

Signals	Complete Removal of Water Vapor from Off-Gas [a]	Partial Removal of Water Vapor from Off-Gas [b]	Saturated Water Vapor in Headspace (HS) [c]	Bulk Water in Broth [d]
MIMS Probe Position	Calibration cell, outside HS	Calibration cell, outside HS	Inside HS	Into broth
H_2O	Fairly constant minimum signal	Fairly constant minimum signal	Fairly constant minimum signal	Fairly constant minimum signal
Ar	Fairly constant, no interference	Fairly constant, no interference	Fairly constant, no interference	Fairly constant but reasonably low compared to HS, no interference
N_2	Fairly constant, no interference	Fairly constant, no interference	Fairly constant, no interference	Fairly constant but reasonably low compared to HS
H_2	Fairly constant, least interference with water vapour	Fairly constant, interference with water vapour	Periodically signal drift and rise; fairly high responses compared to off-gas signals	Periodically signal drift and rise; highly interferes due to high population of water molecule
CO_2	Fairly constant	Constant but occasionally drift	Zig-zag, interfered by stirring speed change	Signal drift and rise; sudden rise some time
EtOH	No quantifiable ethanol signal	Interfere due to condensation	Fairly consistent	Fairly consistent

[a] removal of water vapor using ice bath; [b] removal of water vapor using condenser at room temperature 23 ^{o}C; [c] fermentation temperature ± 3-5 ^{o}C (if not covered with extra insulating jacket); [d] fermentation temperature in ^{o}C

2.1.4 Monitoring of fermentation experiments

After inoculating the reactor, the reaction conditions were maintained at 37 ± 1 °C, pH 7.2 ± 0.02, and stirring speed of 100 rpm. During fermentation, the MIMS was used to monitor H_2 and CO_2 in the head-space at m/z 2 and m/z 22, respectively. Ethanol in the gas-phase was also measured at m/z 31. Simultaneously, discrete samples were taken in 4 hour intervals for off-line analysis of both the gas phase and the liquid phase. Three independent replicate samples (technical replicates) were taken at each time point. In order to retain identical physiological condition, it was difficult to maintain exact time point for biological replicates through out the experiment since a number of tasks were involved at a given time. Therefore, the average of the replicates was shown at each time point if it varied less than 30 minutes (unless otherwise mentioned). Two biological replicate experiments were performed in which the MIMS was used to monitor H_2, CO_2, and ethanol in the reactor head-space. The titration system was used to maintain constant pH and recorded the cumulative hydrogen ion production (HP).

2.1.5 Off-line analytical methods

Off-line analytical methods, such as gas chromatography (GC) for gas phase analysis, high performance liquid chromatography (HPLC) for liquid phase analysis, protein assay for cell biomass analysis, and pH measurements were also conducted.

2.1.5.1 Gas phase analysis

An Agilent 7890A GC System (Agilent Technologies Canada Inc. Mississauga, ON, Canada) equipped with a thermal conductivity detector (TCD) and a PLOT molecular sieve column 30 m by 0.53 m ID was used to verify the concentration of non-condensable gasses (H_2, CO_2) in the reactor off-gas detected by the MIMS. Headspace gas samples (0.5 mL) were

collected with gastight syringe and were immediately analyzed by gas chromatography as described previously (Blunt et al. 2014).

2.1.5.2 Sugar and end-product analysis in liquid phase

Aliquots of cultures were dispensed into micro-centrifuge tubes (Fisher Scientific, Ottawa, ON, Canada) and centrifuged (IEC Micro-MB, International Equipment Company, Chattanooga, TN, USA) at 10,000 x g for 10 min to separate the cell pellets from the supernatants. The supernatants were then transferred into new microcentrifuge tubes and stored in a refrigerator at below 10 ^{o}C for further end-product analysis. The end-product analysis was completed within 24 hrs of finishing the experiment. Sugars, organic acids and ethanol were quantified by an HPLC (Waters, Milford, MA, USA) with a pump (Model 1515), autosampler (Model 2707), and a refractive index detector (Model 2414). A 300 mm x 7.8 mm resin-based column (Aminex HPX-87H, Bio-Rad Laboratories, Mississauga, ON, Canada) was used for analytes separation.

2.1.5.3 Growth and cell protein measurement

The pellets were re-suspended with 0.9 % (w/v) sodium chloride (NaCl) and centrifuged for 10 minutes. The supernatant was discarded and 1 mL of 0.2 M sodium hydroxide (NaOH) was added to re-suspend the pellets. Samples were incubated at 100 ^{o}C in a water bath for 10 minutes, and after cooling down, the supernatants were collected for further processing. Optical densities at 595 nm (PowerWave XS, BIO-TEK, Winooski, VT, USA) were measured until results stabilized and then recorded. Protein content was determined with the Bradford assay (Bradford 1976). The protein data was used to account for cell mass in the carbon balance, approximating biomass as having the composition $C_4H_7O_2N$, and having a molecular weight of 101 g/mol (Islam et al. 2006; Rydzak et al. 2009), because exact elemental composition of *C.*

termitidis is not known. The protein content accounts for approximately 50 % of the bacterial biomass (cell dry weight, CDW), so to convert protein data to biomass yields it was multiplied by 2.

2.1.5.4 Off-line pH measurement

pH of the fermentation broth was measured immediately after sampling for comparison with the on-line titration system. A Beckman Coulter pH meter (Model pHi 410, USA) with ThermoOrion pH probe was used for the off-line pH measurement. The system was calibrated for each set of experiments using two point buffers (pH 4.0 and pH 7.0). It is to be noted that too much disturbance of the sample and prolongation of measurement would result little higher pH compared to actual broth pH; because carbon dioxide leaves broth by such activities.

2.1.6 Total gas production

A gas-phase mass balance was performed, assuming a completely mixed headspace and that the volumetric production of H_2 and CO_2 were negligible in comparison to the sparging rate. Because the system was open and being purged at 20 mL/min, CO_2 and H_2 vented in the off-gas were accounted for by integrating their measured concentrations with respect to time using the trapezoidal rule (Gilat and Subramaniam 2008). It was assumed that the biological rate of gas production was negligible compared to gas flow rate into the reactor, and hence $Q_{g,in} = Q_{g,out}$. The carrier gas used here mixed inert gas mixture (95% N_2 and 5% Ar) and neither of any gas consumed by the fermentation system. In addition to that previously calibrated (data not shown) efficient mass flow controllers (MFCs) were used to maintain constant gas flow. Total gas production was then obtained by adding the dissolved species at a given time. The concentration of H_2 and CO_2 remaining in solution was related to the headspace gas composition using temperature-corrected Henry's coefficients for H_2 and CO_2 (Sander 2015).

Carbon dioxide presents a unique challenge, as it is associated with several dissolved carbonate species, such as CO_2 (aq), H_2CO_3 (aq), HCO_3^- (aq), CO_3^{2-} (aq). These carbonate-bicarbonate species play an important role in any biological system irrespective of operational conditions (aerobic, anoxic and anaerobic), because the system always seeks equilibrium with produced carbon dioxide gas.

$$CO_2\ (g) \rightleftharpoons CO_2\ (aq) \qquad 2.2$$

Then the dissolved species (aq) hydrated according to following equation and formed carbonic acid:

$$CO_2\ (aq) + H_2O \overset{R_{hy}}{\rightleftharpoons} H_2CO_3\ (aq) \qquad 2.3$$

Since the equilibrium coefficient for dehydration reaction (reverse reaction) is much greater than the equilibrium coefficient for hydration reaction (forward reaction), as a consequence carbon dioxide is highly soluble in water compared to nitrogen and other inert gases, therefore, most of the carbon dioxide gas is found as CO_2 (aq) species at STP. Carbonic acid is considered as a weak acid, therefore, it dissociates in the following way at or near neutral pH:

$$H_2CO_3^*\ (aq) \overset{R_{c1}}{\rightleftharpoons} H^+ + HCO_3^-\ (aq) \qquad 2.4$$

$$HCO_3^-\ (aq) \overset{R_{c2}}{\rightleftharpoons} H^+ + CO_3^{2-}\ (aq) \qquad 2.5$$

The reaction rates Rc1 and Rc2 are rapid. Even the rate of hydration of CO_2 (aq), R_{hy}, which is considerably slower than the other acid–base reactions, is significantly faster than the biological process (Royce 1992).

In the context of pH controlled (nearly neutral pH in the present set of experiments) fermentation systems, it can be assumed that these reactions are instantaneous and concentrations can be determined using Henderson-Hasselbalch equation

$$pH = pKa + \log \{C_{A-} / C_{HA-}\} \quad 2.6$$

For a given time, using this equation the concentration of carbonic acid ($C_{H_2CO_3}$), bicarbonate ($C_{HCO_3^-}$), and carbonate ($C_{CO_3^{2-}}$) can be obtained as follows from Equation 2.3, 2.4 and 2.5, since CO_2 is the only directly measurable quantity

$$C_{H_2CO_3} = C_{CO_2}(aq)/K_{hy,} \quad 2.7$$

$$C_{HCO_3^-} = K_{ac1}\, C_{H_2CO_3^*}/10^{-pH} \text{ and} \quad 2.8$$

$$C_{CO_3^{2-}} = K_{ac1}\, K_{ac2}\, C_{H_2CO_3^*}/10^{-2pH} \quad 2.9$$

where, K_{hy}, K_{ac1} and K_{ac2} are the equilibrium constants for Equation 2.3, 2.4 and 2.5, respectively. In the above equations, $C_{H_2CO_3^*}$ is considered as the total analytical concentration of dissolved CO_2, which is equal to the sum of C_{CO_2} (aq) and $C_{H_2CO_3}$ (Stumm and Morgan 1996). Nevertheless, the equilibrium constant (hydration constant) lies far to the left, where less than 0.2 % of H_2CO_3* exist as H_2CO_3 at room temperature (Pratt 2003; Yang et al. 2003). Thus, the total concentration of the dissolved carbonate species (C_T) can be defined as

$$C_T = C_{H_2CO_3^*} + C_{HCO_3^-} + C_{CO_3^{2-}} \quad 2.10$$

By replacing $C_{H_2CO_3^*}$ with C_{CO_2} (aq) + $C_{H_2CO_3}$, the Equation 2.10 can be rearranged as follows:

$$C_T = C_{CO_2}(aq) + C_{H_2CO_3} + C_{HCO_3^-} + C_{CO_3^{2-}} \quad 2.11$$

These equations are used for the determination of carbonate-bicarbonate species produced during fermentation and then total gas production is obtained by the summation of the dissolved species.

2.1.7 Calculation of volumetric, substrate specific, and cell specific end-product synthesis rates

Volumetric production of end-products was calculated in five different phases (as described in Chapter 3); whereas cell specific production rates were calculated at each sampling time point. First couple of data points were excluded from graphical representation, because of high uncertainties in measurements. Volatiles products rates were also calculated from continuous measurement at various growth phases. There is a change in working volume due to discrete sampling, pH control and substrate addition, which eventually affect end-products concentrations, rates, and yields (Johnson et al. 2009). Proper measures were taken for volume correction for liquid phase and gas phase. In a typical fermentation reaction, the volume of the bioreactor (V_R) does not change and can be defined by the following equation

$$V_R = V_L + V_G \qquad 2.12$$

where, V_L is the volume of the liquid phase and V_G is the volume of the gas phase. V_L is, generally, considered as working volume. It is assumed that under standard temperature and pressure these volumes remain constant since neither addition nor loss of any liquid occurs from the working volume. However, in the present set of experiments, due to acidic metabolites synthesis, considerable amount of base is consumed, which can be monitored using automatic titrator. Since the fermentation is performed in a controlled pH (7.20 ± 0.02), therefore, some amount of acid is also consumed due to overshooting of base. Then the working volume of the broth will be increased by $V_{ba} = V_b + V_a$. Here, V_b is the volume change due to base consumption, V_a is the volume due to acid consumption and V_{ba} is the overall volume change (total volume) due to acid and base addition. Considering this situation (here, controlled pH environment), the working volume can be expressed as

$$V_w = V_L + V_{ba} \quad 2.13$$

By replacing the value of V_{ba} in Equation 2.13, the new working volume (V_w) will be

$$V_w = V_L + (V_b + V_a) \quad 2.14$$

In the mean time, the headspace working volume (V_{HS}) will also be decreased by same amount of V_{ba}, therefore,

$$V_{HS} = V_G - V_{ba} \quad 2.15$$

By putting the value of V_{ba} in Equation 2.15, the headspace volume can be obtained as

$$V_{HS} = V_G - (V_b + V_a) \quad 2.16$$

For a given time, when base is added (V_b) to neutralize biologically produced acids, the acidic titrator will not dispense any acid and it will remain zero (Va = 0), vise versa. By putting the values of V_L and V_G into Equation 2.12, the following Equation is obtained:

$$V_R = Vw - (V_b + V_a) + V_{HS} + (V_b + V_a) \quad 2.17$$

From the Equation 2.17, it is observed that to keep the reactor volume constant (since it does not change), the excess liquid volume due to base addition, has to be subtracted from the original headspace volume. Otherwise, significant error will be noticed both in gas phase and in aqueous phase concentration measurement, which is obtained either discretely or continuously. It is also assumed that changes in liquid volume is negligible due to continuous sparging of nitrogen gas; because hydrated headspace gas is passed through the condenser.

2.1.8 Reaction stoichiometry and redox balance

Using reaction stoichiometry, mass balance and electron balances (Gottschalk 1986) were derived to take all major end products into account. In this work, they were used as indicators to test the efficiency of both off-line and on-line results. Like most of the *Clostridia* species, *C.*

termitidis utilizes branched fermentative pathways from the pyruvate node, synthesizing lactate, formate, acetate, ethanol, CO_2, and H_2, as well as a certain amount of cell mass (Figure 1.1). A mass balance can be performed using the residual substrate concentration (here, cellobiose as substrate consumption), cell mass production, and concentrations of end-products to calculate the Carbon Recovery Index (CRI).

$$C_{12}H_{22}O_{11} = H_2 + CO_2 + H\text{-}COOH + CH_3\text{-}COOH + CH_3\text{-}CHOH\text{-}COOH + C_2H_5\text{-}OH + Cell \qquad 2.18$$

This is a simplified form of fermentation equation to describe how substrate (here cellobiose) is distributed to various end-products, where ammonium chloride is the source of nitrogen for bacterial cell growth. It is to be noted that in a controlled pH (= 7.2) fermentation, acidic end-products can be found as their respective conjugate base. The CRI is a useful index to confirm that all the carbon consumed as the substrate can be accounted for in the products. Assuming the elemental composition of the bacterial cellular materials is $C_4H_7O_2N$ (Rydzak et al. 2009), the carbon balance equation can be expressed as

$$\text{CRI} = \frac{4\times C_b + 3\times C_L + 2\times C_E + 2\times C_A + 1\times C_F + 2\times C_{CO2}}{(12\times C_{CB})\ consumed} = 1 \qquad 2.19$$

where, C_b, is concentration of biomass, C_L is concentration of lactic acid, C_F is concentration of formic acid, C_A is concentration of acetic acid, C_{CO2} is concentration of carbon dioxide, and C_{CB} concentration of cellobiose consumed. Their concentrations are measured and compared to theoretical ideal of one. Furthermore, electrons that are removed via the oxidation of glucose ($C_6H_{12}O_6$), must be conserved. By convention, oxygen (reducing agent) and hydrogen (oxidizing agent) are assigned redox values of 1 and -½, respectively (Gottschalk 1986). Each end-product can then be assigned a redox value by subtracting half the number of hydrogen atoms from the number of oxygen atoms present in the compound. A negative redox value indicates that the end-

product is reduced, and a positive redox value indicates the end-product is oxidized. An electron balance can then be performed by dividing the concentrations of the oxidized end-products by the concentrations of the reduced end-products, multiplied by their respective redox value. For *C. termitidis* metabolism, this is shown in the following equation:

$$\frac{O}{R} = \frac{(2\times C_E)+C_{H2}}{(2\times C_{CO2})+C_F} = 1 \qquad 2.20$$

where, C_E is the concentration ethanol and C_{H2} is the concentration of hydrogen. This equation does not describe other sources and sinks of electrons (such as amino acids biosynthesis).

The C_1/C_2 ratio is a mass balance related to the conversion of pyruvate, a three-carbon compound, to acetyl-CoA, which is a two-carbon compound. Pyruvate is reduced to acetyl-CoA via release of either CO_2 or formate. From the acetyl-CoA branch point, carbon flux is either directed to ethanol or acetate. Hence,

$$\frac{C_1}{C_2} = \frac{C_{CO2}+C_F}{C_A+C_E} = 1 \qquad 2.21$$

It has been demonstrated that gas-phase analysis with MIMS can produce reliable real-time data on the stoichiometric amounts of H_2, CO_2, and ethanol synthesized in different growth phases, and that titration signals can be used to quantify proton production, which is a function of the production of CO_2 and organic acids under controlled pH (Blunt et al. 2014).

2.1.9 Statistical analyses

A statistical analysis was performed between the gaseous data obtained discretely and continuously using GC and MIMS, respectively. The comparison will indicate reliability and correlation between the methods and among the biological replicates. Pairwise two tailed t-test was performed with 95% confidence intervals.

2.2 Materials and Methods for Chapter 4

2.2.1 Microorganism, substrate and media preparation

Batch cultures of *C. termitidis* were grown at 37 ± 1 ºC in 50 mL and 500 mL volumes in closed serum bottles. *C. termitidis* was cultured in 1191 medium, which composition has been previously described in Section 2.1.1. Sterile, anaerobic xylose was added as a carbon source to all cultures to a final concentration of 2 g/L. All chemicals for media preparation were purchased either from Fisher Scientific (Ontario, Canada) or Sigma Aldrich Chemical Co. (St. Louis, MO, USA) but yeast extract (New Jersey, USA).

2.2.2 Bioreactor setup

A 7 L round-bottom glass bioreactor with 3 L working volume (Applikon Biotechnology, Foster City, CA, USA) was used in all experiments. The description of the equipped reactor was provided in Section 2.1.2. For agitation, a marine impeller designed stirring apparatus was used. The reactor was then sparged (through L-shape steel tubing with few holes) overnight at a flow rate of 10 mL min^{-1} with an inert carrier gas consisting of 95 % N_2 and 5 % Ar (Praxair, Winnipeg, MB, Canada). Freshly prepared culture was used to inoculate the bioreactor after addition of concentrated filter sterilized xylose.

2.2.3 On-line analytical methods

2.2.3.1 MIMS calibration and operation

A MIMS (Model HPR-40) equipped with a quadrupole mass analyzer (HAL 201 RC), FC detector and SEM detector (Hiden Analytical, Warrington, UK), was used in conjunction with MasSoft 7® software to measure ethanol, H_2, and CO_2 on-line. For gas-phase calibration, a previously described method (sub-section 2.1.3.1 of Chapter 2) was used. After humidification, the combined calibration gas mixture was then cooled using condenser (mounted on the reactor

head plate) from a room temperature water bath that was circulated with a peristaltic pump. The off-gas was sent to a 5 mL glass vial, sealed with a septum and the MIMS probe, at room temperature. The H_2 and CO_2 was measured at m/z ratios of 2 and 22, respectively.

Due to condensation effect, ethanol could not be measured directly from condenser off-gas mixture. Therefore, final ethanol concentration was measured using the standard addition method and compared with discrete HPLC analysis. Ethanol calibration was carried out in a separate, anaerobic bottle containing 180 mL broth from 1191 media at 37 ± 1 °C. A solution of 1 M ethanol was prepared and added to the vessel to final concentrations of 1, 2, 5, 10, and 15 mmol/L. The MIMS probe was used to measure the ethanol signal at m/z 31 and was allowed to equilibrate for at least ten minutes at each concentration step. After the background ion current subtracting each signal of interest was then fitted to the known concentration using linear regression analysis. All regression analyses were performed with Microsoft Excel®.

2.2.3.2 Titration system calibration and operation

The titration system (Scion, Rotorua, New Zealand) was used to maintain constant pH and recorded the cumulative hydrogen ion production (HP) as a function of base addition. The sources and operational details of pH control system can be obtained from Chapter 2, Section 2.1.3.2 and Blunt et al. (2014). The rate of base addition (about 1 M KOH solution) was converted to the HP based on an approach adapted from Pratt et al. (2003), which treated the acid added (about 1 M HCl solution) by the titration system to correct overshooting of base addition. The fundamental purpose of acid/base titration is to control pH when it falls below or rises above the set point. Exact concentration of acid and base was obtained against known concentration of acid/base using potentiometric titration immediate after completion of fermentation.

2.2.4 Fermentation experiments

After inoculating the reactor, the fermentation conditions were maintained at 37 ± 1 °C, pH 7.20 ± 0.02, and gentle stirring at 100 rpm was applied. For perturbed experiment, a concentrated sterile solution of sodium acetate was added through the gas sampling port on the reactor head plate using long needle (sterile) when the culture reached around mid-exponential phase so that final acetate concentration stretched 100 mmol/L. During fermentation, the MIMS was used to monitor H_2 and CO_2 in the off-gas stream at m/z 2 and m/z 22, respectively. Ethanol in the gas-phase was measured at m/z 31. Simultaneously, samples were taken in 1-4 hour intervals for off-line analysis of both the gas phase and the liquid phase. Three biological replicate experiments were performed for control experiment and two for perturbation experiment in which the MIMS was used to monitor H_2 and CO_2 in the reactor off-gas stream.

2.2.5 Off-line analytical methods

The off-line analytical methods, such as GC for gas phase analysis, HPLC for soluble products analysis, protein assay for cell biomass analysis, and pH measurements were also conducted for both controlled and perturbed experiments. The detailed descriptions were provided in section 2.1.5.

2.2.6 Total gas production

For total gas production, a gas-phase mass balance was performed and described in section 2.1.6.

2.2.7 Calculation of volumetric, and substrate specific rates of end-products

Volumetric production of gases were calculated in two different stages (exponential phase before and after control and perturbed experiments, respectively); whereas volumetric production rates of soluble end-products were calculated at stationary phase (20-24 h pi).

Appropriate measures were taken for volume correction, which was described in Chapter 2, Section 2.1.7.

2.2.8 Reaction stoichiometry and statistical analyses

Using reaction stoichiometry, mass balance, and electron balances (Gottschalk 1986) can be derived to indicate that all major end-products have been adequately accounted for. In this work, they were used as indices to test the efficacy of both off-line and on-line results. Detailed methods of analysis can be obtained from section 2.1.8. Also, a statistical analysis was performed for both control and perturbed experiment, which will provide correlation, variability and significance between them. Comparative analysis of hydrogen ion production (from end-products profile) between control and perturbed experiments was performed using on-line titration system. T-tests were performed with two independent means.

2.3 Materials and Methods for Chapter 5

2.3.1 Media, microorganism and substrate

Preparation of 1191 media and substrate was performed in this chapter according to previously described methods in Chapter 2, section 2.1.1. Sterile concentrated cellobiose was used in all experiments for the culture of *C. termitidis*. Freshly prepared cultures were maintained by routinely transferring inocula into fresh media (10 % v/v).

2.3.2 Experimental setup

Experimental setup, including preparation of inocula and set-up of the bioreactor was executed in accordance with the methods described in Chapter 2, section 2.1.2. Initial cellobiose concentration was maintained 2 g/L for both inocula preparation and bioreactor set-up.

2.3.3 Calibration of MIMS for ethanol measurement

A single calibration strategy using the MIMS probe was evaluated for simplicity. In a previous study, Blunt (2013) showed that no significant differences were observed in the slope of ethanol concentrations when measured by *in-situ* or *ex-situ* calibration. *In-situ* calibration was performed in post-fermentation broth containing *C. termitidis* cells, cellular debris, and metabolic end-products. A 3 L culture of *C. termitidis* with the same temperature, sparging rate, and stirring rate as the fermentation experiments was used for the *in-situ* calibration. A three-point standard addition method of calibration was used by adding a solution of 10 M ethanol to the bioreactor to a maximum final concentration of 15 mmol/L. The m/z 31 signal was then monitored by placing MIMS probe in both headspace and broth until a stable equilibrium was reached. The signal was monitored with MIMS at m/z 31 and allowed ten minutes to attain a stable equilibrium. A linear regression was then performed on the baseline-subtracted signals using Microsoft Excel®.

2.3.4 Calibration for headspace and dissolved gases

The calibration for headspace gases was described in Chapter 2, section 2.1.3 Calibration for dissolved gases was performed *in-situ*, both before and after the fermentation process. The MIMS probe, disinfected with a solution of HCl (0.1 M, pH 1.0), rinsed with sterile deionized water to remove the acid, and then immersed half way down in the liquid phase and two centimeters away from the reactor wall. For the pre-fermentation calibration, the reactor was set up as described in Chapter 2, Section 2.1.2. Once anaerobic condition was achieved and the baseline was stable, the pre-fermentation calibration took place at the same temperature, sparging rate, and stirring rate as the fermentation experiments. Known concentrations of H_2 and CO_2 were prepared with the mass flow controllers (MFC) and bubbled though the liquid for several

hours, or until a stable equilibrium was reached. The monitored signals were CO_2 at m/z 22 and H_2 at m/z 2, and the pH was recorded simultaneously. The liquid-phase concentration of gases was obtained from the headspace composition through Henry's Law, using the values from Sander (2015), described by Blunt (2013). These values related to the baseline-subtracted m/z 2 and m/z 22 signals. After calibration, the N_2 sparging and stirring rates were then increased to strip the dissolved gas species out of the system, and the fermentation was started when the baseline was stable. Similarly, the post-fermentation calibration began only when the dissolved gas signals returned to baseline levels, which required the H_2 and CO_2, to be stripped from the liquid phase and purged from the headspace.

2.3.5 Fermentation experiments

Two sets of experiments were performed in duplicate for liquid phase analysis of ethanol, dissolved H_2, and dissolved CO_2. The first set of experiment was carried out with identical temperature, pH, sparging, and stirring conditions described in Chapter 2, Section 2.1.4. The second set of experiment was aimed at (to some extent) avoiding H_2 and CO_2 mass transfer limitations at the interface between the liquid phase and gas phase. In this experiment, agitation was increased to 200 rpm from 100 rpm, sparging was increased to 400 mL/min (high sparging rate, HSR) from 20 mL/min (low sparging rate, LSR). Ethanol, H_2 and CO_2, were monitored at m/z 31, m/z 2, and m/z 22, respectively. Data for off-gas composition and reagent addition (acid and base) via titration was continuously acquired. Off-line liquid and gas-phase samples were taken every four hours for analysis of gaseous end-products, soluble end-products, and protein assays.

2.3.6 On-line liquid phase analysis

The bioreactor was inoculated in accordance with the methodology previously described in Chapter 2, section 2.1.2. The dissolved species signals were monitored until the concentrations had returned to baseline levels such that post-fermentation calibration could be performed. The concentration of each component was found from interpolation of the baseline-subtracted signals from the calibration curves described in Chapter 2, sections 2.3.3 and 2.3.4. All regression analyses were performed with Microsoft Excel®. Soft ionization was employed to minimize fragmentation, and detection of multiple ion fragments was accomplished using the FC detector on the mass spectrophotometer.

2.3.7 Off-line analytical procedures

All off-line analytical procedures, including analysis of the gas-phase with GC, analysis of soluble end-products in the liquid phase with HPLC, and analysis of the cell protein, were conducted as described in Chapter 2, sub-sections 2.1.5.1, 2.1.5.2, and 2.1.5.3, respectively.

2.3.8 Reaction stoichiometry and statistical analyses

Data obtained from discrete measurements (LSR and HSR) was used to understand metabolic changes using reaction stoichiometry, mass balance, and electron balances. A comparative statistical analysis was performed for all end-products obtained during fermentation including their yields with 95 % confidence intervals. This analysis will test the efficacy of both off-line and on-line results. Furthermore, a statistical analysis was also performed for the reaction stoichiometry to see if there was any significant change occurred due to the presence of dissolved gases under LSR and HSR fermentation environment. In both cases, t-tests were performed using two independent means.

2.4 Materials and Methods for Chapter 6

2.4.1 Experimental setup and data generation

The data generated from Chapter 3 was used to validate the hypothesis that one can estimate in real-time the concentration of formate, acetate and lactate on the basis of TOGA generated data.

2.4.2 Data treatment: The use of CRI, C1/C2 and O/R ratios and stoichiometric algorithm

The data (discrete and continuous) obtained from Chapter 3 were used here to test the hypothesis of end-products estimations. Since *C. termitidis* utilizes branched fermentative pathways from the pyruvate node, synthesizing lactic acid, formic acid, acetic acid, ethanol, CO_2, H_2, and cell mass, a mass balance is performed using cellobiose consumption. The CRI, C1/C2 and O/R ratios were calculated using previously described equations in section 2.1.8 of Chapter 2. For this data treatment, the real-time continuous gas phase data obtained using MIMS probe were used. Similar strategies were also applied when the growth of *C. thermocellum* was monitored on 2 g/L cellobiose at 60 ^{o}C (Blunt 2013). In this study, a combination of real-time, on-line data measured by the TOGA, and discrete off-line measurements (HPLC and GC) to determine C_1/C_2 ratios and the O/R balance, concentrations of non-volatile end-products (formic acid and acetic acid) were calculated using Equation 2.20 and Equation 2.21. Lactic acid was ignored, as it was not produced under the conditions tested in that study. Estimations of the formic acid concentrations agreed reasonably with discrete off-line measurements of formate by HPLC, but estimations of the acetic acid concentrations were far from the discrete measurements. This may have been due to systematic errors in the on-line measurements under the *C. thermocellum* growth conditions tested, such as unstable CO_2 signal, inaccurate off-line

calibrations, over estimation in off-line acetic acid data, under estimation of on-line ethanol data. Furthermore, any instability of on-line signal can cause errors in the estimation algorithm.

During *C. termitidis* growth, simultaneous on-line data was collected for H_2, CO_2 and ethanol by placing the MIMS probe just above the liquid surface. Care was taken to avoid foaming, a major fermentation fouling agent, so that it would not contaminate the MIMS probe membrane. Agitation was not altered over the entire course of fermentation. As fluctuations in temperature can cause variations in MS signals, which ultimately can affect the estimation algorithm, the bioreactor was covered with an additional insulating jacket to avoid temperature changes (drift).

Raw signals may be converted into concentrations by using proper calibration, which is done under similar conditions, or as close as possible, to the experimental conditions. Thus, MS signals may be normalized to the background. It is also required to use averaged O/R values throughout entire growth phase of simulation. The O/R index may be rearranged to predict formate concentrations as a function of H_2, CO_2 and ethanol using Equation 2.20 as follows:

$$C_F = (2 \times C_E) + C_{H_2} - (2 \times C_{CO_2}) \qquad 2.22$$

where, C_E is the concentration of ethanol, and C_{H_2} is the concentration of H_2. Following this equation, acetate concentrations may be obtained from the C1/C2 ratio as a function of CO_2, ethanol and formic acid (from Equation 2.21).

$$C_A = C_F + C_{CO_2} - C_E \qquad 2.23$$

Furthermore, lactic acid may be predicted from the titration signals (base consumption) used during the course of fermentation, if no other acid produced. Lactic acid production is proportional to proton production and is a function of CO_2 and organic acids production (after the pyruvate node). Thus,

$$C_L = C_{H+\ ion} - (C_F + C_A + C_{CO_2}) \quad 2.24$$

where, C_L concentration of lactic acid, $C_{H+\ ion}$ concentration of H^+ ion obtained from base consumption, C_F concentration of formic acid, C_A concentration of acetic acid, and C_{CO_2} concentration of carbon dioxide. By applying these calculations (Equation 2.22, Equation 2.23 and Equation 2.24), the concentrations of formic acid, acetic acid and lactic acid produced by *C. termitidis* while growing on cellobiose were predicted.

2.4.3 Statistical analyses

Data obtained from discrete measurements (Chapter 3) was used to understand metabolic changes using reaction stoichiometry, mass balance, and electron balances. Then, estimated signals (for fomate, acetate) were used to find subtle changes with statistical analysis. A statistical analysis (co-relation, regression analysis) was performed for both discrete off-line and continuous on-line measurements (real-time and predicted). In addition, reliability and variability between biological replicates were also presented. A comparative analysis of hydrogen ion production between titrimetric and metabolic acids synthesis was performed using t-test method of two independent means. The overall analysis of these data will test the efficacy of both off-line and on-line results including estimated ones.

Chapter 3

Continuous Monitoring of *Clostridium termitidis* Volatile Fermentation End-products Reveals Previously Undetected Metabolic Shifts

Abstract

Metabolic shifts may be associated with physicochemical environment changes during growth of many types of cells. An ability to monitor in real time changes in microbial end-product secretion may sometimes enhance our understanding of microbial physiology. *Clostridium termitidis* was grown in a 7 L, pH controlled (7.20 ± 0.02) bioreactor with 1191 medium containing a high substrate load (10 g/L cellobiose), at 37 ± 1 ^{o}C. Growth and end-product concentrations (H_2, CO_2, ethanol) in the fermentation reaction headspace were monitored in real-time for about 60 hours using a membrane inlet mass spectrometry (MIMS) probe. Discrete measurements of headspace gases (H_2, CO_2, ethanol) by gas chromatography (GC) and soluble aqueous phase end-products (formate, acetate, lactate, ethanol) by high performance liquid chromatography (HPLC) were conducted in parallel. *C. termitidis* growth phases were identified using both optical density measurement and real-time continuous measurement of H_2 gas. Volumetric production rates, and the substrate (cellobiose) consumption rates were calculated. A number of key shifts in end-product generation (H_2, CO_2, formate, ethanol) were identified, which occurred during the early stationary phase of growth (24-32 h post-inoculation, pi). Based on the data, it was concluded that electron and carbon flow in *C. termiditis* was directed towards ethanol synthesis during early stationary phase to maintain redox balance. Low CO_2 production was compensated by synthesis of formate during stationary phase. H_2 synthesis was also reduced at this growth stage. The lactate production rate did not vary significantly during stationary phase. This set of experiments has provided more acurate information on metabolic shifts in *C.*

termitidis, which provides greater insight into the conditions that enhance synthesis of different end-products of interest.

3.1 Introduction

In the recent past, biological degradation of lignocellulosic compounds drew global attention for several reasons. Lignocellulosic biomass is the most abundant and low cost feedstock source. It is a sustainable way of displacing petroleum based organics such as plastics and transportation fuels, through its conversion via fermentation to biofuels, such as H_2, ethanol, or butanol. For biofuel synthesis, cellulolytic bacteria degrade lignocellulosic biomass to fermentable sugars via a number of enzymatic hydrolysis mechanisms that transform the cellulose into cellodextrins, hexoses, and pentoses described by many authors (Schwarz 2001; Lynd et al. 2002; Munir et al. 2014). These simple sugars are then utilized by bacterial cells in a number of metabolic pathways, such as Embden-Meyerhof-Parnas (EMP), Pentose Phosphate (PP), Entner-Doudoroff (ED) depending on the organism.

Some bacterial species utilize a single pathway, whereas others utilize combination of more than one pathways. This is encoded in the genome of bacterial species and pathway selections and flux are regulated by surrounding growth conditions through thermodynamic constraints and genetic regulation. Among cellulolytic bacteria, *C. thermocellum*, a thermophile, has been investigated widely for its feasibility in consolidated bioprocessing (CBP) under various growth conditions (Islam et al. 2006; Argyros et al. 2011; Islam 2013; Agbor et al. 2014; Thompson and Trinh 2017). Among mesophiles, *C. cellulolyticum*, and *C. phytofermentans* have been the most extensively studied for their potentials for CBP. *C. cellulolyticum* has been investigated systematically under both carbon and nutrient-limiting growth conditions (Guedon et al. 1999a; 1999b; Guedon et al. 2000; Guedon et al. 2002) using continuous cultures to understand its metabolism (Giallo et al. 1983; 1985, Desvaux et al. 2001; Desvaux 2004). In continuous cultures with cellobiose, excess carbon flowed to glycogen (overflow storage

compounds) through glucose-1-phosphate, while excess carbon from glucose-6-phosphate stimulated the production of a variety of alternative end-products, including pyruvate, lactate, and ethanol. More recently, *spo0A* mutants, which cannot sporulate have been shown less sensitive to environmental stresses from carbon overload (Li et al. 2014).

Prior to Guedon et al. (1999b, 2000) *C. cellulolyticum* was described as a slow growing cellulolytic bacterium, where the growth was monitored without pH regulation and control of shaking conditions (Giallo et al. 1983). More detailed investigations were performed later, using batch bioreactors and chemostat techniques (Payot et al. 1998, 1999). These studies determined the nutritional requirements of *C. cellulolyticum*, and demonstrated the benefits of pH controlled cultures on cell growth and catabolic reactions (Guedon et al. 1999b, 2000; Desvaux 2004). These studies utilized discrete measurements (samples taken at specific time-intervals) of fermentation end-products over the course of the experiments. Despite continuous feeding and monitoring of the growth of *C. cellulolyticum* for 28 days, the system did not show/identify metabolic shifts.

Another cellulolytic bacterium, *C. phytofermentan*s, was isolated from forest soil of Massachusetts. It can ferment a wide variety of substrates (Warnick et al. 2002) and produces ethanol, acetate, CO_2 and H_2 as the major end-products, when cultured on either avicel or cellobiose (Ren et al. 2007). Formate and lactate were minor end-products. The ethanol synthesis was almost double (13.6 mmol/L) compared to the ethanol produced by *C. celllulolyticum* (8.2 mmol/L) using 5 g/L cellobiose with similar fermentation condition. Since *C. phytofermentans* has no cellulosomes, this organism cleaves cellulose using enzymes secreted into the medium (Tolonen et al. 2014). As with most other cellulolytic ethanol producing anaerobes (Carere et al.

2012), the bifunctional alcohol dehydrogenase (ADHE) plays a key role in ethanol production in the wild type strains (Mukherjee et al. 2014; Tolonen et al. 2015).

Clostridium termitidis is a mesophilic cellulolytic bacterium obtained from the gut of the termite, *Nasutitermes lujae*. The first study of *C. termitidis* was performed in batch cultures (Hethener et al. 1992), where the organism was tested with a wide-range of substrates. Two decades later, more detailed metabolic (proteomic) investigations were performed in batch cultures and in pH controlled stable cultures under carbon-sufficient conditions with cellobiose and α-cellulose (Ramachandran et al. 2008; Ramachandran 2013). In *C. termitidis*, hydrogen is synthesized via pyruvate ferridoxin oxido-reductase (PFOR) and ferredoxin, and NADH-dependent bifurcating hydrogenase, whereas ethanol is synthesized by the bifunctional ADHE enzyme (Munir et al. 2016; Lal and Levin 2016). The volumetric hydrogen production rate and the specific hydrogen production rate were reported to be 0.44 ± 0.02 mmol/L of culture/h hexose eqv., and 3.30 ± 0.28 mmol/g of protein/h, respectively. By way of comparison, the volumetric hydrogen production rate of *C. thermocellum* reached 1.20 mmol/L of culture/h hexose equivalents. The volumetric ethanol production rate and specific ethanol production rate for *C. termitidis* were determined to be 0.26 ± 0.14 mmol/L of culture/h hexose eqv., and 1.38 ± 0.38 mmol/g of protein/h, respectively. Again, by way of comparison, *C. cellulolyticum* (Guedon et al. 2000; Desvaux 2004) produced ethanol at a specific rate of 1-2 mmol ethanol/g of cells/h depending on soluble substrate loads (here cellobiose), whereas *C. thermocellum* displayed a maximum volumetric rate 0.90 mmol/L of culture/h hexose eqv. and specific rate of 3.91 mmol ethanol/g of protein/h (Blunt et al. 2014).

Munir et al. (2014) performed a comparative analysis of carbohydrate active enzymes in batch fermentation reactions (in serum bottles) under carbon-sufficient conditions. These

enzymes were unique, secreted extracellulary, and have potential to degrade a wide- variety of complex to simple carbohydrates. Furthermore, correlation of transcriptomic and proteomic data with growth and fermentation profiles identified a number of putative carbon-catabolism pathways in *C. termitidis* (Munir et al. 2015; Munir et al. 2016). Information on carbon and electron distribution among end-products under carbon-limiting and carbon-excess conditions for *C. termitidis* is still unknown.

In general, the branched mixed acid fermentation pathways utilized by many cellulolytic *Clostridium* species limit efficiency of ethanol production. Changes in culture conditions, such as pH, nutrient availability, and end-product concentrations, can result in changes in microbial metabolism, as the cells adjust to maintain intracellular redox-balance. As illustrated by studies of *C. cellulolyticum* (Giallo et al. 1983; Payot et al. 1998, 1999; Guedon et al. 1999b, 2000; Desvaux 2004), analysis of samples taken at regular intervals of cell growth may not sufficient to detect rapid metabolic shifts. Understanding how carbon and electrons are distributed to the various fermentation end-products during different phases of growth may provide insight into the metabolism of *C. termitidis.* The objective of this study was to demonstrate that real-time on-line monitoring can provide insight into carbon and electron flow in response to changing growth conditions, complementing discrete off-line measurements of fermentation end-products,. These experiments were conducted with high initial concentrations of a soluble substrate, cellobiose, in 1191 medium, under pH controlled conditions.

3.2 Materials and Methods

The materials and methods for this Chapter 3 are described in section 2.1 of Chapter 2.

3.3 Results

3.3.1 Proof of concept of on-line monitoring techniques: Measuring H^+ ion production relative to gaseous CO_2 evolved

Generally, an HPLC is used to identify and quantify fermentation end-products dissolved in the aqueous phase (fatty acids, alcohols, and sugars). In addition, produced CO_2 creates acidic environment, if present in excess quantities, can have detrimental impact on cell growth and proliferation (Frick and Junker 1999); but it also generates carbonate buffer system with controlled pH (Pratt et al. 2003). Many researchers (Holwerda et al. 2013; Magnusson et al. 2009) adjusted the pH (using acid or base) during fermentation aiming to have better biofuel synthesis. However, both studies lack utilization of base consumption data. It would be worthwhile to have a secondary analytical tool to check reliability of HPLC measurements; otherwise, it might affect carbon balance and oxidation-reduction (O/R) balance. A precise titration system (such as the one that is part of the TOGA unit) may provide opportunity to monitor any pH dependent attribute or profile for fermentation.

Before initiating biological process monitoring, an experiment was designed to monitor chemical gas (CO_2) production from a single source with minimum interactions in a typical bioreactor. The titration was performed in a 7.0 L reactor with 3.0 L working volume of 12.7 mmol/L $KHCO_3$ titrated with approximately 1 M HCl, and CO_2 gas production was monitored using the MIMS probe. The results are shown in Figure 3.1 and summarized in Table 3.1.

Good agreement (1.0 % error only) was obtained for the titration of $KHCO_3$ solution against HCl, which was further confirmed by off-gas CO_2 measurement using the TOGA (1.3 % error only) (Table 3.1). Figure 3.1 shows carbonate speciation of potassium bicarbonate solution using real-time on-line measurements. Since $KHCO_3$ is a salt of weak acid and a strong base,

A)

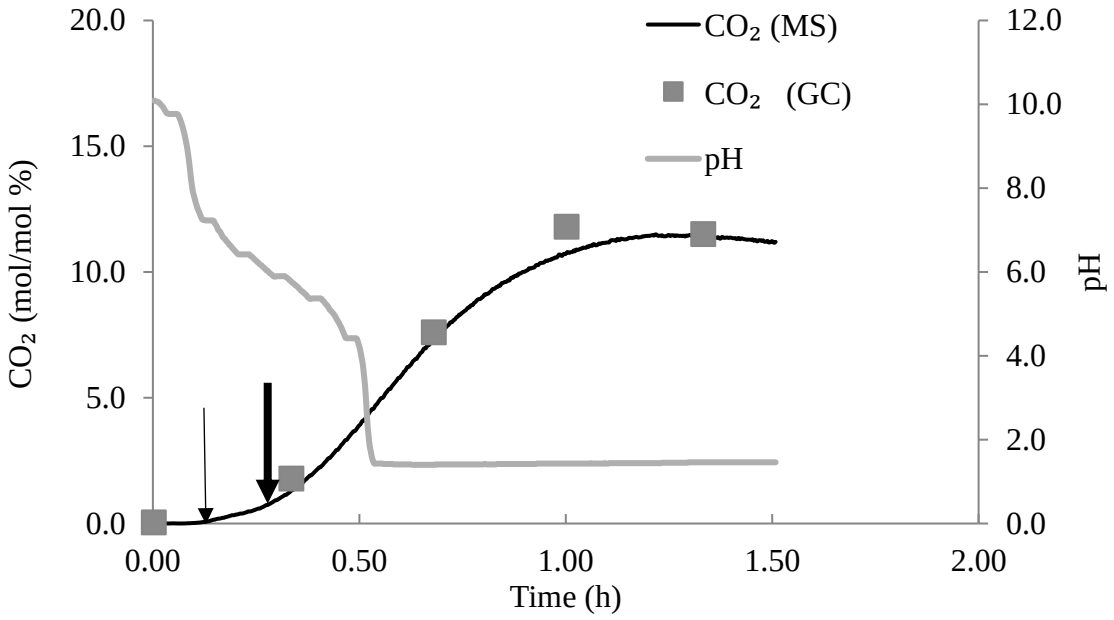
20.0
15.0
10.0
5.0
0.0
CO₂ (mol/mol %)
12.0
10.0
8.0
6.0
4.0
2.0
0.0
pH
CO₂ (MS)
CO₂ (GC)
pH
0.00
0.50
1.00
1.50
2.00
Time (h)

B)

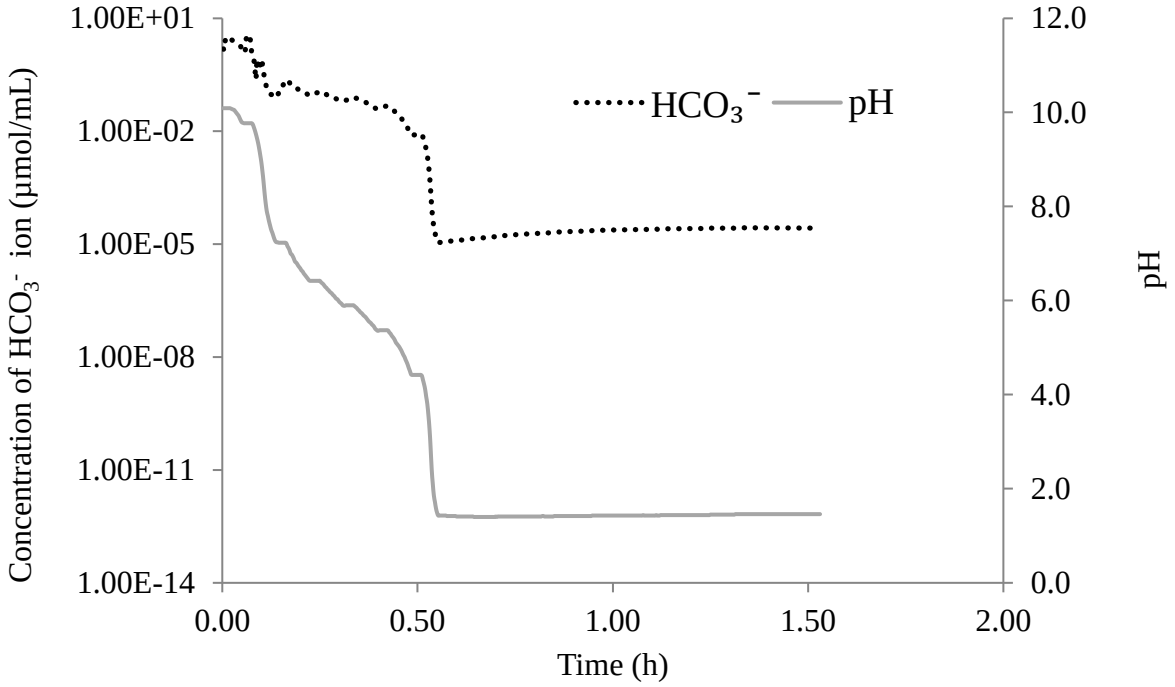
1.00E+01
1.00E-02
1.00E-05
1.00E-08
1.00E-11
1.00E-14
Concentration of HCO3- ion (µmol/mL)
12.0
10.0
8.0
6.0
4.0
2.0
0.0
pH
HCO3⁻
pH
0.00
0.50
1.00
1.50
2.00
Time (h)

C)

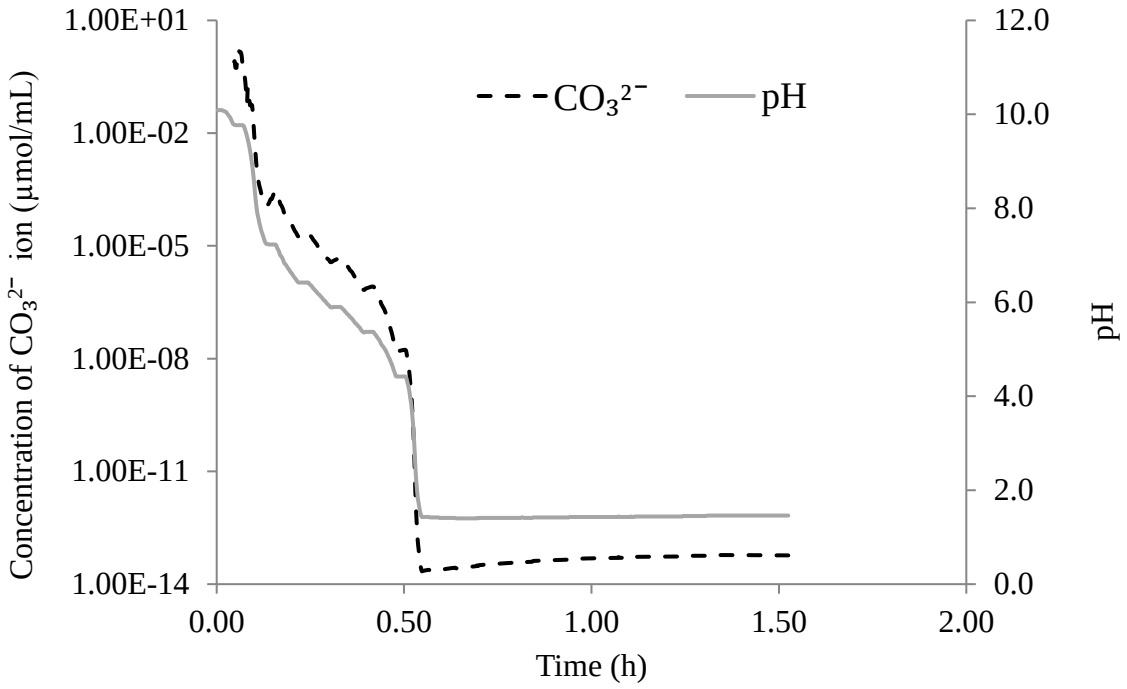

Figure 3.1 Chemical gas production monitoring using TOGA. A) Production of CO_2 from 3.0 L of 0.0127 M $KHCO_3$ solution at room temperature (23 ± 1 ^oC) while adding 0.981 M HCl. Agitation was 100 rpm. Concentration of B) bicarbonate and C) carbonate as compared to pH change during the course of reaction. In Figure 3.1A, the thin vertical arrow indicates basic pH region with no sign of headspace CO_2, and the thick vertical arrow indicates neutral pH region, where HCO_3^- equilibrated with CO_2 and H_2CO_3.

Table 3.1 Chemical production of CO_2 using the TOGA system.

Method	**Volume of $KHCO_3$**	**$KHCO_3$ concentration**	**Volume of HCl consumed**	**HCl concentration**	**Theoretical CO_2**	**Measured* CO_2**	**Percent Error**
	mL	M	mL	M	mol/L	mol/L	%
Titration	3000	0.0127	39.2±1.0%	0.981	...	...	1.01
Off-Gas	...	...	...	...	0.0127	0.0129±1.31%	1.34

*Total carbonate-bicarbonate species recovered using Henry's law and Henderson-Hasselbalch equation

when $KHCO_3$ is dissolved into the water, it dissociates as follows: $KHCO_3 \leftrightarrow K^+ + HCO_3^-$; $H_2O \leftrightarrow H^+ + OH^-$. Due to high alkalinity of K^+ ion the overall solution pH turns into basic (pH > 10), which shifts the chemical equilibrium as follows: $H_2O + CO_2 \leftrightarrow HCO_3^- + OH^- \leftrightarrow H_2O + CO_3^{2-}$. Therefore, significantly low concentration of CO_2 is expected to notice in the headspace at the early stage of reaction. Figure 3.1A clearly shows no sign of CO_2 near the basic pH zone (down thin arrow). However, the release of CO_2 started gradually as the pH approached 7, where HCO_3^- equilibrated with CO_2 and H_2CO_3 (down thick arrow). CO_2 continued to evolve as the pH dropped to as low as 2. Hence, the following equation became dominant $HCO_3^- + H^+ \leftrightarrow H_2CO_3 \leftrightarrow H_2O + CO_2$. Figures 3.1B and 3.1C show the estimated bicarbonate and carbonate concentrations, respectively, over the entire course of the titration using the Henderson-Hasselbalch equation 2.6, described in Chapter 2. These observations could not be revealed when off-line GC data (discretely obtained) were plotted at approximately 20 minutes intervals.

3.3.2 Growth characteristics

Fermentation on cellobiose was carried out in a pH controlled 7 L bioreactor in 1191 medium under carbon-excess condition. Figure 3.2A illustrates the growth of *C. termitidis* under carbon-excess (10 g/L) conditions. There was no initial lag phase observed, because the cells were serially subcultured prior to inoculation of the reactor. From the very beginning, cells grew exponentially until 16 hours post-inoculation (h pi). Thereafter, cell growth reached a second slower exponential phase (indicated as phases II and III: 16 – 32 h pi), there was still a considerable amount of residual cellobiose (approximately 70 % of the cellobiose remained in the culture medium). Maximum OD (32h pi) obtained was 1.92 ± 0.12 when about 50 % of initial cellobiose was consumed, at which point the cells entered into stationary phase. As expected, as the cell population (OD) increased, the cellobiose consumption rate gradually

increased (see Figure 3.6, below). The highest volumetric cellobiose consumption rate was observed 2.75 ± 0.12 mmol/L/h (hexose equivalent) near the end of the second exponential phase (III: 24 – 32 h). While phase II and phase III cannot be distinguished on the basis of growth, shifts in production of various end products was observed at the point of transition between these 2 phases (see sections 3.3.3 and Figure 3.3A). When *C. termitidis* was cultured either on 2 g/L or 1 g/L cellobiose, cells entered stationary phase when carbon became limiting in the culture medium between 24 - 32 h pi and 16-24 h pi, respectively (Figure 3.2B and Figure 3.2C). The growth kinetics of *C. termitidis* based on protein concentration under carbon limiting to carbon-excess conditions were shown in supplementary Figure S3.1. Ramachandran (2013) also reported similar observation on 2 g/L cellobiose. In the current experiment (with an initial cellobiose concentration of 10 g/L), carbon was not limiting. The maximum average OD_{600} and protein concentrations were 1.92 ± 0.08 and 0.16 ± 0.01 mg/mL of culture, respectively, which was more than double the concentrations observed when *C. termitidis* grew on 2 g/L cellobiose. Cellobiose consumption continued throughout stationary phase continued up to 52 h. The cell density started decreasing at around 52 h pi, as cellobiose was depleted in the culture medium.

A)

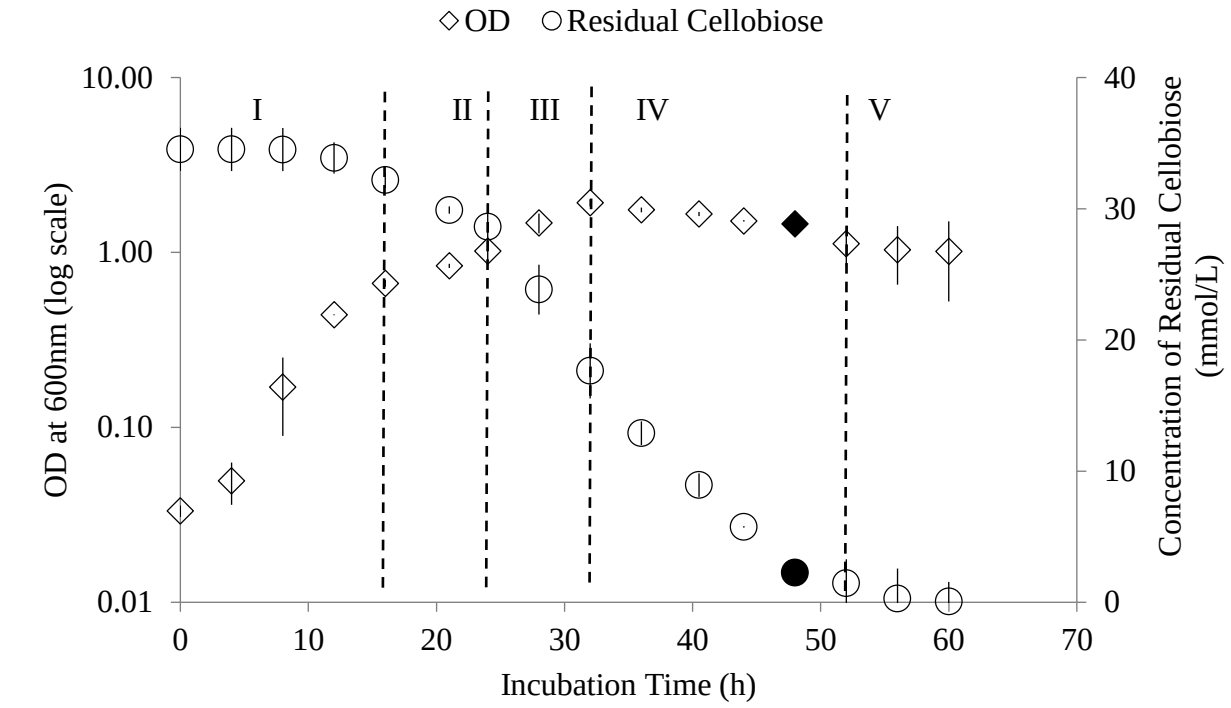
OD
Residual Cellobiose
I
II
III
IV
V
10.00
1.00
0.10
0.01
OD at 600nm (log scale)
40
30
20
10
0
Concentration of Residual Cellobiose (mmol/L)
0
10
20
30
40
50
60
70
Incubation Time (h)

B)

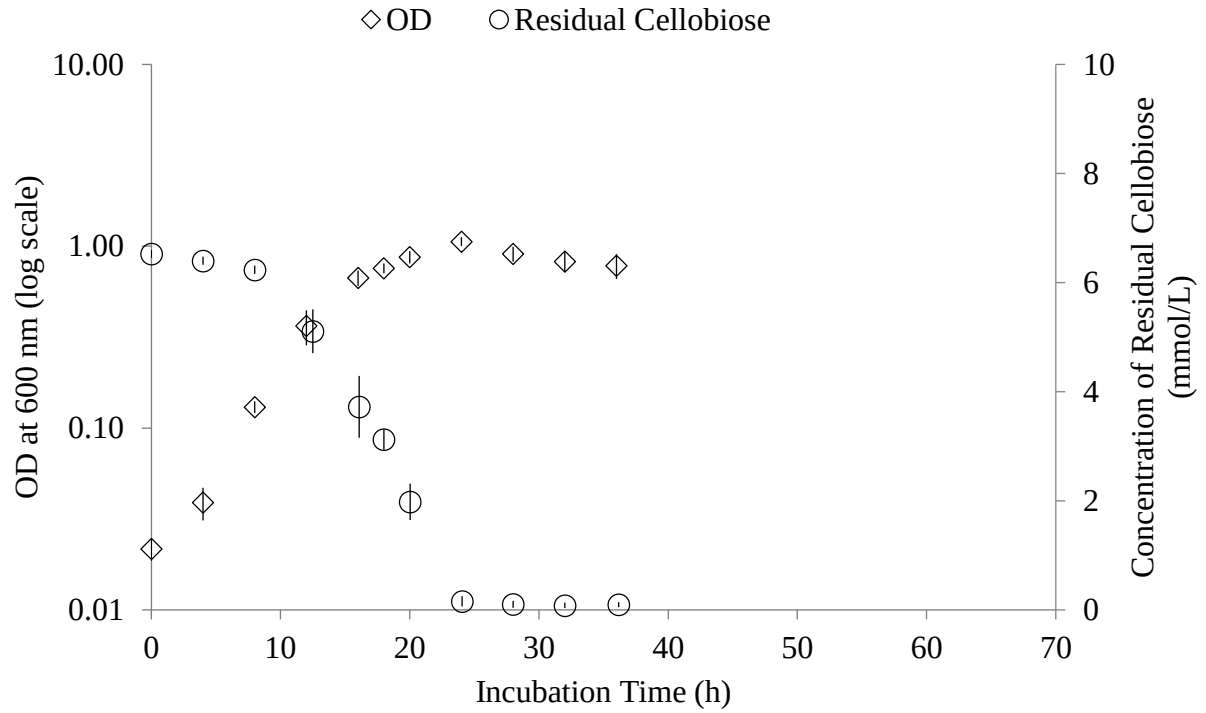
OD
Residual Cellobiose
10.00
1.00
0.10
0.01
OD at 600 nm (log scale)
10
8
6
4
2
0
Concentration of Residual Cellobiose (mmol/L)
0
10
20
30
40
50
60
70
Incubation Time (h)

C)

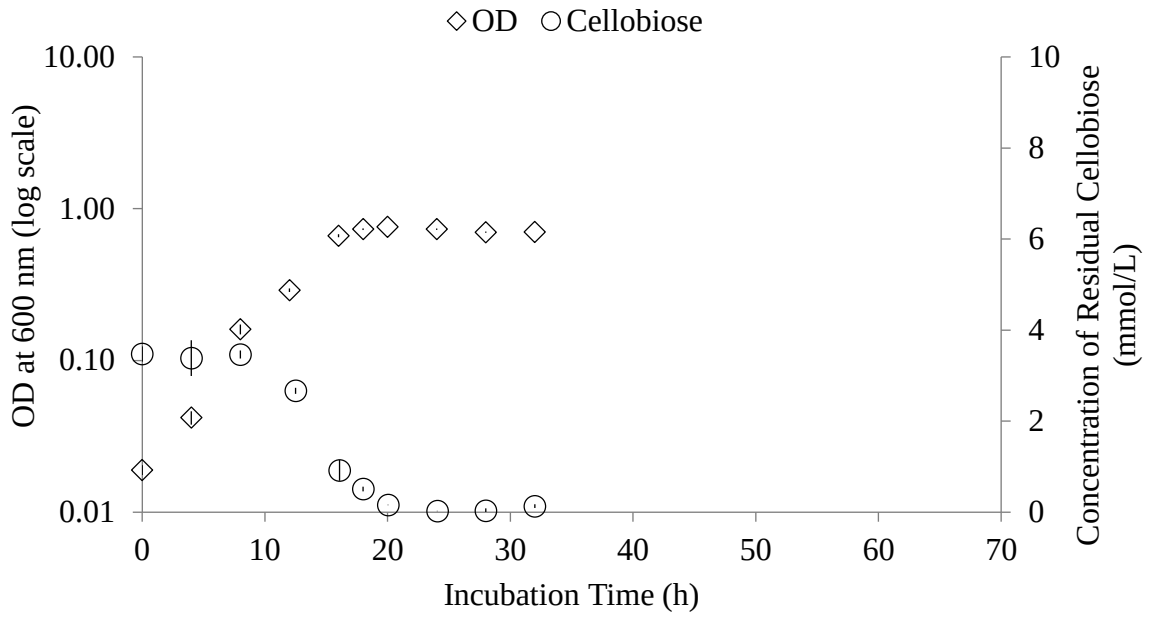

Figure 3.2 Growth of *C. termitidis* on A) 10 g/L, B) 2 g/L and C) 1 g/L cellobiose in a 7 L reactor with 3.0 L working volume in, 1191 media. Growth temperature was 37 ± 1 ^{o}C and covered with insulated jacket. pH was controlled to 7.20 ± 0.02 using about 1 M KOH and 1M HCl. Roman numerals separated by dashed vertical lines in Figure 3A indicate various growth phases: I, exponential phase; II, late exponential phase; III*, early stationary phase; IV, stationary phase; V, cell declining phase. For simplicity, the data were averaged if the variation of a discrete time point was ≤ (less than or equals to) 0.5 h from two replicate fermentor runs. Solid diamond (♦) and solid circle (●) represent single data points from one biological experiment. * The phase III is indistinguishable from phase II on the basis of OD measurement, but are clearly visible on the basis of end product synthesis (Figure 3.3A)

3.3.3 End-product synthesis

3.3.3.1 Gas production

When cultured with cellobiose, *C. termitidis* synthesized H_2 and CO_2, which is consistent with other studies of *C. termitidis* (Hethener et al. 1992; Ramachandran 2013), as well as other cellulolytic bacteria, such as *C. cellulolyticum* (Guedon et al. 1999; Desvuax et al. 2000). The evolved gas concentrations were measured in the headspace that was purged by a constant flow of inert gas mixture (95 % N_2 & 5 % Ar). Figure 3.3 shows the production of H_2, CO_2 and ethanol (raw signals) over the course of entire fermentation where *C. termitidis* was grown on 10 g/L, 2 g/L and 1 g/L cellobiose from continuous measurement using the TOGA. Gas synthesis patterns are different under these three growth conditions, so do their rates (Table 3.2). In the presence of 10 g/L cellobiose, *C. termitidis* rapidly produced H_2 within the early exponential phase, up to 16 h pi. The H_2 production slowed down through the first half of the second growth phase (phase II: 16 – 24 h pi) into the latter half (phase III: 24 – 32 h pi). A sudden and significant decrease in H_2 production occurred between 31 h pi and 34 h pi as the cells entered stationary phase. The H_2 production rate plateaued and remained steady between 34 h pi and approximately 48 h pi, and then began to decrease again until the cellobiose substrate was totally consumed, at around 52 h pi.

Figure 3.4 shows the concentrations of these end-products (calculated from the raw output from the TOGA presented in Figure 3.3A). Hydrogen synthesis by *C. termitidis* displayed a gradual and continuous increase throughout the fermentation reaction. CO_2 production slowly increased up to 24 h pi, and appeared to plateau during the early stationary phase (III: 24 – 32 h pi), and then continued to rise again up to 52 h pi. Ethanol synthesis remained low from the time of inoculation to 24 h pi, and then gradually and continuously increased up to 52 h pi.

A)

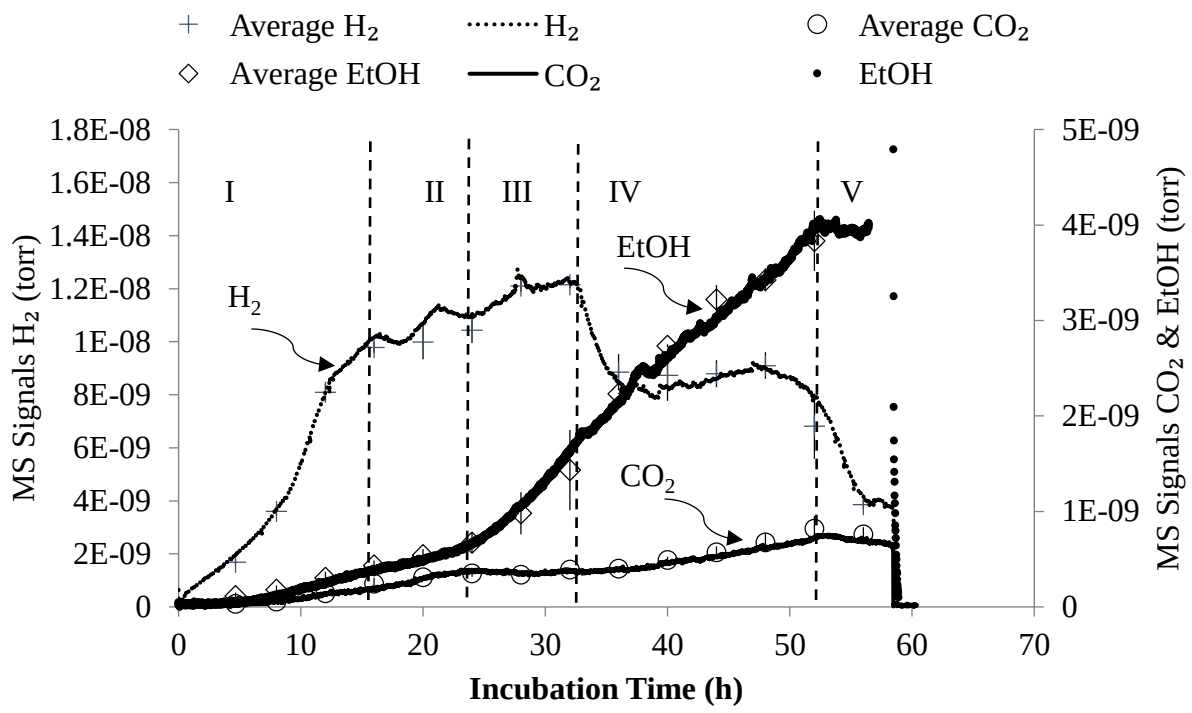
Average H_2
H_2
Average CO_2
Average EtOH
CO_2
EtOH
I
II
III
IV
V
EtOH
H_2
CO_2
MS Signals H_2 (torr)
MS Signals CO_2 & EtOH (torr)
1.8E-08
1.6E-08
1.4E-08
1.2E-08
1E-08
8E-09
6E-09
4E-09
2E-09
0
5E-09
4E-09
3E-09
2E-09
1E-09
0
0
10
20
30
40
50
60
70
Incubation Time (h)

B)

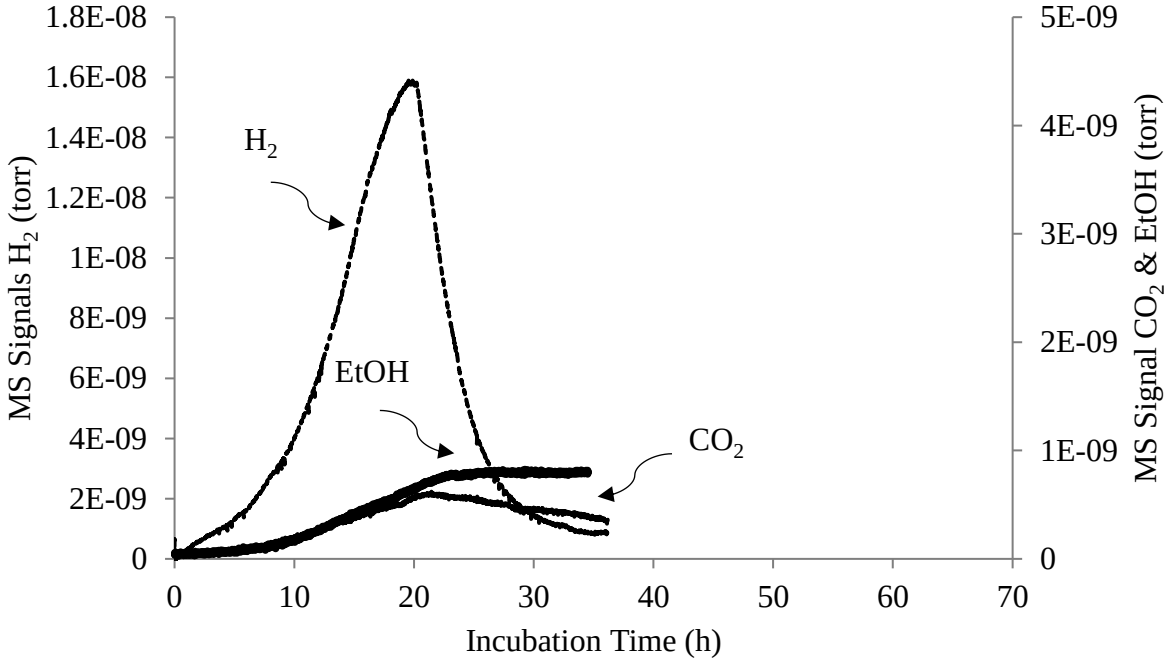
H_2
EtOH
CO_2
MS Signals H_2 (torr)
MS Signal CO_2 & EtOH (torr)
1.8E-08
1.6E-08
1.4E-08
1.2E-08
1E-08
8E-09
6E-09
4E-09
2E-09
0
5E-09
4E-09
3E-09
2E-09
1E-09
0
0
10
20
30
40
50
60
70
Incubation Time (h)

C)

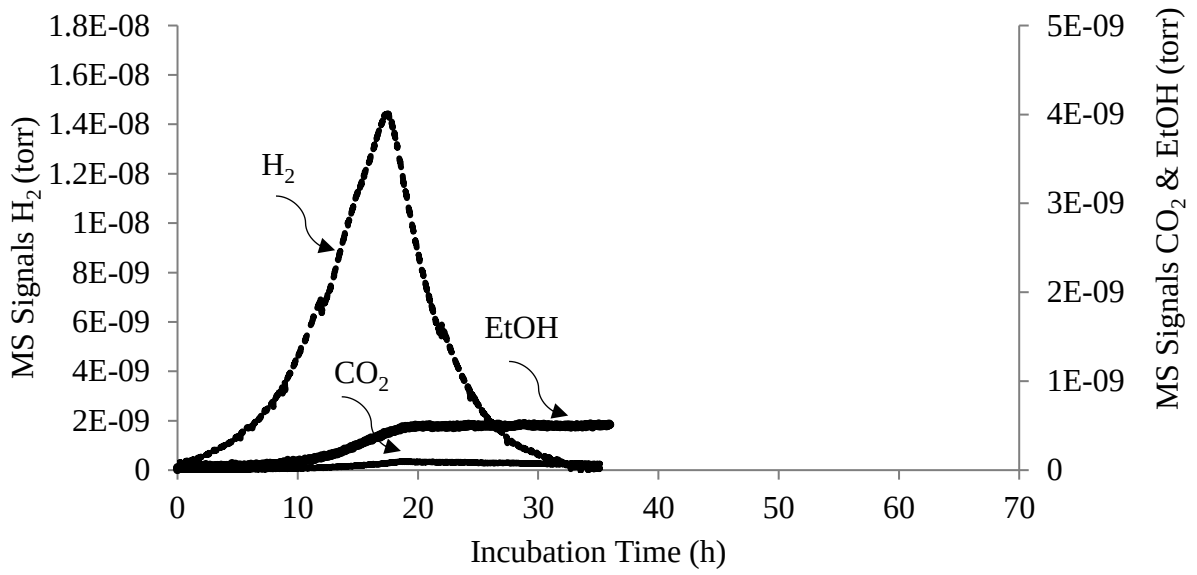

Figure 3.3 Raw data from continuous head-space monitoring using the MIMS for *C. termitidis* cultured with A) 10 g/L cellobiose. Continuous lines represent one replicate while the discrete points represent selected time points where the data from the various biological replicates were averaged. Gas phase data obtained from B) 2 g/L cellobiose and C) 1 g/L cellobiose with similar bioreactor environment. Dotted line – H_2, continuous line – CO_2, dot only (•) – ethanol, black cross (x) – mean H_2, open circle (○) – mean CO_2, and diamond (◊)– mean ethanol. Error bar represents standard deviations of two biological replicates. Roman numerals (I –V) separated by dashed vertical lines in Figure 3.3A indicate various growth phases, as descrived in Figure 3.2.

A)

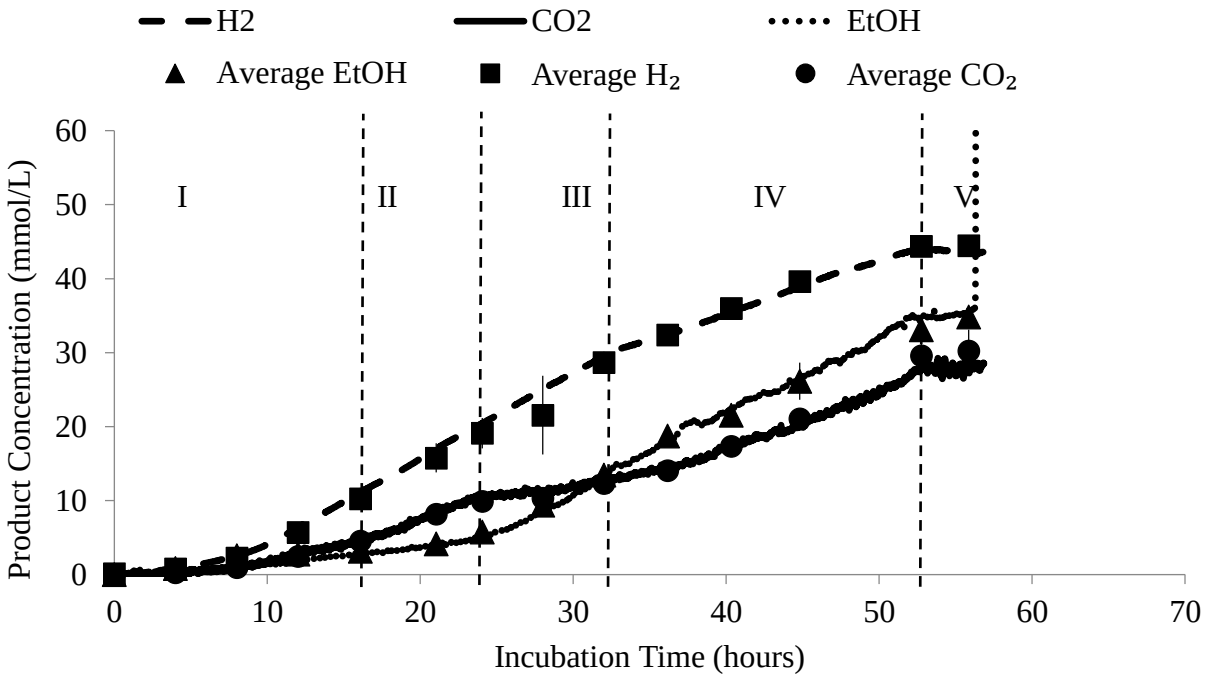
H2
CO2
EtOH
Average EtOH
Average H_2
Average CO_2
I
II
III
IV
V
Product Concentration (mmol/L)
Incubation Time (hours)
0
10
20
30
40
50
60
70

B)

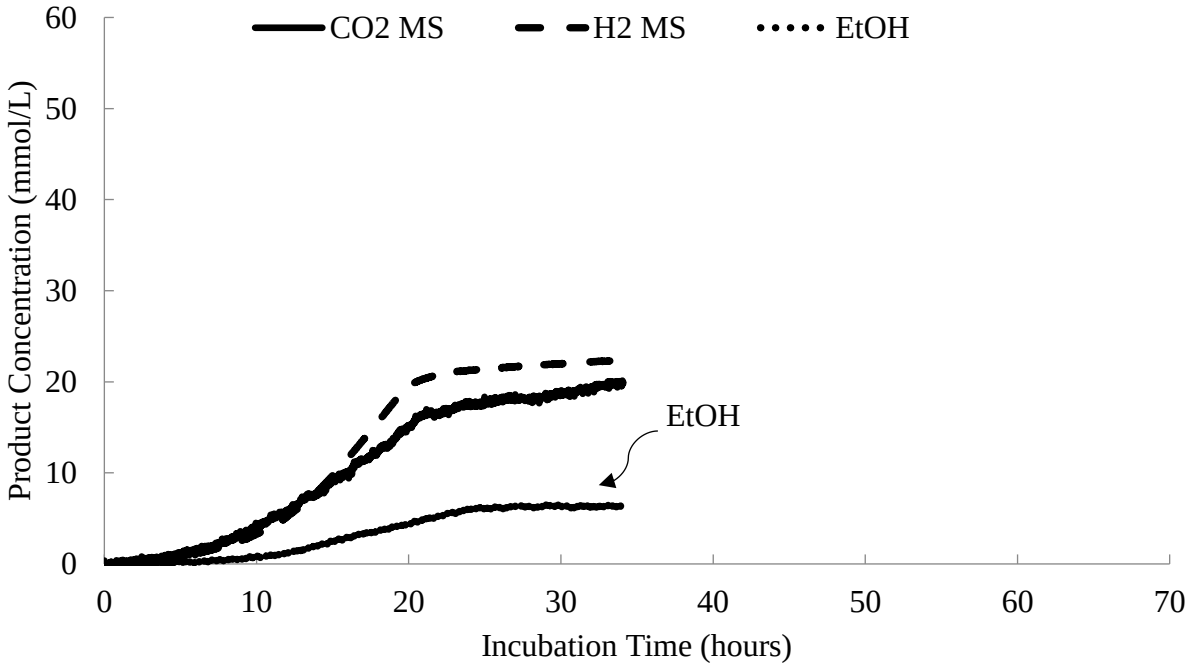
CO2 MS
H2 MS
EtOH
EtOH
Product Concentration (mmol/L)
Incubation Time (hours)
0
10
20
30
40
50
60
70

C)

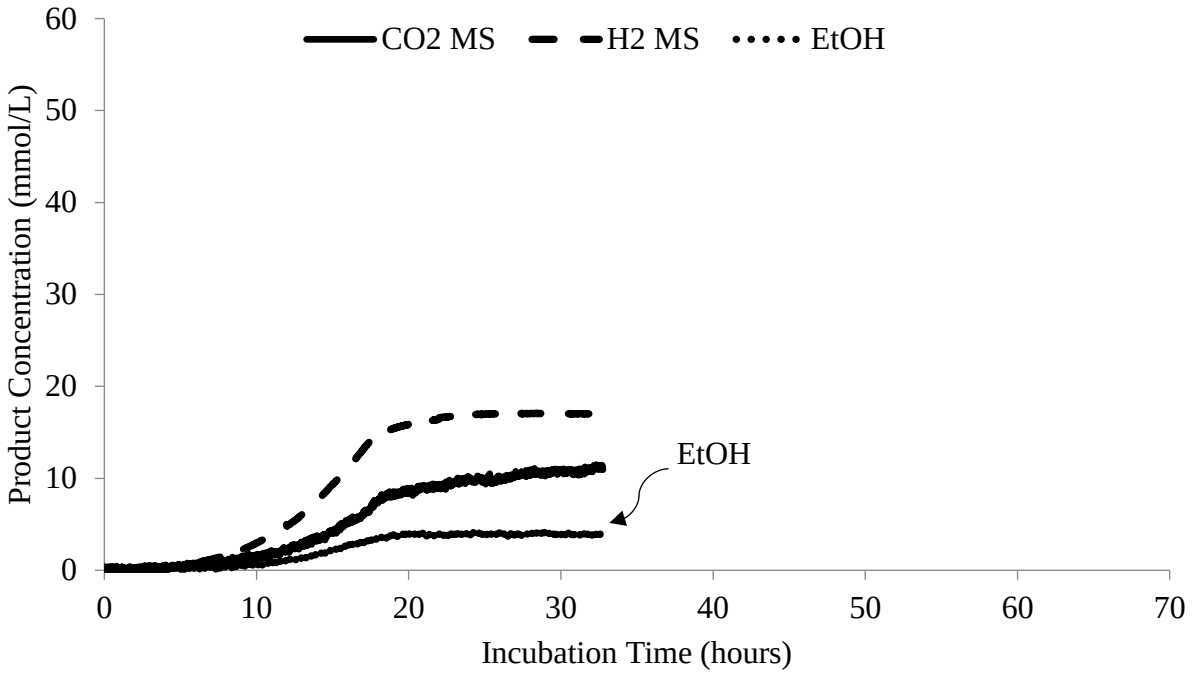

Figure 3.4 Concentrations of H_2, CO_2, and ethanol derived from the raw MIMS data (shown in Figure 3.3). The on-line MIMS measurements of H_2 (gas phase) - dashed line, CO_2 (gas phase) – continuous line and EtOH (gas phase) – dotted line. Discrete points, arbitrarily selected on replicate continuous measurements, indicate average value of two biological replicates with error bars. *C. termitidis* was grown in 1191 media in a 7 L reactor on A) 10 g/L cellobiose at pH 7.20 ± 0.02 and 37 ± 1 ^{o}C. Gas phase data obtained from B) 2 g/L cellobiose and C) 1 g/L cellobiose with similar bioreactor environment. Roman numerals (I –V) separated by dashed vertical lines indicate various growth phases, as descrived in Figure 3.2.

CO_2 production steadily increased within the first 16 h pi, while in the late exponential phase (II: 16 – 24 h pi) the CO_2 production rate decreased, resulting in no accumulation of CO_2 in the bioreactor head-space. CO_2 production barely increased during early stationary phase (III: 24 – 32 h pi), but CO_2 synthesis increased through the stationary phase (IV: 32 – 52 h pi), then dropped off at around 52 h pi, due to lack of substrate. Synthesis of H_2, CO_2 and ethanol followed different patterns when *C. termitidis* was grown on 2 g/L and 1 g/L cellobiose with similar growth environment (Figure 3.3B and Figure 3.3C). For the gas measurement, a discrete method was also applied using GC in addition to real-time on-line technique to confirm the results measured by the TOGA. A detailed statistical analysis was performed to check variability of GC and MS techniques and discussed in section 3.4.3.

3.3.3.2 Acetate and ethanol synthesis

As *C. termitidis* metabolism follows a branched fermentative pathways, it is necessary to evaluate carbon distribution in each branch. In a bioreactor, under carbon-sufficient condition (2 g/L cellobiose), carbon flow was directed towards C2 and C1 fermentation end-products (CO_2, formate, acetate, and ethanol), but predominantly acetate with the increased biomass under carbon-limiting conditions (Table 3.3). Previous study (Ramachandran 2013) showed that significant amount of lactate (C3) produced in addition to C1 and C2 products. Predominant synthesis of acetate with increased biomass indicated that the cellobiose was not only used for energy generation but also biomass production, which is common in most cellulolytic *Clostridium* species (Chung 1976; Islam et al. 2006; Ren et al. 2007; Rydzak et al. 2009), especially *C. cellulolyticum* (Desvaux 2004).

Table 3.2 Comparison of volumetric gas and ethanol production rates in mmol/L/h (hexose equivalent) among selected mesophilic *Clostridium* species.

***Clostridium* species**	**Substrate**	**Growth Condition**	**Growth Phase**	**H_2**	**CO_2**	**EtOH**	**Reference**
C. termitidis	Cellobiose 10 g/L	Reactor pH controlled	Stationary 32-52 h	2.29 ± 0.04	1.88 ± 0.34	2.06 ± 0.11	This study
	Cellobiose 2 g/L	Reactor pH controlled	Stationary 24-36 h	1.76 ± 0.02	1.34 ± 0.16	0.48 ± 0.02	This study
	Cellobiose 2 g/L	Reactor pH controlled	Stationary 28-40 h	0.44 ± 0.02	0.30 ± 0.08	0.26 ± 0.14	Ramachandran 2013
	Cellobiose 2 g/L	Balch tube pH uncontrolled	Stationary 28-40 h	0.52	0.66	0.36	Ramachandran et al. 2008
	Cellobiose 1 g/L	Reactor pH controlled	Stationary 16-20 h	2.19 ± 0.29	1.13 ± 0.06	0.62 ± 0.05	This study
C. cellobioparum	Cellobiose 5 g/L	Serum bottle pH uncontrolled	Stationary 24-72 h	1.76	1.08	0.33	Ren et al. 2007[a]
C. acetobutylicum	Cellobiose 5 g/L	Serum bottle pH uncontrolled	Stationary 24-72 h	2.18	1.12	0.07	Ren et al. 2007[a]
C. cellulolyticum	Cellobiose 5 g/L	Serum bottle pH uncontrolled	Stationary 24-72 h	1.69	1.03	0.34	Ren et al. 2007[a]

a = data derived from Ren et al. 2007.

Table 3.3 Comparison of volumetric yields (mmol/L) of end-products among selected mesophilic *Clostridium* species.

***Clostridium* species**	**Substrate**	**Growth Condition**	**Growth Phase**	**H_2**	**CO_2**	**EtOH**	**Formate**	**Acetate**	**Lactate**	**Cell biomass (CDW)**	**Reference**
C. termitidis	Cellobiose 10 g/L	Reactor pH controlled	32-52 h	42.77±2.93	27.46±5.59	32.23±1.25	46.16±4.44	48.63±0.50	5.22±0.79	3.37±0.20	This study
	Cellobiose 2 g/L	Reactor pH controlled	24-36 h	21.10±0.14	15.86±1.90	5.83±0.30	8.50±1.60	15.70±0.30	1.90±0.70	1.90±0.19	This study
	Cellobiose 2 g/L	Reactor pH controlled	28-40 h	11.98±0.06	8.25±1.01	3.37±0.48	6.66±0.25	13.17±1.53	4.98±0.84	1.52±0.06	Ramachandran 2013
	Cellobiose 2 g/L	Balch tube pH uncontrolled	28-40 h	4.6	5.6	3.7	4.2	5.9	2.0	1.56	Ramachandran et al. 2008
	Cellobiose 1 g/L	Reactor pH controlled	16-20 h	15.89±2.28	8.50±0.50	3.90±0.38	6.20±0.10	8.50±0.60	0.90±0.50	1.37±0.03	This study
C. cellobioparum	Cellobiose 5 g/L	Serum bottle pH uncontrolled	Stationary 24-72 h	42.3	26.0	7.8	<0.2	15.9	NM	6.7	Ren et al. 2007[a]
C. acetobutylicum	Cellobiose 5 g/L	Serum bottle pH uncontrolled	Stationary 24-72 h	52.3	26.8	1.7	<0.2	14.2	NM	9.5	Ren et al. 2007[a]
C. cellulolyticum	Cellobiose 5 g/L	Serum bottle pH uncontrolled	Stationary 24-72 h	40.6	24.8	8.2	0.2	18.6	NM	6.2	Ren et al. 2007[a]

a = data derived from Ren et al. 2007; NM = Not measured; CDW = cell dry weight;

Figure 3.5 provides various end-products distribution over the course of fermentation, which were measured at discrete timepoints using HPLC. As the cellobiose consumption increased during exponential phase, the acetate synthesis increased rapidly compared to ethanol synthesis (Figure 3.5). Although both acetate and ethanol concentrations continued to increase by phase II, the increase in ethanol concentration was significantly lower than the acetate concentration. However, at phase III, both acetate and ethanol production increased sharply. While the rate of growth through phases II and III were identical (Figure 3.2), these 2 phases are distinguished by their distinct differences in end-product generation characteristics. The highest cellobiose consumption was also observed at this growth phase (Figure 3.6). Acetate synthesis gradually increased at a slower rate throughout the stationary phase (phase IV), whereas ethanol synthesis increased at a faster rate but did not vary significantly during stationary phase.

3.3.3.3 Formate synthesis

C. termitidis encodes a *pfl* gene that produces the enzyme, pyruvate formate lyase (PFL) in pyruvate catabolic reactions. This enzyme converts pyruvate to acetyl-CoA with the synthesis of formate during fermentation. In this set of experiments, formate was initially synthesized slowly during exponential phase growth. Concentrations of formate then increased sharply at the beginning of stationary phase (III), followed by a slow increase throughout the stationary phase (Figure 3.5). It is to be noted that the phase III does not exist on the basis of OD in Figure 3.2, but clearly visible based on end-products synthesis (Figure 3.3A).

The proportion of carbon going to acetate and ethanol increased during early stationary phase of growth. In addition to C2 products, C1 products (formate and CO_2) also increased over the course of the fermentation reaction. This indicated that *C. termitidis* produced ethanol and acetate from pyruvate via acetyl-CoA, via two branched fermentative pathways: PFL and PFOR.

A)

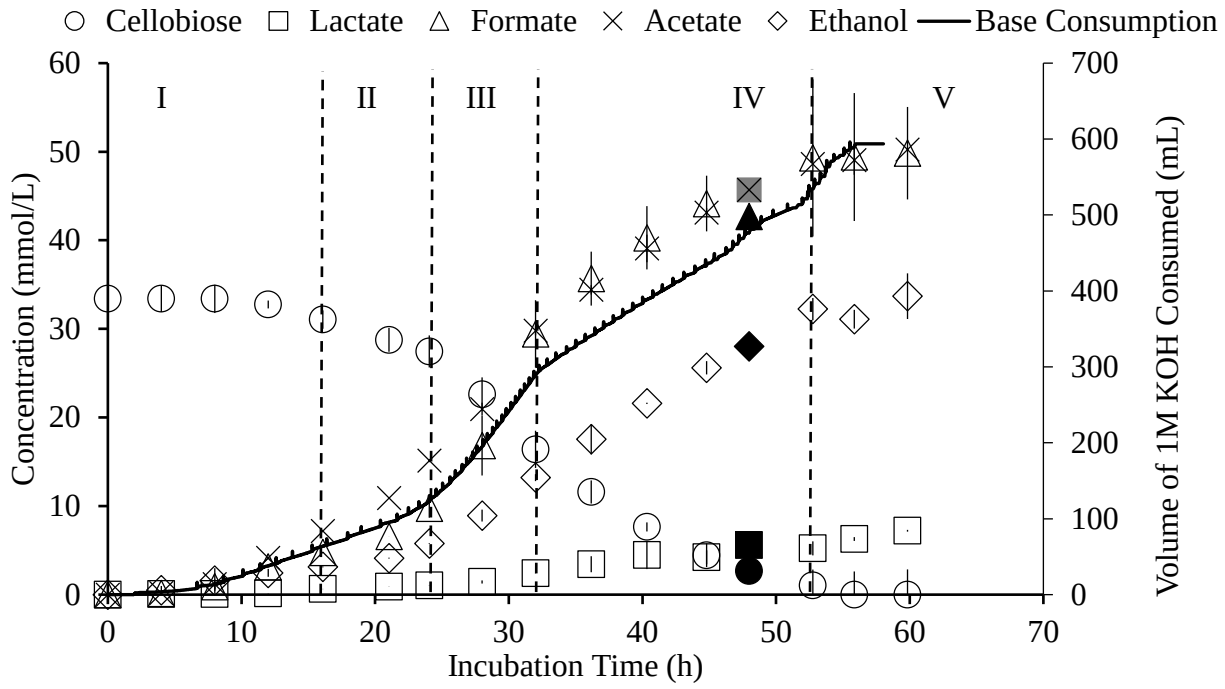
Cellobiose
Lactate
Formate
Acetate
Ethanol
Base Consumption
I
II
III
IV
V
Concentration (mmol/L)
Volume of 1M KOH Consumed (mL)
Incubation Time (h)
0
10
20
30
40
50
60
70
0
100
200
300
400
500
600
700

B)

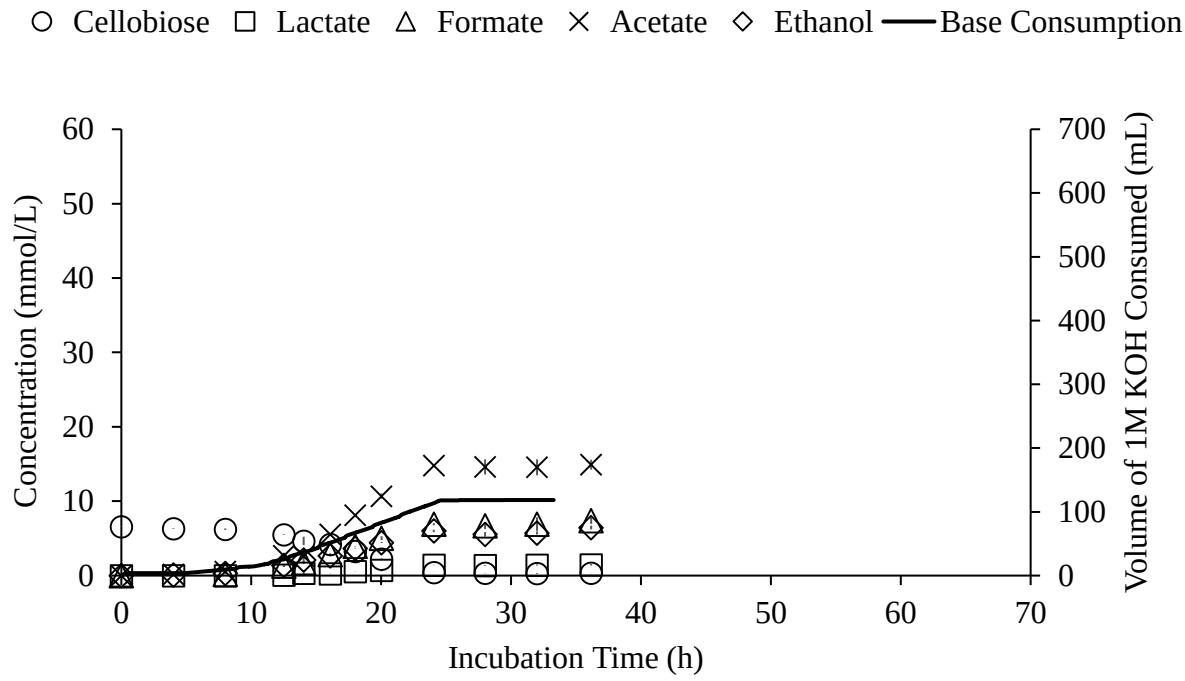
Cellobiose
Lactate
Formate
Acetate
Ethanol
Base Consumption
Concentration (mmol/L)
Volume of 1M KOH Consumed (mL)
Incubation Time (h)
0
10
20
30
40
50
60
70
0
100
200
300
400
500
600
700

C)

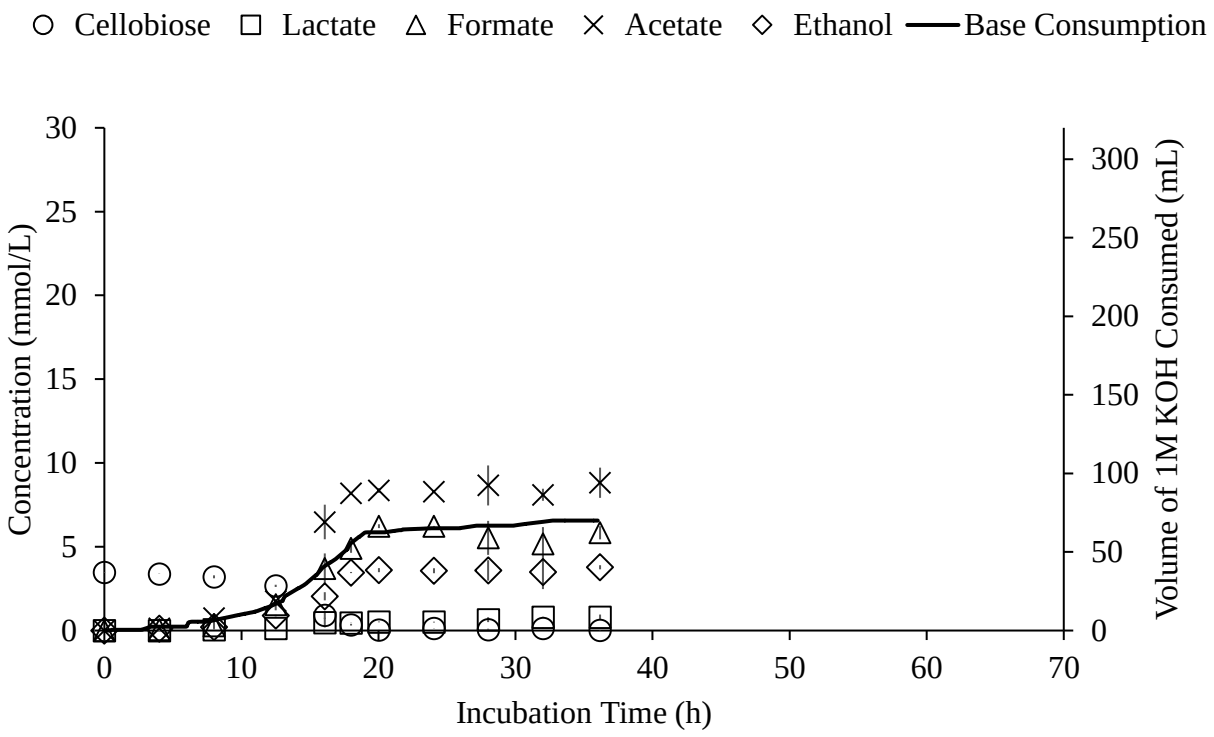

Figure 3.5 End-product distribution by *C. termitidis* grown on A) 10 g/L cellobiose B) 2 g/L and C) 1 g/L under pH controlled conditions. Black line indicates base consumption over the course of reaction. Error bars represents standard deviations of biological replicates. Roman numbers (I –V) indicate various growth phases mentioned in Figure 3.2. Open circle (○) – cellobiose, open square (□) – lactate, open triangle (Δ) - formate, cross (x) – acetate, open diamond (◊) – ethanol, black line – base consumption. All analytes were calculated based on discrete measurements, except base consumption, which was obtained from continuous measurements. Roman numerals (I –V) separated by dashed vertical lines in Figure 3.5A indicate various growth phases, as descrived in Figure 3.2.

3.3.3.4 Lactate synthesis

Lactate production was not observed until 16 h pi, when the rate of cellobiose consumption increased. Lactate synthesis is believed to be the result of pyruvate catabolism by the lactate dehydrogenase (LDH) enzyme in *C. termitidis*, irrespective of carbon source (pentose or hexose sugar) (Munir 2015). In the present experiment (with 10 g/L cellobiose), lactate was produced during the exponential phase and gradually continued increasing to a maximum value of 5.22 ± 0.79 mmol/L (volumetric yield) in the stationary phase. The maximum volumetric production of lactate was obtained 1.90 ± 0.70 mmol/L in the present study using 2 g/L cellobiose at the stationary phase. When *C termitidis* was cultured on 1 g/L cellobiose, only 0.90 ± 0.50 mmol/L lactate was produced.

3.3.4 Substrate consumption and product synthesis rate

3.3.4.1 Volumetric rates

Figure 3.6 provides phase-wise volumetric consumption rate of cellobiose and volumetric production rates of various end-products including increase in biomass measured as cell protein (see Supplementary Figure S3.1). The volumetric cellobiose consumption rate gradually increased as the amount of biomass increased through exponential phase to stationary phase. The highest volumetric cellobiose consumption rate was obtained 2.75 ± 0.12 mmol/L/h (hexose equivalent). Then, it was gradually decreased when the cells reached stationary phases.

Gaseous products were measured both discretely and continuously, and they were used in volumetric rates calculation (Figure 3.6A and B; supplementary Figure S3.2). The volumetric H_2 synthesis rate increased slightly from exponential phase-I to phase-III (Figure 3.6). Here, the maximum volumetric production rate (hexose equivalent) of H_2 was achieved 2.29 ± 0.04 mmol/L/h (Table 3.2) and then it was decreased during stationary phase-IV and V. The

volumetric CO_2 synthesis rate did not follow the trend of H_2 synthesis rate. However, it increased gradually from exponential phase-I to phase-II and then decreased again. The CO_2 synthesis rate gradually increased again throughout the stationary phase and reached to a maximum value of 1.88 ± 0.34 mmol/L/h. Table 3.2 provides volumetric rate comparison of *C. termitidis* with other mesophilic *Clostridium* species. The volumetric synthesis rates of H_2 and CO_2 were not very far off from rates obtained using 2 g/L cellobiose (about 1.5 times) in the present study. It was 5-fold higher for H_2 and 6-fold higher for CO_2 than previously observed data (Ramachandran 2013) with cellobiose under carbon-sufficient conditions. Other cellulolytic bacteria produced hydrogen at an approximately 30 % slower rate under high initial cellobiose load (5 g/L) (Ren et al. 2007) compared to *C. termitidis* on 10 g/L cellobiose in the present study.

The highest volumetric synthesis rate of formate, acetate and ethanol was observed during phase III (Figure 3.6), which was corroborated with cellobiose consumption rate at this growth phase. Here, a 4-fold ethanol synthesis rate was observed compared to the rate during exponential growth phase. Although volumetric synthesis rates for formate and acetate decrease significantly during phase IV and phase V, but volumetric ethanol synthesis rate remained constant during stationary growth phases. 0.23 ± 0.01 mmol/L/h was the highest protein synthesis rate observed during early stationary growth phase of *C. termitidis*.

A)

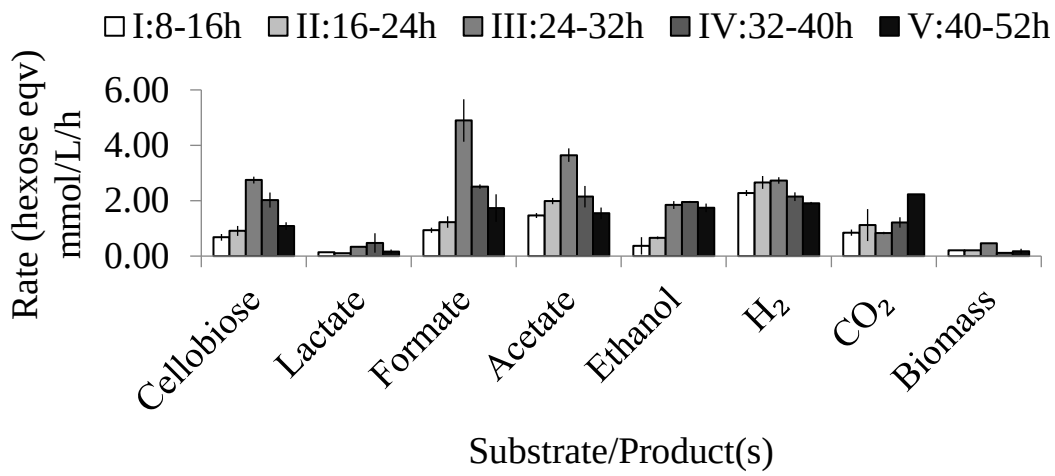

B)

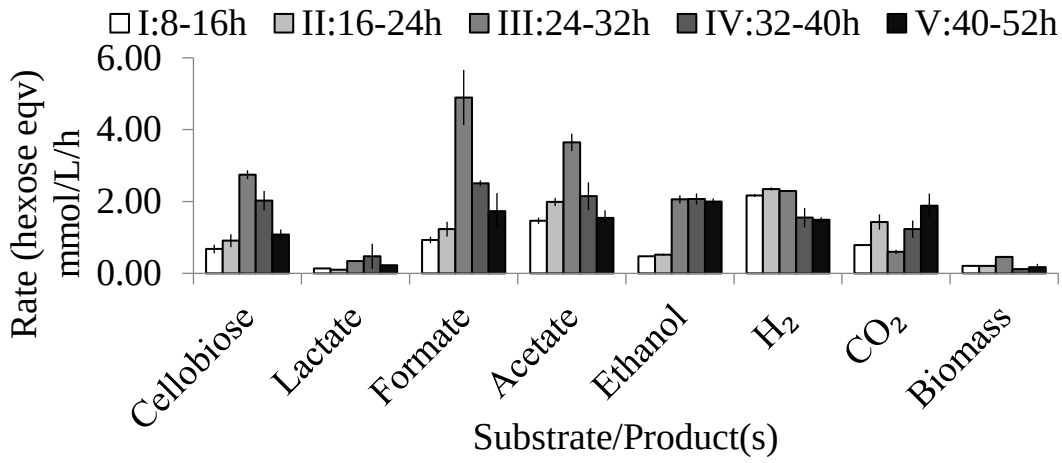

Figure 3.6 Phase-wise volumetric consumption rate of cellobiose and production rates for lactate, formate acetate, ethanol, H_2, and CO_2 at different phases of the *C. termitidis* fermentation reaction. Soluble products were measured using HPLC. Volatile products rates measured A) at discrete time points using GC and B) continuously using MIMS probe. 8-16 h: exponential phase (I); 16-24 h: late exponential phase (II); 24-32 h: early stationary phase (III); 32-40 h: stationary phase (IV) and 40-52 h: stationary phase (V).

3.3.4.2 Cell-specific rates of fermentation end-product synthesis

Cell-specific rates of end-product synthesis were also used to evaluate metabolic shifts observed during various phases of *C. termitidis* growth (Figure 3.7 and Figure 3.8). *C. termitidis* synthesized H_2, acetate, ethanol, formate, and CO_2 as the predominate end-products throughout the fermentation and their distribution varied with growth phase. Synthesis of these products was observed from the beginning of fermentation and continued to rise in phase II, 16-24 h pi. Lactate production became significant near mid-exponential phase (Phase I). This observation was in agreement with other studies (Ramachandran 2013; Munir 2015) including present study with low initial substrate concentration.

Soluble end-products and off-gases (H_2 and CO_2) produced by *C. termitidis* in each growth phase were measured by both discrete and on-line, real-time methods using the TOGA. They are presented in Figure 3.4 and Figure 3.5. Cellobiose (as residual cellobiose) and base consumption are also shown in each growth phase. As expected, the production rate of various end-products are not same throughout the different phases of the fermentation. Therefore, the cell-specific production rates of metabolites are calculated for each end-product at the end of the different phases (Figure 3.7), based on the growth curve (Figure 3.2 and supplementary Figure S3.1) and gas phase monitoring (Figure 3.3).

The highest cellobiose consumption rate was observed in early stationary phase (2.38 ± 0.14 mmol/g of protein/h) among all other growth phases (Figure 3.7A). The specific lactate production rate increased slightly in the early stationary phase compared to exponential phase, but did not vary significantly throughout the stationary growth phase.

The highest cell-specific production rates of acetate, hydrogen, and CO_2 were found to be 4.84 ± 0.46 mmol/g of protein/h, and 7.47 ± 0.98 mmol/ g of protein/h, and 2.72 ± 0.48 mmol/ g

of protein/h respectively, in exponential phase. The ethanol production rate (1.57 ± 0.02 mmol/ g of protein/h) was considerably higher in early stationary phase and remained steady throughout the entire stationary phase. The highest specific production rate of formate was not observed in phase I of growth, but in phase III consistent with its partial replacement of Hydrogen and CO_2 production, which was decreases in that phase.

3.3.5 Product yields

3.3.5.1 Volumetric yields

H_2: The volumetric yield of H_2 was 42.77 ± 2.93 mmol/L of culture in this study using 10 g/L cellobiose (Table 3.3), which was about 4-fold higher than previous study conducted with 2 g/L cellobiose in a pH-controlled reactor and 10-fold higher than the study conducted in Balch tubes (Ramachandran et al. 2008). In batch cultures, low yield of H_2 was obtained because of acid production by the culture, and high partial pressures into Balch tubes. Thus, dissolved H_2 may have affected hydrogenase activity. This was also observed in previous investigations, where *C. thermocellum* (Islam et al. 2006) and *C. cellobioparum* (Chung 1976) were grown on 4.5 g/L and 5.0 g/L cellobiose respectively. *C. thermocellum* produced 15.18 mmol/L H_2, whereas *C. cellobioparum* produced 18.83 mmol/L. Both studies suggested that produced H_2 gas was sufficient for growth inhibition. Similar concentrations of H_2 (ca. 20 mmol/L) were obtained at the early stationary phase of growth for *C. termitidis* in the present study. When *C. termitidis* was cultured on 2 g/L cellobiose in a pH controlled bioreactor, the volumetric yield was obtained 21.10 ± 0.14 mmol/L. This amount was about 2-fold lower when compared to gas obtained on cellobiose excess condition (10 g/L).

A)

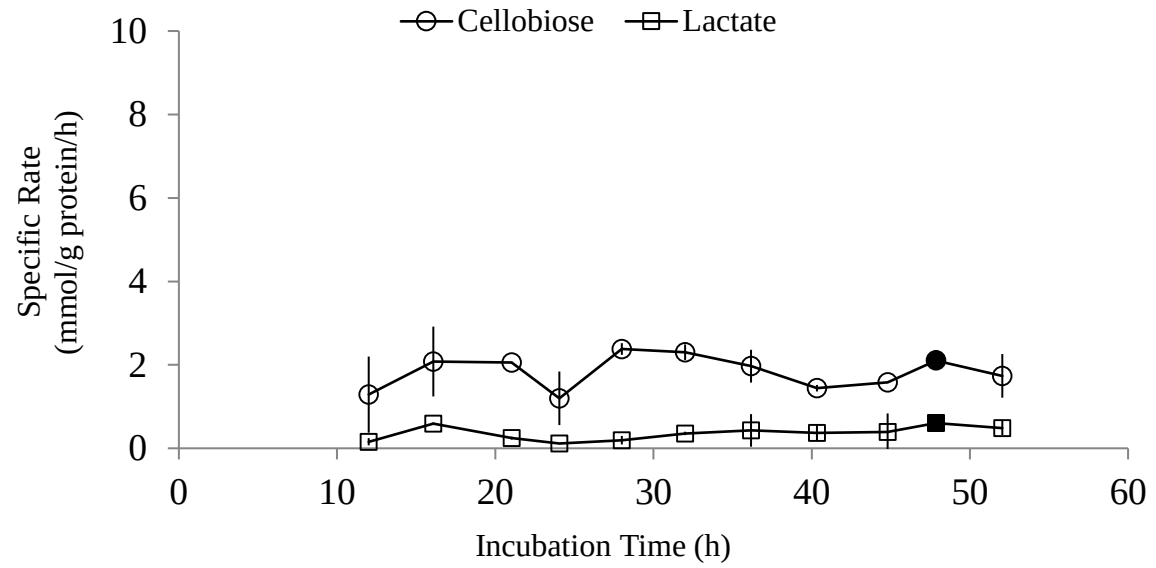
Cellobiose
Lactate
Specific Rate (mmol/g protein/h)
Incubation Time (h)
0
2
4
6
8
10
0
10
20
30
40
50
60

B)

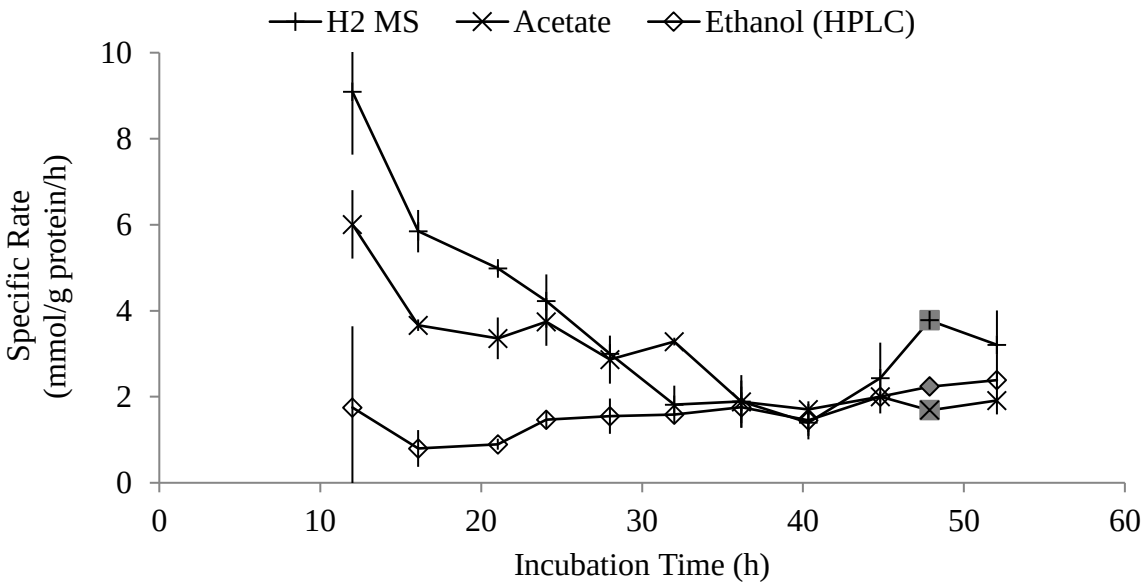
H2 MS
Acetate
Ethanol (HPLC)
Specific Rate (mmol/g protein/h)
Incubation Time (h)
0
2
4
6
8
10
0
10
20
30
40
50
60

C)

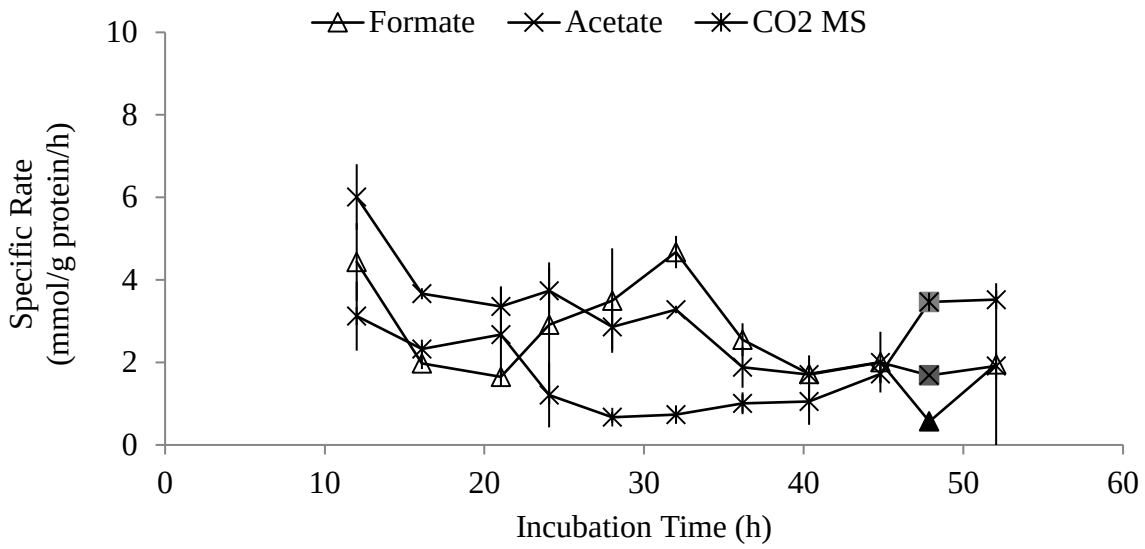
Formate
Acetate
CO2 MS
Specific Rate (mmol/g protein/h)
Incubation Time (h)
0
2
4
6
8
10
0
10
20
30
40
50
60

D)

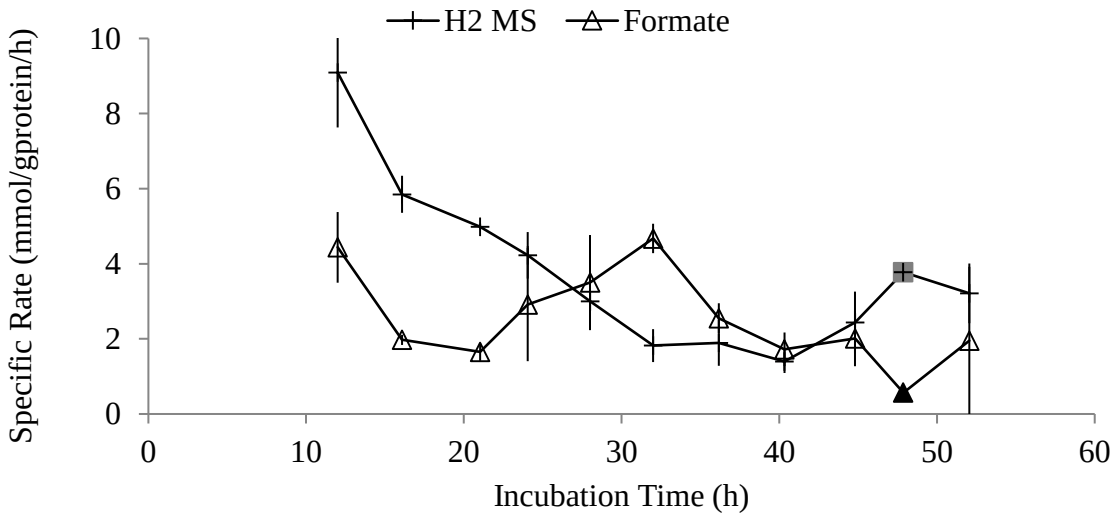
H2 MS
Formate
Specific Rate (mmol/gprotein/h)
Incubation Time (h)
0
2
4
6
8
10
0
10
20
30
40
50
60

Figure 3.7 Variation in cell-specific rates of end-product synthesis by *C. termitidis* during different growth phases. A) rates of H_2, acetate, and ethanol synthesis; B) rates of formate, acetate, and CO_2 synthesis; C) rates of H_2 and formate synthesis; D) rates of cellobiose consumption and lactate synthesis. Plus (+), H_2 measured by Mass Spectrometry (MS); cross (x), acetate measured by HPLC; circle (○), cellobiose measured by HPLC; square (□), lactate measured by HPLC; star (*), CO_2 measured by MS; diamond (◊), ethanol measured by HPLC; triangle (Δ), formate measured by HPLC; solid lines are associated with scattered plot of data. The first few data points were excluded due to high variability in measurement. Error bars represents standard deviations of two biological replicates. Solid fills (plus, cross, square, star, diamond, triangle) indicate single biological replicate at that time point.

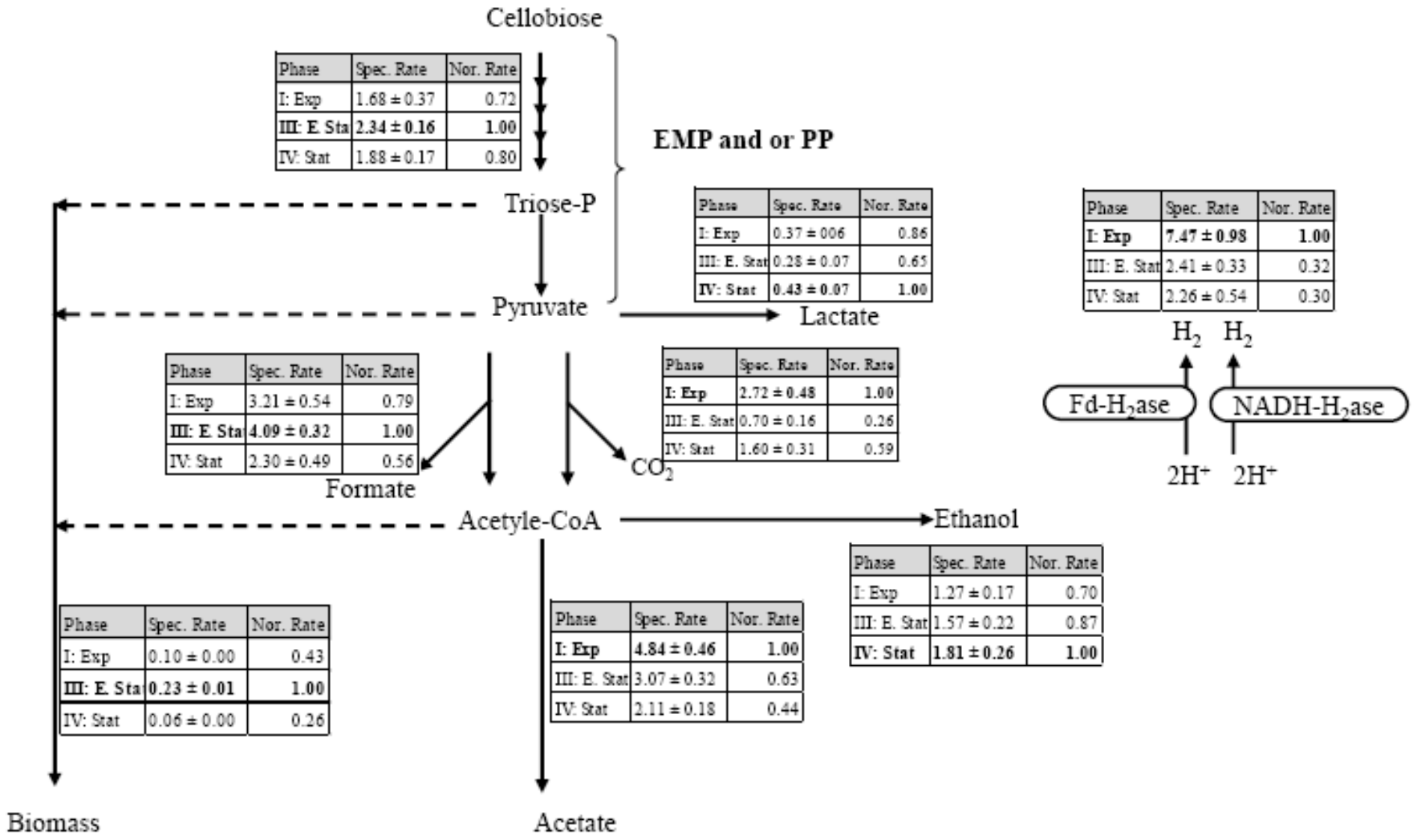

Phase	Spec. Rate	Nor. Rate
I: Exp	1.68 ± 0.37	0.72
III: E. Sta	**2.34 ± 0.16**	**1.00**
IV: Stat	1.88 ± 0.17	0.80

Phase	Spec. Rate	Nor. Rate
I: Exp	0.37 ± 006	0.86
III: E. Stat	0.28 ± 0.07	0.65
IV: Stat	**0.43 ± 0.07**	**1.00**

Phase	Spec. Rate	Nor. Rate
I: Exp	**7.47 ± 0.98**	**1.00**
III: E. Stat	2.41 ± 0.33	0.32
IV: Stat	2.26 ± 0.54	0.30

Phase	Spec. Rate	Nor. Rate
I: Exp	3.21 ± 0.54	0.79
III: E. Sta	**4.09 ± 0.32**	**1.00**
IV: Stat	2.30 ± 0.49	0.56

Phase	Spec. Rate	Nor. Rate
I: Exp	**2.72 ± 0.48**	**1.00**
III: E. Stat	0.70 ± 0.16	0.26
IV: Stat	1.60 ± 0.31	0.59

Phase	Spec. Rate	Nor. Rate
I: Exp	1.27 ± 0.17	0.70
III: E. Stat	1.57 ± 0.22	0.87
IV: Stat	**1.81 ± 0.26**	**1.00**

Phase	Spec. Rate	Nor. Rate
I: Exp	0.10 ± 0.00	0.43
III: E. Sta	**0.23 ± 0.01**	**1.00**
IV: Stat	0.06 ± 0.00	0.26

Phase	Spec. Rate	Nor. Rate
I: Exp	**4.84 ± 0.46**	**1.00**
III: E. Stat	3.07 ± 0.32	0.63
IV: Stat	2.11 ± 0.18	0.44

Figure 3.8 Pyruvate catabolic pathways and cell specific rates of substrate consumption and product synthesis during exponential (I), early stationary (III), and stationary (IV) growth phases of *C. termitidis* cultured with 10 g/L cellobiose. Cells were grown in 1191 media, with pH controlled to 7.20 ± 0.02 using base, in a 7 L reactor with a 3.0 L working volume. The second column in the Table indicates average value of cell specific rates (mmol/g of protein/h & mmol/L/h for biomass only) during the growth phase with standard deviations from two biological replicates. Third column indicates normalized value to the highest specific rates obtained (bold). The cell specific rate cannot be calculated for biomass, therefore, the volumetric rate was used. For protein data conversion (mg/mL into mmol/L), 1 mg of protein/mL of culture = 2 g of biomass (CDW)/L of cluture = (2 g/L)/(101 g/mol) = 2*9.90E-3 mol/L = 19.80 mmol/L biomass (CDW); since, the aproximate molecular weight is 101 g/mol.

Ethanol and acetate: Ethanol yield was 32.23 ± 1.25 mmol/L and it was the highest yield (~10 times higher) obtained from previously reported data (3.37 ± 0.48 mmol/L) using 2 g/L cellobiose. However, a 2-fold ethanol yield (5.83 ± 0.30 mmol/L) was obtained in the present study when *C. termitidis* was cultured on 2 g/L cellobiose. The volumetric acetate yields were obtained 48.63 ± 0.50 mmol/L and 15.70 ± 0.30 mmol/L when *C. termitidis* was cultured on 10 g/L and 2 g/L cellobiose, respectively. This acetate yield was observed 8.50 ± 0.60 mmol/L when cultured on 1 g/L cellobiose. Previous study (Ramachandran 2013) reported that maximum acetate production was observed not in stationary phase but exponential phase using 2 g/L cellobiose. Carbon flux was distributed to ethanol and lactate at this stage.

3.3.5.2 Substrate consumption and biomass yield

Figure 3.2 showed the close relationship between cellobiose consumption and *C. termitidis* growth. The cellobiose consumption rate gradually increased through exponential phase into phase III reaching a maximum value of 2.38 ± 0.14 mmol/g of protein/h. Then it decreased gradually until all the cellobiose was completely consumed (Figure 3.7). When *C. termitidis* was grown under carbon-excess (10 g/L cellobiose) conditions, the maximum average cell protein concentration obtained was 0.21 ± 0.02 mg/mL at the end of phase-III (see Figure S3.1). However, the substrate-specific cell protein yields varied with the cell growth phase. For example, the substrate-specific cell protein yield obtained during exponential growth phase (at 16 h pi) was 0.09 ± 0.01 mol/mol of hexose equivalents, which decreased to 0.05 ± 0.02 mol/mol of hexose equivalents during phase III (at 32 h pi), and then to 0.02 ± 0.00 mol/mol of hexose equivalents as expected from stationary phase (at 52 h pi) (Table 3.4). However, when *C. termitidis* was grown on 2 g/L and 1 g/L cellobiose in a bioreactor in the present study, the cell protein yield were obtained 0.08 ± 0.02 mol/mol of hexose equivalents and 0.11± 0.03 mol/mol

Table 3.4 Substrate-specific yields (mol of product/mol of hexose equivalent) of various end-products at exponential, early stationary and stationary phase (present study) and compared with mesophilic *Clostridium* species (in stationary phase).

Mesophiles	Growth Phase	Lactate	Formate	CO_2	H_2	EtOH	Acetate	Cell Protein	Reference
C. termitidis(10g/L)	I: 16 h Exponential	0.09 ± 0.01	0.71 ± 0.09	0.77 ± 0.02	2.00 ± 0.17	0.47 ± 0.07	1.07 ± 0.14	0.09 ± 0.01	This study
	II: 24 h Late exponential	0.06 ± 0.01	0.60 ± 0.18	0.59 ± 0.22	1.45 ± 0.05	0.35 ± 0.06	0.92 ± 0.16	0.06 ± 0.01	This study
	III: 32 h Early stationary	0.06 ± 0.01	0.75 ± 0.16	0.33 ± 0.08	0.89 ± 0.01	0.34 ± 0.04	0.76 ± 0.08	0.05 ± 0.02	This study
	IV: 52 h Stationary	0.08 ± 0.02	0.75 ± 0.10	0.45 ± 0.07	0.85 ± 0.07	0.49 ± 0.02	0.75 ± 0.03	0.02 ± 0.00	This study
C. termitidis(2g/L)	24-32 h Stationary	0.12 ± 0.04	0.58 ± 0.05	1.27 ± 0.08	1.83 ± 0.11	0.51 ± 0.05	1.25 ± 0.03	0.08 ± 0.02	This study
C. termitidis(2g/L)	24-32 h Stationary	0.43 ± 0.07	0.57 ± 0.02	0.71 ± 0.09	1.03 ± 0.01	0.29 ± 0.04	1.13 ± 0.13	0.06 ± 0.01	Ramachandran 2013[a]
C. termitidis(1g/L)	20-24h Stationary	0.16 ± 0.08	1.05 ± 0.06	1.65 ± 0.11	2.86 ± 0.21	0.62 ± 0.06	1.28 ± 0.09	0.11 ± 0.03	This study
C. acetobutylicum (5g/L)	48 h Stationary	ND	< 0.02	1.16	2.26	0.07	0.61	**0.41**	Ren et al. 2007[b]
C. cellobioparam (5g/L)	48 h Stationary	ND	< 0.02	1.19	1.94	0.36	0.73	**0.31**	Ren et al. 2007[b]
C. cellulolyticum (5g/L)	48 h Stationary	ND	0.02	1.11	1.82	0.37	0.83	**0.28**	Ren et al. 2007[b]

[a] Data derived from Ramachandran (2013);
[b] Data derived from Ren et al. (2007);
Bold indicates cell biomass instead of cell protein. Cellobiose was used as a substrate in all experiments.

of hexose equivalents, respectively. A previous study by Ramachandran (2013) observed, in batch cultures (on 2 g/L cellobiose) a substrate-specific cell protein yield of 0.06 ± 0.01 mol/mol of hexose equivalents obtained exponential growth phase, which was about 30 % less compared to the present study. Ren et al. (2007) obtained biomass yields 0.41, 0.31, and 0.28 mol/mol of hexose equivalents (Table 3.4) for *C. acetobutylicum, C. cellobioparam,* and *C. cellulolyticum*, respectively, when these species were cultured on 5 g/L cellobiose in batch experiments.

3.3.5.3 Substrate-specific yields of fermentation end-products

Table 3.4 also shows the substrate-specific product yields for *C. termitidis* compared with yields of other mesophilic *Clostridium* species. The H_2 yield was more than double (2.00 ± 0.17 mol/mol of hexose equivalent) during exponential growth phase compared to the yield during stationary growth phases (III and IV). Previous study on 2 g/L cellobiose (Ramachandran, 2013) showed almost half the H_2 yield (1.03 ± 0.01 mol/mol of hexose equivalent) in the stationary phase compared to the yield during the exponential phase of growth (determined in this study). When *C. termitidis* was cultured on 2 g/L and 1 g/L celobiose H_2 yields were 1.83 ± 0.11 and 2.86 ± 0.21 mol/mol of hexose equivalent, respectively.

The highest substrate-specific CO_2 yield (0.77 ± 0.02 mol/mol of hexose equivalent) was obtained during exponential growth phase. The substrate-specific CO_2 yield decreased during early stationary phase (0.33 ± 0.08 mol/mol of hexose equivalent), and then increased again in the late stationary growth phase (Table 3.4). On average, 50 % less yield of CO_2 was observed during stationary phase of growth compared to exponential phase. The substrate-specific yield of CO_2 reported by Ramachandran (2013) was 0.71 ± 0.09 mol/mol hexose equivalent, which was very similar to our observation during exponential growth phase.

The substrate-specific yield of formate did not vary significantly during early stationary growth phase compared to exponential growth phase, and it did not also differ significantly between early stationary phase and late stationary phase. The formate yield was reported 0.57 ± 0.02 mol/mol of hexose equivalent, when *C. termitidis* was cultured on 2 g/L cellobiose at the end of fermentation (Ramachandran 2013). The present study was also observed similar formate yield (0.58 ± 0.05 mol/mol of hexose equivalent) on 2 g/L cellobiose, and a slightly higher yield (1.05 ± 0.06 mol/mol of hexose equivalent) on 1 g/L celobiose. Other studies (Ren et al. 2017) reported extremely low yields of formate (≤ 0.02 mol/mol of substrate hexose equivalent) in *C. acetobutylicum*, *C. cellobioparam*, and *C. cellulolyticum* cultures grown on 5 g/L cellobiose in Balch tubes.

Ethanol yields decreased slightly in early stationary phase compared to the exponential growth phase (0.47 ± 0.07 mol/mol hexose equivalent), and then, increased significantly during late stationary growth phase compared to early stationary phase. The substrate specific ethanol yield (0.51 ± 0.05 mol/mol hexose equivalent) on 2 g/L cellobiose did not vary by much compared to that in exponential growth phase and it was, however, significantly high compared to late or early stationary phase. These yields were almost double those reported by Ramachandran (2013) when *C. termitidis* was cultured on 2 g/L cellobiose. Ethanol yields were significantly lower in *C. acetobutylicum* and *C. cellobioparam* compared to the present study. Acetate yields were almost 30 % less in stationary growth phase compared to the yields during exponential growth phase. The acetate yields on low initial substrate concentration (2 g/L and 1 g/L cellobiose) was significantly high compared to that yields at various growth phases of 10 g/L cellobiose. No significant variation of lactate yields were noticed between exponential (0.09 ± 0.01 mol/mol of hexose equivalent) and stationary (0.08 ± 0.02 mol/mol of hexose equivalent)

growth phase. While low substrate specific lactate yields were obtained (0.12 ± 0.04 mol/mol of hexose equivalent and 0.16 ± 0.08 mol/mol of hexose equivalent on low initial carbon loads) in the present study, Ramachandran (2013) achieved comparatively high yield of lactate (0.43 ± 0.07 mol/mol of hexose equivalent) with *C. termitidis* cultured with 2 g/L cellobiose. Ren et al. (2007) did not measure lactate in *C. acetobutylicum*, *C. cellobioparam*, and *C. cellulolyticum* cultured with 5 g/L cellobiose.

3.3.6 Carbon recovery index and redox balance

Figure 3.9 shows carbon recovery and redox balance for *C. termitidis* over the entire fermentation period under excess cellobiose condition. For soluble end-products, data used from discrete measurement using HPLC, whereas continuous MS data used for gaseous substances.

3.3.6.1 Carbon recovery

On an average carbon recovery was 83.9 ± 0.09 % for the entire growth phase of *C. termitidis* on 10 g/L cellobiose (Figure 3.9A). However, while carbon recovery was close to 0.94 (i.e. 94 %) during exponential phase, it was far from 1 (about 65 – 70 %) during stationary phase (Figure 3.9A).

3.3.6.2 C1/C2 ratios

In this experiment, C1/C2 ratio was close to 1 (1.01 ± 0.07) throughout the growth period except for first few discrete data points (Figure 3.9B). This indicated that other than the pyruvate to lactate, reductive pathway, pyruvate to ethanol and acetate via oxidative (PFOR) and non-oxidative (PFL) pathways were accounted for. Any missing carbon flux from pyruvate and other upstream nodes could not be account for in this study. Previous studies reported C1/C2 ratios of 0.81 ± 0.12 with cellobiose (Ramachandran 2013). Lower values represent either C1 (formate or CO_2) under-estimation or C2 (acetate or ethanol) over-estimation.

A)

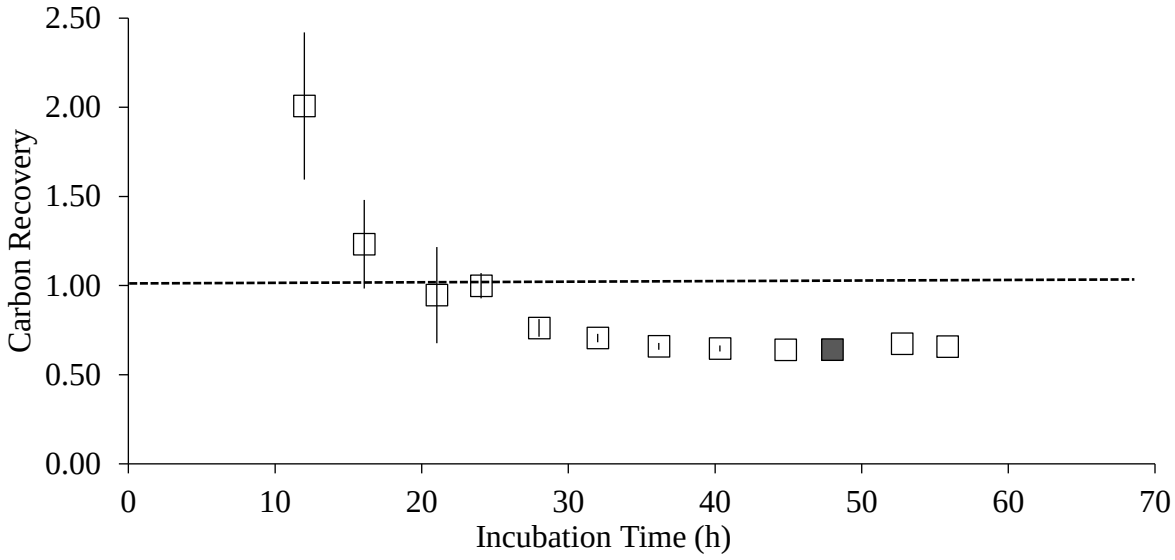
2.50
2.00
1.50
1.00
0.50
0.00
Carbon Recovery
0
10
20
30
40
50
60
70
Incubation Time (h)

B)

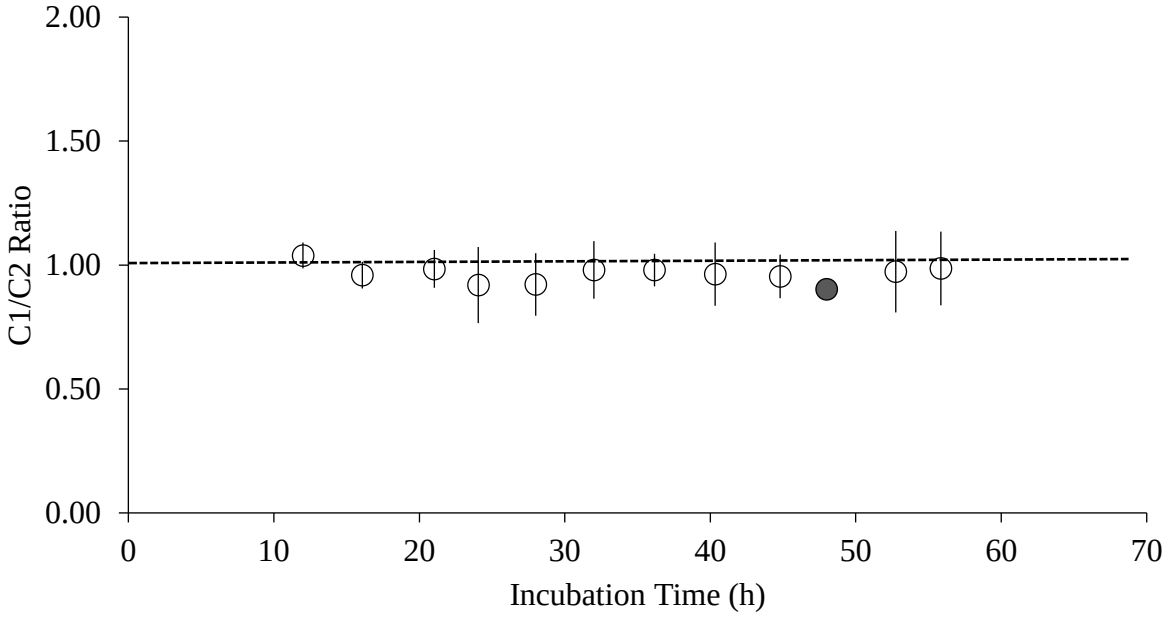
2.00
1.50
1.00
0.50
0.00
C1/C2 Ratio
0
10
20
30
40
50
60
70
Incubation Time (h)

C)

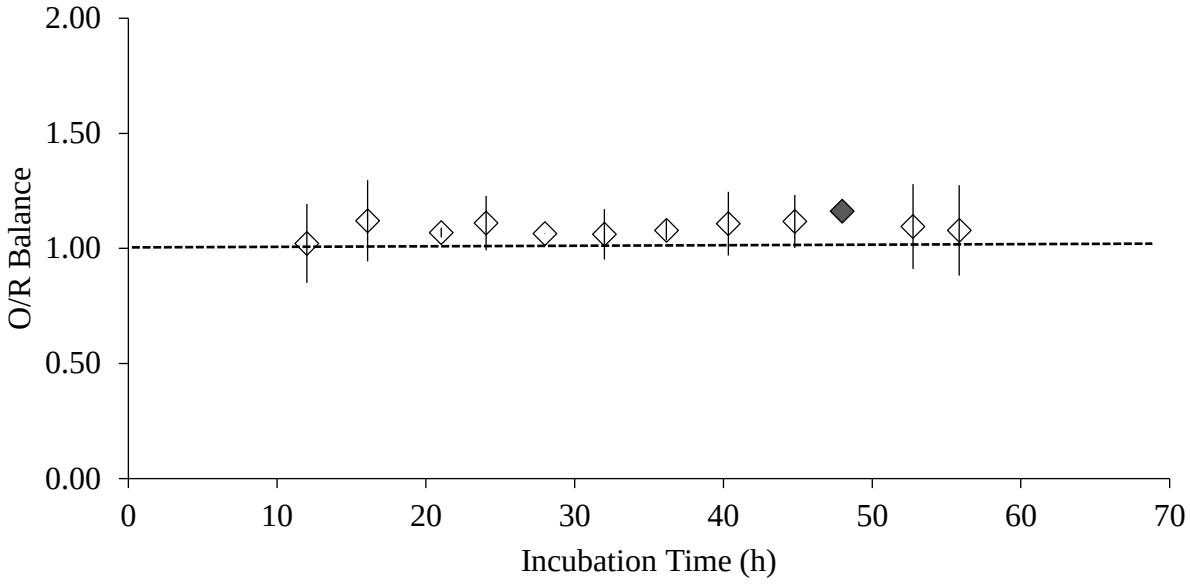

Figure 3.9 Reaction stoichiometry derived from discrete measurement over the course of fermentation. A) carbon recovery; B) C1/C2 ratio; and C) O/R balance. Solid data points (square, circle, diamond) indicate a single biological replicate. Dotted lines indicate the constant ratio 1.

3.3.6.3 O/R balance

The O/R ratio varied between 0.96 ± 0.02 and 2.34 ± 0.03 over the entire period of the fermentation reaction (Figure 3.9C). Higher O/R values were obtained at the very beginning of growth. This may have been due to an under-estimation of reduced end-products, such as hydrogen and ethanol, which may have resulted from saturation of gas in the culture medium (Pauss et al. 1990) at the early stage of fermentation, plus evaporation of ethanol during off-line quantification, or an over estimation of CO_2 (an oxidized end-product). High O/R balances (1.36 ± 0.13) reported in the previous study, with carbon-sufficient conditions indicate high reduced product (hydrogen or ethanol) over low oxidized products (CO_2 or formate) (Ramachandran 2013).

3.3.7 Product ratios

As *C. termitidis* metabolism follows branched fermentative pathways, it is necessary to evaluate carbon flow distribution in each branch. To maintain reaction stoichiometry, electron sinks such as H_2 and ethanol play a significant role in pyruvate catabolism reactions, not only in *Clostridia* species, but also in other species.

Ratios of hydrogen to carbon dioxide concentrations (H_2:CO_2 ratios) calculated for *C termitidis* growth were found to vary from 0.4 to slightly > 1 during the exponential and stationary phases, respectively, under carbon-sufficient conditions (Ramachandran 2013). In the present study, the H_2:CO_2 ratio was 2.5 in the early exponential phase, decreased to 2.0 in late exponential phase, rose again to 2.4 in early stationary phase, and then gradually decreased to 1.5 in late stationary phase (Figure 3.10A). With high cellobiose load (10 g/L), the H_2:acetate ratio was 1.5 during exponential growth phase, gradually decreased to approximately 1.0 during early stationary growth phase, and remained at approximately 1 throughout stationary growth phase

A)

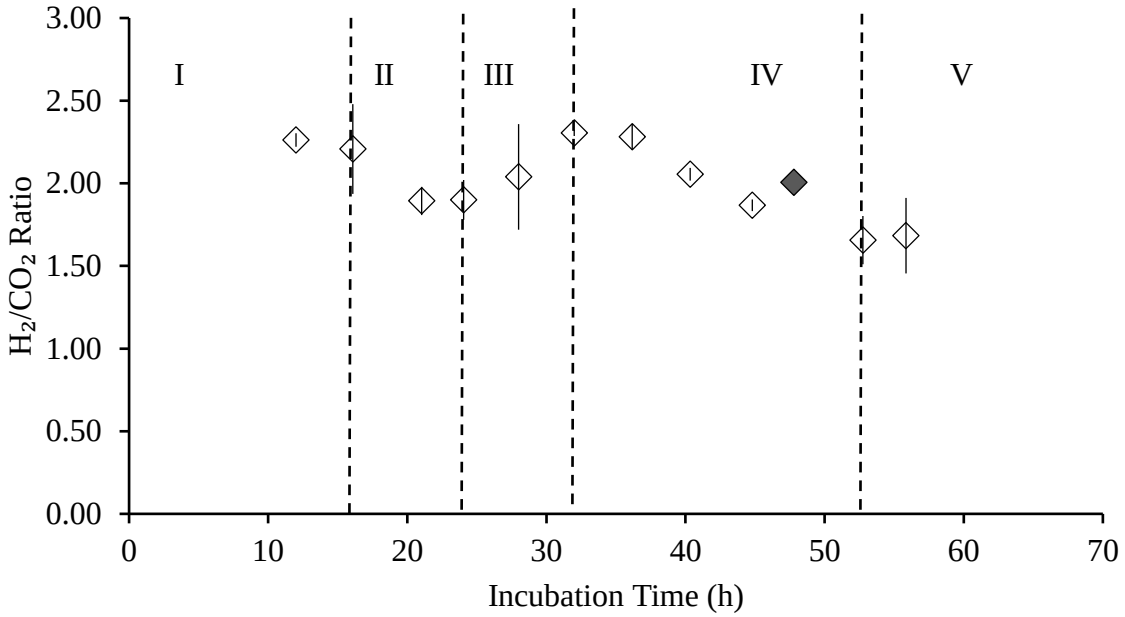
3.00
2.50
2.00
1.50
1.00
0.50
0.00
H2/CO2 Ratio
I
II
III
IV
V
0
10
20
30
40
50
60
70
Incubation Time (h)

B)

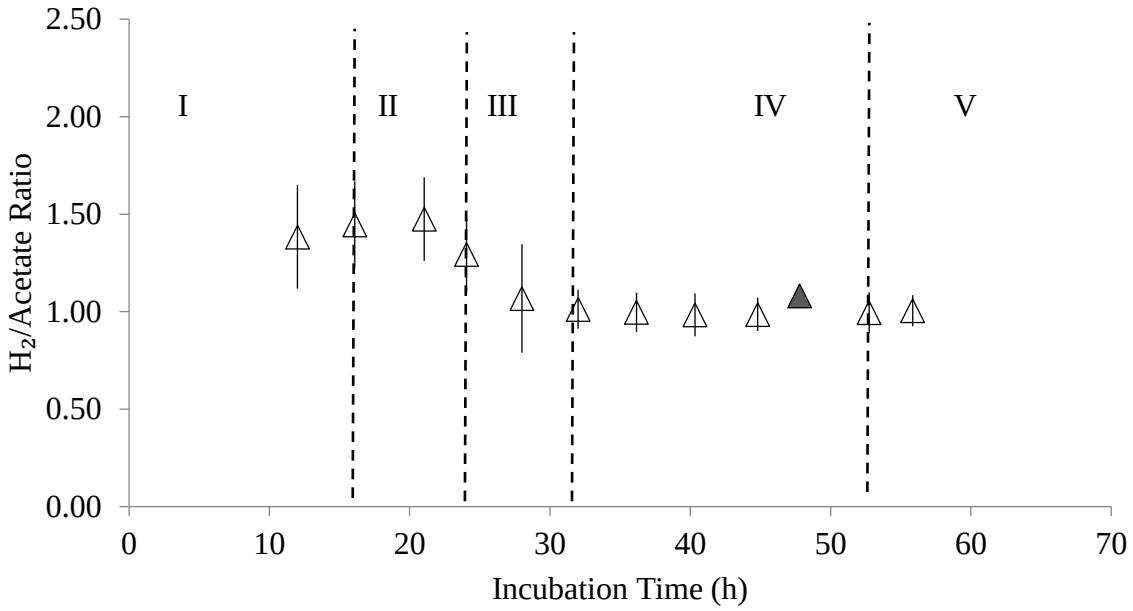
2.50
2.00
1.50
1.00
0.50
0.00
H2/Acetate Ratio
I
II
III
IV
V
0
10
20
30
40
50
60
70
Incubation Time (h)

C)

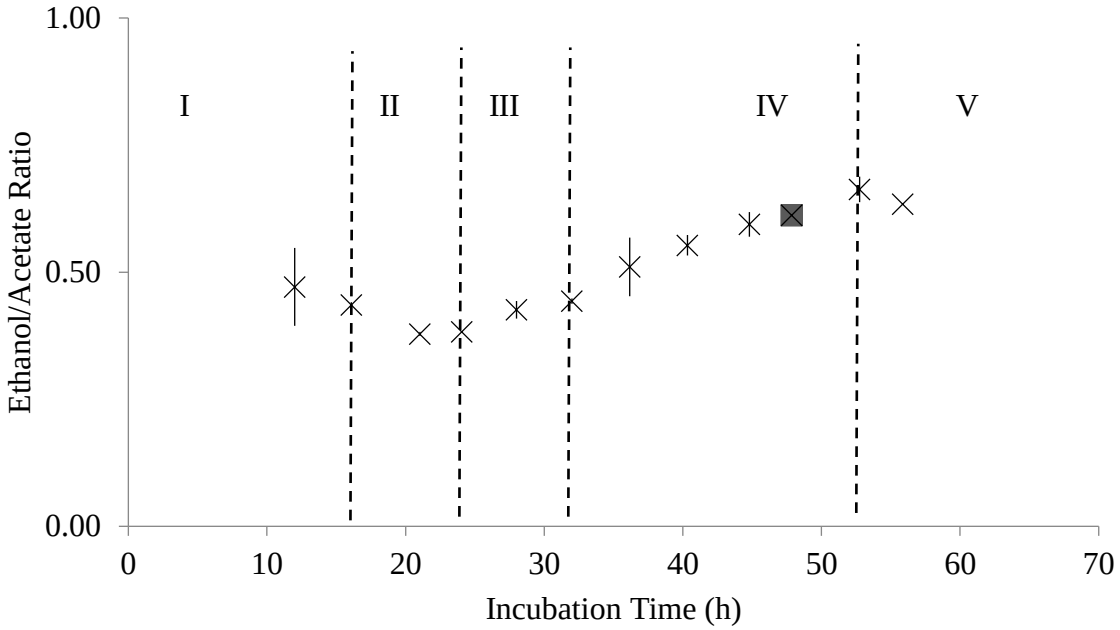
1.00
0.50
0.00
Ethanol/Acetate Ratio
I
II
III
IV
V
0
10
20
30
40
50
60
70
Incubation Time (h)

D)

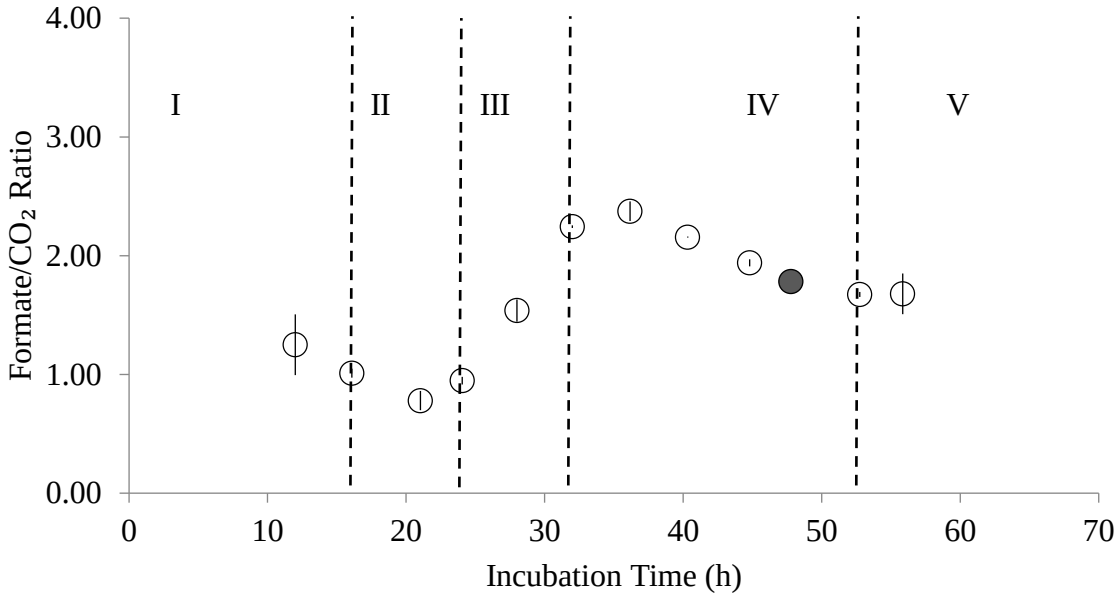
4.00
3.00
2.00
1.00
0.00
Formate/CO_2 Ratio
I
II
III
IV
V
0
10
20
30
40
50
60
70
Incubation Time (h)

Figure 3.10 Product ratios over the course of fermentation reaction. A) diamond (◊), H_2:CO_2 (hydrogen to carbon dioxide ratio); B) triangle (Δ), H_2:Ac (hydrogen to acetate ratio); C) cross (x), EtOH:Ac (ethanol to acetate ratios); and D) open circle (○), Fo:CO_2 (formate to carbon dioxide ratio). The first few data points were excluded due to high variability in measurements. Solid fills (diamond, triangle, cross, circle) indicate single biological replicate. Roman numerals (I –V) separated by dashed vertical lines indicate various growth phases, as descrived in Figure 3.2.

(Figure 3.10B). The ethanol to acetate ratio was approximately 0.40 during the exponential growth phase and increased to 0.68 in late stationary growth phase (Figure 3.10C). Ramachandran (2013) reported that maximum acetate production was observed in exponential phase, not in stationary phase. *C. termitidis* initially synthesized formate at a rate of 3.21 ± 0.54 mmol/g of protein/h during exponential phase. However, the rate of formate synthesis increased to 4.09 ± 0.32 mmol/g of protein/h in early stationary growth phase, resulting in a sharp increase in the formate to CO_2 ratio (Figure 3.10D). The rate of CO_2 synthesis then decreased to approximately, 0.70 ± 0.16 mmol/g of protein/h in early stationary phase, and finally increased to about 1.60 ± 0.31 mmol/g of protein/h in late stationary phase, resulting in a slow decline in the formate to CO_2 ratio (from 2.5 to about 2.0 in Figure 3.10D).

3.4 Discussion

3.4.1 Reliability and validation of real-time monitoring systems

Prior to performing the biological experiment, the chemical reaction was performed using $KHCO_3$ in a bioreactor where all other possible interferences from biological aspects were absent to assess reliability and validation of real-time off-gas monitoring system. This is a fast chemical reaction compared to biological reaction (i.e. the growth of *C. termitidis*) that produces CO_2 upon addition of hydrochloric acid. CO_2 was chosen because it is one of the gases generated by *C. termitidis*, and because it is in equilibrium with carbonate and bicarbonate dissolved in the liquid phase in a pH dependent manner. During titration of $KHCO_3$ solution with HCl, sharp chemical changes (due to carbonate species formation) in the aqueous phase left signatures in the headspace CO_2 gas (obtained from on-line continuous measurement), which was observed initially as bumps and later continuous rise (Figure 3.1A). At the very beginning of titration (basic pH region), OH^- ion helped to hold CO_2 by forming HCO_3^- into aqueous phase, and

therefore no chance of escaping CO_2 in the headspace. This is the reason why it did not show the presence of significant amount of CO_2 in that region. But, neutral to acidic pH release of CO_2 was noticed clearly in the headspace of the reactor. Although GC and TOGA data are highly co-related for CO_2 and other carbonate species (HCO_3^-, CO_3^{2-}) ($0.990 \leq R^2 \leq 1.000$ with 95% confidence intervals and standard error limits of slopes $0.068 \leq SE \leq 0.258$ in Table S3.1), these observations are not visible from the data obtained by discrete sampling by GC within the first twenty minutes of the fermentation reaction, with a critical pH range ($10 \leq pH \leq 6.0$). The discrete GC method sampled only one time point, whereas TOGA sampled twenty time points within twenty minutes (one per minute). Therefore, the observation of these chemical changes (HCO_3^-, CO_3^{2-}) in real-time was used to validate the use of the TOGA system. Based on the $KHCO_3$ test a narrow percentage of error (1.01 to 1.34 % in Table 3.1) between theoretical and experimental values of CO_2 indicate great reliability of the real-time on-line monitoring system for gaseous end-products. Consistency of real-time off-gas (here CO_2) measurement by acidification and titrimetric information provide confidence in performing biological experiments. Compared to present open pH controlled batch experiments of *C. termitidis* on 2 g/L cellobiose (and previous study by Ramachandran 2013), this study conducted five times higher carbon loading conditions (10 g/L) and employed on-line gas phase monitoring along with discrete measurements. Therefore, any noticeable changes could be detected in real-time throughout the growth phases in end-products synthesis pattern.

3.4.2 OD and growth phases measured by other means

By using OD as a conventional growth measurement tool, it was possible to identify biphasic growth of *C. termitidis* on 10 g/L cellobiose, where only three growth phases were observed. They were exponential phase, early stationary phase, and stationary phase.

Nevertheless, when it was looked into the real-time continuous gas phase data, five different growth phases (phase I to V in Figure 3.3) were noticed. Without measuring real-time on-line information, the transition point between phase II and phase III of *C. termitidis* would not have been noticed. This information helped analyzing the behavior of *C. termitidis* under various growth conditions. Furthermore, among the cumulative gas production (H_2 and CO_2 on 10 g/L cellobiose in a pH controlled bioreactor in Figure 3.4), which were obtained from real-time on-line continuous measurement, H_2 production was incomparable with the growth curves discretely obtained using conventional methods and shown in Figure 3.2 and Figure S3.1. Since production of H_2 obtained from processed (e.g. assumption, integration) information of real-time continuous data. The cumulative production curve of CO_2 does not signify or represent the growth curve, because it forms several interactive species in the broth including carbonate ones.

3.4.3 Discrete versus continuous information

C. termitidis produced two major types of metabolites – gaseous and water soluble upon consumption of cellobiose. Gaseous metabolites were monitored both by discrete and continuous methods using GC and MIMS, respectively. Whereas, water-soluble metabolites were monitored discretely using HPLC method. Therefore, it is essential to check reliability of the gaseous data obtained from both discretely and continuously.

Discrete gaseous (H_2 and CO_2) data points achieved using GC generally may not represent the continuity of fermentation reaction depending on the number of time points and the selection of times of sampling. On the other hand, gaseous (H_2 and CO_2) data points obtained from MIMS probe represent numerous data, which signify continuity of fermentation reaction. Hence, integration involves the area bounded by the curve of the function, the axis and upper and lower limits. This area can be given as the sum of much smaller areas included in the bounded

area. This is why little higher value is expected during integration of a continuous data set compared to summation of discrete points of a typical fermentation reaction. When GC data are plotted against corresponding MS data, the following Figures 3.11(A & B) were obtained for H_2 and CO_2, respectively. Ideally, each set of data should inclined to the diagonal line i.e $C_{MS} = C_{GC}$, where C_{MS} and C_{GC} represent concentration of gaseous metabolites using MS and GC, respectively. But in reality, the GC data set is slightly different (falls behind, shortened or low) compared to the MS data. Because, the discretely sampled data (GC) is likely to be prone to differences arising from the sample handling, depressurization and measurement techniques used.

To check statistical significance of the difference between the data obtained from MIMS probe and GC, a pairwise two-tailed t-test and Pearson correlation were performed for both H_2 and CO_2 gas (Table 3.5). For biological replicate (BR) 1 and 2, the two-tailed P values for CO_2 are 0.0094 and 0.0073, respectively, which are statistically significant. The two-tailed P values for H_2 are 0.0092 and 0.0005 for BR1 and BR2, respectively and they are statistically significant too. Therefore, gaseous data obtained from MIMS probe were strongly correlated with GC data with slight differences. We have used the MIMS data for most of the calculations in the studies presented in this chapter, unless otherwise mentioned.

A)

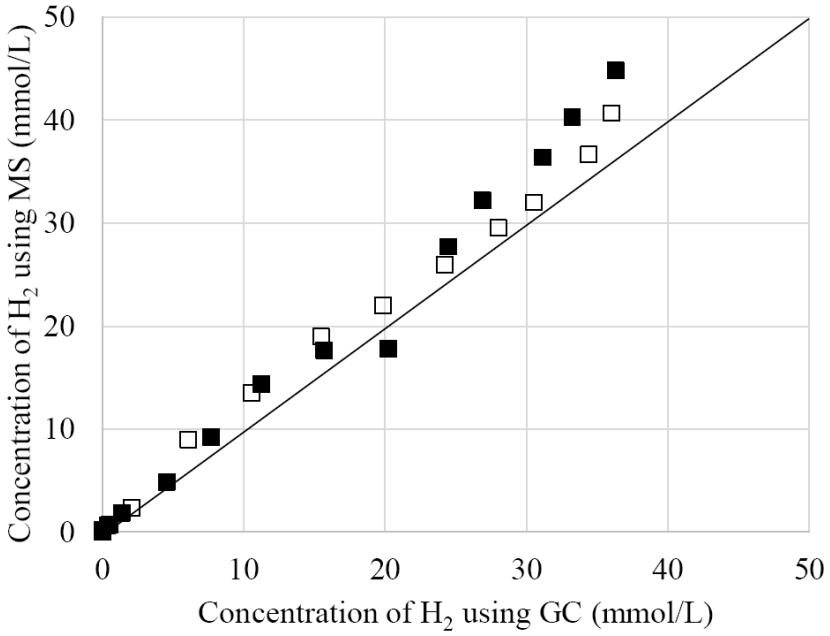

B)

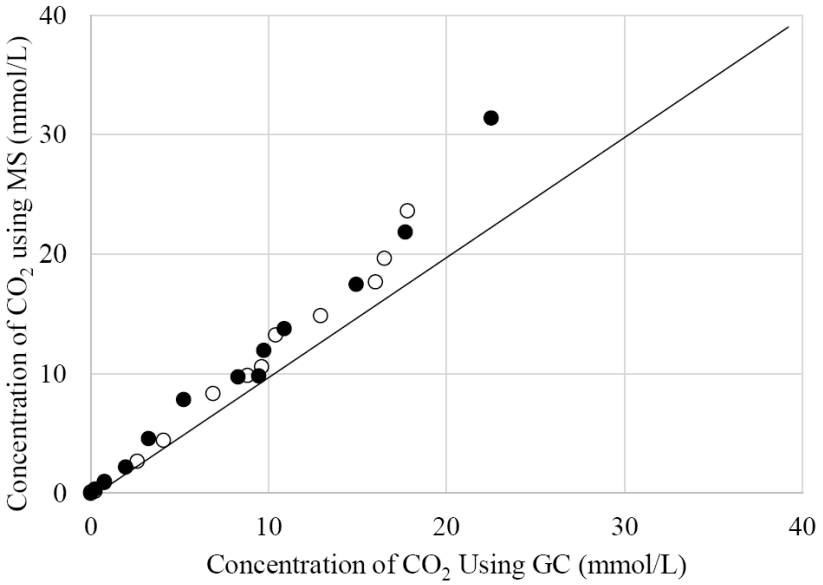

Figure 3.11 Comparison of discrete and continuous data obtained using GC and MIMS for A) H_2 and B) CO_2. Closed circle and square represent biological replicate 1 and open circle and square represent biological replicate 2. Pairwise two tailed t-test results are shown in Table 3.5.

3.4.4 Carbon flow distribution into metabolic end-products

Analysis of carbon flow distribution (growth phase-wise) provides in-depth information on metabolic switches. In this study, *C. termitidis* produced acetate, ethanol, formate, and CO_2 as the major fermentation end-products throughout fermentation regardless of initial cellobiose load, but their distribution varied along with growth. During exponential growth phase, only approximately 10 % of the cellobiose was consumed, with about 82 % of this carbon was converted to the major end-products (acetate, ethanol, CO_2, and formate). However, CO_2 was generally considered as off-gas in fermentation process. Synthesis of these products was observed from the beginning of fermentation and continued to rise as more biomass was produced (II: 16 – 24 h pi). Lactate production became significant near mid-exponential phase. This observation was in agreement with other studies (Ramachandran 2013; Munir 2015).

Table 3.5 Statistical comparison between discrete and continuous data for H_2 and CO_2 obtained using GC and MIMS (pairwise two tailed t-test and Pearson correlation coefficient).

Statistical Parameters	**CO_2**		**H_2**	
Biological replicate (ID)	BR1	BR2	BR1	BR2
Two-tailed P value	0.0094	0.0073	0.0092	0.0005
Mean difference	2.0846	1.4985	2.6862	1.9875
95% confidence intervals	0.6147 to 3.5545	0.4865 to 2.5104	0.7968 to 4.5755	1.0914 to 2.8836
t	3.0900	3.2262	3.0977	4.8816
Degree of freedom, df	12	11	12	11
Standard error of diff.	0.675	0.464	0.867	0.407
N	13	12	13	12
Pearson correlation coefficient, R	0.9917	0.9933	0.9924	0.9965
R^2	0.9835	0.9866	0.9849	0.9930
Inference/Comment	significant & strong positively correlated	significant & strong positively correlated	significant & strong positively correlated	significant & strong positively correlated

By the end of phase III (24 – 32 h pi), approximately 45 % of the cellobiose had been consumed and about 51 % of the substrate carbon consumed was converted to acetate, ethanol, and formate. The rest of the cellobiose (45 %) was consumed in the stationary phase (IV: 32 – 52 h pi) and about 55 % of the carbon substrate consumed was converted to acetate, ethanol, and formate (Figure 3.5). This analysis suggests that a considerable amount of cellobiose was going somewhere other than the main end-products. The contribution of substrate carbon to the formation of cell mass/protein decreased substantially during the stationary phase compared to exponential phase (6.49 % to 2.17 %). This is a 67% reduction, which implies that conversion of carbon to C2 products (acetate and ethanol) synthesis was favorable. It is clear that production rates of various end-products such as H_2, CO_2 and acetate were reduced substantially, whereas gradually increased for ethanol throughout fermentation (Figure 3.5, Figure 3.8).

3.4.5 Pyruvate catabolic reactions

In contrast to present open pH controlled batch experiments with *C. termitidis* cultured with 2 g/L cellobiose, this study grew *C. termitidis* with 10 g/L cellobiose in an open bioreactor, to assess the metabolic impact of higher carbon loading. The carbon flux distribution observed for *C. termitidis* grown on 10 g/L cellobiose relative 2 g/L in this work is further supported by the following observations.

There was a competition between CO_2 and formate synthesis during the growth of *C. termitidis* under pH controlled conditions (pH 7.2). During exponential phase, CO_2 synthesis was favoured (formate: CO_2 ratio near 1). At phase III, synthesis of formate was favoured (formate: $CO_2 > 1$). In the present study, this ratio was 0.54 and 0.76 on 2 g/L cellobiose and 1 g/L cellobiose, respectively. This ratio was, however, obtained 0.81 when *C. termitidis* was cultured on 2 g/L cellobiose in previous study (Ramachandran 2013).

The proportion of both C1 (formate and CO_2) and C2 (acetate and ethanol) fermentation end-products increased gradually during the growth of *C. termitidis*. This observation was also supported by concomitant decreased in H_2 and CO_2 synthesis. Here, most of the electron and reducing equivalent was consumed with the formation of ethanol. As the reaction proceeded towards late stationary phase, the formate: CO_2 ratio decreased, which suggest greater flux through the PFOR pathway and less flux through PFL pathway.

Acetyl Co-A to acetate or ethanol: Once acetyl Co-A is formed through either PFL or PFOR pathways then there is a competition between ethanol and acetate formation. Experimental data show a gradual increase of ethanol to acetate ratio, (Figure 3.10C) provides supporting evidence of competing nature of metabolic pathways present in *C. termitidis* at this node. Here, ethanol synthesis was highly favourable (a 4-fold increased rate) after early stationary growth phase-III and continued to form ethanol with constant rate (volumetric rate and cell specific rate) until full consumption of cellobiose was over. At this stage, molar yields of H_2 and acetate decreased compared to the molar yields during exponential phase (Table 3.4). When average values of product ratios were reported (Brener and Johnson 1984, Magnusson et al. 2009, Ramachandran 2013), it was difficult to assess metabolic shifts (if any at all) during the growth of organism.

Pyruvate to lactate: The volumetric and specific lactate production rate increased slightly in the early stationary phase compared to exponential phase, but did not vary significantly throughout the stationary growth phase. This indicates that *C. termitidis* does not direct carbon significantly towards lactate synthesis, even though this pathway is energetically favourable in *C. thermocellum* (Islam et al. 2006; Rydzak et al. 2009; Freier et al. 1988). Ramachandran (2013) reported 4.98 mmol/L of lactate when *C. termitidis* was cultured on 2 g/L cellobiose with

maximum volumetric rate 0.44 ± 0.02 mmol/L/h in a pH (7.2) controlled batch reaction. Allosteric regulations could be the cause of high lactate synthesis. Significantly, high lactate (5.75 mmol/L) was observed on cellobiose excess conditions when *C. thermocellum* cultured in batch experiment in tubes (Islam et al. 2006). Acidic growth environment might have played regulating lactate dehydrogenase activities (LDH), which ultimately lead to synthesis of high lactate yield. Very low lactate yield (< 2.00 mmol/L of culture) was reported when *C. thermocellum* cultured with 10 g/L either cellobiose or cellulose in pH controlled batch reactor (Ellis et al. 2012).

Carbon overflow at the pyruvate branch-point was also observed for the growth of *C. cellulolyticum* under carbon-excess condition (Guedon et al. 2000). In this study, the highest cellobiose consumption rate (0.95 mmol/L/h hexose equivalent) was observed under the set conditions of chemostat culture. Very low ethanol synthesis rate (0.57 mmol/L/h hexose equivalent) was reported. Most of the carbon flow was directed towards lactate and acetate synthesis at the rate of 0.83 mmol/L/h hexose equivalent and 1.08 mmol/L/h hexose equivalent, respectively.

3.4.6 Carbon recovery index and redox balance

Although there was good carbon recovery in biomass and the major products measured in the exponential phase, the mass balance was less during stationary phase. This implies that there was some unaccounted carbon still present in the broth. When *C. termitidis* was grown on 2 g/L cellobiose in a bioreactor, the carbon recovery was observed 97 ± 5.0 %. In compared to carbon recovery of *C. termitidis*, when *C. thermocellum* grew on high cellobiose and cellulose in defined media, carbon recovery was reported 63.7 ± 10.3 % Ellis et al. (2012). Here, only ethanol, acetate and lactate were accounted for, because other products, including amino acids

were building up in the medium. Indeed, more than 92.3 % carbon recovery was reported when they accounted C1-C3 along with cell mass and other dissolved species (> 10 %), such as pyruvate, malate, extra cellular proteins, and free amino acids. Guedon et al. (2000) also reported that when *C. cellulolyticum* grew on excess cellobiose, numerous soluble products, such as exopolysaccharides, cellotriose, extracellular proteins, and free amino acids, were formed and much improved carbon recovery (> 94 %) could be ascertained when they were accounted for in the carbon balance. Detailed investigations are required to further close the carbon balance, when *C. termitidis* is growing on high cellobiose and other substrates.

The overall reaction stoichiometry, such as C1/C2 ratio (1.01± 0.02) and O/R balance (1.08 ± 0.03), of the *C. termitidis* fermentation on 10 g/L cellobiose, was reasonable except the 4 h and 8 h time points at the beginning of the experiment. During those time points, very low concentrations were measured both discretely and continuously, and therefore, high variability in their measurements was observed. For that reason, these data points were excluded from the specific rate calculations (see Figure 3.7). Furthermore, consistent C1/C2 ratios close to 1 indicated that all products of pyruvate catabolism were mostly accounted. The C1/C2 and O/R ratios were used to develop a stoichiometric algorithm, which will be discussed in Chapter 6.

3.5 Conclusion

Although metabolic changes or shifts may not be accurately detected using discrete measurements, metabolic shifts can be effectively detected and analyzed using continuous measurements of bio-analytes, which is helpful in explaining metabolic changes along with other information from discrete measurement. Real-time, continuous H_2 production can be used as an analogue to a growth curve (in place of OD_{600} and/or protein assay) for this experiment. When insoluble substrates are used (Islam 2013; Munir 2015; Ramachandran 2013; Ellis et al. 2012;

Thompson and Trinh 2017) for fermentation, OD measurements or protein essay can be challenging. On-line gas measurement could be used as growth indicator instead.

Transition from hydrogen synthesis to ethanol synthesis occurred during phase III, which was difficult to observe from discrete measurements. This transition was not even observed/existed in either carbon-limited or carbon-sufficient growth conditions, because carbon was depleted. In *C. termitidis* cultured under carbon-excess conditions, carbon and electron flow in pyruvate catabolism was balanced chiefly by H_2 and acetate synthesis during exponential phase via PFOR, and then by synthesis of formate (via PFL) and ethanol in the early stationary phase of the growth. Low CO_2 and H_2 production in stationary phase was balanced by increasing formate synthesis.

Further research is required to close the carbon balance for *C. termitidis* growth under low to high substrate where extra cellular metabolites, such as pyruvate, amino acids can be accounted for. With the help of on-line monitoring tool, this study shows that it is possible to more precisely predict when and under which conditions metabolic switches occur. The on-line method using the TOGA system that were testing through the current chapter would be useful during industrial biofuel production, as they can direct strategies for substrate feeding and fermentation management.

Chapter 4

End-Product Induced Metabolic Shift Monitoring During Growth of *Clostridium termitidis* on Xylose Using Titrimetric and Off-Gas Analysis (TOGA)

Abstract

Conventional off-line analytical techniques have been used for understanding microbial physiology in many bioprocesses, such as the microbial synthesis of biofuels. Perturbation studies are useful in understanding changes in microbial metabolism and reaction mechanisms. It may be, however, challenging to monitor rapid changes in metabolic pathway utilization (metabolic shifts) using off-line analytical techniques. Using an on-line, titrimetric and off-gas analysis (TOGA) system to provide real-time information on changes to microbial metabolism and end-product synthesis during fermentation, metabolic shifts induced by end-product inhibition were evaluated in *Clostridium termitidis,* a mesophilic cellulose and xylan degrading bacterium capable of H_2 and ethanol synthesis. Cells were grown in 1191 medium containing 2 g/L xylose in a pH controlled 7 L bioreactor, with a 3 L working volume. The system was subjected to a perturbation by adding acetate (final concentration 100 mmol/L), one of the end-products of cellulose fermentation to the mid-exponential phase culture, at a concentration of 8-fold higher than observed from the fermentation of 2 g/L xylose. The TOGA system was used to monitor the effects of adding excess acetate on gas production from the fermentation reaction in real-time. While growth was only slightly affected, ethanol production increased by 13-18 % after the perturbation, in comparison with control studies in which no acetate was added. Acetate and H_2 production decreased 18-23 % and 16-19 % respectively, indicating that there was no net metabolism change after the addition of the acetate. Thus, the TOGA system may be used as a monitoring tool for real-time metabolic shifts associated with fermentation processes. This can

assist with optimization studies and reveal new strategies for maximizing biofuel yields from cellulosic biomass.

4.1 Introduction

C. termitidis produces significant amounts of acetate (ranges from 25-40 % mol/mol of substrate carbon equivalent) in addition to hydrogen, carbon dioxide, formate, ethanol, and lactate, while growing on variable substrate loads (carbon-limited to carbon-excess) (Ramachandran 2013; Munir 2015; Chapter 3 of present thesis). Considering inhibition or promotion, it is useful to study the effect of end-product concentrations on growth (if any) and end-product synthesis patterns compared to other organisms under similar conditions (Roe et al. 1998; Rydzak et al. 2011). Therefore, the question addressed in this chapter is how the sudden addition of a particular fermentation end-product, such as acetate, impacts metabolic pathway utilization and overall end-product synthesis patterns during the growth of *C. termitidis.*

Traditional off-line analytical techniques have been used for understanding microbial physiology in many bioprocesses, such as the microbial synthesis of biofuels (Herrero et al. 1985b; Freier et al. 1988; Zheng and Yu 2005; He et al. 2009; Rydzak et al. 2011). Studies of metabolic shifts are useful in understanding changes in microbial metabolism and reaction mechanisms. It is, however, challenging to monitor immediate perturbations in metabolic pathway using off-line analytical techniques. Rydzak et al. (2011) showed that end-product addition (acetate, lactate, hydrogen) re-directed carbon and electron flow in *C. thermocellum* to maintain oxidation/reduction balance (O/R index) and C1/C2 ratios. The reported observations were made based on final end-product concentrations and enzymes assays during stationary phase. Using these measurement parameters, it was difficult to observe the immediate effects of these end-product additions on *C. thermocellum*'s growth, unless there were significantly large perturbations in the metabolic pathways of interest.

Studies also showed that some end-products can have negative impacts on desired end-product synthesis patterns (Herreo et al. 1985a; Freier et al. 1988), while others may have a positive impact on ethanol, acetate, propionate, and valerate synthesis (Zheng and Yu 2005). Most of these studies used discrete spectrophotometric methods to monitor microbial growth, which may over-estimate actual growth due to inability of distinguishing between live and dead cells.

Careful choice of experimental design (Zanzotto et al. 2004; Baylor and O'Rourke 2005) and efficient monitoring tools may provide in-depth information on metabolic shift studies. Data presented in Chapter 3 suggested the use of H_2 off-gas as an alternative method for monitoring cell growth. We hypothesize that continuous off-gas analyses could be used to monitor microbial growth as an alternative to discrete optical density (OD) measurements. We also hypothesize that, together with measurement of changes in metabolic end-product concentrations, continuous off-gas monitoring may be used to analyze changes in microbial metabolism during cell growth.

The TOGA systems is a proven analytical technique for monitoring of wastewater treatment systems (Pratt et al. 2003) with mixed organisms. It also demonstrated competition of acetic acid uptake between polyphosphate accumulating organisms (PAOs) and glycogen accumulating organisms (GAOs) under anaerobic growth conditions and synthesis of poly-hydroxybutyrate. Furthermore, there was a close relation of GAOs with PAOs and well demonstrated with the measurement of HPR and CPR using stoichiometric model for both organism. Recently, it has been reported that the TOGA system can be used to monitor end-product synthesis patterns during cellulose fermentation reactions by *C. thermocellum* (Blunt et al. 2014). Previous studies with *C. thermocellum* also suggest that presence of high acetate (Herreo et al. 1985a; Freier et al. 1988; Rydzak et al. 2011) and high ethanol (Brown et al. 2011)

in the fermentation broth may divert carbon-flux towards higher ethanol production from the pool of acetyl–CoA and may leave a signature in off-gas synthesis. *C. phytofermentans* (adapted ethanol-tolerant strain) reduced ethanol yield due to abolishment of bifunctional acetaldehyde-CoA/alcohol dehydrogenase (Tolonen et al. 2015). Thus, these studies suggest that metabolic perturbations may be monitored using off-gas analysis with the TOGA system.

A simplified representation of pyruvate catabolic reactions in *C. termitidis* cultured with xylose is shown in Figure 4.1 (Hethener et al. 1992; Ramachandran 2013; Munir 2015). This is similar to that of *C. thermocellum*, which has been shown to produce hydrogen, carbon dioxide, formate, acetate and ethanol, and under certain conditions, lactate. The objective of the current study was to see how acetate induced metabolic shifts in *C. termitidis* can be ascertained using the TOGA systems as a perturbation monitoring tool, compared with conventional analytical tools (e.g. spectrophotometry, chromatography). In this study, the TOGA system was used as an on-line system to provide real time information on changes in microbial metabolism and end-product synthesis patterns during fermentation of *C. termitidis* on xylose.

4.2 Materials and Methods

C. termitidis was grown in 1191 medium containing 2 g/L xylose in a pH controlled 7 L bioreactor, with a 3 L working volume. The system was also subjected to a perturbation by adding exogenous acetate and monitored using both off-line and on-line methods. Three control and two perturbation experiments were performed. Detailed description of materials and methods are provided in section 2.2 of Chapter 2.

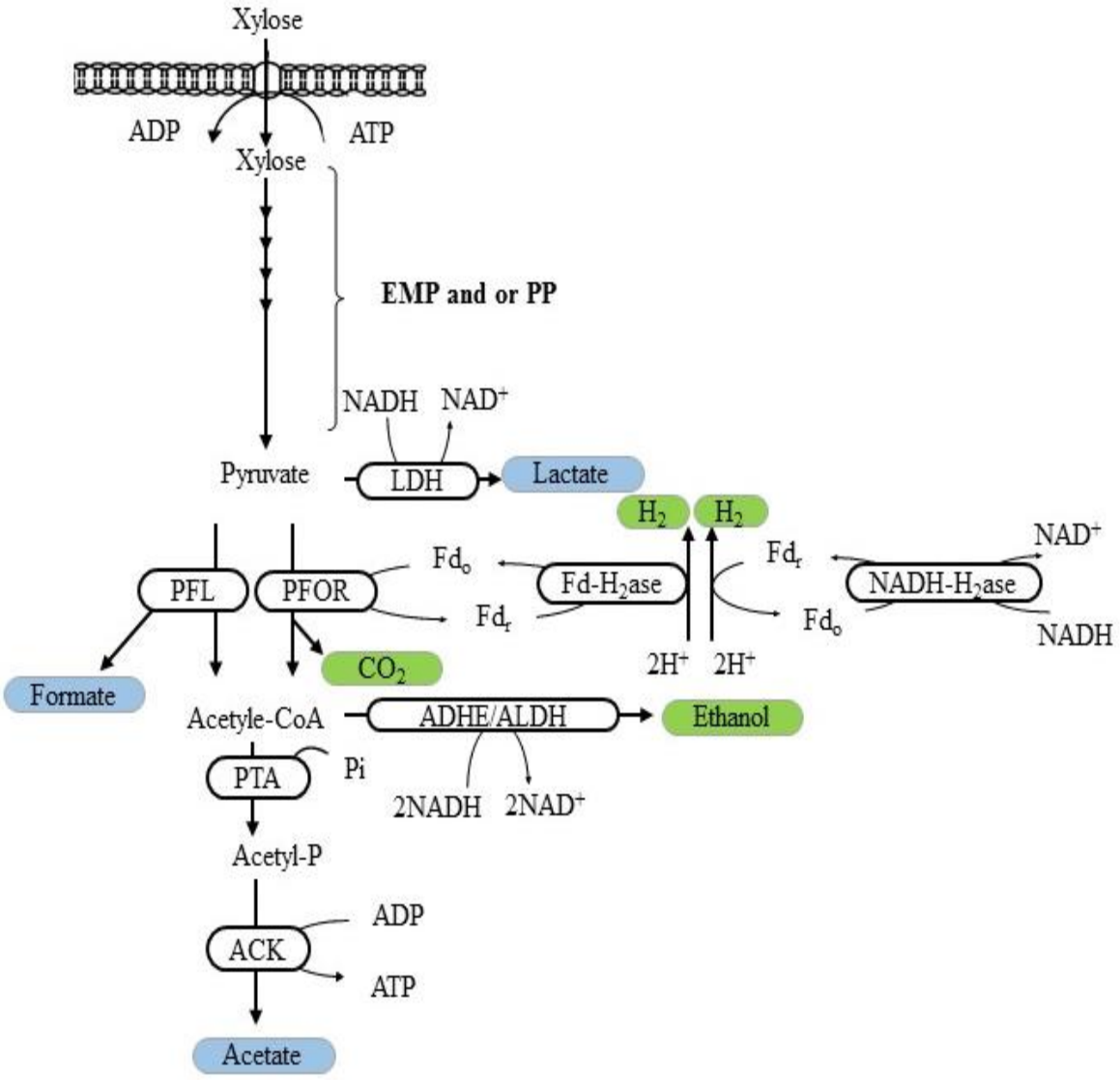

Figure 4.1 Simplified diagram of pyruvate catabolic reactions in *Clostridium termitidis*. Green boxes indicate end-products that can be monitored on-line using TOGA, while blue boxes are not at neutral pH. LDH, lactate dehydrogenase. PFL, pyruvate:formatelyase; PFOR, pyruvate:ferredoxin oxidoreductase; ADH-E, bifunctional acetaldehyde-alcohol dehydrogenase; PTA, phosphotransacetylase; ACK, acetate kinase; Fd-H_2ase, ferredoxin hydrogenase; NADH H_2ase, NADH hydrogenase (adapted from Munir et al. 2016a).

4.3 Results

4.3.1 Effect of acetate addition on growth and pH

Batch cultures of *C. termitidis* were conducted in bioreactors under anaerobic conditions. In a control set of experiments, *C. termitidis* was cultured in 1191 medium containing 2 g/L xylose, without the addition of acetate. In the "perturbed" set of experiments, *C. termitidis* was cultured in 1191 medium containing 2 g/L xylose, in the presence of elevated concentrations of sodium acetate (100 mmol/L) (Figure 4.2). Both sets of experiments were performed under controlled pH at 7.20 ± 0.02 and atmospheric pressure. No lag was observed in either the control or perturbed experiment.

After addition of acetate, no significant changes in growth were observed in either the control or perturbed experiment. The final OD of the control experiment (0.83 ± 0.09) was slightly higher than the final OD of the perturbed experiment (0.71 ± 0.05). In addition to OD measurement, cell protein contents were also measured (Figure 4.2B). The protein contents extracted from the control versus the perturbed experiment were 0.78 ± 0.01 mmol/L and 0.81 ± 0.04 mmol/L (20 -24 h pi), respectively. The major difference between the control and perturbed fermentation reactions was a sudden fast pumping of acid (to adjust pH) just after addition of sodium acetate into the fermentation broth (Figure S4.1).

A)

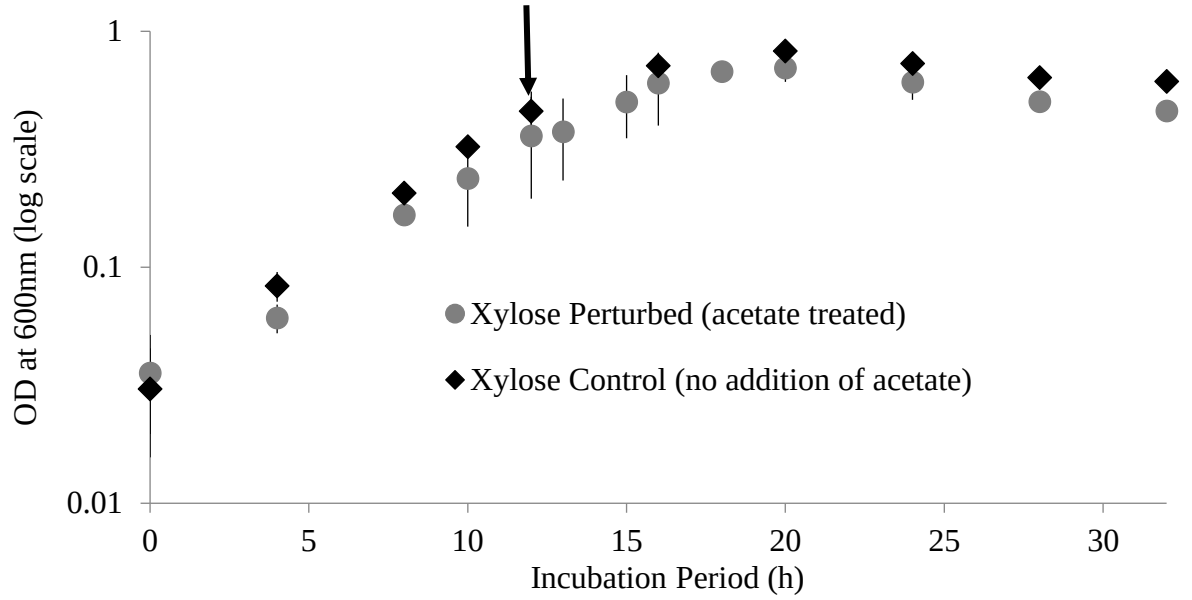
1
0.1
0.01
OD at 600nm (log scale)
0
5
10
15
20
25
30
Incubation Period (h)
Xylose Perturbed (acetate treated)
Xylose Control (no addition of acetate)

B)

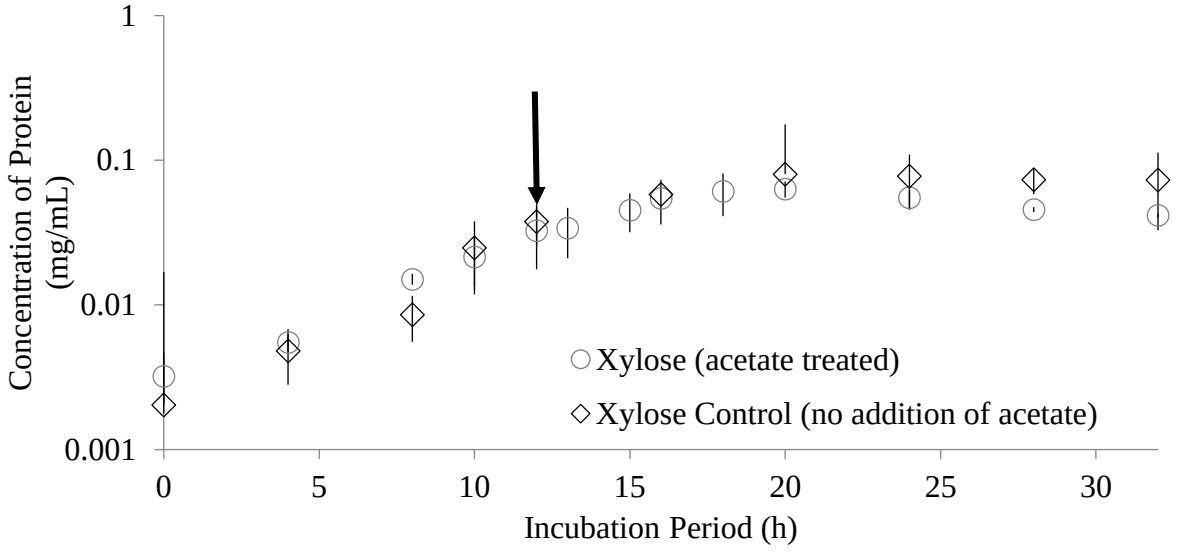
1
0.1
0.01
0.001
Concentration of Protein (mg/mL)
0
5
10
15
20
25
30
Incubation Period (h)
Xylose (acetate treated)
Xylose Control (no addition of acetate)

Figure 4.2 Growth of *C. termitidis* on 2 g/L xylose without the addition of acetate (unperturbed control: black diamonds) compared to growth of *C. termitidis* on 2 g/L xylose after the addition of acetate (perturbed experiment: grey circles). A) OD at 600 nm and B) protein assay. The black arrow indicates the addition of acetate to the culture (perturbed experiment) at mid-log phase (12 h).

4.3.2 Effect of acetate addition on gas production

C. termitidis produces H_2 and CO_2 when cultured on xylose, and concentrations of these gases were monitored over the entire growth period (Figure 4.3). After addition of sodium acetate, H_2 production dropped compared to control experiment (Figure 4.3A), but then gradually increased and reached to its maximum value (5.49 ± 0.44 mol %). At early to mid-exponential phase (8 -12 h pi), production of H_2 and CO_2 between control and perturbed experiment were not significantly different (region C of supplementary Figure S4.2 and Figure S4.3). However, mid-exponential to early stationary phase (12 – 18 h pi) considerable variations were noticed (region P of supplementary Figure S4.2 and Figure S4.3), and the rate of H_2 production in the perturbed fermentation was slower (0.97 ± 0.04 mmol/L/h) than the rate of H_2 production in the control fermentation (1.10 ± 0.06 mmol/L/h) (Table 4.1). Overall H_2 production decreased 16-19 % compared to control experiment (Table 4.2).

Production of CO_2 gas for both control (dark line) and acetate induced (grey line) experiments may be seen in Figure 4.3B. CO_2 was produced at a constant rate (0.56 ± 0.16 mmol/L/h) throughout entire exponential growth phase in control experiment, whereas CO_2 was produced at a slower rate (0.42 ± 0.01 mmol/L/h) after addition of sodium acetate at mid-exponential phase (Table 4.1). At or near stationary phase, a slight increase in CO_2 production was noticed in the perturbed experiment. Overall, CO_2 production decreased by 10-15 % in the perturbed fermentation reaction (Table 4.2).

4.3.3 Effect of sodium acetate addition on end-product distribution

Growth of *C. termitidis* was sustained, despite the addition of sodium acetate at a concentration of 8-fold greater (100 mmol/L) than achieved during a normal fermentation on 2 g/L xylose. The immediate effect of the perturbation was a change in the rates of H_2 and CO_2

A)

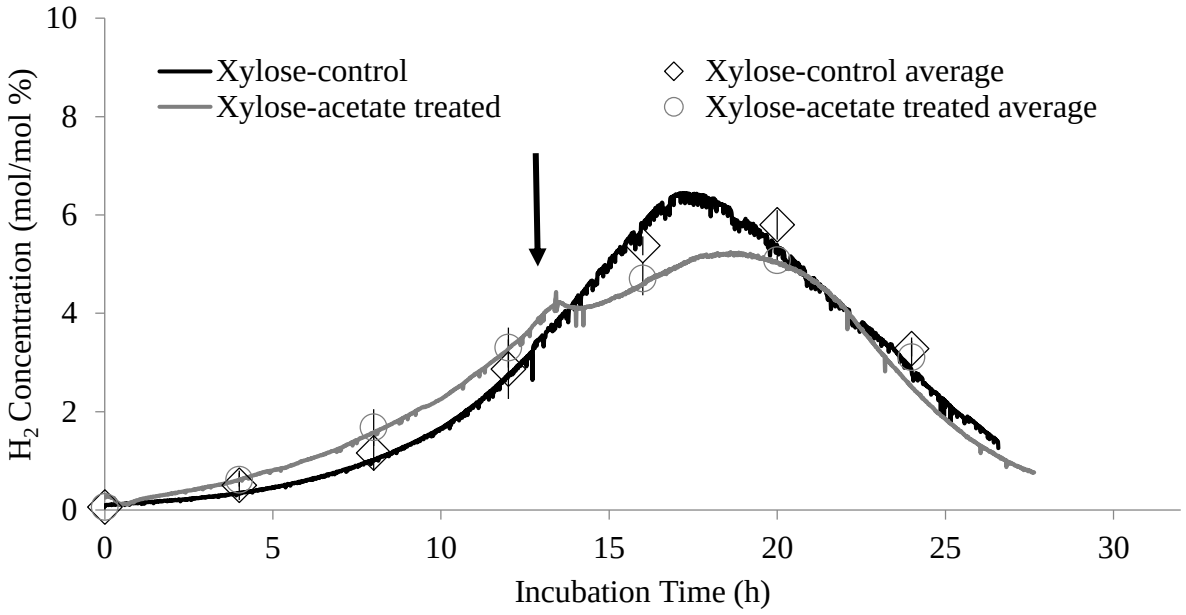
Xylose-control
Xylose-acetate treated
Xylose-control average
Xylose-acetate treated average
H_2 Concentration (mol/mol %)
Incubation Time (h)
0
2
4
6
8
10
0
5
10
15
20
25
30

B)

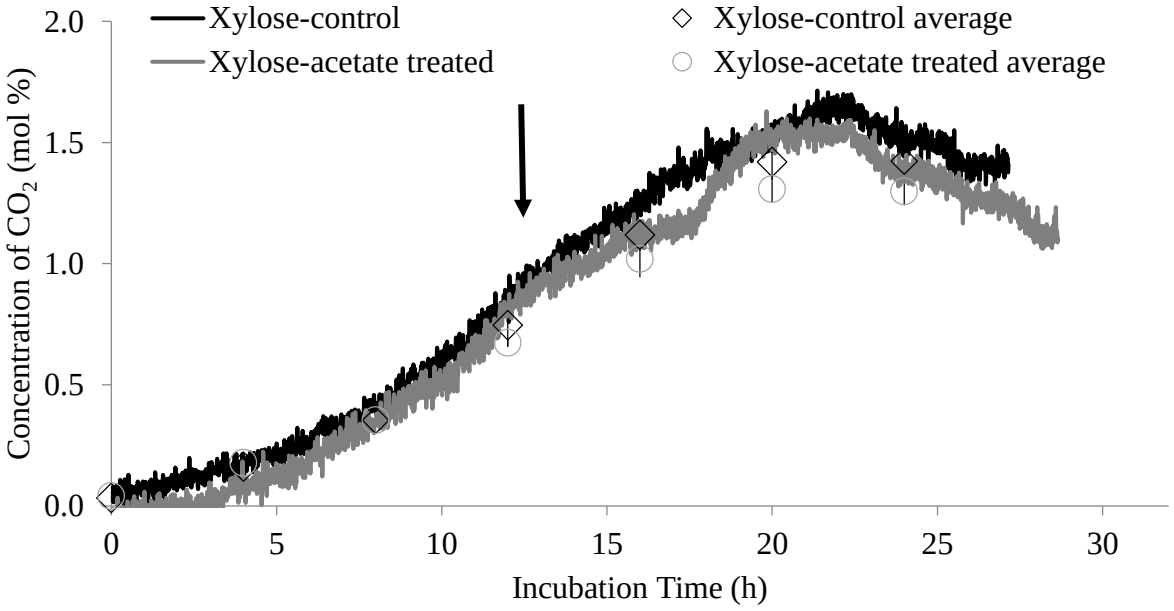
Xylose-control
Xylose-acetate treated
Xylose-control average
Xylose-acetate treated average
Concentration of CO_2 (mol %)
Incubation Time (h)
0.0
0.5
1.0
1.5
2.0
0
5
10
15
20
25
30

Figure 4.3 Production of A) H_2 and B) CO_2 during the growth of *C. termitidis* on 2 g/L xylose under control (black line) and perturbed-acetate treated (grey line) experiment. Open diamonds and open circles represent average discrete points, obtained from continuous measurements, of cultures without the addition of acetate (control, unperturbed experiment) and cultures to which acetate was added (perturbed experiments), respectively, with error bars. The black arrow indicates the addition of acetate to the culture (perturbed experiment) at mid-log phase (12 h).

Table 4.1 Variation of gas production rates between control and perturbed experiments.

Experiment	N	Production Rate (µmol/mL/h) @ 12-18h pi					
		H_2			CO_2		
		Rate	Average	SD	Rate	Average	SD
Control	1	1.15	1.10	0.06	0.56	0.56	0.16
	2	1.12			0.72		
	3	1.03			0.40		
Perturbed	1	0.94	0.97	0.04	0.43	0.42	0.01
	2	0.99			0.41		
Statistical Analysis/ Comment		$t = 2.69$, $p = 0.074$, significant at $p < 0.10$			$t = 2.73$, $p = 0.112$, insignificant at $p < 0.10$		

N= Biological replicates; SD= Standard deviation; t = Two tailed t-test was performed with two independent means; @ = Starting immediately after the time of perturbation

Table 4.2 Final end-product concentrations from *C. termitidis* grown on 2 g/L xylose using the addition of 100 mmol/L Na-acetate at exponential phase (12 h). All results are compared at stationary phase (20 -24 h pi).

Events	N	pH	Lactate	Formate	Acetate	EtOH	H_2	CO_2	Cell Protein	Carbon Recovery	C1/C2	O/R
			mmol/L	mmol/L	mmol/L	mmol/L	mmol/L	mmol/L	mmol/L			
Xylose Control 2 g/L (no acetate)	1	7.19	1.33	12.33	13.82	5.12	10.77	5.75	0.77	0.90	0.95	0.88
	2	7.20	0.99	11.67	14.95	5.49	10.33	6.31	0.78	0.93	0.88	0.88
	3	7.21	1.59	10.44	12.97	5.10	11.82	5.36	0.79	0.85	0.87	1.04
	Avg	7.20	1.30	11.48	13.91	5.24	10.97	5.81	0.78	0.89	0.90	0.93
	SD	0.01	0.30	0.96	0.99	0.22	0.77	0.48	0.01	0.04	0.04	0.09
Xylose Perturbed 2 g/L (acetate treated)	1	7.20	0.61	10.03	11.41	5.91	8.90	4.94	0.83	0.77	0.86	1.04
	2	7.20	0.69	9.95	10.67	6.14	9.21	5.21	0.78	0.76	0.90	1.05
Production flux $^{\Psi}$ shift %			(-) 47-53	(-)13	(-)18-23	(+)13-18	(-)16-19	(-)10-15	(+) 6			
Statistical Analysis/ Comment			t = 2.89, p = 0.063, significant @ p<0.05	t = 2.08, p = 0.128, insignificant @ p<0.10	t = 3.64, p = 0.035, significant @ p<0.05	t = -4.27, p = 0.024, significant @ p<0.05	t = 3.30, p = 0.046, significant @ p<0.05	t = 1.98, p = 0.142, insignificant @ p<0.10	t = -1.25, p = 0.301, insignificant @ p<0.10	t = 4.23, p = 0.024, significant @ p<0.05		

Ψ : Negative sign (-) means decrease and positive sign (+) means increase; N = Biological replicates; t = Two tailed t-test was performed with two independent means between control and perturbed experiments. 1 mg of protein/mL of culture = 9.90 mmol/L

synthesis (Figure 4.3 and Table 4.1). Ethanol production increased by 13-18 % after perturbation compared with the control. In contrast, on the basis of off-line discrete sample measurements, the final acetate concentrations in the perturbed fermentation were 18-23 % lower than the final acetate concentrations in the control reactions. Formate production marginally increased, about 8 %, in the stationary phase of the perturbed experiment compared to control. Lactate production did not increase as an immediate effect of perturbation, rather 50 % less lactate was obtained in perturbed experiment compared to control experiment at stationary phase (Table 4.2; see also Supplementary Figure S4.4 for all products).

4.4 Discussion

4.4.1 Growth and pH

Generally, acetate is excreted as acetic acid by the cell during fermentation to minimize proton balance into the cytoplasm, and is neutralised externally by base in a pH control (pH near 7) environment. Therefore, constant build up of acetate ion into the broth sometimes carries positive impact on cells growth (PAOs, GAOs Pratt et al. 2003) by consuming it as a substrate, while in other organism which may create acidic environment in the cytoplasm under acidic growth environment (*E. coli* Roe et al. 1998; *C. thermocellum* Herrero et al. 1985a; Herrero et al. 1985b). Cell growth of *C. termitidis* was not significantly affected (insignificant at $p < 0.10$ in Table 4.2) by the additional amount of external acetate ion that was very unlikely to permeate through the cell membrane by forming acetic acid upon accepting a H^+ ion. Even the amount of acetate that entered by passive diffusion process may not sufficient enough to decrease cytoplasmic pH, which can negatively effect biosynthesis if the acid concentration is high (Herrero et al. 1985b; Roe et al. 1998). Herrero et al. (1985b) reported growth inhibition when *C. thermocellum* was exposed to elevated concentration (200 mmol/L) of acetate. Both cytoplasmic

pH and the acetate concentration were monitored using discrete measurements in their study. Just after addition of acetate, increased amount of cytoplasmic acetate was noticed, which was responsible for sudden drop of pH. Internal pH gradually increased from 7.0 to 7.4 as the cells were adapted to the growth condition during fermentation. In the present study, fast consumption of acid by fermentation broth was observed in the perturbed compared to control experiment, due to the basic nature of Na-acetate solution (pH = 8.84), which again might show slightly lower value due to the presence of CO_2 in the broth as dissolved form even with N_2 sparging (Schmitz 2002). The basic nature of fermentation broth was, however, reduced/diminished by the addition of HCl solution using the automatic titrator (Figure S4.1).

Presence of elevated concentrations of organic acids affect the growth of many organisms including *Clostridia* species and have been reported by other authors (Roe et al. 1998; Ramachandran et al. 2008; Islam et al. 2006) in batch experiments. When organisms grow on pH uncontrolled buffered systems, the organic acids produced (such as acetic acid, formic acid, lactic acid, butyric acid) can reach its maximum concentration beyond the buffering zone and hence arrest the growth by reducing the capacity of cell building blocks (Herrero et al. 1985a). In our experiments (control and perturbed), pH was maintained 7.20 ± 0.02 throughout entire growth phase. Therefore, neither the produced organic acids nor added acetate salt have an impact on the culture pH.

As the pH remained constant (7.20 ± 0.02) in both control and acetate induced experiments, therefore, it did not have any impact either on growth of *C. termitidis*. Rydzak et al. (2011) also did not notice any significant change in pH when *C. thermocellum* was cultured in both control and acetate induced experiments using 1.1 g/L cellobiose in batch. On average, pH dropped from 7.2 to 6.65 and 6.63 respectively at stationary phase. These changes may have

been occurred due to the buffering capacity of 1191 media, and this there was no impact on the end-products produced under both conditions of the experiments. No significant changes were noticed in optical densities and cell proteins in the experiments performed under both conditions. Furthermore, the selected acetate concentration (100 mmol/L or about 8-times greater than acetate produced in control experiment using 2 g/L xylose) did not arrest the growth of *C. termitidis* in this experiment, while other studies showed that excessive use of acetate (200 mmol/L) in the perturbed experiment arrested the growth of *C. thermocellum* (Freier et al., 1988). In fact, our objective was to see the effect of acetate-induced metabolic changes, not arresting the growth. What we have noticed from this experiment is that no differences observed in growth curve using conventional analytical technique (spectrophotometry), while the system was perturbed (Figure 4.2). This observation was consistent with other reports in the literature (Rydzak et al. 2011; Roe et al. 1998).

4.4.2 Gas synthesis

4.4.2.1 H_2 synthesis

In *C. termitidis* growth, significantly reduced H_2 production (16 – 19 % with $p < 0.05$) was observed as a consequence of exogenous acetate addition compared to control experiment. The observed reduction of H_2 production (cumulative) was calculated based on TOGA measurements. Reduction of H_2 synthesis is not uncommon during the growth of mesophilic or thermophilic *Clostridia* species (Guedon et al. 1999; Rydzak et al. 2011; Zheng et al. 2014). *C. cellulolyticum* showed steady decrease in H_2/CO_2 ratio, when organism was cultured in synthetic medium, gradually from low to elevated concentration of cellobiose. Elevated substrate feeding increased acetate concentration. During acetate induced *C. thermocellum* culture, Rydzak et al. (2011) suggested that exogenous acetate did not affect carbon and electron flux at the

pyruvate/lactate/acetyo-CoA branch point, rather it redirected acetyl-CoA towards ethanol, during which NADH was reoxidized and left less reducing equivalent for H_2 synthesis. *C. termitidis* possess several hydrogenases including energy conserving membrane bound Fe-Ni hydrogenase (Ramachandran 2013; Munir et al. 2016; Lal and Levin 2016), which is highly expressed in xylose fermentation (Munir et al. 2016).

4.4.2.2 CO_2 synthesis

CO_2 was synthesized when pyruvate is degraded via PFOR pathway and produced acetyl-CoA. Slow synthesis rate of CO_2 (although insignificant at $p < 0.10$, Table 4.1) indicated that this PFOR pathway may have slightly affected due to the added acetate. Unlike H_2, widely interactive CO_2 forms several species (bicarbonate, carbonate) in fermentation broth, which are dependent on pH. Liberation of CO_2 from aqueous surface (or dehydration process) is a slow process and can easily be affected by internal reactor environment, which generally appears as a noisy signal compared to H_2 gas. In the previous Chapters 3, we have observed that to minimize the effect of CO_2 synthesis reduction, *C. termitidis* has an alternative option to follow PFL pathway, which produce less reducing equivalents. Again, acetate modulated growth of *C. thermcellum* showed no significant change in PFOR activities at late exponential phase (Rydzak et al. 2011) suggesting that organism may have capable of using alternative thermodynamically efficient pathways to minimize such effect.

4.4.3 Acetate modulated/induced end-product distribution

At slightly acidic or near neutral pH growth environment, acetate ion can be incorporated into the cell by partition of undissociated form of the acid in the membrane bilayer and passive diffusion into the cytoplasm (Herrero et al. 1985b; Pratt et al. 2003; Li 2013). The acid form of acetate can slowly permeate the cell membrane, resulting in a build-up of acetyl-CoA, which

accumulates temporarily as the cell adapts to the immediate impact of acetate addition (Roe et al. 1998). Consequently, the organism may have used alternative thermodynamically favourable pathways by slow process of H_2 synthesis. This phenomenon may be observed in Figure 4.3, which is supported by significant reduction of H_2 and acetate synthesis. To minimize this effect, cells may have redirected acetyl-CoA, which would normally converted to acetate by acetate kinase (ACK), towards ethanol by Adh-E, a bifunctional acetaldehyde-alcohol dehydrogenase. Le Chatelier's principle states that when a system experiences a disturbance, such as a change in end-product concentration, or a change in temperature, or pressure, it will respond to restore a new equilibrium state. Other studies, have also shown that elevated concentrations of acetate enhance the growth of organism by utilizing it as a substrate and re-directing carbon flux through other metabolic pathways (Chung 1976; Pratt et al. 2003) but not necessarily changes in enzyme activities (Rydzak et al. 2011). However, exogenous acetate addition did not show any sign of enhancing growth in the present study.

4.4.4 Carbon recovery index and redox balance

Carbon recovery index and redox balance provide the opportunity to evaluate experimental errors (if any) along with shortcoming of experimental design. When closely looked into the Table 4.2 for carbon recovery and C1/C2 ratio in perturbed experiments, it showed comparatively poor carbon recovery (0.77 ± 0.01) than the control experiments (0.89 ± 0.04). Statistically, these variations are significant at $p < 0.05$. This implied that either some carbon was missing due to experimental shortcomings in soluble product quantification or some unaccounted carbon was still present into the fermentation broth due to exogenous acetate addition. When compared the volumetric yields of H_2 and CO_2 produced from xylose fermentation with the gases obtained from cellobiose fermentation, significant amount of H_2 and

CO_2 were missing or under estimated in both control and perturbed experiments, probably due to supersaturation of gases into the fermentation broth under the applied bioreactor conditions, especially sparging technique (L-shape steel tubing with few holes at the end) with mild agitation (100 rpm). This tube allowed generating few large bubbles that went straight upwards with very short residence time into the broth. Underestimation of these gases, certainly affect both carbon recovery, C1/C2 ratio and redox balance, that were observed in the present study.

4.4.5 Salting effect

In the perturbed experiment, there might have extra sodium ion present due to addition of sodium acetate into the 1191 growth media. The excess concentration of sodium salt would not be more than 100 mmol/L. Because during titration potassium hydroxide was used and its additional concentration would be around 40 mmol/L. These concentrations (sodium and potassium ions) do not exit the limit of growth inhibition studied for other organisms (Zhao et al. 2016; Rydzak et al. 2011). Rydzak et al. (2011) showed that there was no significant impact of 80 mmol/L NaCl addition on growth and end-product distribution for *C. thermocellum*. Likewise, *C. acetobutylicum* showed insignificant growth inhibition when the culture was treated with an additional 5 g/L (85 mmol/L) NaCl compared to control experiment where no salt was added (Zhao et al. 2016). However, when the organism was treated with 10 g/L NaCl, growth inhibition was not only observed (15.05 ± 1.94 % less biomass yield), but also decreased yields of other metabolites, such as acetone, butanol, and ethanol were recorded. Therefore, we assume that there might have been negligible to no impact of Na^+ ion on the growth of *C. termitidis* (as also revealed by end-products distribution patterns, see Figure S4.4) under the conditions applied in this study.

4.4.6 Comparative analysis of the HP between control and perturbed experiments

Table 4.3 provides a comparative analysis of the HP between control and perturbed experiments. On an average 101.0 ± 6.4 % of the H^+ ion recovered by the titration system and the difference between HP from end-products synthesis and net OH^- (base) consumption was insignificant. When net base consumption of perturbed experiments was compared with control experiments, a significantly low amount of base ($t = 5.79$, $p = 0.010$) was consumed during perturbed experiments. This indicates that significantly low acidic end-products were synthesized during perturbed experiments. In fact, low production of acetate and lactate were observed in perturbed experiments compared to control experiments, which were corroborated with significantly low xylose specific yields, respectively (supplementary Table S4.1). Furthermore, when H^+ ion produced from end-products synthesis of perturbed experiments (2 biological replicates) and compared with net OH^- (base) consumption (within biological replicates), significant difference was noticed (88.1 ± 0.9 % recovery; $t = 15.15$ and significant at $p < 0.01$). This means some amount of acidic end-products were unaccounted or missing, either due to masking of lactate and formate peaks during HPLC analysis or some amount of unaccounted CO_2 was still saturated into the broth under applied growth conditions.

Table 4.3 Comparative analysis of hydrogen ion production (from end-products profile) between control and perturbed experiments using on-line titration system. T-tests were performed with two independent means.

Events	N	Working volume	Net OH- added	Lactate	Formate	Acetate	CO_2	H+ ion eqv. produced	Proton recovery	Statistical analysis/ Comment
		L	mmol	mmol	mmol	mmol	mmol	mmol	%	
Xylose Control 2 g/L (no acetate)	1	3	97.8	4.0	37.0	41.5	17.3	99.7	101.9	t = - 0.28, p = 0.397, insignificant @ p < 0.05
	2	3	95.3	3.0	35.0	44.9	18.9	101.8	106.8	
	3	3	96.7	4.8	31.3	38.9	16.1	91.1	94.2	
	Average	3	96.6	3.9	34.4	41.7	17.4	97.5	101.0	
	SD		1.3	0.9	2.9	3.0	1.4	5.7	6.4	
Xylose Perturbed 2 g/L (acetate treated)	1	3	91.3	1.8	30.1	34.2	14.8	81.0	88.7	t = 15.16, p = 0.002, significant @ p < 0.01
	2	3	91.0	2.1	29.9	32.0	15.6	79.6	87.4	
	Average	3	91.2	2.0	30.0	33.1	15.2	80.3	88.1	
	SD		0.2	0.2	0.2	1.6	0.6	1.0	0.9	
Statistical Analysis/ Comment			t = 5.79, p = 0.010, significant @ p < 0.05					t = 3.48, p = 0.040, significant @ p < 0.05		

N = Biological replicates, SD = Standard deviation, t = Two tailed t-test was performed with two independent means

4.5 Conclusion

Here, we demonstrated that the effect of the addition of exogenous acetate can be monitored with the help of the TOGA system on real-time metabolic shifts associated with fermentation processes. The presence of elevated concentrations of acetate during fermentation of *C. termitidis* increased ethanol yields and decreased H_2 yields significantly. To maintain a stoichiometric balance, such as C1/C2 ratio and O/R ratio due to the presence of excess acetate, the end-product distribution changed. In a pH controlled fermenting environment, the presence of a high concentration of added acetate during *C. termitidis* culture is beneficial to ethanol synthesis. This TOGA technique, along with end-product addition, can assist with optimization studies under various physico-chemical conditions and can potentially reveal new strategies for maximizing biofuel yields from cellulosic biomass.

Chapter 5

Effects of Dissolved Gas Concentrations on *Clostridium termitidis* Fermentation End-product Synthesis Patterns

Abstract

Clostridium termitidis synthesizes ethanol and organic acids (formate, acetate, lactate), as well as hydrogen (H_2) and carbon dioxide (CO_2) when cultured with soluble substrates such as simple sugars, or insoluble substrates such as cellulose. While H_2 and CO_2 are synthesized as a consequence of microbial metabolism, it is unclear whether the concentrations of H_2 and CO_2 in the culture medium and/or headspace influence overall ethanol production. To address this question, *C. termitidis* was grown on 2 g/L cellobiose in 1191 media in a bioreactor with pH control, at 37 ^{o}C. To evaluate the effect of dissolved gasses on microbial metabolism and fermentation end-product synthesis patterns, cultures were sparged with nitrogen (N_2) gas at a high rate (400 mL/min), with moderate stirring (200 rpm), to rapidly remove dissolved gases. Control cultures were sparged with N_2 at a lower rate (20 mL/min) and low stirring speed (100 rpm). Concentrations of H_2, CO_2, and EtOH fermentation end-products were monitored in both the headspace and aqueous phase in-real time by membrane inlet mass spectrometry (MIMS). Discrete samples were also analyzed off-line to determine concentrations of all fermentation products (formate, acetate, lactate, ethanol) in the aqueous phase by HPLC. The volumetric yields of H_2 and CO_2 increased significantly, in cultures with high sparging (Re 17,500) compared to the cultures with low sparging (Re 8,700). It also appeared that formate synthesis was favourable rather than H_2 and CO_2 at low sparging, with much less impact on ethanol vs acetate synthesis. Ethanol production significantly decreased (12 % to16 %) in cultures with high sparging. Supersaturation of H_2 and high concentrations of CO_2 were observed in the aqueous

phase under both experimental conditions. It was revealed that carbon and reducing equivalents were directed towards the pyruvate ferredoxin oxidoreductase (PFOR) pathway as opposed to the pyruvate formate lyase (PFL) pathway as a result of rapid mass transfer. Low turbulent growth environment favours higher ethanol yield via PFL pathway, whereas high turbulent growth environment disfavours ethanol yield due to re-direction of carbon and reducing equivalent flux towards PFOR pathway.

5.1 Introduction

Bacterial fermentation reactions are dynamic biological processes. Both gaseous (hydrogen, carbon dioxide, methane) and aqueous (alcohols, organic acids) fermentation end-products may be synthesized and accumulate to different concentrations depending on growth environment. The presence of these fermentation gases can have a direct or indirect impact on synthesis of soluble products (Lamed et al. 1988; Thauer 1998; Bothun et al. 2004; Zhang et al. 2012; Carere et al. 2014; Thompson and Trinh 2017). Direct measurement of dissolved gas species is usually conducted with discrete samples that are analyzed by gas chromatography (Heinzle et al. 1990; Carere et al. 2014; Blunt et al. 2014; Islam et al. 2015). However, concentrations of dissolved gases, especially those with low solubility like hydrogen (H_2) and methane (CH_4), are routinely estimated using Henry's Law, which assumes dissolved species are at equilibrium with the bioreactor headspace.

Estimation of dissolved gases using Henry's Law from off-gas measurements is often inaccurate (Pauss et al. 1990), due to mass transfer limitations. The mass transfer properties for common gases including H_2, nitrogen (N_2), oxygen (O_2), and CH_4 show extremely low solubility in water (Table 5.1) due to poor dipole moment and week van-der Waal's forces. In contrast, carbon dioxide (CO_2), hydrogen sulphide (H_2S), ammonia (NH_3), and ethanol (EtOH) show comparatively high solubility due to strong dipole moment and H-bonding (Table 5.1). Ethanol has strong physico-chemical interactions with water and has a very high Henry's Law constant ($2.3x10^2$ M/atm) (Sander 2015) and is impossible to remove from aqueous phase via sparging/stripping process. Liquid to gas phase and gas to liquid phase mass transfer limitations may occur for many reasons, such as viscosity, hydrostatic pressure, agitation, bubble size,

Table 5.1 Mass transfer properties of various gases produced in biological process.

Gases	Intrinsic properties	$K^{\theta}{}_{H}$ M/atm	Pure gases solubility ¥ g/Kg of water at 40 °C, 1 atm	Removal from aqueous phase
H_2	Low physico-chemical interactions	$7.8x10^{-4}$	0.00138	Easy AG/HSR
N_2	Low physico-chemical interactions	$6.5x10^{-4}$	0.0014	Easy AG/HSR
O_2	Moderate physico-chemical interactions	$1.2x10^{-3}$	0.031	Moderate AG/HSR, MB
CH_4	Low physic-chemical interactions	$1.4x10^{-3}$	0.016	Moderate AG/HSR, MB
CO_2	Highly associated with physico-chemical interactions	$3.4x10^{-2}$	1.00	Moderate AG, MB, IBRT
H_2S	Highly associated with physico-chemical interactions	$1.0x10^{-1}$	2.4	Difficult AG, MB, IBRT
NH_3	Highly associated with physico-chemical interactions	$5.8x10^{1}$	320	Difficult AG, MB, IBRT
EtOH	Strong physico-chemical interactions	$2.3x10^{2}$	Infinite	Impossible to remove under the conditions mentioned above

$K^{\theta}{}_{H}$ =Henry's law constant at standard temperature and pressure (Sander 2015); ¥ Source: https://www.engineeringtoolbox.com/gases-solubility-water-d_1148.html
AG/HSR: agitation/high sparging rate, AG/HSR & MB: agitation/high sparging rate & micro bubbling, AG, MB & IBRT: agitation, micro bubbling & increased bubbles residence time

residence time, and physico-chemical interactions (Lamed et al. 1988; Pauss et al. 1990; Bredwell & Worden 1998; Bothun et al. 2004; Kraakman et al. 2011; Risso 2018).

Poor liquid to gas phase mass transfer can play a critical and significant role in bioethanol synthesis (Zhang et al 2012; Blunt et al 2015). It has been suggested that poor H_2 transfer results in elevated H_2 concentration in aqueous phase, which via feed-back inhibition, can result in decreased hydrogenase activity, and increased NADH/NAD^+ ratios, which can result in increased ethanol or lactate synthesis (Lamed et al. 1988; Rydzak et al. 2011; Zhang et al. 2012). The presence of elevated concentrations of dissolved CO_2 can also impact fermentation end-product synthesis patterns (Park et al. 2005; Rydzak et al. 2011). Therefore, it is essential to evaluate individual microbial metabolism in connection to mass transfer barriers (if any) and thereby adapt techniques for trading off undesirable bioproducts, which may enhance the efficiency of a particular bioprocess.

Supersaturation is a common phenomenon, generally observed in biological processes that involves gas synthesis. It is described as the ratio of the actual measured dissolved gas concentration to the concentration that is predicted by Henry's Law at a state of equilibrium and has been quantified by many authors (Pauss et al. 1990; Zhang et al. 2013; Blunt et al. 2015). This is also known as the Supersaturation Factor (S_f) (Kraemer and Bagley 2006), and is defined by the following Equation 5.1.

$$Sf = \frac{[gas]_{aq}}{[gas]^*_{aq}} \qquad 5.1$$

where, $[gas]_{aq}$ = the actual dissolved gas concentration; and $[gas]_{aq}^*$ = the concentration of a dissolved gas species at thermodynamic equilibrium, predicted/estimated by Henry's Law. It should be close to unity when no significant mass transfer limitations are present, indicating that

the biological production rate of the gas alone is the limiting factor in the transfer of gases from the liquid phase to the headspace. If S_f is greater than 1, mass transfer limitations occurs. When *C. termitidis* cultured in a batch experiment with carbon-sufficient condition and carbon-excess condition, where growth is not affected due to lack of substrate and assuming no deficit in nutrients, then quasi-steady state and steady-state condition will be achieved, respectively. For a particular kind of gas in a given environment (here, carbon-sufficient or carbon-excess condition), the saturation factor is dependent on the volumetric mass transfer coefficient, (k_La), and it is defined by the following equation (Pauss et al. 1990):

$$k_L a = \frac{Q_v}{K_H R_c T(Sf-1)} \qquad 5.2$$

where, Q_v, the volumetric gas production rate, which is the ratio of the gas flow rate to the liquid volume, K_H = Henry's Law constant (mol/L/atm); R_c = ideal gas constant = 0.8206 L atm/mol/K; T = temperature (K).

The term, k_La, is generally used to describe the transfer of gases from liquid phase to gas phase, or vice-versa (Kawase et al. 1992; Muller et al. 2012). The coefficient is comprised of k_L, the film coefficient, which is mostly dependent on properties of solvent and solute gas, and a, which is the area of gas-liquid interface normalized to the liquid volume, and is dependent on hydrodynamic conditions (Pauss et al. 1991; Kawase et al. 1992).

Clostridium termitidis is a mesophilic anaerobic bacterium that synthesizes ethanol and organic acids (formate, acetate, lactate), as well as hydrogen (H_2) and carbon dioxide (CO_2) when cultured with soluble substrates such as simple sugars or insoluble substrates such as cellulose. While H_2 and CO_2 are synthesized as a consequence of microbial metabolism, it is unclear whether the concentrations of H_2 and CO_2 in the culture medium and/or headspace

influence overall ethanol production. In other words, do concentrations of dissolved H_2 and CO_2 influence microbial metabolism, and can they enhance or inhibit ethanol production during the growth of *C. termitidis*?

To address these questions, *C. termitidis* was grown on 2 g/L cellobiose in 1191 media in a 7 L bioreactor with pH control, at 37 ^{o}C. To evaluate the effect of dissolved gasses on microbial metabolism and fermentation end-product synthesis patterns, cultures were sparged with N_2 gas at a high rate (400 mL/min, with stirring at 200 rpm), to rapidly remove dissolved gases, or at a lower rate (20 mL/min, with stirring at100 rpm). Concentrations of H_2, CO_2, and EtOH fermentation end-products were monitored in both the headspace and aqueous phase in-real time by membrane inlet mass spectrometry (MIMS). Discrete samples were also analyzed off-line to determine concentrations of all fermentation products (formate, acetate, lactate, ethanol) in the aqueous phase by HPLC.

The hypothesis underlying this work was that continuous, real-time, and quantitative measurements of H_2 and CO_2 concentrations in the aqueous phase using the MIMS system would enable comparisons with predicted dissolved gas concentrations from headspace gas, and these data, combined with discrete off-line measurements of all fermentation end-products, could be used to explain how fermentation end-product synthesis patterns are influenced by dissolved H_2 and/or CO_2 concentrations.

5.2 Materials and Methods

C. termitidis were grown on 2 g/L cellobiose in a pH controlled bioreactor under low and high turbulent growth environment and their progress were monitored using both discrete and continuous techniques. At least two biological replites were performed in each set of experiment. Detailed description of materials and methods were described in section 2.3 of Chapter 2.

5.3 Results

5.3.1 Growth of *C. termitidis*

The growth of *C. termitidis* was monitored in open-batch cultures containing 2 g/L cellobiose in 1191 media continuously sparged with high N_2 (400 mL/min with agitation 200 rpm) and low N_2 (20 mL/min with agitation 100 rpm). The growth curves for *C. termitidis* cultures exposed to low sparging rate (LSR) and high sparging rate (HSR) are shown in Figure 5.1. A lag phase of approximately 7-8 hrs was observed in the HSR cultures, whereas no lag was noticed in the LSR cultures. After lag cell mass continuously increased with a growth rate of 0.06 h^{-1}. Under LSR, cell mass increased exponentially with a growth rate of 0.05 h^{-1} and followed increasing with a slower rate thereafter. The growth rates were calculated based on OD measurement. A final cell density (OD_{600}) of 0.98 ± 0.05 was achieved in the LSR cultures, while the final cell density of the HSR culture was 1.10 ± 0.05. Thus, a slight difference was observed in the final cell densities for the two experimental conditions (LSR versus HSR). Similar trends were observed in the protein data. The growth of *C. termitidis* was, unaffected by pH thanks to continuous pH control during growth (LSR, HSR)

A)

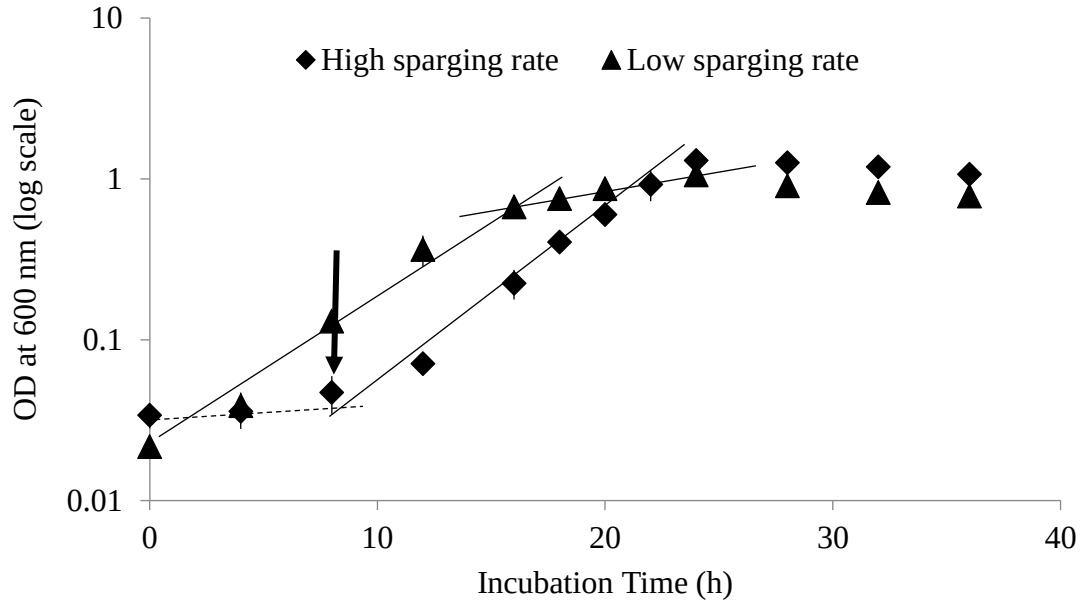
High sparging rate
Low sparging rate
OD at 600 nm (log scale)
10
1
0.1
0.01
0
10
20
30
40
Incubation Time (h)

B)

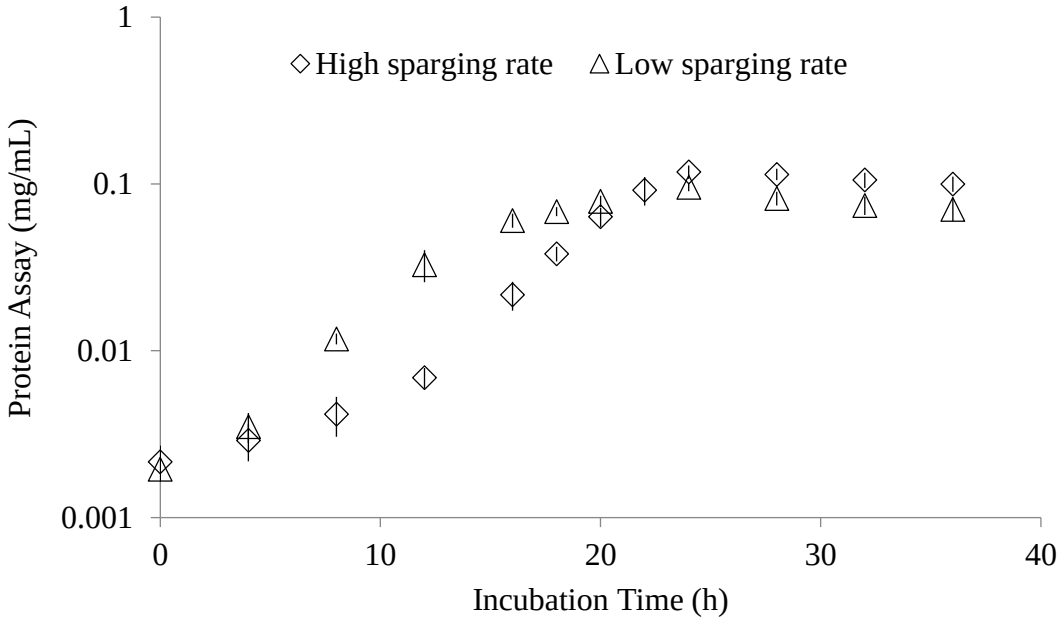
High sparging rate
Low sparging rate
Protein Assay (mg/mL)
1
0.1
0.01
0.001
0
10
20
30
40
Incubation Time (h)

Figure 5.1 Growth of *C. termitidis* on 2 g/L cellobiose with low N_2 sparging rate (20 mL/min with 100 rpm stirring: triangles) and high sparging rate (400 mL/min with 200 rpm stirring: diamonds) in a 7 L bioreactor (3 L working volume) using A) OD and B) protein assay. The vertical arrow indicates lag only with high sparging rate growth environment.

5.3.2 Analysis of dissolved gases

The response of the MIMS probe to the dissolved gas concentrations was found to be linear for the range tested, with regression coefficients ranging $0.867 < R^2 < 0.988$. Greater deviations from regression co-efficient indicate existence of highly turbulent conditions where gases were rapidly removed from the bioreactor by the high sparging rate. In this case, high signal to noise ratio was expected. Upon applying the MIMS calibration curves to the baseline-subtracted signals acquired during the fermentation process, it was observed that the results were directly measured with the MIMS probe. Moreover, the results obtained using the MIMS probe were different/inconsistent from the results obtained from off-gas analyses of discrete samples, and the application of Henry's Law, (Figures 5.2 & 5.3). From aqueous phase measurement, it was observed that the growth looked dynamic in nature (in other words, growth changes over the period of time) between 0 to 15 hrs pi. The growth, however, seemed in steady-state after 15 hrs pi (stationary phase), which would not be revealed until aqueous phase measurement of H_2 signal was obtained during LSR (purple line in Figure 5.2). This pattern of growth was not observed adequately from CO_2 signals (purple line in Figure 5.3). Therefore, in particular, the signals of H_2 (aq) and CO_2 (aq) were far under-estimated when thermodynamic equilibrium was assumed in entire growth period of *C. termitidis* on 2 g/L cellobiose (Figure 5.4 and Figure 5.5). Under HSR, the concentration of dissolved and headspace H_2 was quickly (5 -10 minutes) diminished when cellobiose was fully consumed (end of stationary phase) compared to LSR.

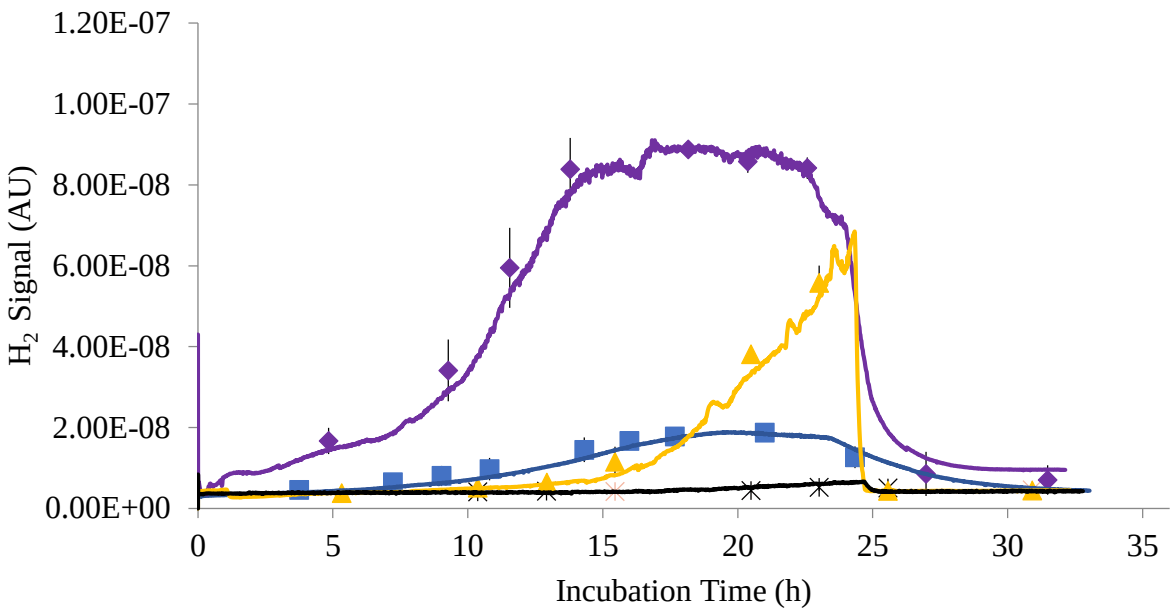

Figure 5.2 Production of H_2 by *C. termiditis* cultures under low sparging rate (LSR: 20 mL/min, 100 rpm) and high sparging rate (HSR: 400 mL/min, 200 rpm) conditions measured in the headspace and aqueous phase in real-time by the MIMS probe. Purple line, H_2 signal in aqeuous phase under LSR conditions; Yellow line, H_2 signal in the aqueous phase under HSR conditions; Blue line, H_2 signal in headspace under LSR conditions; Black line, H_2 signal in the headspace under HSR conditions. For simplicity, discrete points, obtained from continuous measurements, represent average value of two biological replicates with error bars (SD).

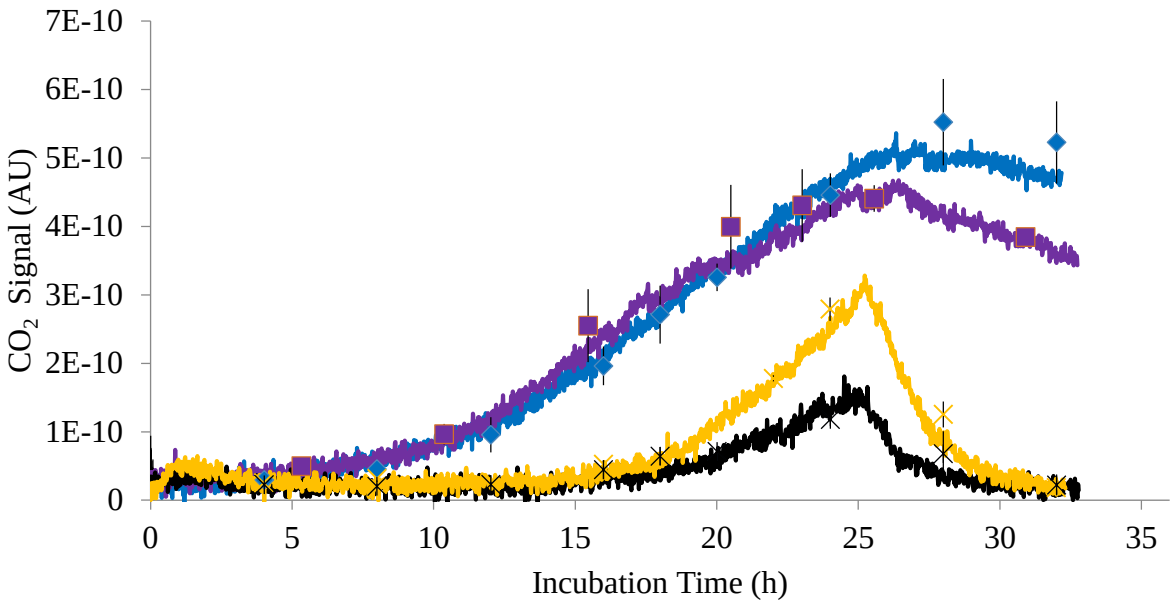

Figure 5.3 Production of CO_2 by *C. termiditis* cultures under low sparging rate (LSR: 20 mL/min, 100 rpm) and high sparging rate (HSR: 400 mL/min, 200 rpm) conditions measured in the headspace and aqueous phase in real-time by the MIMS probe. Purple line, CO_2 signal in aqeuous phase under LSR conditions; Yellow line, CO_2 signal in the aqueous phase under HSR conditions; Blue line, CO_2 signal in in headspace under LSR conditions; Black line, CO_2 signal in the headspace under HSR conditions. For simplicity, discrete points, acquired from continuous measurements, represent average value of two biological replicates with error bars (SD).

A)

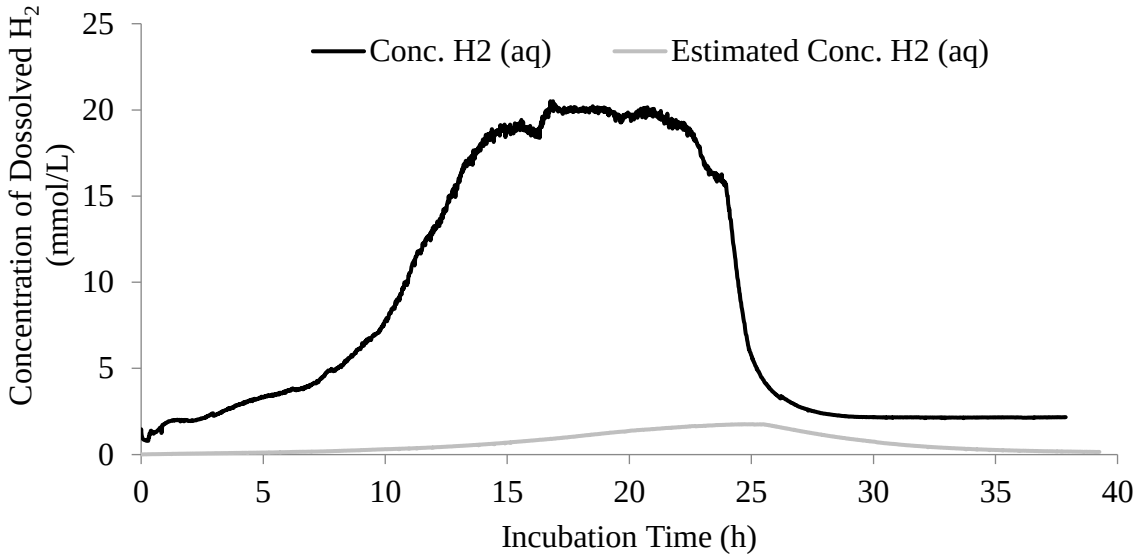
Conc. H2 (aq)
Estimated Conc. H2 (aq)
Concentration of Dossolved H_2 (mmol/L)
Incubation Time (h)
0
5
10
15
20
25
30
35
40

B)

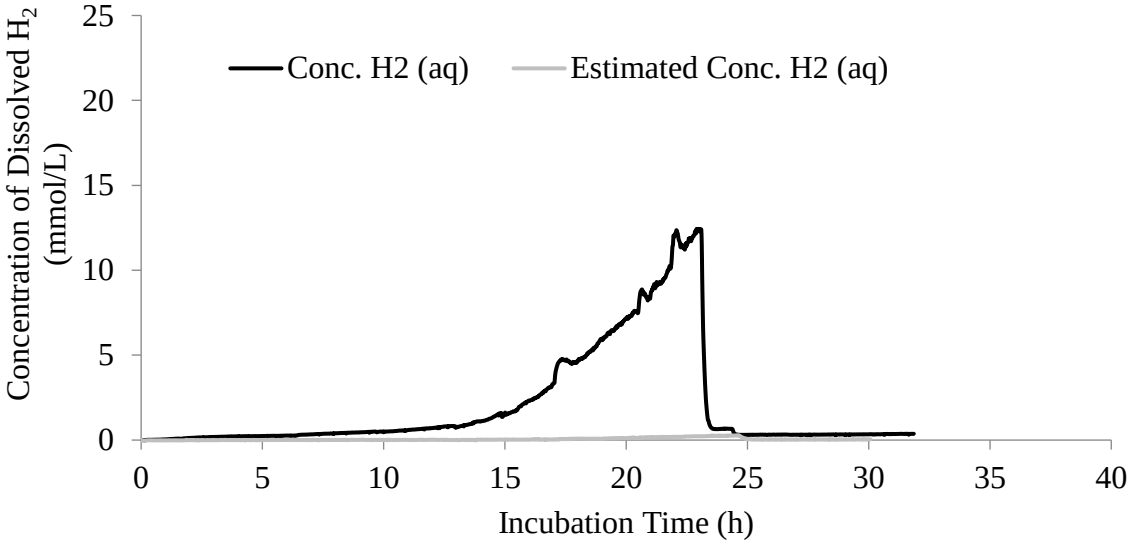
Conc. H2 (aq)
Estimated Conc. H2 (aq)
Concentration of Dissolved H_2 (mmol/L)
Incubation Time (h)
0
5
10
15
20
25
30
35
40

Figure 5.4 Concentrations of dissolved H_2 A) in LSR (20 mL/min, 100 rpm) and B) in HSR (400 mL/min, 200 rpm) in the cultures of *C. termitidis* on 2 g/L cellobiose, pH 7.20 ± 0.02. The black line indicates actual H_2 concentrations measured directly in the aqueous phase. The grey line indicates the estimated H_2 concentration in the headspace using Henry's Law based on headspace composition. For simplicity, only data from a single experiment are presented, although two biological replicates were performed and shown in Figure 5.2.

A)

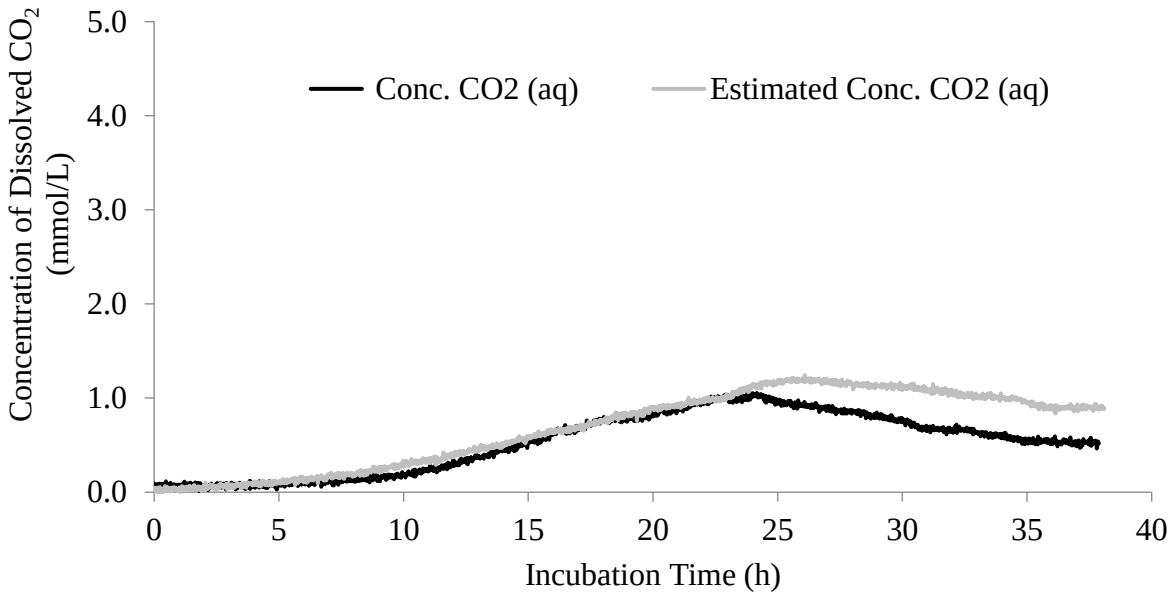
Concentration of Dissolved CO_2 (mmol/L)
5.0
4.0
3.0
2.0
1.0
0.0
Conc. CO2 (aq)
Estimated Conc. CO2 (aq)
0
5
10
15
20
25
30
35
40
Incubation Time (h)

B)

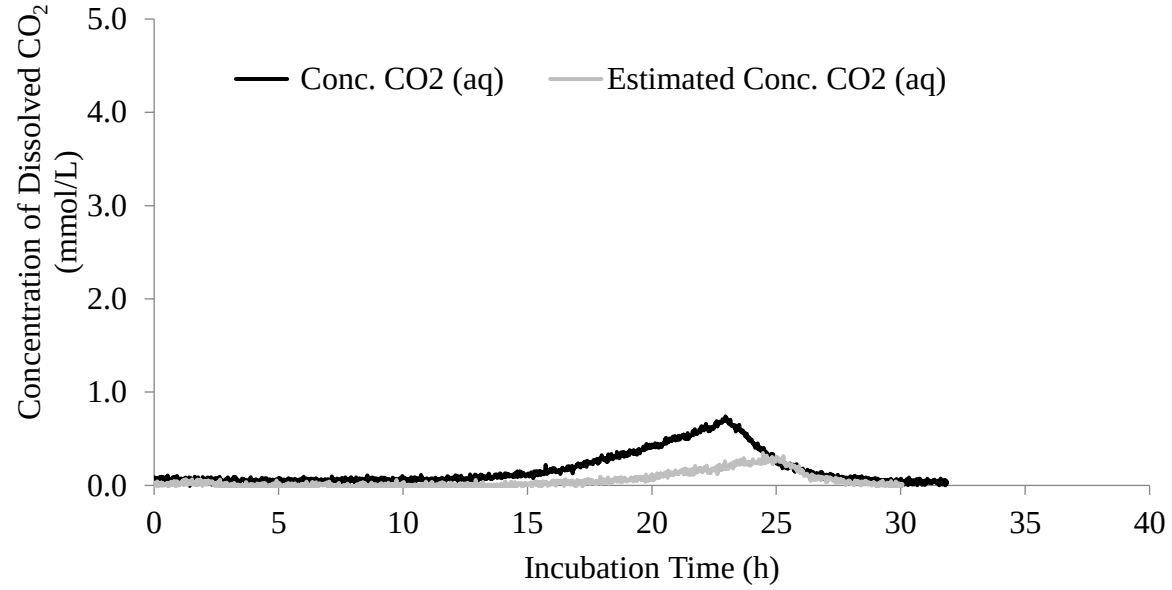
Concentration of Dissolved CO_2 (mmol/L)
5.0
4.0
3.0
2.0
1.0
0.0
Conc. CO2 (aq)
Estimated Conc. CO2 (aq)
0
5
10
15
20
25
30
35
40
Incubation Time (h)

Figure 5.5 Concentration of dissolved CO_2 A) in LSR (20 mL/min, 100 rpm) and B) in HSR (400 mL/min, 200 rpm) in the cultures of *C. termitidis* grown with 2 g/L cellobiose under controlled pH at 7.20 ± 0.02. The black line indicates the measured CO_2 concentration in the aqueous phase. The grey line indicates the CO_2 concentration in the in headspace, estimated using Henry's Law based on headspace composition. For simplicity, only data from a single experiment are presented, although two biological replicates were performed and shown in Figure 5.3.

5.3.2.1 Aqueous H_2 analysis

Figure 5.4 shows the measured and estimated dissolved H_2 concentrations in the LSR culture (Re ≈ 8700, stirring at 100 rpm) and in the HSR culture (Re ≈ 17500, stirring at 200 rpm). The dissolved H_2 concentration estimated from the headspace partial pressure, using Henry's Law (Stumm and Morgan 1996), was much lower than the actual dissolved gas concentration measured using the MIMS probe (Figure 5.4A). Underestimation of dissolved H_2 was also noticed in the HSR (Re ≈ 17500, agitation 200 rpm) cultures (Figure 5.4B). Consequently, the assumption that H_2 gas synthesized by *C. termitidis* during cellobiose fermentation reaction is near equilibrium appears to be inaccurate.

While concentrations of dissolved H_2 was underestimated by Henry's Law in both the LSR and HSR cultures (Figures 5.4A and 5.4B), supersaturation of H_2 in the aqueous phase (H_2 aq) was detected in both conditions. Although stable concentrations were obtained in the mid-exponential to early stationary phase of growth in the LSR culture, a higher saturation factor (S_f ≈10 - 100) was observed in the HSR culture (Figure 5.6).

5.3.2.2 Aqueous CO_2 analysis

In LSR cultures, the measured concentration of dissolved CO_2 did not vary greatly from the CO_2 concentration in the headspace estimated using Henry's Law (Figure 5.5A). It was, however, took long time to eliminate either from aqueous phase or gas phase. The CO_2, saturation factor (S_f) was approximately little over than unity ($1 \leq S_f \leq 2$) between exponential to late stationary growth phase (i.e. 5-20 hrs pi) and within the limited standard error of measurement (grey open diamonds in Figure 5.6A).

In contrast, the measured CO_2 concentration was slightly greater in the HSR cultures during stationary phase (Figure 5.5B). Statistically this variation was significant (Table 5.2). The

Table 5.2 *C. termitidis* fermentation end-product synthesis patterns in cultures with LSR and HSR conditions.

Experiment	Biol. Rep.	Cellobiose	Lactate	Formate	Acetate	EtOH (HPLC)	H_2 (MS)	CO_2 (MS)	Protein
	Unit	mmol/L	mmol/L	mmol/L	mmol/L	mmol/L	mmol/L	mmol/L	mmol/L
Low Sparging Rate	Average (N=4)	6.23	1.72	8.08	14.96	5.83	21.26	14.88	0.89
	SD	0.20	0.29	0.90	2.16	0.30	0.42	0.46	0.01
High Sparging Rate	Average (N=4)	6.35	1.02	2.64	14.33	5.16	29.80	22.02	1.20
	SD	0.13	0.56	2.16	0.79	0.11	1.54	0.49	0.07
Statistical Analysis		t = -1.03, p=0.337, insignificant @p<0.05	t = 2.46, p=0.044, significant @p<0.05	t = 5.18, p=0.001, significant @p<0.05	t = 0.55, p=0.598, insignificant @p<0.05	t = 4.27, p=0.004, significant @p<0.05	t = -12.06, p<0.0001, significant @p<0.05	t = -22.47, p<0.0001, significant @p<0.05	t = -10.09, p<0.0001, significant @p<0.05

SD = Standard deviations; t = Two tailed t-test with two independent means; 1 mg of protein/mL of culture = 9.90 mmol/L, since the approximate molecular weight of cell biomass is 101 g/mol of cells

A)

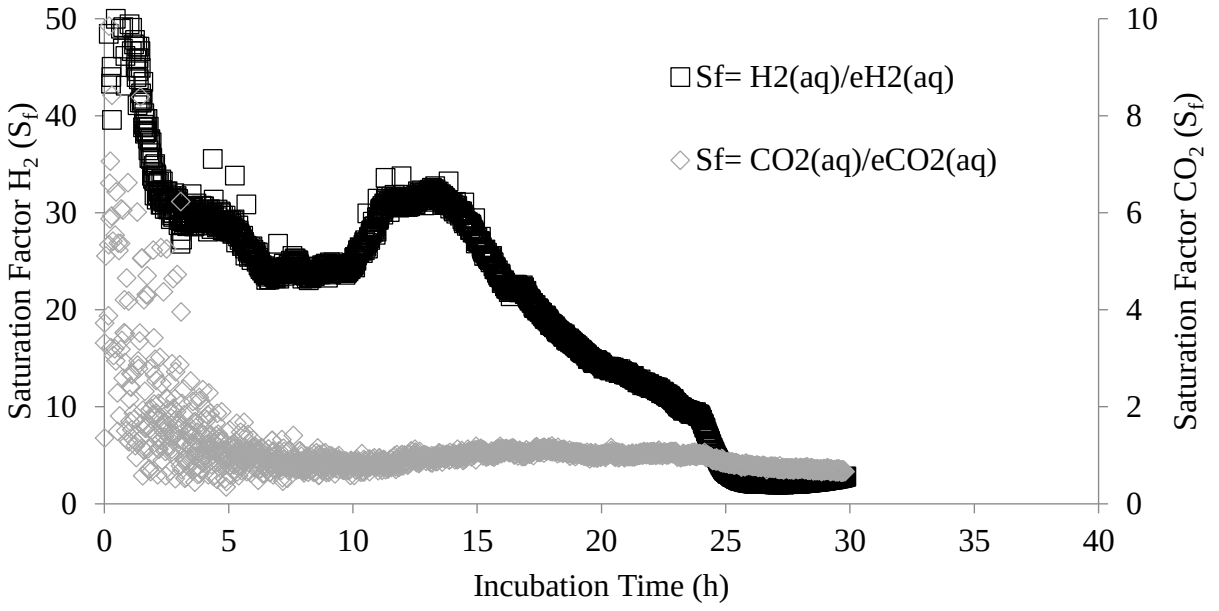
Saturation Factor H_2 (S_f)
Saturation Factor CO_2 (S_f)
Incubation Time (h)
Sf= H2(aq)/eH2(aq)
Sf= CO2(aq)/eCO2(aq)
0
10
20
30
40
50
0
2
4
6
8
10
0
5
10
15
20
25
30
35
40

B)

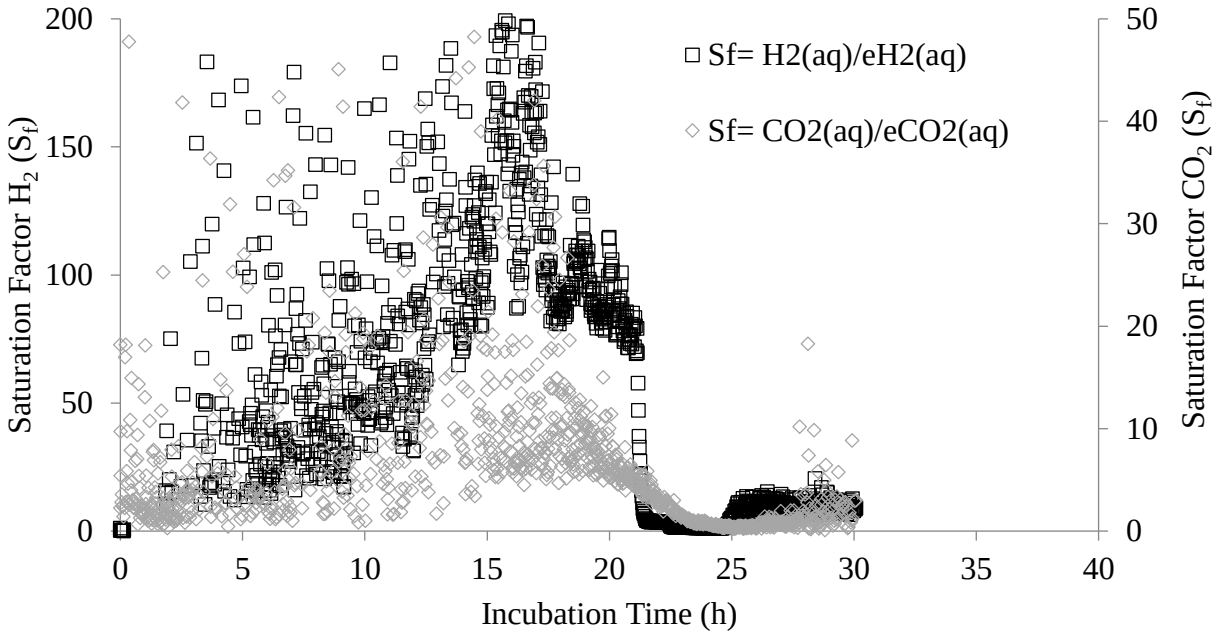
Saturation Factor H_2 (S_f)
Saturation Factor CO_2 (S_f)
Incubation Time (h)
Sf= H2(aq)/eH2(aq)
Sf= CO2(aq)/eCO2(aq)
0
50
100
150
200
0
10
20
30
40
50
0
5
10
15
20
25
30
35
40

Figure 5.6 Saturation factor (S_f) for dissolved gases A) in LSR (20 mL/min, Re = 8700, 100 rpm) and B) HSR (400 mL/min, Re = 17500, 200 rpm) experiments. (□) open black squares represent saturation factor for H_2; (◊) open grey diamonds represent saturation factor for CO_2.

S_f values varied greatly in the early exponential phase, but became more consistent in late exponential phase, and then decreased in the stationary phase (Figure 5.6B).

5.3.3 Ethanol analysis

Ethanol possesses a very high Henry's Law constant ($2.30x10^2$ M/atm), therefore, it shows infinite solubility in water. The raw signals obtained either by headspace or by liquid phase measurement showed minimum variability (qualitatively). For that reason, it was necessary to evaluate any changes in applied ethanol calibration either headspace or liquid phase measurement. The slopes generated from either calibration approach described in section 2.3.3 of Chapter 2 were within the range of 1.08×10^{-10} to 1.23×10^{-10}, and were not significantly different ($t = - 0.63$, at $p < 0.05$). This indicates that the *ex-situ* calibration method produced the same result as the *in-situ* calibration method for highly soluble volatiles (ethanol in this case) and can be used as a simpler and faster method of calibration. The response of the instrument was linear for the range of ethanol concentrations tested, with all regression coefficients (R^2) exceeding 0.998.

The ethanol concentrations obtained during the growth of *C. termitidis,* using on-line measurements with the MIMS probe, are shown in Figure 5.7. The average ethanol concentrations were 5.83 ± 0.30 for the LSR cultures and 5.16 ± 0.11 for HSR cultures, which were obtained by HPLC measurement (Table 5.2). These values were slightly higher when measured by the MIMS probe. The maximum ethanol concentration (stationary phase) detected by the MIMS probe in the LSR cultures and HSR cultures were 6.05 ± 0.05 mmol/L (Figure 5.7A) and 5.33 ± 0.07 mmol/L (Figure 5.7B), respectively. The ethanol concentrations either obtained by HPLC or MIMS probe (LSR, HSR) were different from the experiments described (2 g/L cellobiose with sparging rate 3 mL/min and 50 rpm agitation) by Ramachandran (2013),

A)

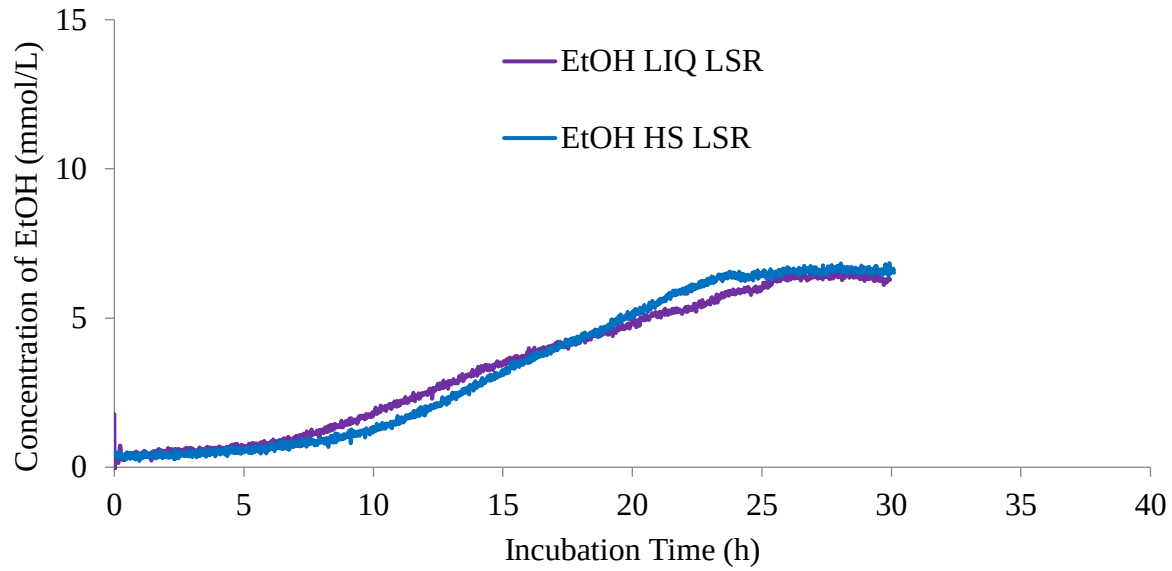
Concentration of EtOH (mmol/L)
15
10
5
0
0
5
10
15
20
25
30
35
40
Incubation Time (h)
EtOH LIQ LSR
EtOH HS LSR

B)

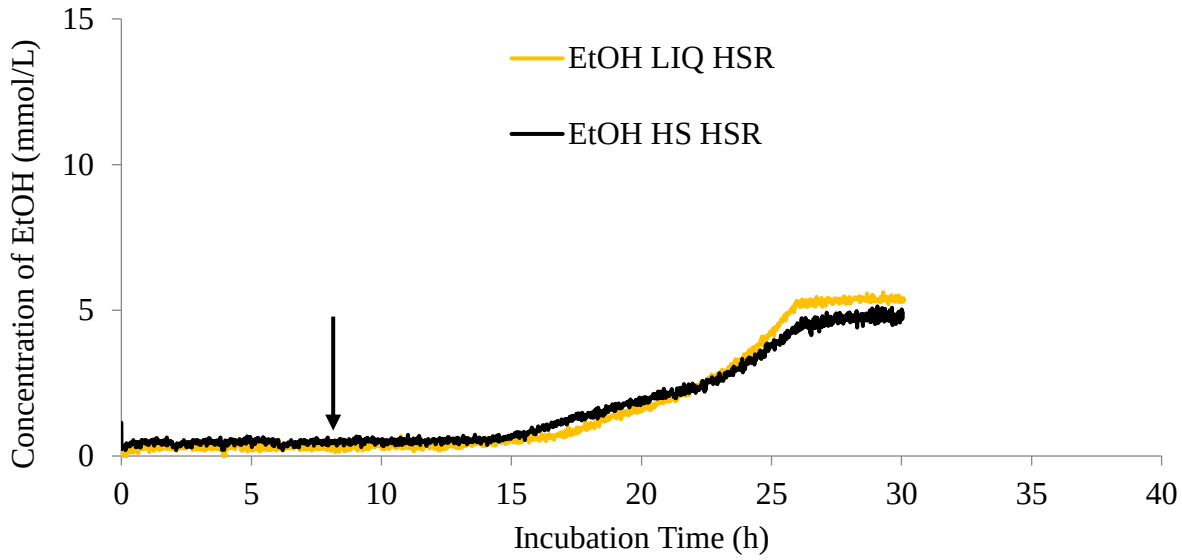
Concentration of EtOH (mmol/L)
15
10
5
0
0
5
10
15
20
25
30
35
40
Incubation Time (h)
EtOH LIQ HSR
EtOH HS HSR

Figure 5.7 Ethanol concentrations measured with MIMS probe in A) LSR (20 mL/min, 100 rpm) cultures and B) HSR (400 mL/min, 200 rpm) cultures of *C. termitidis* on 2 g/L cellobiose in pH controlled 7 L bioreactor. Purple line indicates ethanol in liquid phase with low sparging rate (20 mL/min), blue line indicates ethanol in gas phase with low sparging rate (20 mL/min), yellow line indicates ethanol in liquid phase with high sparging rate (400 mL/min), and black line indicates ethanol measured in headspace using MIMS probe with high sparging rate (400 mL/min). Vertical arrow indicates lag phase.

in which the ethanol concentration measured by HPLC averaged 3.37 ± 0.48 mmol/L. Here, significant portion of cellobiose was converted to lactate under this growth conditions.

5.3.4 The impact of supersaturation on reaction stoichiometry and mass balance

By accounting for the supersaturation of both H_2 and CO_2, it was found that the average carbon recovery and C1/C2 ratios did not vary significantly (Table 5.3; see also Figure S5.4). The average carbon recovery and C1/C2 ratios in the LSR experiment were 97 ± 5.0 % and 1.11 ± 0.09, respectively, while the average carbon recovery and C1/C2 ratios in the HSR experiment were 100 ± 4.0 % and 1.27 ± 0.13, respectively. The O/R ratios also did not change: the O/R ratio in the LSR culture was 0.87 ± 0.03, while the O/R ratio of the HSR culture was 0.86 ± 0.06.

5.4 Discussion

5.4.1 Effects of sparging and agitation on growth

Based on the OD measurement, the growth rate of *C. termitidis* was high during HSR compared to the growth rate under LSR. Although a slight difference was observed between the final OD_{600} for the two experimental conditions (LSR versus HSR), the difference between protein assay was significantly different ($t = -10.09$, $p < 0.0001$, significant @ $p < 0.05$ Table 5.2) at 24h. The substrate specific protein yields were also varied significantly (Table 5.4). Turbulence, sheer, and fast micro aeration of nitrogen may have hampered initial growth of *C termitidis* under HSR conditions. Carere et al. (2014) also reported slightly higher biomass yield (3.6 mmol/L) during high sparging rate of N_2 compared to the yield (3.3 mmol/L) at low sparging rate of N_2, when *C. thermocellum* was cultured on 2 g/L cellobiose in a 14 L bioreactor with 7 L working volume. Nevertheless, it was unclear whether the biomass yield difference was significant or not. Cellobiose consumption rate was reported much slower during high N_2 sparging.

Table 5.3 Carbon recovery index and product ratios under LSR and HSR growth conditions

Experiment	Biol. Rep. Unit	C-Recovery	C1/C2	O/R	Ethanol/Acetate
Low Sparging Rate	Average (N=4)	0.97	1.11	0.87	0.40
	SD	0.05	0.09	0.03	0.06
High Sparging Rate	Average (N=4)	1.00	1.27	0.86	0.36
	SD	0.04	0.13	0.06	0.02
Statistical Analysis		t = 0.68, p=0.521, insignificant @p<0.05	t = - 2.14, p=0.069, insignificant @p<0.05	t = 0.32, p=0.755, insignificant @p<0.05	t = 3.77, p=0.009, significant @p<0.05

Data derived from Table 5.2; SD = Standard deviations; t = Two tailed t-test with two independent means

Table 5.4 Substrate (cellobiose) specific yields (mol/mol hexose equivalent) of *C. termitidis* fermentation end-products in cultures with LSR and HSR conditions. Statistical analysis was performed between two experimental conditions (LSR and HSR).

Expt	Biol. Rep.	Lactate	Formate	Acetate	EtOH (HPLC)	H_2 MS	CO_2 MS	Protein
Low Sparging Rate	Average (N=4)	0.14	0.65	1.16	0.47	1.72	1.19	0.07
	SD	0.02	0.06	0.08	0.02	0.07	0.06	0.00
High Sparging Rate	Average (N=4)	0.08	0.21	1.13	0.41	2.35	1.74	0.09
	SD	0.05	0.17	0.04	0.01	0.10	0.05	0.00
Statistical Analysis		t = 2.14, p=0.075, insignificant @p<0.05	t =4.76, p=0.003, significant @p<0.05	t =0.16, p=0.880, insignificant @p<0.05	t = 5.42, p=0.002, significant @p<0.05	t = -10.28, p<0.0001, significant @p<0.05	t = -13.62, p<0.0001, significant @p<0.05	t = -8.66, p<0.0001, significant @p<0.05

SD = Standard deviations; t = Two tailed t-test with two independent means;

Protein yield expressed as moles of protein per mole of hexose equivalent

5.4.2 Supersaturation of H_2

Supersaturation of H_2 was observed during both experimental conditions (LSR and HSR) in the present study, which has similarity with other study for H_2 concentrations in a biohydrogen producing bioreactor with anaerobic digester sludge with and without N_2 sparging (Kramer and Bagley 2006). The movement of H_2 from the liquid phase to the gas phase was affected due to mass transfer limitations (especially, LSR growth environment) in the present study. Large variations were observed during early stage of reaction due to its dynamic nature and higher turbulence in HSR reaction environment. Similar findings ($S_f \approx 11$) were reported for H_2 by Kraemer and Bagley (2006) in cultures with relatively high sparging rates (150 mL/min) during biohydrogen synthesis. In a methanogenic bioreactor, which was operated at mesophilic temperature (32-35 ^oC), hydrogen saturation factor was reported within the range of 19 – 102 (Pauss and Guiot 1993). Significantly, higher volumetric yield of H_2 was obtained during HSR compared to LSR (Table 5.2) in the present study. Carere et al. (2014) reported higher H_2 yield (16.4 mmol/L) at HSR (1200 mL/min) compared to yield (13.9 mmol/L) at LSR (120 mL/min) during the culture of *C. thermocellum*; but lacked reporting the evidence of any H_2 supersaturation.

5.4.3 Supersaturation of CO_2

The finding of supersaturation factor ($1 \leq S_f \leq 2$ for CO_2) under LSR is consistent with Kraemer and Bagley (2006), who reported limited supersaturation of CO_2 in a mixed culture fermentation for hydrogen producing reactor at 25 °C. In that study, S_f values of 1.6-1.7 were found to occur regardless of the N_2 sparging rate applied, which varied from 0 to 160 mL/min in a reactor with a 2 L working volume and a 1 L headspace volume.

Under HSR, the S_f values obtained late exponential to stationary growth phase (≈ 5 to 8) are in agreement with the findings of Pauss et al. (1990), who reported that the mass transfer of CO_2 and other highly soluble gases is not limited under most conditions in anaerobic methanogenic processes. This suggests that the liquid phase was in a state of quasi-equilibrium/steady-state equilibrium with the gas phase for this set of conditions, and CO_2 measurements were dictated by thermodynamics, rather than mass transfer rates, and should therefore be independent of agitation or aeration rates (Oeggerli and Heinzle 1994). This observation was also partially supported by the value of mass transfer coefficients (k_La) obtained in either condition (Supplementary Figure S5.2). Although significant variations in k_La (CO_2) were observed during early stage of growth (HSR), comparatively stable k_La (CO_2) were obtained during stationary growth phase, where steady-state equilibrium was assumed. It is not unusual to obtain variable k_La. Literatures suggest that bubble size, agitation, turbulence and sparging rate affect k_La determination (Bredwell and Worden 1998; Worden and Bredwell 1998; Risso 2018). Thus, reliable estimations can be made for total CO_2 production by measuring either the headspace or the liquid-phase signal alone, since good carbon recovery, C1/C2 and O/R ratios were obtained either LSR or HSR and their variations between growth conditions were statistically insignificant (Table 5.3).

5.4.4 Effects of rapid removal of dissolved gases on their yields

The total H_2 production increased significantly (about 40 %) when supersaturation was taken into account, and less accumulation of H_2 was observed in the aqueous phase in the HSR culture experiment compared to LSR culture experiment. In the LSR cultures, the total volumetric yield of H_2 production, measured at the end of the growth phase, increased from 21.26 ± 0.42 mmol/L to 29.8 ± 1.54 mmol/L when supersaturation was factored in (significant

when t = - 12.06 at $p < 0.05$). Substrate specific yields of H_2 were 1.72 ± 0.07 mol/mol hexose equivalent and 2.35 ± 0.10 mol/mol hexose equivalent for LSR and HSR, respectively. These variations are significant at $p < 0.05$. Owing to the relatively large amount of CO_2 dissolved into the liquid phase, the slight supersaturation of CO_2 in the LSR experiment (≈ 1.2) resulted in total CO_2 production to increase from 14.88 ± 0.46 mmol/L to 22.02 ± 0.49 mmol/L when supersaturation was accounted for, an increase more than 48 %.

5.4.5 Effects on organic acid synthesis

C. termitidis produces acetic acid, formic acid and lactic acid when cultured with cellobiose/xylose through pyruvate catabolic reactions. Changing its growth environment, their yields also altered, which was observed in previous Chapters (3 and 4). In this section, we shall find how significantly (if any) these organic acids synthesis vary due to manipulation of gas sparging rates. Formate synthesis decreased significantly ($t = 5.18$ at $p < 0.05$) in the HSR experiment compared with the LSR experiment, so did the formate yields (Table 5.4). This may have been due to the fact that under HSR conditions (high mass transfer rates) dissolved gases were quickly removed. The rapid removal of H_2 (resulting in low H_2 partial pressures) enhanced carbon and electron flow from pyruvate to acetyl-CoA synthesis via the pyruvate ferredoxin oxidoreductase (PFOR) pathway. This thermodynamically favourable process may have diverted carbon and electrons away from pyruvate formate lyase (PFL) pathway, resulting in a 67 % reduction in formate synthesis. Acetate yields did not vary significantly ($t = 0.16$, $p < 0.05$ Table 5.4) between LSR and HSR growth environments. Furthermore, reducing equivalents utilized for H_2 synthesis were diverted away from lactate and ethanol synthesis, resulting in a significant amount 25 – 70 % ($t = 2.46$ at $p < 0.05$) decrease in lactate synthesis and a 12 - 16 % decrease in ethanol synthesis.

5.4.6 Effects of fast removal of dissolved gas on ethanol synthesis

The maximum ethanol concentration in the HSR cultures was 5.16 ± 0.11 mmol/L. This amount was significantly low ($t = 4.27$, $p < 0.05$) compared to the ethanol obtained (5.83 ± 0.30 mmol/L) from cultures with HSR. Low production of ethanol relative to acetate final concentration may be the result of mass transfer driving forces (such as sparging rate, agitation, and bubble size). Due to increased shear stress from vigorous stirring adversely impacting growth, which was observed by Blunt et al. (2015), when *C. thermocellum* was cultured in a reaction environment with moderate agitation (200 rpm) with surface mixing. Nevertheless, in the present set of experiments significant change in growth was noticed in terms of total protein content (Table 5.2) and its yield (0.07 and 0.09 mol/mol hexose equivalent for LSR and HSR, respectively). This observation rejects the hypothesis of cell lysis under the present sets of experiments where no surface mixing was applied.

Foaming also increased significantly during stationary growth phase in the HSR cultures, where a high cascade of N_2 micro-bubbles was visually noticed. Foaming may have been developed due to biofilm formation during stationary phase of growth. The ethanol/acetate ratio decreased slightly (but significantly $t = 3.77$ at $p < 0.05$) from 0.40 ± 0.06 in the LSR cultures to 0.36 ± 0.02 in the HSR cultures. This observation was corroborated with lower ethanol production in HSR culture (5.33 ± 0.07 mmol/L, Figure 5.7B) compared with ethanol production (6.05 ± 0.05 mmol/L, Figure 5.7A) in the LSR cultures, measured in both the headspace and the aqueous phase by the MIMS probe. Therefore, reduced amount of ethanol may have obtained under HSR compared to LSR due to existence of turbulent environment that drives higher mass transfer and allows electron and reducing equivalents towards H_2 synthesis, rather than ethanol or lactate synthesis. Furthermore, comparatively low mass transfer resistance for both H_2 and

CO_2 under HSR growth environment (supplementary Figure S5.3) allowed quick removal dissolved gases, which may have also played a significant role in reducing ethanol yield. Low volumetric yields of ethanol were noticed during bioethanol synthesis using 2 g/L cellobiose with *C. thermocellum* due to elevated mass transfer conditions: Re 23000, 200 rpm and sparging rate 100 mL/min and or cell lysis (Blunt et al. 2015). Carere et al. (2014) observed 14 % decreased in final ethanol concentration when sparging rate of *C. thermocellum* cultures switched from 120 mL/min to 1200 mL/min. When cultures sparged with low N_2 and high N_2, ethanol to acetate ratios were decreased from 0.6 to 0.5. A significant decrease (30 %) in specific activity of alcohol dehydrogenase enzyme was noticed in cultures with high sparging compared to low sparging with N_2 gas.

5.5 Conclusion

In cultures with a high sparging rate (HSR, where less mass transfer resistance existed), rapid removal of dissolved gases from the aqueous phase during growth of *C. termitidis* on cellobiose resulted in an increase in H_2 and CO_2 production and a decrease in ethanol, formate, and lactate production. The most significant change was in the production of formate and the formate to CO_2 ratio. However, the rate at which H_2 gas was removed from the headspace was not the same as the rate at which it was removed from the aqueous phase, as revealed by continuous, real-time monitoring with the MIMS probe. Measurement of the fermentation end-products at discrete time points using off-line methods (GC for headspace gases, and HPLC for aqueous phase products), was less accurate than the MIMS probe measurements (especially, dissolved gases), leading to potentially inaccurate understanding of the rapid changes in *C. termitidis* metabolism during growth. Based on more detailed analyses of end-product synthesis patterns provided by continuous, real-time monitoring with the MIMS probe, it is possible to

conclude that rapid removal of CO_2 and H_2 allow carbon and reducing equivalents to flow from pyruvate to acetyl-CoA via the PFOR pathway, and away from synthesis of formate via the PFL pathway, and that this partially restricted redirection of electron and carbon flow towards ethanol synthesis. Furthermore, cultures with LSR growth environment, where comparatively high mass transfer resistance existed, was favourable for ethanol and lactate synthesis.

Chapter 6

Estimation of Formate, Acetate and Lactate Yields in *Clostridium termitidis* under Variable Substrate Loads Using a Stoichiometric End-product Algorithm

Abstract

The study of microbial metabolism under various environmental conditions involves tedious and labour intensive research, especially when replicated biological experiments are required. Appropriate instrumentation is also required to validate research hypotheses. Incorporating many measurement and analytical techniques may be an option; but this adds to the time and cost of the study. Indicators of metabolic activity, such as the C1/C2 ratio of fermentation end-products, the carbon recovery index (CRI), and the oxidation/reduction (O/R) ratio are useful in understanding microbial metabolism and how carbon and electrons are partitioned to various metabolic end-products. Unfortunately, many scientific reports on microbial fermentation do not report these indicators, making it difficult to fully understand the metabolic processes at work. Without a deeper understanding of these processes, it is difficult to optimize fermentation processes to maximize yields of desired products. As an alternative, we have developed a stoichiometric end-product algorithm, where real-time, on-line measurements of gaseous (H_2, CO_2, ethanol) metabolites produced during growth of *C. termitidis* and real-time titrimetric information on acid/base balance were used to predict the yields of non-volatile metabolites (formate, acetate, lactate) in a pH controlled bioreactor. Good agreement between the predicted and observed yields of these metabolites was obtained (below 5 % uncertainty) in both exponential and stationary phases of *C. termitidis* cultures. Greater uncertainty was observed in the late stationary phase of growth. The estimation algorithm was applicable when reliable on-line data was obtained under suitable physico-chemical conditions of bacterial growth.

Furthermore, the algorithm was able to notify, both qualitatively and quantitatively, trends in metabolic processes, such as when a particular end-product was produced, as well as increases or decreases in synthesis (metabolic shifts). The algorithm was also incorporated real-time titrimetric information that could be used for proton balance, therefore, allowed lactate estimation in addition to formate and acetate estimation.

6.1 Introduction

In a given reaction (chemical or biochemical), the stoichiometric co-efficients of the reaction products are very useful to establish the molar ratios between reactants and products. These co-efficients can be whole numbers or fractions, depending on types of reactions, their reaction intermediates, and the final products. Reactions in biological systems are more complex in nature compared to general chemical reactions. In biological systems, numerous reactions take place to fulfill the requirement of biochemical cycles. To understand the nature of biochemical cycles, scientists often use various biomarkers (gaseous or aqueous) to monitor reactions either with discrete, off-line measurements, or with real-time, on-line techniques, or a combinations of both.

In most papers on fermentation reported in the recent scientific literature (Holwerda et al. 2013; Holwerda and Lynd 2013; Munir et al. 2015; Munir et al. 2016; Thompson and Trinh 2017), indicators of metabolic activity, such as C1/C2 ratios of fermentation end-products, the carbon recovery index (CRI), and the oxidation/reduction (O/R) balance, are rarely reported. In most cases limited information on fermentation end-product concentrations or yields is available. Data on reaction stoichiometries can provide insights into carbon and electron flux through different metabolic pathway nodes (Sauer 2006; Liu et al. 2012) and enable a deeper understanding of the relationships between substrate utilization and product synthesis (Holwarda et al. 2013; Holward and Lynd 2013), as well as how these parameters relate to transcriptomic and proteomic analyses (Munir et al. 2015; Munir et al. 2016) during fermentation.

Although membrane inlet mass spectrometry (MIMS) was efficient in measuring volatile end-products (Pratt et al. 2003), it was unable to measure non-volatile products such as formate, acetate, lactate, pyruvate at, or near, neutral pH, either in gas phase or liquid phase. Johnson et al.

(1997) measured ethanol, acetate, and lactate simultaneously in the fermentation broth using a MIMS probe, by bringing down the pH below 1 with HCl (with the help of a custom built flow injection analyzer). Diamantis et al. (2006) measured continuously volatile products in anaerobic fermenters using an on-line capillary gas chromatography at pH 5. These acidic conditions do not only affect the growth of microorganisms, but also the response of other volatile end-products, such as ethanol and CO_2. Therefore, it is necessary to find an alternative way of measuring non-volatile dissolved acids in addition to volatile end-products without compromising optimum growth conditions of the microorganism of interest.

On-line monitoring is essential for understanding real-time dynamics of microbial metabolism. The titrimetric and off-gas analysis (TOGA) system is a state-of-the-art instrument that combines mass spectrometry (MS), with a mass flow controller (MFC) and titrator. The TOGA system is ideal for detecting and quantifying concentrations of volatile fermentation end-products. We have developed a stoichiometric end-product algorithm (section 2.4.2) that uses real-time, continuous data on concentrations of volatile end-products as well as the titrimetric information to calculate the concentrations of non-volatile end-products (which cannot be measured in real-time).

6.2 Materials and Methods

The data obtained from Chapter 3 was used to validate the hypothesis that one can estimate, in real-time, the concentration of formate, acetate, and lactate on the basis of continuous data generated using TOGA. It is to be noted that for the fermentation of cellobiose, *C. termitidis* was cultured in 1191 media with 3 L working volume in a pH controlled bioreactor environment. The initial substrate concentrations were 10 g/L, 2 g/L, and 1 g/L. Detailed descriptions materials and methods are available in Chapter 2, Sections 2.1 and 2.4.

6.3 Results

6.3.1 Hydrogen, carbon dioxide and ethanol analysis

For predicting soluble metabolites, the real-time continuous data for H_2, CO_2 and ethanol were used. These data were obtained placing the MIMS probe above the liquid phase inside the reactor headspace. Most of the signals were quite stable and clear, even in the presence of high water vapour concentrations. However, the H_2 and CO_2 raw signals were noisy. This was attributed due to interference from water vapour at the MIMS probe surface, which was beyond the scope of our current discussion. A regression analysis was performed for H_2, CO_2 and ethanol between the MIMS signals of biological replicates, and was found reasonably correlated to each other (supplementary Table S6.1). 95 % of the signal population falls with in confidence intervals 1.003 and 1.372 for the slopes with standard error limit 0.001 to 0.004. The majority of the variability between the replicates in H_2, and CO_2 measurements originated from the late stationary phase measurements. Furthermore, there might have some degree of suppersaturation of product gases (H_2 and CO_2) into the broth, which did not quantify. Suppersaturation of H_2 creates positive environment for enhenceing ethanol synthesis, which has been shown during the growth *C. termitidis* on 2 g/L cellobiose in Chapter 5. During gas-phase measurements, ethanol provided comparatively good/decent signals (slope = 0.999, standard error 0.002 with R^2 = 0.992), confirming that ethanol vapour was in thermodynamic equilibrium with the liquid phase (Oeggerli and Heinzle 1994).

6.3.2 Estimation of formate and acetate concentrations

Since the data (H_2, CO_2, and ethanol) showed reasonable agreement among the biological replicates, therefore by placing these data in Equation 2.22 and Equation 2.23 the predicted formate and acetate concentrations were obtained, and presented in Figure 6.1. Formate and

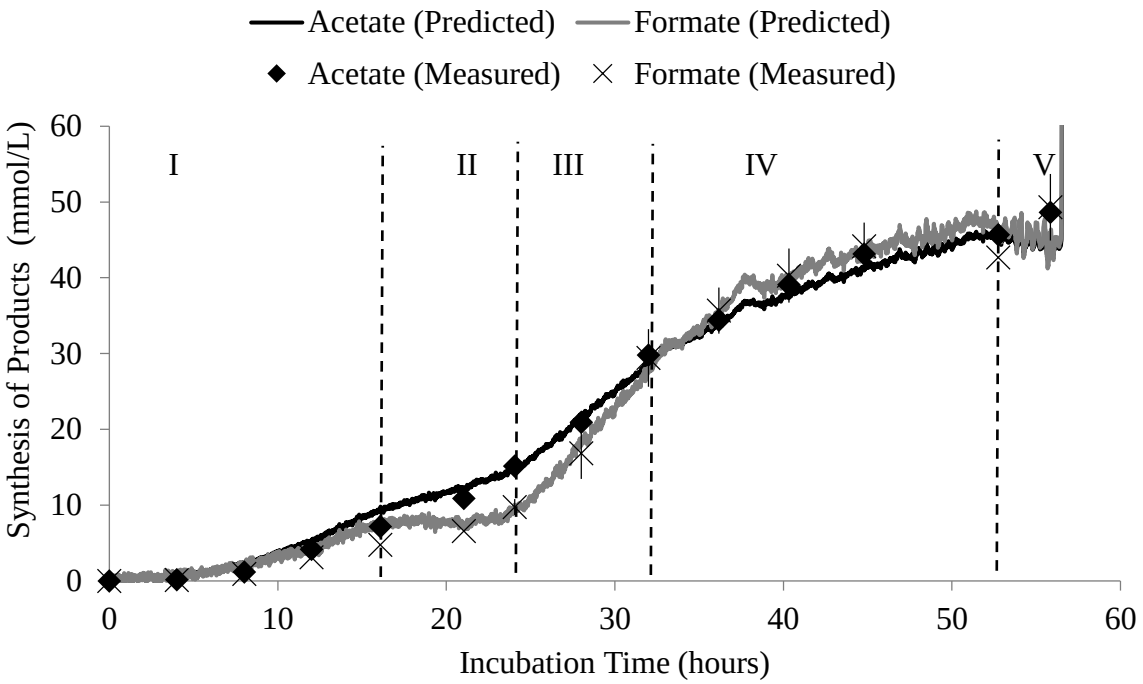

Figure 6.1 Estimations of formate and acetate synthesis patterns over the growth phases of *C. termitidis* cultured with cellobiose under carbon-excess condition. Concentrations of formate and acetate were calculated using the proposed stoichiometric algorithm using on-line MIMS measurements of H_2, CO_2, and ethanol. Average concentrations of acetate and formate measured off-line by HPLC are indicated with discrete points. Roman numbers (I –V) indicate various growth phases, as specified in Chapter 3, Figure 3.2.

acetate production followed a similar trend during the exponential growth phase. There was no significant increase in formate production during the late exponential phase II (between 16 h and 24 h pi). Concentrations of both formate and acetate synthesis increased rapidly in early stationary phase III (between 24 and 32 h pi), and then decreased significantly in stationary phase IV (between 32 h and 52 h pi).

When continuous predicted data were compared with discrete data (obtained from off-line HPLC) for formate and acetate concentration, a reasonable agreement was observed (Figure 6.2). Although the biological replicate 1 showed better correlations (slope = 0.899, std. error = 0.018, $R^2 = 0.996$, $p < 0.05$ for formate; and slope = 0.910, std. error = 0.019, $R^2 = 0.995$, $p < 0.05$ for acetate), slight deviations were observed with biological replicate 2 near end of stationary growth phase IV (supplementary Table S6.2). Due to high instrument noise at the early stages (growth phase I) of the fermentation reaction, the algorithm predicted some values to be negative. This is not possible, and consequently, these results were assigned a default value of zero. Furthermore, Figure 6.3 shows that the predicted levels of formate and acetate are in acceptable agreement with corresponding biological replicates throughout the entire growth phase of *C. termitidis*. Deviations, occurred in the late stationary phase, were due to generation of foaming, which may caused poor gas transfer during headspace measurement.

A)

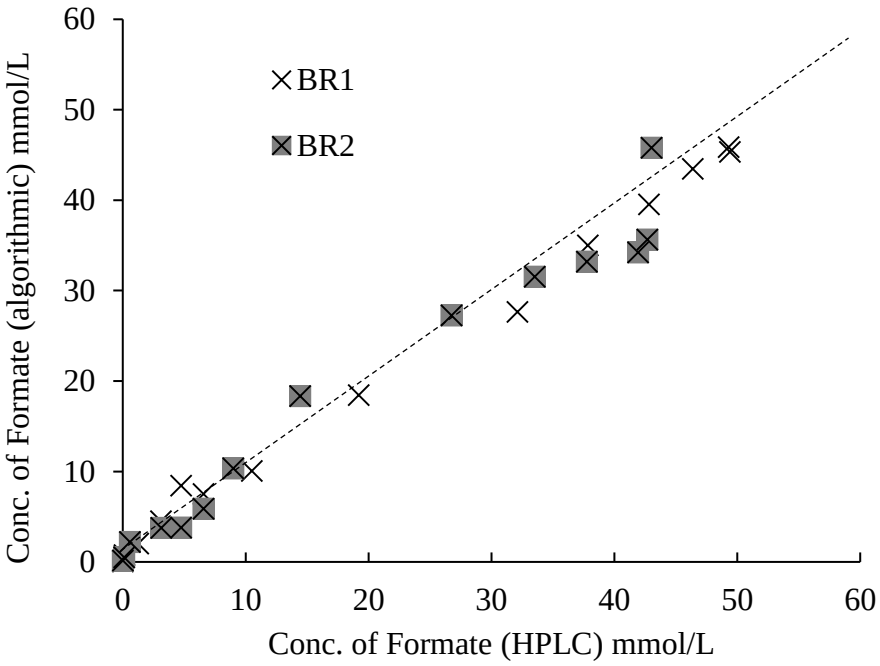
Conc. of Formate (algorithmic) mmol/L
Conc. of Formate (HPLC) mmol/L
BR1
BR2
0
10
20
30
40
50
60

B)

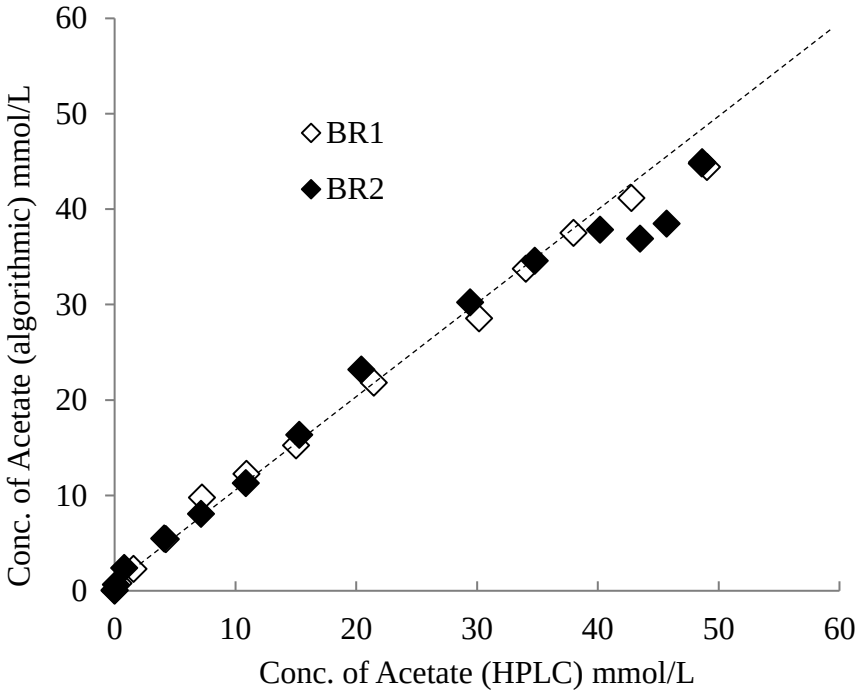
Conc. of Acetate (algorithmic) mmol/L
Conc. of Acetate (HPLC) mmol/L
BR1
BR2
0
10
20
30
40
50
60

Figure 6.2 Correlation between estimated (algorithmic) and HPLC data A) formate and B) acetate throughout entire growth phase of *C. termitidis* with two biological replicates. Cross (x) and open diamond (◊) for biological replicate 1 (BR1) and filled cross (x) and filled diamond (♦) for biological replicate 2 (BR2).

A)

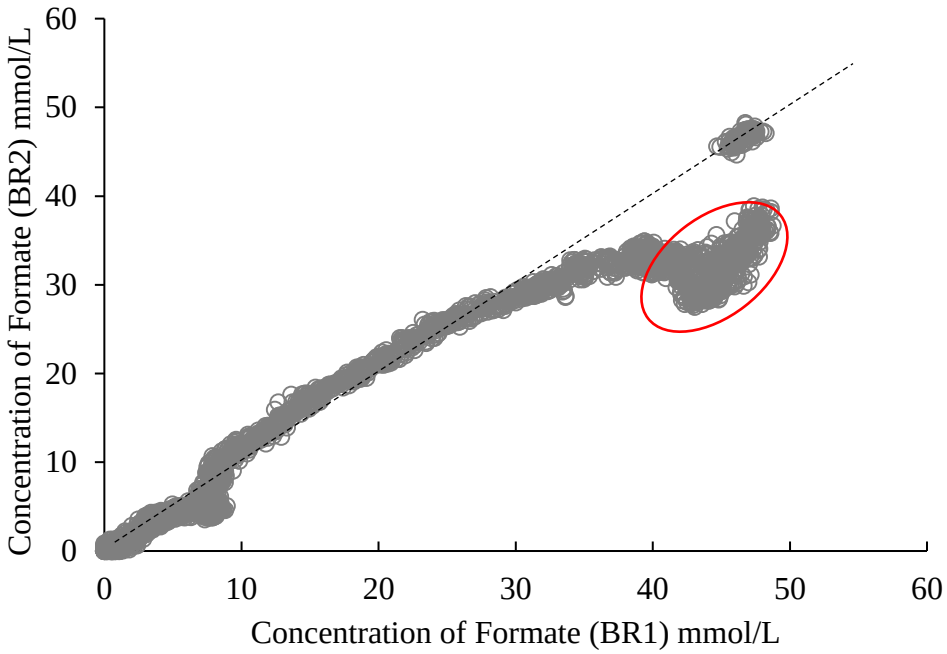
Concentration of Formate (BR2) mmol/L
0
10
20
30
40
50
60
Concentration of Formate (BR1) mmol/L

B)

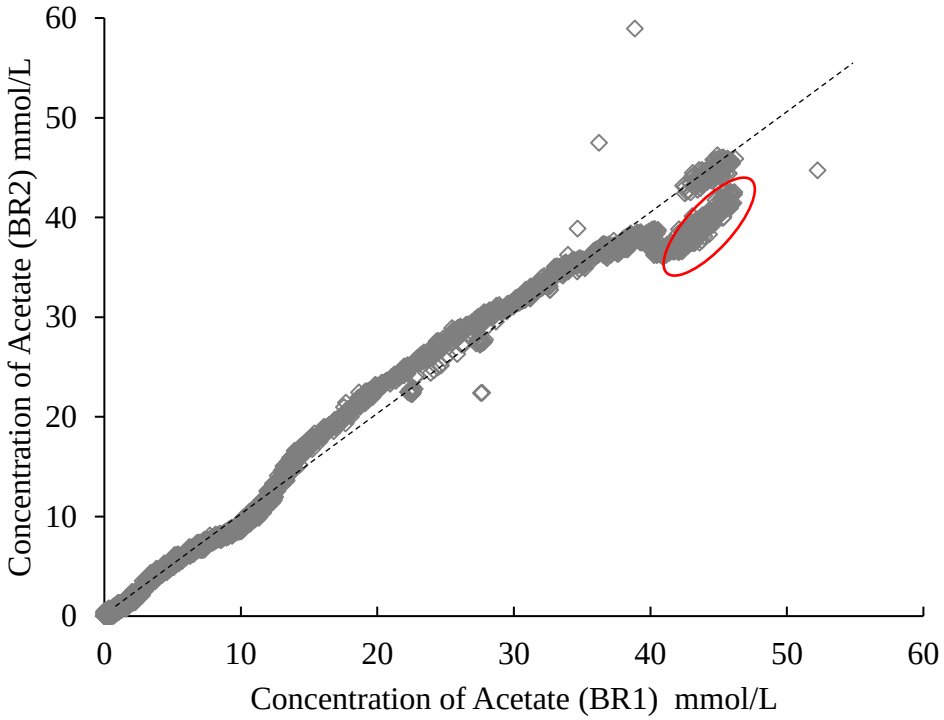
Concentration of Acetate (BR2) mmol/L
0
10
20
30
40
50
60
Concentration of Acetate (BR1) mmol/L

Figure 6.3 Correlation of estimated (algorithmic) data A) formate and B) acetate between two biological replicates throughout entire growth phase of *C. termitidis*. Open circle (○) and open diamond (◊) represents formate and acetate, respectively for biological replicate 1 and 2. Red circles represent deviated regions in late stationary phase due to biological replicate 2.

6.3.3 Estimation of lactate concentrations

Figure 6.4 shows the trend of lactate production (using the estimation algorithm) throughout the entire growth phase, as well as lactate concentrations obtained by discrete, off-line HPLC measurements. The predicted concentrations were slightly higher than the concentrations determined by off-line measurement (Figure 6.4A), which needed some modifications in the algorithm. Figure 6.4B showed lactate synthesis originated from modified algorithm, which discussed later in Section 6.4.4. Both measurement techniques confirmed that lactate did not produce until *C. termitidis* growth environment reached mid to late exponential phase. The final concentration of lactate was obtained 5.2 ± 0.8 mmol/L (Table 6.2).

6.3.4 Reaction stoichiometry using estimated signals

Until the use of continuous, real-time, on-line measurement of volatile fermentation end-products, it has not been possible to detect the subtle and rapid shifts in microbial metabolism in response to changes in external and/or internal growth environments. In the previous sections (Sections 6.3.2 and 6.3.3), we observed changes in formate, acetate, and lactate synthesis patterns using O/R and C1/C2 ratios. In this section, we shall describe much deeper information about metabolic changes during the growth of *C. termitidis* by using other reaction stoichiometric ratios, such as H_2:CO_2; formate:CO_2; H_2:acetate; EtOH:acetate.

Figure 6.5 and Figure 6.6 show changes in reaction stoichiometry along with production variations (Figure 6.7) of H_2, CO_2, formate, and ethanol over the course of the fermentation reaction. Furthermore, to assess pyruvate catabolic reactions in real-time and how it vary over the course of fermentation in various growth phases, a stoichiometric comparison is derived and shown in Table 6.1. From the discrete measurements (Chapter 3), some of these changes could not be revealed properly or precisely. For example, synthesis of formate remained steady in late

exponential phase II; and beginning of early stationary phase III, both ethanol and formate synthesis rose sharply until continuous product ratios were obtained. Furthermore, how H_2:acetate ratio rose from early exponential phase I to end of late exponential phase II (1 to 1.5 in Figure 6.6 A) was unnoticeable with discrete measurement. Steady rise of ethanol to acetate ratios (0.3 to 0.7) was observed after end of late exponential phase II.

The carbon recovery index, calculated using on-line measurements, off-line measurements, or a combination of both methods, did not exceeded 80 %, which implies that there might have some metabolites (intermediates or end-products) present in the broth or accumulated in the cell that were not accounted for.

A)

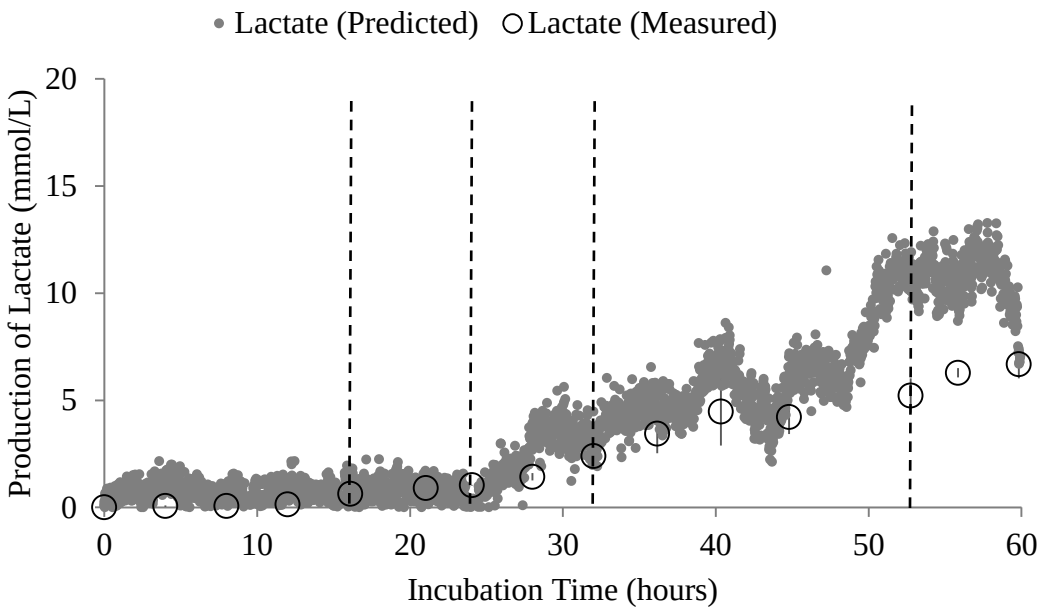
Lactate (Predicted)
Lactate (Measured)
Production of Lactate (mmol/L)
0
5
10
15
20
0
10
20
30
40
50
60
Incubation Time (hours)

B)

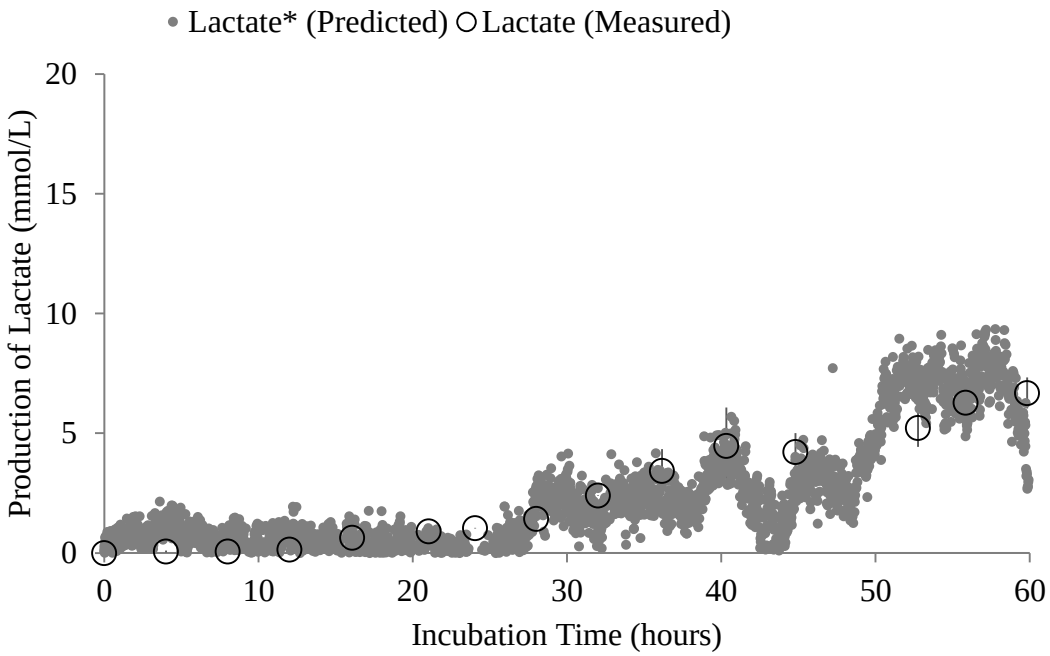
Lactate* (Predicted)
Lactate (Measured)
Production of Lactate (mmol/L)
0
5
10
15
20
0
10
20
30
40
50
60
Incubation Time (hours)

Figure 6.4 Estimation of lactate synthesis using the stoichiometric algorithm, with concentrations obtained by discrete HPLC measurement. Grey solid circle (●) represents predicted lactate concentration A) using Equation 2.24, and B) using Equation 6.1, and open circle (○) discrete HPLC concentrations of lactate. Average values of two biological replicates are represented here for all data.

A)

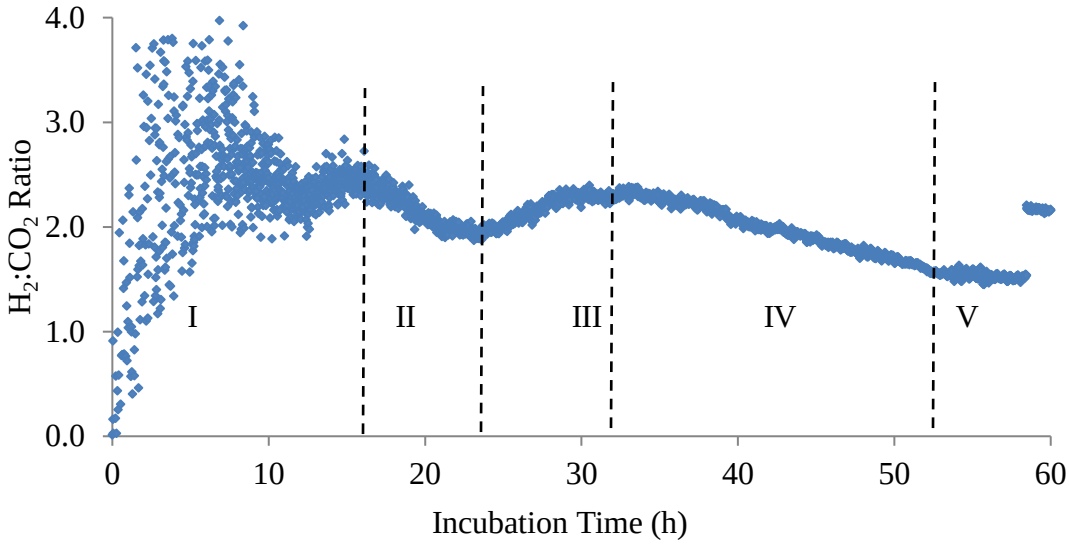

B)

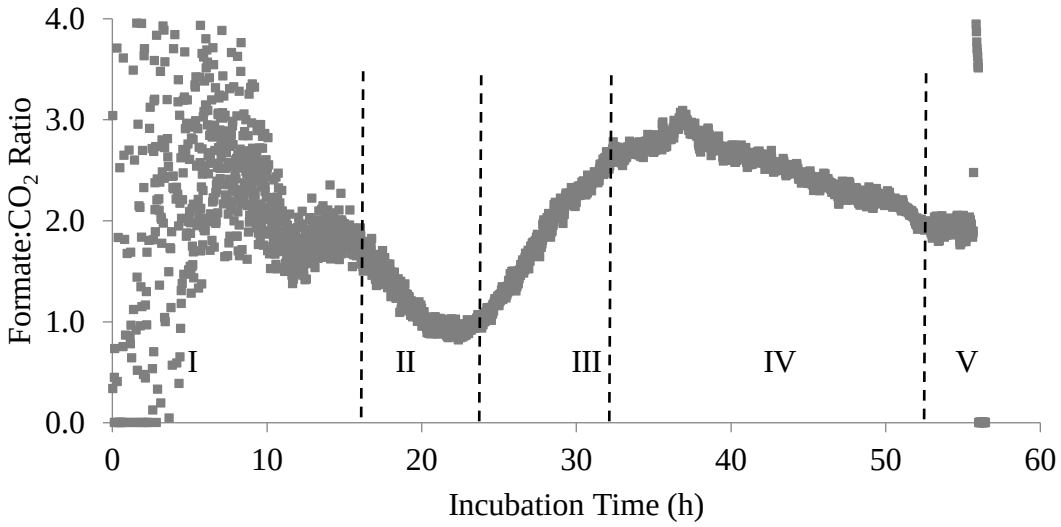

Figure 6.5 Hydrogen:carbon dioxide (H_2:CO_2) and formate:carbon dioxide (Formate:CO_2) ratios derived from real-time, on-line MIMS measurements using estimation algorithm over the course of *C. termitidis* fermentation in various growth phases (I-V). A) Shifts in hydrogen:carbon dioxide (H_2:CO_2) ratios; and B) Shifts in formate:carbon dioxide (Formate:CO_2) ratios.

A)

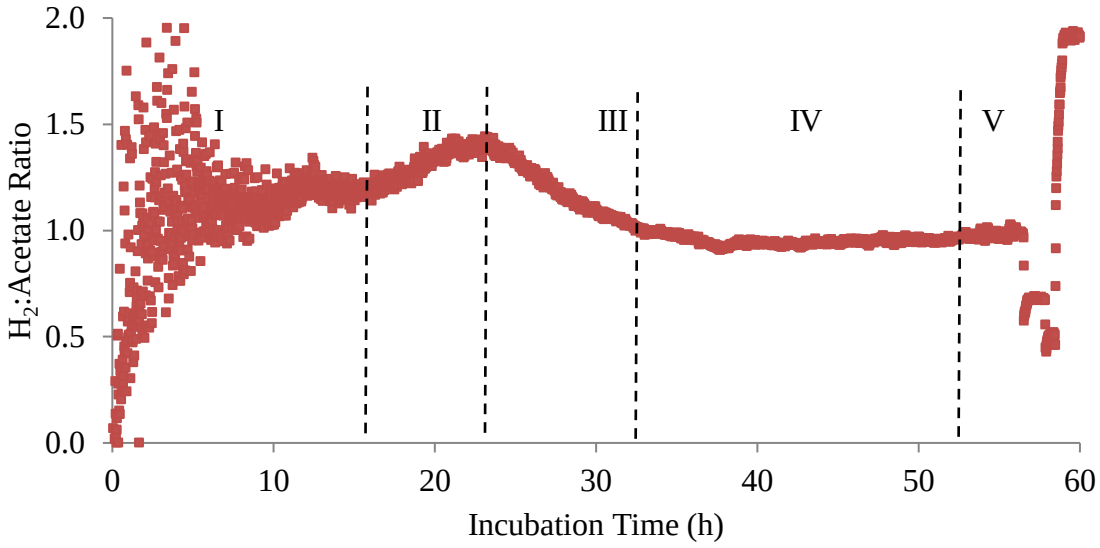

B)

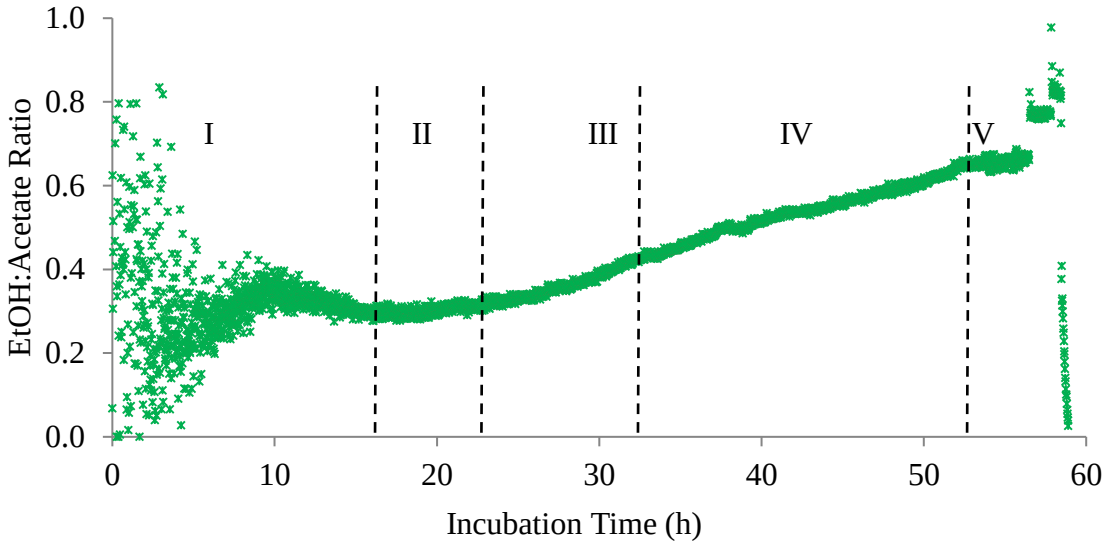

Figure 6.6 Hydrogen:acetate (H_2:Acetate) and ethanol:acetate (EtOH:Acetate) ratios derived from real-time, on-line MIMS measurements using estimation algorithm over the course of the *C. termitidis* fermentation reaction in various growth phases (I-V). A) Shifts in hydrogen:acetate (H_2:Acetate) ratios; and B) ethanol:acetate (EtOH:Acetate) ratios.

A)

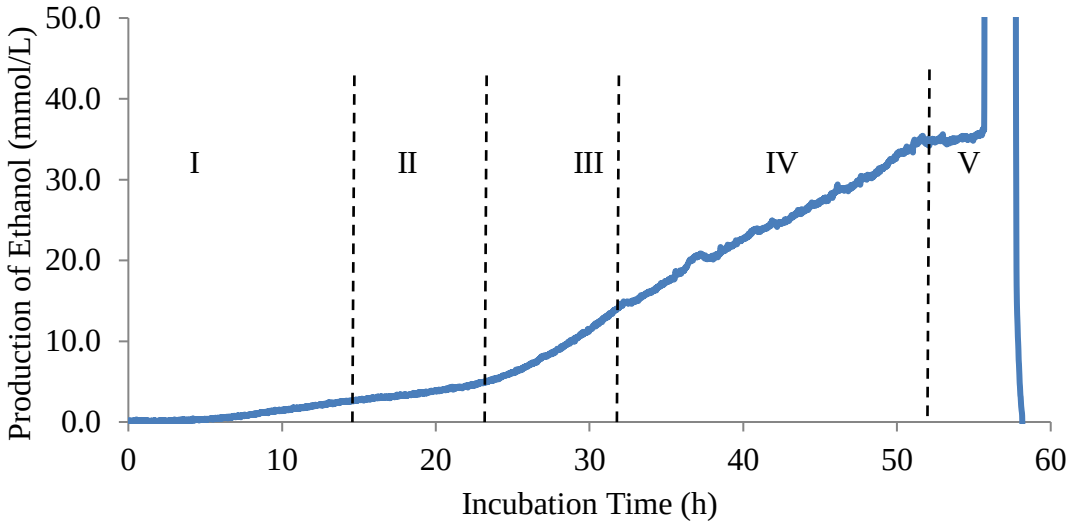

B)

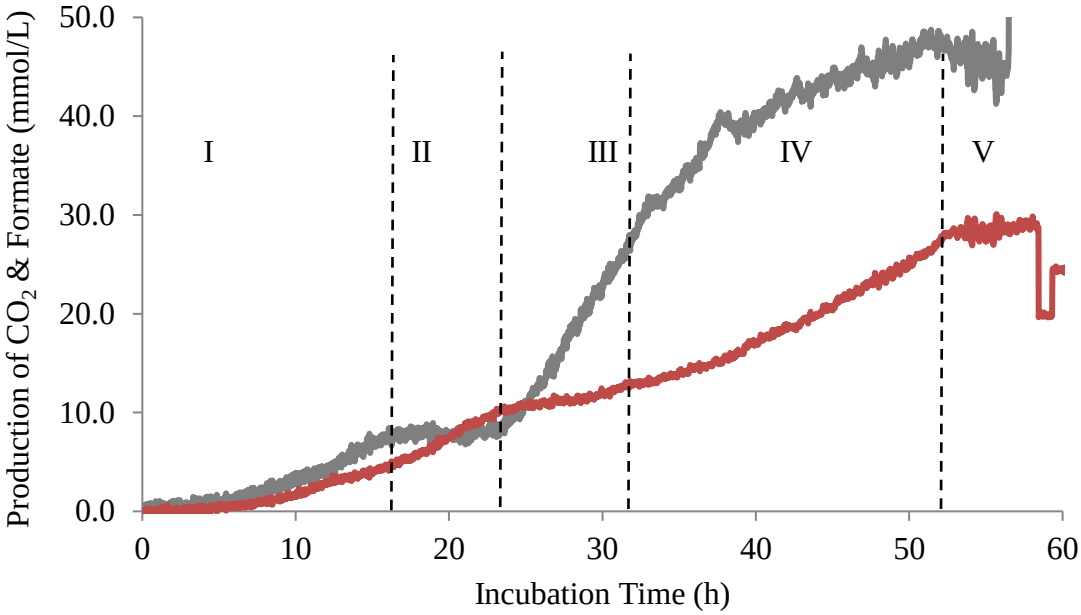

Figure 6.7 Metabolic shifts in various growth phases (I-V) during *C. termitidis* fermentation derived using estimation algorithm and from direct MIMS probe measurement. A) Production of ethanol (blue); B) production of predicted formate (grey) and carbon dioxide (brick red).

Table 6.1 Variation of product ratios under various growth phases of *C. termitidis* along with changes in end-product synthesis on 10 g/L cellobiose load (derived from Figure 6.5, Figure 6.6 and Figure 6.7).

Substrate Load (g/L)	Growth Phase	H_2:CO_2	Fo:CO_2	H_2:Ac	Et:Ac	Formate	CO_2	Ethanol
10	I	High > 2	High 3.0 – 1.8	Low 1.3 – 1.2	Low 0.2 – 0.3	Gradual increase	Gradual increase	Gradual increase
	II	Decrease 2	Decrease 1.8 – 1.0	Increase 1.2 – 1.5	Increase 0.3 – 0.3	Remained constant	Increase	Increase
	III	Increase > 2	Increase 1.0 – 2.5	Decrease 1.5 – 1.0	Increase 0.3 – 0.4	Sharp rise	Remained steady	Sharp rise
	IVa	Decrease 2	Increase 2.5 – 3.0	Constant 1.0 – 1.0	Increase 0.4 – 0.5	Gradual rise	Gradual rise	Increase constant rate
	IVb	Decrease 1.5	Decrease 3.0 - 2.0	Constant 1.0 – 1.0	Decrease 0.5 - 0.7	Slow rise	Gradual rise	Increase constant rate

IVa = 32 – 40 hrs pi and IVb = 40 – 52 hrs pi, while both represent stationary growth phase. Fo = formate; Ac = acetate; Et = ethanol

Table 6.2 Variation of *C. termitidis* growth phases along with various acids and H^+ ion production under variable substrate (cellobiose) loads[¥].

Substrate load [Ψ] (g/L)	Lag phase	Exponential phase	Decline phase	Lactate mmol/L	Acetate mmol/L	Formate mmol/L	CO_2 mmol/L	H^+ ion mmol/L	Acid recovery %	Unknown metabolites (H^+ ion eqv) %
10	0 h	4 - 16 h	52 - 53 h	5.2 ± 0.8	48.6 ± 0.5	46.2 ± 4.4	27.5 ± 5.6	133.9 ± 1.0	95.2 ± 2.1	4.8 ± 2.1
2	4 – 5 h	8 - 18 h	23 - 24 h	1.2 ± 0.2	13.9 ± 0.7	7.5 ± 0.7	14.2 ± 0.8	38.4 ± 1.3	95.4 ± 3.1	4.6 ± 3.1
1	2 h	6 - 14 h	16 h	0.5 ± 0.1	8.5 ± 0.9	6.2 ± 0.1	8.5 ± 0.5	24.0 ± 0.7	98.0 ± 0.4	2.0 ± 0.4

¥ = These experiments were performed in a bioreactor under pH controlled (7.20 ± 0.02) conditions; Ψ = Represents biological replicates (N=2) except for 2 g/L, where N=3.

6.3.5 Applicability of estimation algorithm under carbon-limited and carbon-sufficient conditions

The stoichiometric algorithm is also used to predict formate, acetate, and lactate concentrations in *C. termitidis* fermentation reactions under carbon-limited (1 g/L cellobiose) and carbon-sufficient (2 g/L cellobiose) conditions (Figure 6.8 and Figure 6.9) and are summarised in Table 6.2. Both conditions had a 2 to 5 hour lag phase, which delayed the onset of formate, acetate, and lactate (data not shown here) synthesis. Similar lag was also observed in ethanol synthesis. However, predicted concentrations of acetate and formate were in reasonable agreement with the concentrations of acetate and formate determined by off-line, HPLC measurement (shown as discrete points with error bars in the figures). No significant shifts in *C. termitidis* metabolism were observed under either carbon-limited or carbon-sufficient conditions.

6.4 Discussion

Reliably obtained real-time data (H_2, CO_2, EtOH and HP) used in stoichiometric algorithm, which are important in explaining pyruvate catabolic reactions (statistical analysis point of view).

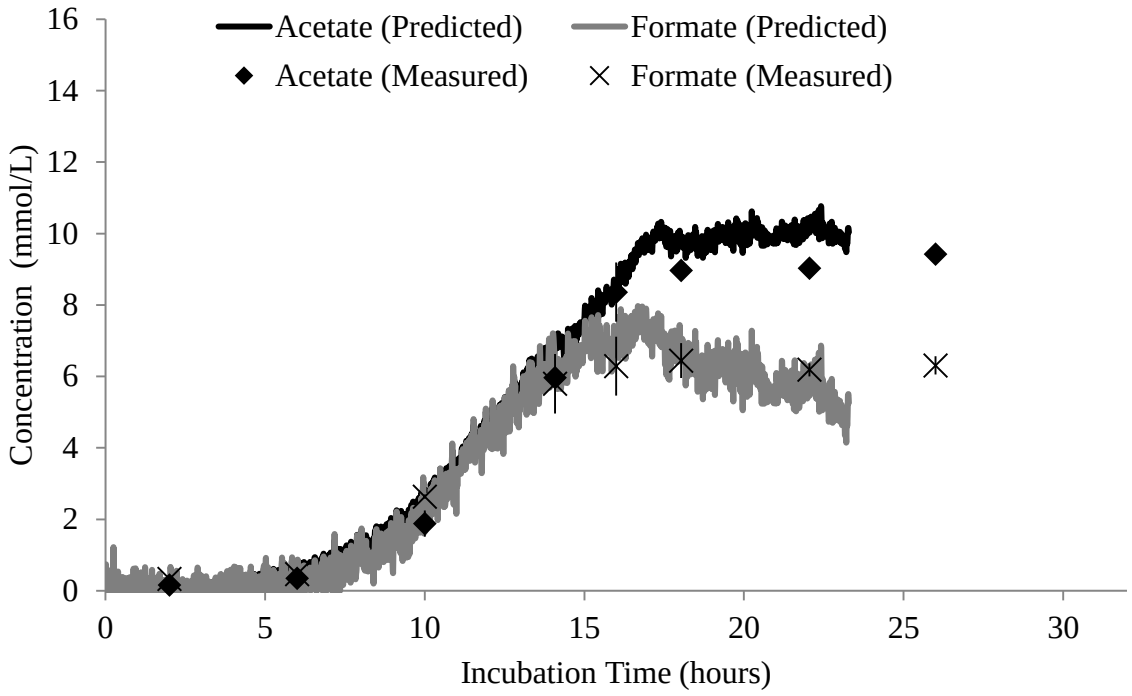

Figure 6.8 Formate and acetate concentrations produced by *C. termitidis* cultured with 1 g/L cellobiose in a 7 L bioreactor. Solid black line, acetate concentrations predicted by the stoichiometric algorithm based on on-line MIMS measurements of H_2, CO_2, and ethanol; Solid grey line, formate concentrations predicted by the stoichiometric algorithm based on on-line MIMS measurements of H_2, CO_2, and ethanol; Black diamonds (♦), acetate concentrations determined by discrete, off-line HPLC measurements; Crosses (x), formate concentrations determined by discrete, off-line HPLC measurements. Discrete points represent the means of two biological replicates. Vertical lines through the discrete points represent standard error bars.

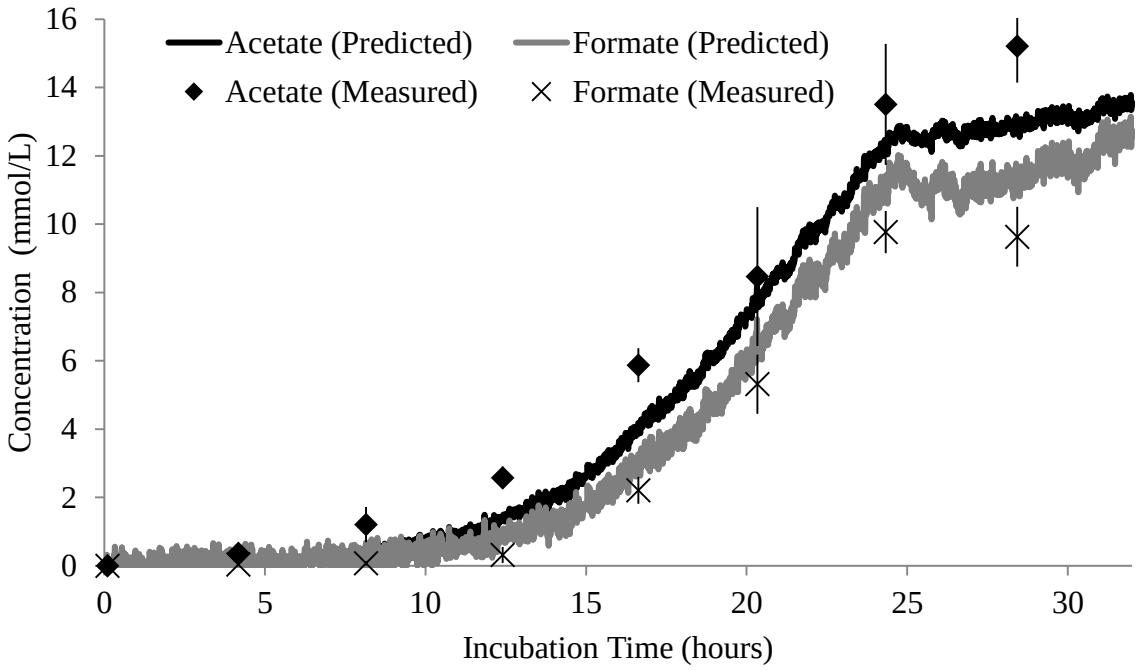

Figure 6.9 Formate and acetate concentrations produced by *C. termitidis* cultured with 2 g/L cellobiose in a 7 L bioreactor. Solid black line, acetate concentrations predicted by the stoichiometric algorithm based on on-line MIMS measurements of H_2, CO_2, and ethanol; Solid grey line, formate concentrations predicted by the stoichiometric algorithm based on on-line MIMS measurements of H_2, CO_2, and ethanol; Black diamonds (♦), acetate concentrations determined by discrete, off-line HPLC measurements; Crosses (x), formate concentrations determined by discrete, off-line HPLC measurements. Discrete points represent the means of two biological replicates. Vertical lines through the discrete points represent standard error bars.

6.4.1 Changes of pyruvate catabolic reactions growth phase-wise

C. termitidis associates pyruvate catabolic reactions in two main nodes while consuming cellobiose. First, pyruvate/acetyl-CoA/lactate branch point, where pyruvate catabolic reactions involve synthesis of a) CO_2, acetyl-CoA and reduced ferredoxin using PFOR, b) formate and acetyl-CoA using PFL, and c) lactate using LDH. Later, acetyl-CoA/ethanol/acetate branch point, where acetyl-CoA catabolism involves ethanol synthesis using bifurcating ADH-E with NADH reoxidation, and acetate synthesis using PTA/ACK with ATP generation. Furthermore, high H_2:CO_2 ratio (2.5) in exponential phase indicates that *C. termitidis* used all possible ways (Fd-H_2ase, NADH-H_2ase) to synthesis H_2 and its synthesis varies over the course of fermentation indicates the adjustment of these hydrogenase activities accordingly. In the following sections (6.4.2 to 6.4.4), how carbon, electrons and reducing equivalents shifted from one node to another node (under various growth phases) will be discussed.

6.4.2 Formate estimation

There was no significant increase in formate production during the late exponential phase II (between 16 h and 24 h pi). Because carbon flux probably started shifting from pyruvate to lactate synthesis using LDH at this growth stage. In addition, the continuous use of the PFOR pathway over the PFL pathway may have resulted in the maximum synthesis rate of CO_2. These results were corroborated with constant decline of formate to CO_2 ratio (1.8 to 1.0). Concentrations of formate synthesis increased rapidly in early stationary phase III (between 24 and 32 h pi) due to preferential use of PFL pathway over PFOR pathway by the *C. termitidis*, which has been supported by increased formate to CO_2 ratio (1.0 to 2.5). The synthesis rate of formate decreased significantly during stationary phase IV (between 32 h and 52 h pi), probably due to low influx of cellobiose.

Formate synthesis was surpassed acetate synthesis near the end of the early stationary phase III (around 32 h pi) due the preferential use of the PFL pathway over the PFOR pathway. At or near late stationary (IV) and decline phase (V), formate and acetate concentrations were slightly underestimated in biological replicate 2 (Figure 6.2A), as the on-line MIMS signals diverged from discrete off-line HPLC measurements. This may have been due to instability in the on-line CO_2 signal (probably foaming caused weak mass transfer) as the cultures approached stationary phase. Blunt (2013) also observed unstable and oscillatory signals, when estimating formate and acetate produced by *C. thermocellum* in stationary phase. This implied that the estimation algorithm was unable to explain biochemical reactions precisely that took place late stationary and decline phase. Blunt (2013) also observed that instability in the MS signal for CO_2 was due to predominantly the presence of water vapour in the measurement matrix and that it affected the ability of the algorithm to predict acetate and formate concentrations during the growth of *C. thermocellum* at 60 ^{o}C. Thus, the algorithm was extremely sensitive to variations in gas phase measurements (e.g. H_2, CO_2 concentrations), so confidence in calibration methodology and accuracy of measurement was critical.

6.4.3 Acetate estimation

Estimations of acetate concentrations based on on-line MIMS measurements showed minor deviations (minimum error) with respect to discrete, off-line HPLC measurements, which showed that acetate concentrations were reasonably stable thorough the growth phase (Figure 6.2B). Acetate is produced to keep up ATP generation so that cells can use this energy for substrate consumption as observed in *C. cellulolyticum* (Guedon et al. 1999).

Although the carbon flux started shifting from pyruvate to lactate synthesis during late exponential growth phase II, acetate synthesis kept increasing with slower rate. Because portion

of acetyl-CoA, produced from either PFOR or PFL pathways, was shifted towards ethanol synthesis using bifunctional alcohol dehydrogenase (AdhE). These results were corroborated with constant decline of formate to CO_2 ratio (1.8 to 1.0). Concentrations of acetate synthesis increased rapidly during early stationary phase III (between 24 and 32 h pi) due to preferential use of PFL pathway over PFOR and LDH pathways and followed by increased ethanol synthesis, which has been supported by increased formate to CO_2 ratio (1.0 to 2.5) and continual increase of ethanol to acetate ratio (0.3 to 0.4). The synthesis rate of acetate decreased significantly during stationary phase IV (between 32 h and 52 h pi), probably due to the use of electron and reducing equivalents towards ethanol synthesis via ADHE pathway over PTA/ACK pathway, which has been clearly observed from continuous rise of ethanol to acetate ratios 0.4 to 0.7 (Figure 6.6B and Table 6.1).

In the present set of experiments (Figure 6.6A and Table 6.1), conditions were less suitable for ethanol production when the H_2:acetate ratio was > 1 (Phase I, Phase II, and at the beginning of phase III), possibly because a significant portion of the electrons were used during H_2 synthesis. On the other hand, when th H_2:acetate was ratio near 1 (end of Phase III and through out Phase IV), the available electrons (which were not being used for H_2 synthesis) were available for ethanol synthesis. Therefore, higher ethanol synthesis was observed as the H_2:acetate ratio approached 1 and it was maintained throughout stationary phase (Phase IV). At the same time, formate was produced favorably to compensate less H_2 and CO_2 synthesis, because 1 mole formate is equivalent to 1 mole H_2 plus 1 mole CO_2.

It is possible that measurement error associated with each of the input variables in the algorithm are compounded and result in slightly deviated estimation of acetate. In particular, error in CO_2 measurements seem to have the most detrimental effect on the algorithm output

(Equation 2.23). The measurement of CO_2 could be improved by accounting for salting-out effect of the dissolved gases in ionic media (Goldberg et al. 2002; Schumpe 1993; Stumm and Morgan 1996; Weisenberger and Schumpe 1996). The algorithm itself could be improved by employing a filter to remove some of the extraneous values associated with instrument noise, which are commonly incorporated into software sensors (Chéruy 1997; de Assis and Filho 2000). The only filtering technique employed in this study was to remove negative values.

6.4.4 Lactate estimation

Conversion of pyruvate to lactate via NADH dependent LDH diverts reducing equivalents away from H_2 and ethanol synthesis. It is generally observed in *Clostridia* species under high substrate loads (Guedon et al. 1999; Ellis et al. 2012). The reducing equivalents NADH and ferredoxin reductase (Fd_r) are generated by the oxidative decarboxylation of pyruvate to acetyl-CoA via PFOR. NADH and ferredoxin reductase are oxidized to NAD^+ and ferredoxin oxidase (Fd_o) during H_2 and ethanol synthesis. Lactate synthesis rate did not change significantly, because probably its synthesis was independent of pH in the present study. Literatures also suggests that synthesis of lactate may be independent of Fd:NADH as it is allosterically regulated at fructose-1,6-biphosphate (FBP) (Guedon et al. 1999) and acidic pH may enhance LDH activities (Desvaus et al. 2001) which ultimately ended up with high lactate synthesis (data not shown here).

The predicted concentrations of lactate synthesis were slightly higher than the concentrations determined by off-line HPLC measurement using Equation 2.24 (Figure 6.4A), because the stoichiometric algorithm does not take into account other products, such as pyruvate or other acids (e.g. butyrate, succinate), which have been observed to be secreted by other mesophilic *Clostridium* species, such as *C. cellulolyticum*, *C. cellobioparam*, and *C.*

acetobutylicum (Ren et al. 2007; Giallo et al. 1983). Thus, Equation 2.24 was not be able to determine lactate concentrations under all fermentation conditions, and an alternative algorithm may be required to predict the true lactate concentrations produced. In the present experiments with *C. termitidis*, significant lactate synthesis was not observed until the fermentation reaction reached the late exponential phase II, and the lactate synthesis rate did not vary significantly through the stationary phase, which was observed in Chapter 3. On an average 5.22 ± 0.79 mmol/L lactate was produced by the end of the fermentation reaction.

Analysis of H^+ ion equivalents, determined by the amount of base used to maintain the culture pH, indicated that the acid strength of the *C. termitidis* culture medium was approximately 5 % greater than that contributed by the synthesis of acetate, formate, and lactate, suggesting that other, unknown, acidic metabolites were produced by *C. termitidis* when it was cultured with 10 g/L cellobiose. Although this change was significant at $p < 0.10$ for 10 g/L cellobiose, it was insignificant for 2 g/L and 1 g/L substrate (Table 6.2, Table S6.3, and Figure S6.1). Previous studies of fermentation reactions containing *Clostridium* species, including *C. cellulolyticum*, *C. cellobioparam*, *C. acetobutylicum*, and *C. thermocellum*, showed that extra-cellular fermentation products, such as pyruvate, butyrate, and/or malate were produced under carbon-excess conditions (Ellis et al. 2012; Liu et al. 2012; Ren et al. 2007; Desvaux 2005). Therefore, it may be reasonable to assume approximately 2-5 % deviation of the total H^+ ion equivalents from the late exponential phase to late stationary phase concentrations of lactate. Revised lactate estimation Equation 2.24 can be written as follows

$$C_L = C_{H+\ ion} - (C_F + C_A + C_{CO_2}) - C_U\ (H^+ \text{ ion equivalent}) \qquad 6.1$$

where, C_L concentration of lactate, $C_{H+\ ion}$ concentration of H+ ion obtained from base consumption, C_F concentration of formate, C_A concentration of acetate, C_{CO2} concentration of carbon dioxide, and C_U concentration of unknown metabolites (H^+ ion equivalent).

Differences between lactate concentrations predicted by the stoichiometric algorithm and the H^+ ion concentrations based on base-titration (Table 6.2) supports the hypothesis of the presence of unaccounted metabolites in the culture broth. The estimations of H^+ ion concentrations were off by 2 % to 5 % (H^+ ion equivalent), depending on substrate load, perhaps due to the production of acid end-products (pyruvate and other acids) that resulted in greater consumption of KOH under carbon-excess conditions.

This experiment was performed at least twice and must be replicated several times to gain more confidence in the measured values. Nonetheless, the algorithm was able to estimate formate concentrations within a reasonable degree of error, and also converged on the final measured acetate concentrations, albeit earlier estimations were higher than the measured values. On a qualitative basis, the algorithm was able to reveal trends, such as when a particular end-product, such as acetate or formate, was produced, when it increased or decreased, and when it stopped being produced.

6.5 Conclusion

By placing the MIMS probe in the reactor headspace immediately above the liquid surface, it was able to collect real-time, continuous, measurements of volatile fermentation end-products (H_2, CO_2, and ethanol) in the gas phase, and use these data along with titration data to predict concentrations of non-volatile fermentation end-products (formate, acetate, and lactate). Despite the high proportion of water vapour in the measurement matrix, the on-line MIMS measurements were in good agreement with off-line measurements by HPLC. The carbon

recovery index, C1/C2 ratios, and O/R balance were all close to the theoretical values, for both the on-line and off-line measurements. Low carbon recovery in both on-line and off-line measurements indicated that there may have been additional, unaccounted for end-products present in the aqueous phase, as observed for other *Clostridium* species, like *C. thermocellum*, *C. cellulolyticum, and C. cellobioparam* (Holwerda et al. 2014; Ellis et al. 2012; Desvaux 2004; Desvaux 2005; Ren et al. 2007), needs further investigations.

An algorithm was developed to predict formate and acetate from the on-line measurements of H_2, CO_2, and ethanol. Lactate was also detected off-line, so it was necessary to incorporate it into the algorithm with the H^+ ion production (HP). The proposed algorithm was able to predict acetate, formate, and lactate concentrations that were reasonably close to those measured by HPLC analysis. Estimations of the acetate, formate, and lactate concentrations produced by *C. termitidis* were more accurate compared to attempts to predict concentrations of these end-products in *C. thermocellum* (Blunt 2013) and less cumbersome compared to other methods of organic compounds measurement (Chauvatcharin et al. 1995; Diamantis et al. 2006; Demeestere et al.2007).

Thus, this stoichiometric algorithm could become a powerful tool to follow all of *C. termitidis* end-products in real-time either directly or indirectly through TOGA. The algorithm has demonstrated potential as both qualitative and quantitative tool for on-line monitoring of metabolic shifts in *C. termitidis* during cellobiose fermentation, which has important implications with respect to industrial process control (Tarkiainen et al. 2005). However, further study is necessary to develop this approach as an effective quantitative tool for fermentation of other substrates, such as cellulose. The proposed algorithm could be further improved by quantifying unknown metabolites and incorporating some degree of saturation factor for H_2 and

CO_2, and in addition to incorporation of a filter to remove unnecessary values in the algorithm input variables.

Chapter 7

Conclusions and Future Perspectives

7.1 Research objectives, hypotheses, and observed outcomes

The aim of the present research was to demonstrate changes in microbial metabolism as a consequence of changing growth conditions, which ultimately reflected metabolic shifts in end-product synthesis patterns. Differences in end-product synthesis resulting from metabolic shifts may be detected at the end of a fermentation reaction (stationary phase), or during the fermentation reaction based on analyses of samples taken at discrete time points within the growth (log) phase or the transition from log to stationary phase. However, analyses of samples taken at discrete time points are often insufficient due to limited number of sampling points, which may miss significant changes in metabolism that may have occurred between sample time points. A deeper understanding of microbial metabolism and the mechanisms responsible for changes in end-product synthesis patterns may be acquired by continuous monitoring. Thus, the primary goal of the research was to develop and validate analytical tools so that the characterization of instantaneous changes in metabolic flux (measured as changes in end-product synthesis patterns) can be achieved under various physico-chemical conditions.

To achieve this goal, detailed investigations of *Clostridium termitidis* fermentation using cellobiose were performed in various growth conditions (excess cellobiose, acetate induced, dissolved gas removal) and their outcomes are described below, under the heading of hypotheses. Before testing the hypotheses, the titration of $KHCO_3$ experiment was performed in a reactor environment, and was monitored both off-line (discretely) and on-line (continuously) techniques. The reliable and effective outcome of carbonate and bicarbonate species monitoring using continuous data, has led us to proceed with biological experiments. Discretely obtained

and analyzed data lack interpretation of those changes due to insufficient sampling points. The Titration and Off-Gas Analysis (TOGA) system was used as an on-line monitoring tool for headspace and liquid phase analysis of gases (H_2, CO_2 and ethanol) in addition to other analytical tools commonly used for fermentation metabolites analysis. *C. termitidis* was chosen as the model organism for this work because its genome has been sequenced (Lal et al. 2013) and its various growth characteristics have been studied recently (Ramachandran et al. 2008; Munir et al., 2014, 2015, 2016).

Hypothesis 1: Metabolic shifts in microbial metabolism are associated with physicochemical changes in cells growth environment. For the commercial viability, the growth of *C. termitidis* was studied at high substrate loads and compared with low substrate loads. We hypothesized that **under carbon-excess condition, re-distribution of fermentation end-products will occur through pyruvate catabolic reactions of *C. termitidis* compared to that in carbon-limited condition.** Therefore, the growth of *C. termitidis* was studied on high substrate load (10 g/L cellobiose) in a 7 L bioreactor under pH controlled condition and monitored using both on-line and off-line methods. In Chapter 3, it was shown that the growth of *C. termitidis* was highly dependent on substrate availability during its various growth phases. When *C. termitidis* was cultured in carbon-limited (1 g/L) to carbon-sufficient conditions (2 g/L), it produced acetate, formate and ethanol with slower rates, but at higher carbon loadings, such as 10 g/L cellobiose, these fermentation end-products produced comparatively higher rates, and they are dominant end-products under all conditions.

To clarify when and how these changes occurred during the growth of *C. termitidis*, substrate specific yields and cell specific production rates were calculated at various growth phases in Chapter 3. These analyses revealed that a number of key metabolic switches occurred

during the early stationary phase of growth (24-32 h pi). At early stationary phase, the CO_2 and H_2 production rates significantly decreased, while the specific ethanol and formate production rates increased significantly. Decreased CO_2 production and increased formate synthesis suggested that carbon flux shifted from the PFOR pathway to the PFL pathway. To maintain redox balance and the carbon balance, electron and carbon flow shifted from the PFOR pathway to the PFL pathway, resulting ultimately in increased ethanol production by *C. termitidis.* Lactate production rate did not vary significantly during stationary growth phase. Therefore, the first hypothesis was supported by data demonstrating the growth characteristics and metabolic shifts of *C. termitidis,* and evaluating associated ethanol synthesis rates and yields. Furthermore, a 4-fold increase in ethanol synthesis rate in early stationary phase compared to exponential phase suggests the active role of the pyruvate node in *C. termitidis* metabolism, as it regulates the competition between PFOR vs PFL pathways under high substrate loading.

Hypothesis 2: Perturbation studies are useful in understanding changes in microbial metabolism and reaction mechanisms. It is, however, tedious to monitor changes in metabolic pathway perturbations using off-line analytical techniques. *C. termitdis* follows branched fermentative pathways through pyruvate catabolic reaction and produces hydrogen, acetate, formate, carbon dioxide and ethanol while utilizing simple to complex sugars. It was hypothesized that **presence of exogeneous acetate during the exponential growth phase may divert C-flux towards ethanol production.** In response *C. termitdis* may rearrange its end-product distribution and synthesize a specific ratio of gaseous end-products. To test this hypothesis, cells were grown in 1191 medium containing 2 g/L xylose in a pH controlled 7 L bioreactor, with a 3 L working volume. The system was subjected to a perturbation by adding

acetate (resultant concentration 100 mmol/L) into the mid-exponential phase of culture, at a concentration of 8-fold higher than achieved from the fermentation of 2 g/L xylose.

In Chapter 4, it was demonstrated that the effect of adding exogenous end-products can be monitored with the help of the TOGA system for real-time metabolic shifts associated with the fermentation processes. Presence of elevated concentration of acetate during fermentation of *C. termitidis* showed immediate change (decrease) in H_2 synthesis rate, which ultimately leads to enhanced ethanol yields and decreased H_2 yields. To maintain stoichiometric balance in the presence of excess acetate, as measured by the C1/C2 ratio and the O/R ratio, the end-product distribution changed according to thermodynamic principles. This technique can assist with optimization studies under various physico-chemical conditions and reveals new strategies for maximizing biofuel yields from cellulosic biomass.

Hypothesis 3: Gaseous metabolites such as H_2 and CO_2 are present in the fermentation broth as dissolved form in the liquid phase, as well as in the headspace during fermentation. In large volumes of liquid culture medium, broth density (viscosity), foaming, and biofilm formation may limit mass transfer of the gases from liquid to gas phase during the fermentation reaction. Previous studies suggest that the concentrations of gaseous metabolites play a role in end-product synthesis. Significant elimination of dissolved gases can be accomplished either physically or chemically. Therefore, it was hypothesized that **quick removal of metabolic dissolved gaseous (by means of physical methods) will increase H_2 production and decrease ethanol production during the growth of *C. termitidis* in a pH controlled bioreactor.** In Chapter 5, the MIMS probe was used for analyses of fermentation end-products in *C. termitidis* cultures in both the aqueous phase and the bioreactor headspace. Because, the estimation of gaseous metabolites in aqueous phase from headspace analysis using Henry's Law is not always

accurate, the main objective was to measure dissolved H_2 and CO_2 directly from the liquid phase along with ethanol. If the aqueous phase was supersaturated with dissolved gases, then the effect of this regulation on microbial metabolism was evaluated.

Conditions of low and high mass transfer were provided by means of changes in agitation and sparging with nitrogen gas. In the high mass transfer experiment, agitation was increased from 100 rpm to 200 rpm, and nitrogen sparging was increased from 20 mL/min to 400 mL/ min without surface mixing. Ethanol was successfully measured in both cases and the results showed concentrations of 6.05 ± 0.05 mmol/L and 5.33 ± 0.07 mmol/L under low mass transfer and high mass transfer condition, respectively. There was about a 12 to 16% decrease in ethanol synthesis under high mass transfer (high rates of agitation and sparging) conditions compared to low mass (low rates of agitation and sparging) transfer conditions.

It was determined that super-saturation of H_2 occurred under both experimental conditions, despite a wide variations in k_La under high mass transfer conditions, resulting in a significant amount of H_2 that was not accounted for. Because supersaturation still occurred under high mass transfer conditions, which was not detrimental to cell growth, H_2 supersaturation may be inevitable in this system. Some supersaturation of CO_2 occurred under low mass transfer conditions, with no CO_2 supersaturation detected under high mass transfer conditions. When CO_2 supersaturation was present, however, the relatively high solubility of CO_2, can result in significant under-estimation of the total CO_2, even in cases with small supersaturation ratios of 1.2.

Ethanol, and CO_2 can be accurately quantified from the liquid phase, but supersaturation prevented accurate quantification of total H_2 (using headspace measurement), for which there was supersaturatated between 10 and 100 times the value expected at thermodynamic

equilibrium. This work demonstrates the value of TOGA, particularly the MIMS component, to obtain information in fermentation applications that few other instruments are able to study. Chapter 5 presented data supporting the third hypothesis, revealing which gaseous end-products are supersaturated, and how this can affect microbial metabolism in *C. termitidis*.

Hypothesis 4: To validate the fourth research hypothesis, that **continuous measurement of selected volatile biomarkers can be used to predict the overall changes in fermentation end-product synthesis,** Chapter 6 described a stoichiometric algorithm for the estimation of end-products those can not be measured in the gas phase by using simultaneous data on H_2, CO_2 and ethanol, obtained with the MIMS probe in the reactor headspace. The proposed algorithm could accurately predict acetate, formate, and lactate concentrations, although some noise was detected in the H_2 and CO_2 signal as the culture approached stationary phase due to unknown reason at this moment. Lactate concentrations were predicted using H^+ ion production rates measured from base consumption by on-line titration with a partially modified algorithm. Thus, the algorithm can be used as a qualitative tool as well as quantitative tool for fermentation processes and subtle changes in *C. termitidis* growth using only volatile gas measurements. This work fulfills the fourth objective inferring immeasurable end-products from products that can be measured using on-line method, showing that the MIMS probe combine with a stoichiometric algorithm can be used as a bioprocess engineering monitoring tool. This is an important bioprocess engineering achievement of the present work.

Thus the main objective, to develop and validate analytical tools so that the characterization of instantaneous changes in metabolic flux can be explained under various physico-chemical conditions, was ascertained or achieved by applying several observing methods in chemical and biological changes. For example, monitoring of chemically produced

CO_2, and tracking of *C. termitidis* growth under carbon-limited to carbon-excess conditions using both off-line (discrete) and on-line (continuous) techniques were used to check reliability and endorse analytical tools. Discrete methods such as off-gas measurement using GC, cells growth measurement using OD and protein assay, soluble end-products measurement using HPLC showed some degree of limitations in explaining chemical and metabolic changes due to insufficient sampling points and, which sometime suffers reproducing reliable results.

During titration of $KHCO_3$, chemical CO_2 produced so rapidly, therefore, adapting faster sampling frequency than one sampling per twenty minutes using GC was tedious and cumbersome task. Whereas, TOGA provided one sampling per minute (20-times more than the discrete GC technique) in both off-gas and pH measurements, which clearly helped in explaining carbonate/bicarbonate and carbonic acid/carbon dioxide equilibrium in aqueous as well as gaseous phase.

The off-gas measurement using continuous sampling techniques with MIMS probe and titrimetric systems helped to observe subtle changes during culture of *C. termitidis* under various growth conditions. In contrast, discrete sampling (OD, protein assay, GC, HPLC) four hours intervals was inadequate to see some changes (described above). It even sometime missed invaluable information. Furthermore, continuous data obtained from stoichiometric estimation algorithm facilitated us to understand how metabolic fluxes switch among themselves to maintain redox balance.

7.2 Engineering significance

Clostridium termitidis and other cellulolytic bacteria, like *C. thermocellum*, have the ability to convert cellulosic wastes into H_2 and ethanol, which could be used as biofuels. While the idea of converting waste into usable energy is laudable, it is important to evaluate this

technology from an engineering point of view to determine if these processes are feasible economically. To address this issue, an attempt has been made to evaluate the engineering significance of the present research.

a) This study has demonstrated that *C. termitidis* is able to synthesize ethanol with the highest specific yield (9.56 ± 0.37 mol/mol of cells DCW) under carbon-excess load (10 g/L cellobiose) compared to carbon-sufficient (2 g/L cellobiose) and carbon-limited (1 g/L cellobiose) loads. This is a significantly greater (4.5 fold) than the specific yield of 2.22 ± 0.32 mol/mol of cells DCW that was previously reported on 2 g/L cellobiose culture (Ramachandran 2013). The specific yield of H_2 was obtained 12.69 ± 0.87 mol/mol of cells DCW under carbon-excess load. The cells entering stationary phase triggered an increased in ethanol production in the presence of excess carbon, which was revealed from continuous measurement of headspace data. Nevertheless, this yield is better than those reported for other mesophilic *Clostridium* species;
b) The applied real-time on-line analytical tool, which generates continuous data, has provided the opportunity to observe insight conditions of *C. termitidis* growth on xylose in the presence of exogeneous acetate that causes the significant improvement of ethanol synthesis;
c) Presence of elevated concentrations of H_2 in the fermentation broth of *C. termitidis* enhances ethanol yield, possibly high H_2 prevents the production of further hydrogen. The thermodynamics decrease for H_2 production from NADH leads to a redirection of electrons to acetyl-CoA generating ethanol. Therefore, it is necessary to provide optimum physical conditions (sparging and agitation) for *C. termitidis* growth so that the culture broth maintains a threshold concentration of dissolved H_2 to maximize ethanol yields;

d) An algorithm to predict concentrations of non-volatile fermentation end-products, based on real-time, on-line measurements of volatile end-product concentrations using the MIMS probe, was applied. This algorithm not only offers an enormous opportunity as a bioprocess engineering monitoring tool to maximize yields of desired end-products, but also to identify subtle metabolic shifts and, potentially, detect the synthesis of unknown soluble metabolites.

7.3 Future perspectives

Selection of industrially viable microorganism has to be done on the basis of their inherent capabilities, such as synthesis of valuable end-products, resilience to surrounding growth environments, utilization of inexpensive and a wide variety of feed stocks. Without recognizing these considerations, the organism of interest cannot be treated as economically important. The work presented in this thesis has provided insights into the biofuel yields and how *C. termitidis* utilizes soluble substrates, here cellobiose and xylose, when it was in excess in pH controlled batch experiments. It seems promising to use *C. termitidis* in fed-batch cultures with nutritional requirements. This organism also has the ability to utilize both pentose and hexose sugars for efficient lignocellulosic conversion into biofuels such and ethanol and hydrogen, and has provided rationale for future studies on its potential utilization in either sequential or co-utilization using a bioreactor. This would require a detailed understanding of bacterial metabolism and its regulatory components and would involve enzyme characterization, metabolic profiling of intracellular metabolites, metabolic flux modeling and genetic engineering if required.

Several studies have explored the use of mixed cultures for efficient ethanol conversion with the use of fermentation intermediates (Gomez-Flores et al. 2017; Wang et al. 2015; Zuroff

et al. 2013; Nakyama et al. 2011). As a mesophile, *C. termitidis* could be used in the implementation of a successful co-culture partnership with methanogens, because it produces reasonable amount of acetate, CO_2 and H_2, which could serve as a substrate.

Studies on dissolved gas removal (especially H_2) by means of physical changes (agitation, sparging) has provided the opportunity to learn about how quick removal of dissolved H_2 reduces ethanol yield; but it was difficult to remove dissolved CO_2 because of its greater solubility and carbonate chemistry. It might be interesting to try quick CO_2 removal, providing acidic environments during the growth of *C. termitidis* and evaluate how substrate is being utilized. Furthermore, as a result of variations in substrate utilization, which may result from acidic growth environment, biofuel synthesis yield is expected to vary. Successful demonstration of real-time on-line monitoring of gaseous metabolites and its utilization in estimation of soluble metabolites has provided the opportunity to extend this stoichiometric algorithm in other bioprocesses so that industrial monitoring can be performed efficiently with minimum available resources.

C. termitidis possesses diverse potential for substrate utilization and its ethanol production capabilities. Investigating and understanding the core metabolism may help identifying approaches to improve its ethanol production and ultimately its industrial relevance. In other studies (Munir et al. 2014; Munir et al. 2015; Lal and Levin 2016), carbon catabolic pathways involved in *C. termitidis* cultured on cellobiose, xylose, xylan, and α-cellulose were investigated in batch fermentation through correlatiton of transcriptomes and proteomes with metabolic profiles. With the help of the present analytical tools used in this research, it may be possible to monitor gene expression profiles of *C. termitidis* and dictate desirable end-product

synthesis under wide variety of lignocellulosic substrates together with biochemical characterization of associated enzymes.

References

Aathithan, S., Plant, J.C., Chaudry, A.N., & French, G.L. (2001). Diagnosis of bacteriuria by detection of volatile organic compounds in urine using an automated headspace analyzer with multiple conducting polymer sensors. *Journal of Clinical Microbiology*, *39*, 2590-2593.

Agbor, V., Zurzolo, F., Blunt, W., Dartiailh, C., Cicek, N., Sparling, R., & Levin, D. B. (2014). Single-step fermentation of agricultural hemp residues for hydrogen and ethanol production. *Biomass and Bioenergy*, *64*, 62–69. https://doi.org/10.1016/j.biombioe.2014.03.027

Amend, J. P., & Shock, E. L. (2001). Energetics of overall metabolic reactions of thermophilic and hyperthermophilic Archaea and bacteria. *FEMS Microbiology Reviews*, *25*(2), 175–243. Retrieved from http://www.ncbi.nlm.nih.gov/pubmed/11250035

Argyros, D. A., Tripathi, S. A., Barrett, T. F., Rogers, S. R., Feinberg, L. F., Olson, D. G., Foden, J. M., et al. (2011). High ethanol titers from cellulose by using metabolically engineered thermophilic, anaerobic microbes. *Applied and Environmental Microbiology*, *77*(23), 8288–94. doi:10.1128/AEM.00646-11

Arnold, S. A., Gaensakoo, R., Harvey, L.M., & McNeil, B. (2002). Use of at-line and in-situ near-infrared spectroscopy to monitor biomass in an indus- trial fed-batch *Escherichia coli* process. *Biotechnology and Bioengineering*, *80*, 405–413.

Bankar, S. B., Survase, S. A., Ojamo, H., & Granström, T. (2013). Biobutanol: The outlook of an academic and industrialist. *RSC Advances*, *3*(47), 24734–24757. https://doi.org/10.1039/c3ra43011a

Bastidas-Oyanedel, J. R., Mohd-Zaki, Z., Pratt, S., Steyer, J. P., & Batstone, D. J. (2010). Development on membrane-inlet mass spectrometry for examination of fermentation processes. *Talanta. 83*,482-492.

Baum, D., Decker, C., & Montoya, J. (2009). Environmental regulation and interest group pressure on petroleum refinery capacity growth in the United States : A regional analysis. *Energy Studies Review*, *16*(1), 1–14.

Baylor, L. C. & O'Rourke, P. E. (2005). Process analytical technology: spectroscopic tools and implementation strategies for the chemical and pharmaceutical industries, ed. K. A. Bakeev, Blackwell, Oxford, Chapter 6, pp. 170–186.

Bender, R., Andreesen, J. R., & Gottschalk, G. (1971). 2-keto-3-deoxygluconate, an intermediate in the fermentation of gluconate by *Clostridia*. *Journal of Bacteriology*, *107*(2), 570–573.

Blanc, B., Gerez, C., & Choudens, S. O. D. (2015). Assembly of Fe / S proteins in bacterial systems: Biochemistry of the bacterial ISC system. Biochimica et Biophysica Acta-*Molecular Cell Research*, *1853*(6), 1436–1447. doi:10.1016/j.bbamcr.2014.12.009

Blank, L. M., & Kuepfer, L. (2010). Metabolic flux distributions: genetic information, computational predictions, and experimental validation. *Applied Microbiology and Biotechnology, 86*(5), 1243–55. doi:10.1007/s00253-010-2506-6

Blunt, W., Dandoroff, R., & McDonald, B. (2010). User guide to the TOGA system, Scion, Rotorua 3046, New Zealand.

Blunt, W. (2011). A novel method for online data acquisition for biofuel production using a titrimetric and off-gas analysis (TOGA) sensor, BSc Thesis, Department of Biosystems Engineering, University of Manitoba, MB, Canada.

Blunt, W. (2013). On-line monitoring of microbial fermentation end-products synthesized by *Clostridium thermocellum* using titrimetric off-gas analysis (TOGA). MSc Thesis, Department of Biosystems Engineering, University of Manitoba, MB, Canada.

Blunt, W., Hossain, M. E., Gapes, D., Sparling, R., Levin, D. B., & Cicek, N. (2014). Real-time monitoring of microbial fermentation end-products in biofuel production with titrimetric off-gas analysis (TOGA). *Biological Engineering Transactions*, *6*(4), 203–219. doi:10.13031/bet.6.10496

Blunt, W., Dartiailh, C., Sparling, R., Gapes, D., Levin, D. B., & Cicek, N. (2017). Microaerophilic environments improve the productivity of medium chain length polyhydroxyalkanoate biosynthesis from fatty acids in Pseudomonas putida LS46. *Process Biochemistry*, *59*(January), 18–25. https://doi.org/10.1016/j.procbio.2017.04.028

Boe, K. (2006). Online monitoring and control of the biogas process. Institute of Environment and Resources, Technical University of Denmark, Denmark.

Boe, K., Batstone, D. J., Steyer, J. P., & Angelidaki, I. (2010). State indicators for monitoring the anaerobic digestion process. *Water Research. 44*(20), 5973–80. doi:10.1016/j.watres.2010.07.043

Bokinsky, G., Peralta-yahya, P. P., George, A., Holmes, B. M., Steen, E. J., & Dietrich, J. (2011). Synthesis of three advanced biofuels from ionic liquid-pretreated switch grass using engineered *Escherichia coli*, *Proceedings of the National Academy of Sciences, 108*(50), 19949–19954. doi:10.1073/pnas.1106958108

Boilot, P., Hines, E., Gardner, J., Pitt, R., John, S., Mitchell J., & Morgan, D.W. (2002). Classification of bacteria responsible for ENT and eye infections using the Cyranose system. *IEEE Sensors Journal, 2*, 247-253.

Bothun, G. D., Knutson, B. L., Berberich, J. A., Strobel, H. J., & Nokes, S. E. (2004). Metabolic selectivity and growth of *Clostridium thermocellum* in continuous culture under elevated hydrostatic pressure. *Applied Microbiology and Biotechnology*, *65*, 149–157. https://doi.org/10.1007/s00253-004-1554-1

Boyd, R.K., Basic, C., & Bethem, R.A. (2008). Trace quantitative analysis by mass spectrometry. John Wiley and Sons, West Sussex, England.

Bradford, M.M. (1976). A rapid and sensitive method for the quantification of micro-gram quantities of protein utilizing the principal of protein-dye binding. *Analytical Biochemistry, 72*, 248–254

Bredwell, M. D., & Worden, R. M. (1998). Mass-transfer properties of microbubbles. 1. Experimental studies. *Biotechnology Progress*, *14*(1), 31–38. https://doi.org/10.1021/bp970133x

Brener, D., & Johnson, B. F. (1984). Relationship between substrate concentration and fermentation product ratios in *Clostridium thermocellum* cultures. *Applied and Environmental Microbiology*, *47*(5), 1126–1129.

Brown, S. D., Guss, A. M., Karpinets, T. V, Parks, J. M., Smolin, N., Yang, S., … Lynd, L. R. (2011). Mutant alcohol dehydrogenase leads to improved ethanol tolerance in *Clostridium thermocellum*. *Proceedings of the National Academy of Sciences of the United States of America*, *108*(33), 13752–7. https://doi.org/10.1073/pnas.1102444108

Carere, C.R., Sparling, R., Cicek N. & Levin, D.B. (2008). Third generation biofuels via direct cellulose fermentation. *International Journal of Molecular Science, 9*, 1342-1360.

Carere, C. R., Rydzak, T., Verbeke, T. J., Cicek, N., Levin, D. B., & Sparling, R. (2012). Linking genome content to biofuel production yields: a meta-analysis of major catabolic pathways

among select H_2 and ethanol-producing bacteria. *BMC microbiology*, *12*(1), 295. doi:10.1186/1471-2180-12-295

Carere, R. C. (2013). Genomics of cellulolytic clostridia and development of rational metabolic engineering strategies. *PhD Thesis, Department of Biosystems Engineering, University of Manitoba, Canada*.

Carere, C. R., Rydzak, T., Cicek, N., Levin, D. B., & Sparling, R. (2014). Role of transcription and enzyme activities in redistribution of carbon and electron flux in response to N_2 and H_2 sparging of open-batch cultures of *Clostridium thermocellum* ATCC 27405. *Applied Microbiology and Biotechnology*, *98*(6), 2829–40. https://doi.org/10.1007/s00253-013-5500-y

Cavinato, A. G., Mayes, D. M., Ge, Z. H., & Callis, J. B. (1990). Noninvasive method for monitoring ethanol in fermentation processes using fiber-optic near-infrared spectroscopy. *Analytical Chemistry*, *62*(18), 1977–82. Retrieved from http://www.ncbi.nlm.nih.gov/pubmed/2240577

Chauvatcharin, S., Konstantinov, K. B., Fujiyama, K., Seki, T., & Yoshida, T. (1995). A mass spectrometry membrane probe and practical problems associated with its application in fermentation processes. *Journal of Fermentation and Bioengineering*, *79*(5), 465–472. https://doi.org/10.1016/0922-338X(95)91263-5

Chéruy A. 1997. Software sensors in bioprocess engineering. *Journal of Biotechnology*, *52*(3)193-199.

Chung, K. (1976). Inhibitory effects of H_2 growth of *Clostridium cellobioparum*. *Applied and Environmental Microbiology*, *31*(3), 342–348.

Clementschitsch, F., & Bayer, K. (2006). Improvement of bioprocess monitoring: development of novel concepts. *Microbial Cell Factories*, *5*, 19. doi:10.1186/1475-2859-5-19

Conway, E. J., Brady, T. G., & Carton, E. (1950). Biological production of acid and alkali. *Journal of Biochemistry*, *47*(1942), 369–374.

Conway, T. (1992). The Entner-Doudoroff pathway: history, physiology and molecular biology. *FEMS Microbiology Reviews*, *103*, 1–28.

Dabrock, B., Bahl, H. & Gottschalk, G. (1992). Parameters affecting solvent production in *Clostridia pasteurianum. Applied and Environmental Microbiology, 58*(4): 1233-1239.

de Assis, A. J., & Filho, R. M. (2000). Soft sensors for on-line bioreactor state estimation. *Computers and Chemical Engineering*, *24*(2),1099-1103

Demain, A. L., Newcomb, M., & Wu, J. H. D. (2005). Cellulase, Clostridia, and Ethanol†. *Microbiology and Molecular Biology Reviews*, *69*(1), 124–154. https://doi.org/10.1128/MMBR.69.1.124

Demeestere, K., Dewulf, J., De Witte, B., & Van Langenhove, H. (2007). Sample preparation for the analysis of volatile organic compounds in air and water matrices. *Journal of Chromatography. A*, *1153*(1-2), 130–44. doi:10.1016/j.chroma.2007.01.012

Desvaux, M., & Petitdemange, H. (2001). Flux analysis of the metabolism of *Clostridium cellulolyticum* grown in cellulose-fed continuous culture on a chemically defined medium under ammonium-limited conditions. *Applied and Environmental Microbiology*, *67*(9), 3846–3851. https://doi.org/10.1128/AEM.67.9.3846

Desvaux, M., Guedon, E., & Petitdemange, H. (2001). Metabolic flux in cellulose batch and cellulose-fed continuous cultures of *Clostridium cellulolyticum* in response to acidic environment. *Microbiology (Reading, England)*, *147*(Pt 6), 1461–71. Retrieved from http://www.ncbi.nlm.nih.gov/pubmed/11390677

Desvaux, M. (2004). Mapping of carbon flow distribution in the central metabolic pathways of clostridium cellulolyticum : direct comparison of bacterial metabolism with a soluble versus an insoluble carbon source. *Journal of Microbiology and Biotechnology*, *14*, 1200–1210.

Desvaux, M. (2005). *Clostridium cellulolyticum*: model organism of mesophilic cellulolytic clostridia. *FEMS Microbiology Reviews*, *29*(4), 741–64. doi:10.1016/j.femsre.2004.11.003

Diamantis, V., Melidis, P., & Aivasidis, A. (2006). Continuous determination of volatile products in anaerobic fermenters by on-line capillary gas chromatography. *Analytica Chimica Acta*, *573–574*, 189–94. https://doi.org/10.1016/j.aca.2006.05.036

Dutta, R., Hines, E.L., Gardner, J.W., & Boilot, P. (2002). Bacteria classification using Cyranose 320 electronic nose. *Biomedical Engineering, (online). 1*, 1-4.

Ellis, L. D., Holwerda, E. K., Hogsett, D., Rogers, S., Shao, X., Tschaplinski, T., Thorne, P., et al. (2012). Closing the carbon balance for fermentation by *Clostridium thermocellum* (ATCC 27405). *Bioresource Technology*, *103*(1), 293–9. doi:10.1016/j.biortech.2011.09.128

Farrell, J., & Rose, A. (1967). Temperature effects on microorganisms. *Annual Review of Microbiology*, *21*, 101–20. https://doi.org/10.1146/annurev.mi.21.100167.000533

Ferreira, B. S., van Keulen, F., & da Fonseca, M. M. R. (1998). Novel calibration method for mass spectrometers for on-line gas analysis-set-up for the monitoring of a bacterial fermentation. *Bioprocess Engineering*,*19*, 289-296.

Fischer, E. & Sauer, U. (2003). Metabolic flux profiling of *Escherichia coli* mutants in central carbon metabolism using GC-MS. *European Journal of Biochemistry*, *270*, 880–891.

Flamholz, A., Noor, E., Bar-Even, A., Liebermeister, W., & Milo, R. (2013). Glycolytic strategy as a tradeoff between energy yield and protein cost. *Proceedings of the National Academy of Sciences of the United States of America*, *110*(24), 10039–10044. https://doi.org/10.1073/pnas.1215283110

Fleming, R. W. & Quinn. L. Y. (1971). Chemically defined medium for growth of *Clostridium thermocellum*, a cellulolytic thermophilic anaerobe, *21*(5), 2904.

Fong, S. S., & Palsson, B. Ø. (2004). Metabolic gene-deletion strains of *Escherichia coli* evolve to computationally predicted growth phenotypes. *Nature Genetics. 36*(10), 1056–8. doi:10.1038/ng1432

Fonknechten, N., Chaussonnerie, S., Tricot, S., Lajus, A., Andreesen, J. R., Perchat, N., … Kreimeyer, A. (2010). *Clostridium sticklandii*, a specialist in amino acid degradation: revisiting its metabolism through its genome sequence. *BMC Genomics*, *11*, 555. https://doi.org/10.1186/1471-2164-11-555

Fowler, Z. L., & Koffas, M. (2010). Microbial biosynthesis of fine chemicals: an emerging technology. In, *The Metabolic Pathway Engineering Handbook: Tools and Applications*. Smolke, C. D. (editor). CRC Press.

Freier, D., Mothershed, C. P., & Wiegel, J. (1988). Characterization of *Clostridium thermocellum* JW20. *Applied and Environmental Microbiology*, *54*(1), 204–211.

Frick, R., & Junker, B. (1999). Indirect methods for characterization of carbon dioxide levels in fermentation broth. *Journal of Bioscience and Biotechnology*, *87*(3), 344-351.

Fuhrer, T., Fischer, E., and Sauer, U. (2005). Experimental identification and quantification of glucose metabolism in seven bacterial species. *Journal of Bacteriology*, *187*, 1581-1590.

Gapes D. & Keller, J. (2001). Analysis of biological wastewater treatment process using multicomponent gas phase mass balancing. *Biotechnology and Bioeng*ineering, *76*, 361-375.

Gapes, D. (2002). External and internal mass transfer in biological wastewater treatment systems, PhD Thesis, Department of Chemical Engineering, The University of Queensland, New Zealand.

Giaever, I., & Keese, C. R. (1993). A morphological biosensor for mammalian cells. *Nature. 366*: 591-592

Giallo, J., Gaudin, C., Belaich, J. P., & Petitdemange, E. (1983). Metabolism of glucose and cellobiose by cellulolytic. *Applied and Environmental Microbiology*, *45*(3), 843–849.

Giallo, J., Gaudin, C., & Belaich, J. P. (1985). Metabolism and solubilization of cellulose by *Clostridium cellulolyticum* H10. *Applied and Environmental Microbiology*, *49*,1216–1221.

Gilat, A., & Subramaniam, V. (2008). Numerical methods for engineers and scientists: an introduction with applications using MATLAB: Wiley, USA.

Ginsburg, E., Salomon, D., Sreevalsan, T., & Freese, E. (1973). Growth inhibition and morphological changes caused by lipophilic acids in mammalian cells. *Proceedings of the National Academy of Sciences of the United States of America*, *70*(8), 2457–61.

Goldberg, R. N., Kishore, N., & Lennen, R. M. (2002). Thermodynamic quantities for the ionization reactions of buffers. *Journal of Physical Chemistry Reference Data*, 31(2), 231-370. http://dx.doi.org/10.1063/1.1416902.

Gombert, A. K., dos Santos, M. M., Christensen, B., & Nielsen, J. (2001). Network identification and flux quantification in the central metabolism of *Saccharomyces* cerevisiae under different conditions of glucose repression. *Journal of Bacteriology*, *183*, 1441–1451.

Gomez-Flores, M., Nakhla, G., & Hafez, H. (2017). Hydrogen production and microbial kinetics of *Clostridium termitidis* in mono-culture and co-culture with *Clostridium beijerinckii* on cellulose. *AMB Express*, *7*(1). https://doi.org/10.1186/s13568-016-0256-2

Gottschalk, G., & Barker, H. A. (1966). Synthesis of glutamate and citrate by *Clostridium kluyveri*. a new type of citrate synthase. *Biochemistry*, *5*(4), 1125–1133.

Gottschalk, G. (1986). Bacterial metabolism, 2nd Edition, Springer-Verlag, NY, USA Chapter 8-Bacterial Fermentation. 208-280.

Gross, J. H. (2004). Mass spectrometry, Published by Springer-Verlag Berlin Heidelberg, Germany.

Guedon, E., Desvaux, M., Payot, S., Petitdemange, H., Gram, B., & Henri, U. (1999). Growth in hibition of *Clostridium cellulolyicum* by an inefficiently regulated carbon flow. *Microbiology*, *145*, 1831–1838.

Guedon, E., Payot, S., Desvaux, M., Petitdemange, H., Scientifique, D., Grignard, V., & Poincare, H. (1999). Carbon and electron flow in *Clostridium cellulolyticum* grown in chemostat culture on synthetic medium. *Journal of Bacteriology*, *181*(10), 3262–3269.

Guedon, E., Desvaux, M., & Petitdemange, H. (2000). Kinetic analysis of *Clostridium cellulolyticum* carbohydrate metabolism: importance of glucose 1-phosphate and glucose 6-phosphate branch points for distribution of carbon fluxes inside and outside cells as revealed by steady-state continuous culture. *Journal of Bacteriology*, *182*(7), 2010–2017.

Guedon, E., Desvaux, M., & Petitdemange, H. (2002). Improvement of cellulolytic properties of *Clostridium cellulolyticum* by metabolic engineering. *Applied and Environmental Microbiology*, *68*(1), 53–58. doi:10.1128/AEM.68.1.53

Hahn-H, B., Jeppsson, H., Olsson, L., & Mohagheghi, A. (1994). An interlaboratory comparison of the performance of ethanol-producing micro-organisms in a xylose-rich acid hydrolysate. *Applied Microbiology and Biotechnology*, *41*, 62–72.

Harms, P., Kostov, Y., & Rao, G. (2002). Bioprocess monitoring. *Current Opinion in Biotechnology, 13*,124-127.

Hayward, M. J., Kotiaho, T., Lister, A. K., Cooks, R. G., Austin, G. D., Narayan, R., & Tsao G.T., (1990). On-line monitoring of bioreactions of *Bacillus polymyxa* and *Klebsiella oxytoca* by membrane introduction tandem mass spectrometry with flow injection analysis sampling. *Analytical Chemistry, 62*,1798-1804.

He, Q., Lokken, P.M., Chen, S. & Zhou, J. (2009). Characterization of the impact of acetate and lactate on ethanolic fermentation by *Thermoanaerobacter ethanolicus*. *Bioresources. Technology*. *100*,5955–596.

Helle, S., & Duff, S. J. B. (2004). Supplementing spent sulfite liquor with a lignocellulosic hydrolysate to increase pentose / hexose co-fermentation efficiency and ethanol yield, Final report, Natural Resources Canada, 580 Booth St.Ottawa, Ontario.

Herrero, A. A., & Gomez, R. F. (1980). Development of ethanol tolerance in *Clostridium thermocellum*: effect of growth temperature. *Applied and Environmental Microbiology, 40*(3): 571–577.

Herrero, A. A., Gomezs, R. F., & Roberts, M. F. (1985a). ^{31}P NMR studies of Clostridium thermocellum: mechanism of end product inhibition by ethanol. *Journal of Biological Chemistry, 260*(12), 7442–7451.

Herrero, A., Gomez, R., Snedecor, B., Tolman, C., & Roberts, M. F. (1985b). Growth inhibition of *Clostridium thermocellum* by carboxylic acids: A mechanism based on uncoupling by weak acids. *Applied Microbiology and Biotechnology, 22*(1), 53–62. doi:10.1007/BF00252157

Hethener, P., Brauman, A., & Garcia, J. (1992). *Clostridium termitidis* sp. nov., a cellulolytic bacterium from the gut of the wood-feeding termite, *Nasutitermes lujae*. *Syst. Applied Microbiology, 15*, 52-58.

Heinzle, E., & Lafferty, R. (1980). A kinetic model for growth and synthesis of poly-β-hydroxybutyric aci (PHB) in *Alcaligenes eustrophus* H16. *European Journal of Applied Microbiology and Biotechnology, 11*, 17–22.

Heinzle, E. (1987). Mass spectrometry for online monitoring of biotechnological processes. *Advanced in Biochemistry and Engineering, 35*,1-45.

Heinzle, E., Oeggerli, A. & Dettwiler, B. (1990) On-line fermentation gas analysis: error analysis and application of mass spectrometry. *Analytica Chimica Acta, 238*, 101-115. https://doi.org/10.1016/S0003-2670(00)80528-0

Heinzle, E. (1992). Present and potential applications of mass spectrometry for bioprocess research and control. *Journal of Biotechnology, 25*,81-114.

Hiden Analytical. (2010).Warrington, United Kingdom,

Hoch, G. & Kok, B. (1963). A mass spectrometer inlet system for sampling gases dissolved in liquid phase. *Archive of Biochemistry and Biophysics, 101*,160-170.

Hoffmann, E. de & Stroobant, V. (2007). Mass spectrometry: principles and applications, 3rd Edition, John Wiley and Sons Ltd. West Sussex, England.

Holwerda, E. K., Ellis, L. D., & Lynd, L. R. (2013). Development and evaluation of methods to infer biosynthesis and substrate consumption in cultures of cellulolytic microorganisms. *Biotechnology and Bioengineering, 110*(9), 2380–8. https://doi.org/10.1002/bit.24915

Holwerda, E. K., & Lynd, L. R. (2013). Testing alternative kinetic models for utilization of crystalline cellulose (avicel) by batch cultures of *Clostridium thermocellum*. *Biotechnology and Bioengineering, 110*(9), 2389–94. https://doi.org/10.1002/bit.24914

Holwerda, E. K., Thorne, P. G., Olson, D. G., Amador-Noguez, D., Engle, N. L., Tschaplinski, T. J., van Dijken, J. P., et al. (2014). The exometabolome of *Clostridium thermocellum* reveals overflow metabolism at high cellulose loading. *Biotechnology for Biofuels*, *7*(1), 155. doi:10.1186/s13068-014-0155-1

Horta, A. C. L., Sargo, C. R., da Silva, A. J., Gonzaga, M. C., dos Santos, M. P., Goncalves, V. M., Zangirolami, T. C., & Giordano, R. C. (2012). Intensification of high cell-density cultivations of *rE. Coli* for production of *S. pneumoniae* antigenic surface protein, PspA3, using model-based adaptive control. *Bioprocess and Biosystems Engineering*, *35*, 1269-1280.

Huang, L. I., Forsberg, C. W., & Gibbins, L. N. (1986). Influence of external pH and fermentation products on *Clostridium acetobutylicum* intracellular pH and cellular distribution of fermentation products. *Applied and Environmental Microbiology*, *51*(6), 1230–1234.

Huber, R., Langworthy, T. A., Knig, H., Thomm, M., Woese, C. R., Sleytr, U. B., & Stetter, K. O. (1986). *Thermotoga maritima* sp. nov. represents a new genus of unique extremely thermophilic eubacteria growing up to 90ºC. *Archive of Microbiology*, *144*, 324–333.

Hungate, R. E. (1944). Studies on cellulose fermentation I. the culture and physiology of an anaerobic cellulose-digesting bacterium. *Journal of Bacteriology*, 499–513.

Husky Energy. (2015). Resilience: Annual Report 2015. Pp. 1-137. Husky Energy, Alberta, Canada.

IEA. (2013). Resources to reserves: oil, gas and coal technologies for the energy markets of the future. pp. 1–268. International Energy Agency, France.

Islam, R., Cicek, N., Sparling, R., & Levin, D. (2006). Effect of substrate loading on hydrogen production during anaerobic fermentation by *Clostridium thermocellum* 27405. *Applied Microbiology and Biotechnology*, *72*(3), 576–83. doi:10.1007/s00253-006-0316-7

Islam, R. (2013). Optimization of direct bioconversion of cellulose into biofuels: medium improvement, scale-up and use of alternative nutrients. PhD Thesis, Department of Biosystems Engineering, University of Manitoba, MB, Canada.

Islam, R., Sparling, R., Cicek, N., & Levin, D. B. (2015). Optimization of influential nutrients during direct cellulose fermentation into hydrogen by *Clostridium thermocellum*. *International Journal of Molecular Sciences*, *16*(2), 3116–32. doi:10.3390/ijms16023116

Johnson, E. A., Madia, A., & Demain, A. L. (1981). Chemically defined minimal medium for growth of the anaerobic cellulolytic thermophile *Clostridium thermocellum*. *Applied and Environmental Microbiology*, *41*(4), 1060–1062.

Johnson, R. C., Srinivasan, N., Cooks, R. G., & Schell, D. (1997). Membrane introduction mass spectrometry in a pilot plant: on-line monitoring of fermentation broths. *Rapid Communication in Mass Spectrometry, 11*,363-367.

Jugder, B. E., Welch, J., Aguey-Zinsou, K. F., & Marquis, C. P. (2013). Fundamentals and electrochemical applications of Ni-Fe -uptake hydrogenases. *RSC Advances*, *3*(22), 8142–8159. https://doi.org/10.1039/c3ra22668a

Karadag, D., & Puhakka, J. A. (2010). Effect of changing temperature on anaerobic hydrogen production and microbial community composition in an open-mixed culture bioreactor. *International Journal of Hydrogen Energy*, *35*(20), 10954–10959. https://doi.org/10.1016/j.ijhydene.2010.07.070

Katzen, R., & Fowler, D. E. (1994). Ethanol from lignocellulosic wastes with utilization of recombinant bacteria. *Applied Biochemistry and Biotechnology*, *45-46*, 697-707.

Kawase Y., Halard B., & Moo-Young M. (1992). Liquid-phase mass transfer coefficients in bioreactors. *Biotechnology and Bioengineering, 39*(11), 1133-1140.

Kell, D. B., Peck, M. W., Rodger, G. & Morris, J. G. (1981). On the permeability to weak acids and bases of the cytoplasmic membrane of *Clostridium pasteurianum*. *Biochemical and Biophysical Research Communications, 99*,81–88.

Kirk, T. K., Higuchi, T., & Chang, H. M. (1980). Lignin biodegradation: microbiology, chemistry and potential applications, Vols. I and II, CRC Press, Boca Raton, FL, USA.

Kraakman, N. J. R., Rocha-Rios, J., & Van Loosdrecht, M. C. M. (2011). Review of mass transfer aspects for biological gas treatment. *Applied Microbiology and Biotechnology*, *91*(4), 873–886. https://doi.org/10.1007/s00253-011-3365-5

Kraemer, J. T., & Bagley, D. M. (2006). Supersaturation of dissolved H_2 and CO_2 during fermentative hydrogen production with N_2 sparging. *Biotechnology Letters*, *28*(18), 1485–1491. https://doi.org/10.1007/s10529-006-9114-7

Lal, S., Ramachandran, U., Zhang, X., Munir, R., Sparling, R., & Levin, D. B. (2013). Draft genome sequence of the cellulolytic , mesophilic , anaerobic. *Genome Announcements*, *1*(3), 4–5. https://doi.org/10.1128/genomeA.00281-13.

Lal, S., & Levin, D. B. (2016). Comparative genomics of core metabolism genes of cellulolytic and non-cellulolytic clostridium species. *Advance Biochemistry and Engineering Biotechnology*. doi:10.1007/10

Lamed, R., & Zeikus, J. G. (1980). Glucose fermentation pathway of *Thermoanaerobium brockii*. *Journal of Bacteriology, 141*,1251–1257

Lamed, R., Setiter, E. V. A., & Bayer, E. A. (1983). Characterization of a cellulose-binding , cellulase-containing complex in *Clostridium thermocellum*. *Journal of Bacteriology*, *156*(2), 828–836.

Lamed, R. J., Lobos, J. H., & Su, T. M. (1988). Effects of stirring and hydrogen on fermentation products of *Clostridium thermocellum*. *Applied and Environmental Microbiology*, *54*(5), 1216–1221.

Landgrebe, D., Haake, C., Höpfner, T., Beutel, S., Hitzmann, B., Scheper, T., Rhiel, M., & Reardon, K. F. (2010). Online infrared spectroscopy for bioprocess monitoring. *Applied Microbiology and Biotechnology, 88*,11-22.

Le Coq, D., Michel, K., Keirsse, J., Boussard-Plédel, Catherine Fonteneau, G., Bureau, B., Le Quéré, J.-M., & Lucas, J. (2002). Infrared glass fibers for in-situ sensing, chemical and biochemical reactions. *C. R. Chimie, 5*, 907–913.

Levin, D., Islam, R., Cicek, N., & Sparling, R. (2006). Hydrogen production by *Clostridium thermocellum* 27405 from cellulosic biomass substrates. *International Journal of Hydrogen Energy*, *31*(11), 1496–1503. doi:10.1016/j.ijhydene.2006.06.015

Levin, D. B., Carere, C., Cicek, N., & Sparling, R. (2009). Challanges for biohydrogen production via direct lignocellulose fermentation. *International Journal of Hydrogen Energy, 34*, 7390-7403.

Li, Y.-F. (2013). An Integrated Study on Microbial Community in Anaerobic Digestion Systems. PhD Thesis, Graduate Program in Environmental Science, The Ohio State University, USA.

Lin, C.-Y., Hung, C.-H., Chen, C.-H., Chung, W.-T., & Cheng, L.-H. (2006). Effects of initial cultivation pH on fermentative hydrogen production from xylose using natural mixed cultures. *Process Biochemistry*, *41*(6), 1383–1390. https://doi.org/10.1016/j.procbio.2006.01.021

Lin, L., Song, H., Tu, Q., Qin, Y., Zhou, A., Liu, W., & Xu, J. (2011). The Thermoanaerobacter glycobiome reveals mechanisms of pentose and hexose co-utilization in bacteria. *PLoS Genetics*, *7*(10), e1002318. https://doi.org/10.1371/journal.pgen.1002318

Liu, L., Zhang, L., Tang, W., Gu, Y., Hua, Q., Yang, S., & Yang, C. (2012). Phosphoketolase pathway for xylose catabolism in *Clostridium acetobutylicum* revealed by ^{13}C-metabolic flux analysis. *Journal of Bacteriology*, *194*(19), 5413–5422. https://doi.org/10.1128/JB.00713-12

Lloyd, D., Bohatka, S., & Szilagyi, J. (1985). Quadrupole mass spectrometry in monitoring and control of fermentations. *Biosensor*, *1*,179-212.

Løvgreen, M. N., Martic, M., Windahl, M. S., Christensen, H. E. M,. & Harris. P. (2011). Crystal structures of the all-cysteinyl-coordinated D14C variant conversion. *Journal of Biological Inorganic Chemistry*, *16*, 763–775. doi:10.1007/s00775-011-0778-7

Lynd, L. R., Baskaran, S., & Casten, S. (2001). Salt accumulation resulting from base added for pH control , and not ethanol , limits growth of *Thermoanaerobacterium thermosaccharolyticum* HG-8 at elevated feed xylose concentrations in continuous culture. *Biotechnology Progress*, *17*(1), 118–125.

Lynd, L. R., Weimer, P. J., Zyl, W. H. Van, Isak, S., & Pretorius, I. S. (2002). Microbial cellulose utilization : fundamentals and biotechnology microbial cellulose utilization : fundamentals and biotechnology. *Microbiology and Molecular Biology Reviews*, *66*(3), 506–577. https://doi.org/10.1128/MMBR.66.3.506

Magnusson, L., Cicek, N., Sparling, R., & Levin, D. (2009). Continuous hydrogen production during fermentation of alpha-cellulose by the thermophillic bacterium *Clostridium thermocellum*. *Biotechnology and Bioengineering*, *102*(3), 759–66. https://doi.org/10.1002/bit.22092

Massé, A., Pringault, O., & de Wit, R. (2002). Experimental study of interactions between purple and green sulfur bacteria in sandy sediments exposed to illumination deprived of near-infrared wavelengths. *Applied and Environmental Microbiology*, *68*(6), 2972–2981. https://doi.org/10.1128/AEM.68.6.2972-2981.2002

Mendham, J., Denney, R.C., Barnes, J. D., & Thomas, M. (2006). Vogel's textbook of quantitative chemical analysis, 6th Ed. Pearson Education Ltd., London, UK.

Monserrate, E., Leschine, S. B., & Canale-parola, E. (2017). *Clostridium hungatei* sp . nov ., a mesophilic, N_2 - fixing cellulolytic bacterium isolated from soil. *International Journal of Systematic and Evolutionary Microbiology*, (2001), 123–132.

Mukherjee, S., Thompson, L. K., Godin, S., Schackwitz, W., Lipzen, A., Martin, J., & Blanchard, J. L. (2014). Population level analysis of evolved mutations underlying improvements in plant hemicellulose and cellulose fermentation by *Clostridium phytofermentans*. *PLoS ONE*, *9*(1). https://doi.org/10.1371/journal.pone.0086731

Müller, S., Murray, D. B., & Machne, R. (2012). A new dynamic model for highly efficient mass transfer in aerated bioreactors and consequences for k_La identification. *Biotechnology and Bioengineering*, *109*(12), 2997–3006. https://doi.org/10.1002/bit.24594

Munir, R. I., Schellenberg, J., Henrissat, B., Verbeke, T. J., Sparling, R., & Levin, D. B. (2014). Comparative analysis of carbohydrate active enzymes in *Clostridium termitidis* CT1112 reveals complex carbohydrate degradation ability. *PloS One*, *9*(8), e104260. doi:10.1371/journal.pone.0104260

Munir, R. (2015). Cellulose hydrolysis and metabolism in the mesophilic, cellulolytic bacterium, *Clostridium termitidis* CT1112. *PhD Thesis, Department of Biosystems Engineering, University of Manitoba, Canada*.

Munir, R. I., Spicer, V., Shamshurin, D., Krokhin, O. V., Wilkins, J., Ramachandran, U., … Levin, D. B. (2015). Quantitative proteomic analysis of the cellulolytic system of *Clostridium termitidis* CT1112 reveals distinct protein expression profiles upon growth on α-cellulose and cellobiose. *Journal of Proteomics*, *125*, 41–53. https://doi.org/10.1016/j.jprot.2015.04.026

Munir, R. I., Spicer, V., Krokhin, O. V., Shamshurin, D., Zhang, X. L, Taillefer, M., Blunt, W., Cicek, N., Sparling, R., & Levin, D. B. (2016a). Transcriptomic and proteomic analyses of core metabolism in *Clostridium termitidis* CT1112 during growth on α-cellulose, xylan, cellobiose and xylose. *BMC Microbiology*, *16*(91), 1–21.

Munir, R., & Levin, D. B. (2016b). Enzyme systems of anaerobes for biomass conversion. *In, Advances in Biochemical Engineering/*Biotechnology, Hatti-Kaul R (Editor). Springer-Verlag. DOI 10.1007/10_2015_5002.

Murray, W. D., & Khan, A. W. (1983). Ethanol production by a newly isolated anaerobe, *Clostridium saccharolyticum*: effects of culture medium and growth conditions. *Canadian Journal of Microbiology*, *29*(3), 342–347. https://doi.org/10.1139/m83-057

Nakayama, S., Kiyoshi, K., Kadokura, T., & Nakazato, A. (2011). Butanol production from crystalline cellulose by cocultured *Clostridium thermocellum* and *Clostridium saccharoperbutylacetonicum* N1-4. *Applied and Environmental Microbiology*, *77*(18), 6470–6475. https://doi.org/10.1128/aem.00706-11

Oeggerli, A., & Henizle, E. (1994). On-line exhaust gas analysis of volatiles in fermentation using mass spectrometry. *Biotechnology Progress* 10:284-290.

Olsson, L., Schulze, U., & Neilsen, J. (1998). On-line bioprocess monitoring – and academic discipline or an industrial tool? *Trends in Analytical Chemistry*, *17*(2):88-95.

Palmqvist, E., & Hahn-Hägerdal, B. (2000). Fermentation of lignocellulosic hydrolysates. II: inhibitors and mechanisms of inhibition. *Bioresource Technology*, *74*(1), 25–33. https://doi.org/10.1016/S0960-8524(99)00161-3

Park, W., & Hyun, S. H. (2005). Removal of headspace CO_2 increases biological hydrogen production. *Environmental Science & Technology*, *39*(12), 4416–4420.

Pauss, A., Andre, G., Perrier, M., & Guiot, S. R. (1990). Liquid-to-gas mass transfer in anaerobic processes: inevitable transfer limitations of methane and hydrogen in the biomethanation process. *Applied and Environmental Microbiology*, *56*(6), 1636–1644.

Pauss, A. & Guiot, A. (1993). Hydrogen monitoring in anerobic sludge bed reactors at various hydraulic regimes and loading rates. *Water and Environmental Resources*, *65*(3), 276-280.

Payot, S., Guedon, E., Cailliez, C., Gelhaye, E., & Petitdemange, H. (1998). Metabolism of cellobiose by *Clostridium cellulolyticum* growing in countinuous culture: evidence for decreased NADH reoxidation as a factor limiting growth. *Microbiology*, *144*, 375-384.

Payot, S., Guedon, E., Desvaux, M., Gelhaye, E., & Petitdemange, E. (1999). Effect of dilution rate , cellobiose and ammonium availabilities on *Clostridium cellulolyticum* sporulation. *Applied Microbiology and Biotechnology*, *52*, 670–674.

Perani, A., Gloria, B., Wang, D., Buffier, A.-S., Berteau, O., Esteban, G., & Scott, A. M. (2011). Evaluation of an online biomass probe to monitor cell growth and cell death. *BMC Proceedings*, *5*(Suppl 8), P16. https://doi.org/10.1186/1753-6561-5-S8-P16

Peters, J. W., Schut, G. J., Boyd, E. S., Mulder, D. W., Shepard, E. M., Broderick, J. B., Adams, M. W. W. (2015). [FeFe]- and [NiFe]-hydrogenase diversity, mechanism, and maturation. *Biochimica et Biophysica Acta - Molecular Cell Research, 1853*(6), 1350–1369. https://doi.org/10.1016/j.bbamcr.2014.11.021

Petitdemange, H., Scientifique, D., Grignard, V., & Poincare, H. (2001). Flux analysis of the metabolism of *Clostridium cellulolyticum* grown in cellulose-fed continuous culture on a chemically defined medium under ammonium-limited conditions. *Applied and Environmental Microbiology*, *67*(9), 3846–3851. https://doi.org/10.1128/AEM.67.9.3846

Pfromm, P. H., Amanor-Boadu, V., Nelson, R., Vadlani, P., & Madl, R. (2010). Bio-butanol vs. bio-ethanol: A technical and economic assessment for corn and switchgrass fermented by yeast or *Clostridium acetobutylicum*. *Biomass and Bioenergy*, *34*(4), 515–524. https://doi.org/10.1016/j.biombioe.2009.12.017

Pine, L., Haas, V., & Barker, H. A. (1954). Metabolism of glucose *by Butyribacterium rettgeri*. *Journal of Bacteriology*, *68*, 227–230.

Pollard, D. J., Buccino, R., Connors, N. C., Kirschner, T. F., Olewinski, R. C., Saini, K., & Salmon, P. M. (2001). Real-time analyte monitoring of a fungal fermentation, at pilot scale, using in situ mid-infrared spectroscopy. *Bioprocess and Biosystems Eng*ineering, *24*,3-24.

Pratt, S. (2003). The development of the TOGA sensor for the study of biological wastewater treatment systems. *PhD Thesis, Department of Chemical Engineering, The University of Queensland, Australia*.

Pratt, S., Yuan, Z., Gapes, D., Dorigo, M., Zeng, R. J., & Keller, J. (2003). Development of a novel titration and off-gas analysis (TOGA) sensor for study of biological processes in wastewater treatment systems. *Biotechnology and Bioengineering*, *81*(4), 482–95. https://doi.org/10.1002/bit.10490

Ramachandran, U., Wrana, N., Cicek, N., Sparling, R., & Levin, D. (2008). Hydrogen production and end-product synthesis patterns by *Clostridium termitidis* strain CT1112 in batch fermentation cultures with cellobiose or α-cellulose. *International Journal of Hydrogen Energy*, *33*(23), 7006–7012. doi:10.1016/j.ijhydene.2008.09.022

Ramachandran, U. (2013). Proteomics and metabolism of mesophilic cellulolytic bacterium, *Clostridium termitidis* strain CT1112, PhD Thesis, Department of Biosystems Engineering, University of Manitoba, Winnipeg, Canada.

Ren, Z., Ward, T. E., Logan, B. E., & Regan, J. M. (2007). Characterization of the cellulolytic and hydrogen-producing activities of six mesophilic Clostridium species. *Journal of Applied Microbiology*, *103*, 2258–2266. doi:10.1111/j.1365-2672.2007.03477.x

Risso, F. (2018). Agitation, mixing, and transfers induced by bubbles. *Annual Review of Fluid Mechanics*, *50*, 25–48. https://doi.org/10.1146/annurev-fluid-122316-045003

Roe, A. J., Laggan, D. M. C., Davidson, I. A. N., Byrne, C. O., & Booth, I. A. N. R. (1998). Perturbation of anion balance during inhibition of growth of *Escherichia coli* by weak acids. *Journal of Bacteriology*, *180*(4), 767–772.

Royce, P. N. (1992). Effect of changes in the pH and carbon dioxide evolution rate on the measured respiratory quotient of fermentations. *Bioechnology and Bioengineering, 40(10),* 1129-1138. https://doi.org/10.1002/bit.260401002

Rudnitskaya, A., & Legin, A. (2008). Sensor systems, electronic tongues and electronic noses, for the monitoring of biotechnological processes. *Journal of Industrial Microbiology and Biotechnology*, *35*(5): 443–451. doi:10.1007/s10295-007-0298-1

Ruess, M., Piehl, H., & Wagner, F. (1975). Application of mass spectrometry to the measurement of dissolved gasses and volatile substances in fermentation. *European Journal of Applied Microbiology*. *1*,323-325.

Russell, J. B., and T. Hino. 1985. Regulation of lactate production in *Streptococcus bovis*: a spiraling effect that leads to rumen acidosis. *Journal of Dairy Science*. 68:1712–1721

Russell, J. B., & Cook, G. M. (1995). Energetics of bacterial growth : balance of anabolic and catabolic reactions. *Microbiological Reviews*, *59*(1), 48–62.

Rydzak, T., Levin, D. B., Cicek, N., & Sparling, R. (2009). Growth phase-dependant enzyme profile of pyruvate catabolism and end-product formation in *Clostridium thermocellum* ATCC 27405. *Journal of Biotechnology*, *140*(3–4), 169–75. https://doi.org/10.1016/j.jbiotec.2009.01.022

Rydzak, T., Levin, D. B., Cicek, N., & Sparling, R. (2011). End-product induced metabolic shifts in *Clostridium thermocellum* ATCC 27405. *Applied Microbiology and Biotechnology*, *92*(1), 199–209. doi:10.1007/s00253-011-3511-0

Rydzak, T., Grigoryan, M., Cunningham, Z. J., Krokhin, O. V., Ezzati, P., Cicek, N., Levin, D. B., et al. (2014). Insights into electron flux through manipulation of fermentation conditions and assessment of protein expression profiles in *Clostridium thermocellum*. *Applied Microbiology and Biotechnology*, *98*(14), 6497–510. doi:10.1007/s00253-014-5798-0

Samuelov, N. S., Lamed, R., Lowe, S., & Zeikus, J. G. (1991). Influence of CO_2-HCO_3^- levels and pH on growth, succinate production, and enzyme activities of *Anaerobiospirillum succiniciproducens*. *Applied and Environmental Microbiology*, *57*(10), 3013–9.

Sander, R. (2015). Compilation of Henry's law constants (version 4.0) for water as solvent. *Atmospheric Chemistry and Physics*, *15*(8), 4399–4981. https://doi.org/10.5194/acp-15-4399-2015

Sauer, U. (2006). Metabolic networks in motion: ^{13}C-based flux analysis. *Molecular Systems Biology, 2*, 1-10.

Scheper, T. H., Hilmer, J. M., Lammers, F., Müller, C., & Reinecke, M. (1996). Biosensors in bioprocess monitoring. *Journal of Chromatography. A. 725*:3-12.

Schgnheit, P., & Schafer, T. (1995). Metabolism of hyperthermophiles. *World Journal of Microbiology and Biotechnology*., *1*, 26–57.

Schmitz, G. (2002). pH of sodium acetate solutions. *Journal of Chemical Education*, *79*(1), 29. https://doi.org/10.1021/ed079p29.1

Schumpe, A. (1993). The estimation of gas solubilities in salt solutions. *Chemical Engineering Science 48*(1):153-158.

Schut, G. J., & Adams, M. W. W. (2009). The iron-hydrogenase of *Thermotoga maritima* utilizes ferredoxin and NADH synergistically : a new perspective on anaerobic hydrogen production. *Journal of Bacteriology*, *191*(13), 4451–4457. doi:10.1128/JB.01582-08

Schwarz, W. H. (2001). The cellulosome and cellulose degradation by anaerobic bacteria. Applied Microbiology and Biotechnology, *56*,634–639.

Shaw, A. J., Podkaminer, K. K., Desai, S. G., Bardsley, J. S., Rogers, S. R., Thorne, P. G., … & Lynd, L. R. (2008). Metabolic engineering of a thermophilic bacterium to produce ethanol at high yield. *Proceedings of the National Academy of Sciences of the United States of America*, *105*(37), 13769–74. https://doi.org/10.1073/pnas.0801266105

Solomon, B. D. (2010). Biofuels and sustainability. *Annals of the New York Academy of Science, 1185*:119–134.

Sonderegger, M., Jeppsson, M., Larsson, C., Gorwa-Grauslund, M.-F., Boles, E., Olsson, L., Spencer-Martins, I. et al. (2004). Fermentation performance of engineered and evolved xylose-fermenting *Saccharomyces cerevisiae* strains. *Biotechnology and Bioengineering, 87*(1): 90–98. doi:10.1002/bit.20094

Soni, M., Bauer, S., Amy, J. W., Wong, P., J, R. G. C., & Bay, P. (1995). Direct determination of organic compounds in water at parts-per-quadrillion levels by membrane introduction mass spectrometry. *Analytical Chemistry*, *67*(8), 1409–1412.

Sparling, R., Islam, R., Cicek, N., Carere, C., Chow, H., & Levin, D. B. (2006). Formate synthesis by *Clostridium thermocellum* during anaerobic fermentation. *Canadian Journal of Microbiology*, *52*, 681–688. https://doi.org/10.1139/W06-021

Sridhar, J., Eiteman, M. A., & Wiegel, J. W. (2000). Elucidation of enzymes in fermentation pathways used by *Clostridium thermosuccinogenes* growing on inulin. *Applied and Environmental Microbiology*, *66*(1), 246–251. https://doi.org/10.1128/AEM.66.1.246-251.2000.

Sridhar, J., & Eiteman, M. A. (2001). Metabolic flux analysis of *Clostridium thermosuccinogenes*. *Applied Biochemistry and Biotechnology*, *94*, 51–69.

Srinivasan, N., Kasthurikrishan, N., Cooks, R. G., Krishnan, M. S., & Tsao, G.T. (1995). On-line monitoring with feedback control of bioreactors using a high ethanol tolerance yeast by membrane inlet mass spectrometry. *Analytica Chimica Acta*, *316*,269-276.

Stainthorpe, A.C., & Williams, R. A. D. (1988). Isolation and properties of *Clostridium thermocellum* from Icelandic hot springs. *International Journal of Systematic Bacteriology*, *38*(1), 119-121.

Strong, P. J., McDonald, B., & Gapes, D. J. (2011). Combined thermochemical and fermentative destruction of municipal biosolids: a comparison between thermal hydrolysis and wet oxidative pre-treatment. *Bioresource Technology*, *102*(9), 5520–7. https://doi.org/10.1016/j.biortech.2010.12.027

Stumm, W., & Morgan, J. J. (1996). Dissolved carbon dioxide. Aquatic Chemistry. New York: John Wiley. USA.

Takahashi, C. M., Gianni, K., & Lima, D. C. (2000). Fermentation of sugar cane bagasse hemicellulosic hydrolysate and sugar mixtures to ethanol by recombinant *Escherichia coli* KO11. *World Journal of Microbiology and Biotechnology*, *16*, 829-834.

Taniguchi, M., Itaya, T., Tohma, T., & Fujii, M. (1997). Ethanol production from a mixture of glucose and xylose by a novel co-culture system with two fermentors and two microfiltration modules. *Journal of Fermentation and Bioengineering, 84*(1): 59–64. doi:10.1016/S0922-338X(97)82787-0

Tarkiainen, V., Kotiaho, T., Mattila, I., Virkajärvi, I., Aristidou, A., & Ketola, R. A. (2005). On-line monitoring of continuous beer fermentation process using automatic membrane inlet mass spectrometric system. *Talanta. 65*(5), 1254–1263.

Temudo, M. F., Mato, T., Kleerebezem, R., & van Loosdrecht, M. C. M. (2009). Xylose anaerobic conversion by open-mixed cultures. *Applied Microbiology and Biotechnology, 82*(2): 231–239. doi:10.1007/s00253-008-1749-y

Thauer, R. K. (1998). Special biochemistry of methanogenesis : a tribute to Marjory Stephenson. *Microbiology*, *144*, 2377–2406.

Thompson, A., & Trinh, C. T. (2017). Overflow metabolism and growth cessation in *Clostridium thermocellum* DSM1313 during high cellulose loading fermentations. *Biotechnology and Bioengineering*, 1–39. doi:10.1002/bit.26374.

Tolonen, A. C., Petit, E., Blanchard, J. L., Warnick, T., & Leschine, S. B. (2014). Technologies to study plant biomass fermentation using the model bacterium *Clostridium phytofermentans*. *Biological Conversion of Biomass for Fuels and Chemicals*, (7), 114–139.

Tolonen, A. C., Zuroff, T. R., Ramya, M., Boutard, M., Cerisy, T., & Curtis, W. R. (2015). Physiology, genomics, and pathway engineering of an ethanol-tolerant strain of *Clostridium phytofermentans*. *Applied and Environmental Microbiology*, *81*(16), 5440–5448. https://doi.org/10.1128/AEM.00619-15

Vallino, J. J. (1991). Identification of branch-point restrictions in microbial metabolism through metabolic flux analysis and local network perturbations, PhD Thesis, Department of Chemical Engineering, Massachusetts Institute of Technology, MA, USA.

Veen, D., Lo, J., Brown, S. D., Johnson, C. M., Tschaplinski, T. J., Martin, M., & Lynd, L. R. (2013). Characterization of *Clostridium thermocellum* strains with disrupted fermentation end-product pathways. *Journal of Industrial Microbiology & Biotechnology*. https://doi.org/10.1007/s10295-013-1275-5

Verbeke, T. J., Dumonceaux, T. J., Wushke, S., Cicek, N., Levin, D. B., & Sparling, R. (2011). Isolates of *Thermoanaerobacter thermohydrosulfuricus* from decaying wood compost display genetic and phenotypic microdiversity. *FEMS Microbiology Ecology*, *78*(3), 473–87. https://doi.org/10.1111/j.1574-6941.2011.01181.x

Verbeke, T. J., Zhang, X., Henrissat, B., Spicer, V., Rydzak, T., Krokhin, O. V., & Sparling, R. (2013). Genomic evaluation of *Thermoanaerobacter spp.* for the construction of designer co-cultures to improve lignocellulosic biofuel production. *PLoS ONE*, *8*(3), e59362. https://doi.org/10.1371/journal.pone.0059362

Vojinović, V., Cabral, J. M. S., & Fonesca, L. P. (2006). Real-time bioprocess monitoring part I: in situ sensors. *Sensors and Actuators.* B. *114*,1083-1091.

Wang, Z., Cao, G., Zheng, J., Fu, D., Song, J., Zhang, J., … Yang, Q. (2015). Developing a mesophilic co-culture for direct conversion of cellulose to butanol in consolidated bioprocess. *Biotechnology for Biofuels*, *8*(1), 1–9. https://doi.org/10.1186/s13068-015-0266-3

Warnick, T. A., Methé, B. A., & Leschine, S. B. (2002). *Clostridium phytofermentans* sp. nov., a cellulolytic mesophile from forest soil. *International Journal of Systematic and Evolutionary Microbiology*, *52*(4), 1155–1160. https://doi.org/10.1099/ijs.0.02125-0

Watrous, J. D., & Dorrestein, P. C. (2011). Imaging mass spectrometry in microbiology. *Nature Reviews Microbiology*, *9*(9), 683–694. https://doi.org/10.1038/nrmicro2634

Weisenberger, S., & Schumpe, A. (1996). Estimation of gas solubilities in salt solutions at temperatures from 273K to 363K. AIChE Journal, *42*(1):298-300

Wiechert, W., Möllney, M., Petersen, S., & de Graaf, A. A. (2001). A universal framework for ^{13}C metabolic flux analysis. *Metabolic Engineering*, *3*(3), 265–83. https://doi.org/10.1006/mben.2001.0188

Wilkins, C. L., & Lay. J. O. (2006). Identification of microorganisms by mass spectrometry. Vol. 169, Published by John Wiley & Sons, Inc., Hoboken, New Jersey, USA.

Wolfe, A. J. (2005). The acetate switch, *Microbiology and Molecular Biology Reviews*, *69*(1), 12-50. doi:10.1128/MMBR.69.1.12

Worden, R. M., & Bredwell, M. D. (1998). Mass-transfer properties of microbubbles. 2. Analysis using a dynamic model. *Biotechnology Progress*, *14*(1), 39–46. https://doi.org/10.1021/bp970131c

Xiao, H., Gu, Y., Ning, Y., Yang, Y., & Mitchell, W. J. (2011). Confirmation and elimination of xylose metabolism bottlenecks in glucose phosphoenolpyruvate-dependent phosphotransferase system-deficient *Clostridium acetobutylicum* for simultaneous utilization of glucose. *Applied and Environmental Microbiology*, *77*(22), 7886–7895. https://doi.org/10.1128/AEM.00644-11

Yang, T. H., Wittmann, C., & Heinzle, E. (2003). Dynamic calibration and dissolved gas analysis using membrane inlet mass spectrometry for the quantification of cell respiration. *Rapid Communications in Mass Spectrometry*, *17*, 2721-2731.

Yusoff, M. N. A. M., Zulkifli, N. W. M., Masum, B. M., & Masjuki, H. H. (2015). Feasibility of bioethanol and biobutanol as transportation fuel in spark-ignition engine: A review. *RSC Advances*, *5*(121), 100184–100211. https://doi.org/10.1039/c5ra12735a

Yutin, N., & Galperin, M. Y. (2013). A genomic update on clostridial phylogeny: Gram-negative spore-formers and other misplaced clostridia. *Environmental Microbiology*, *15*(10), 2631–2641. https://doi.org/10.1111/j.1743-6109.2008.01122.x.Endothelial

Zanzotto, A., Szita, N., Boccazzi, P., Lessard, P., Sinskey, A.J. & Jensen, K.F. (2004). Membrane-aerated microbioreactor for high-throughput bioprocessing, *Biotechnology Bioengineering*. 87: 243–254.

Zeikus, J. G., Wellstein, A. L., & Kirk, T. K. (1982). Molecular basis for the biodegradative recalcitrance of lignin in anaerobic environments. *FEMS Microbiology Letters*, *15*(3), 193–197. doi:10.1111/j.1574-6968.1982.tb00066.x

Zhang, F., Zhang, Y., Chen, M., & Zeng, R. J. (2012). Hydrogen supersaturation in thermophilic mixed culture fermentation. *International Journal of Hydrogen Energy*, *37*(23), 17809–17816. https://doi.org/10.1016/j.ijhydene.2012.09.019.

Zhang, Y., Zhang, F., Chen, M., Chu, P.-N., Ding, J., & Zeng, R. J. (2013). Hydrogen supersaturation in extreme-thermophilic (70°C) mixed culture fermentation. *Applied Energy*, *109*, 213–219. https://doi.org/10.1016/j.apenergy.2013.04.019

Zhang, X., Tu, B., Dai, L., Lawson, P. A., Zheng, Z., Liu, L.-Y., … Cheng, L. (2018). *Petroclostridium xylanilyticum* gen. nov., sp. nov., a xylan-degrading bacterium isolated from an oilfield, and reclassification of clostridial cluster III members into four novel genera in a new *Hungateiclostridiaceae* fam. nov. *International Journal of Systematic and Evolutionary Microbiology*, *68*(10), 3197–3211. https://doi.org/10.1099/ijsem.0.002966

Zhao, X., Condruz, S., Chen, J., & Jolicoeur, M. (2016). A quantitative metabolomics study of high sodium response in *Clostridium acetobutylicum* ATCC 824 acetone-butanol-ethanol (ABE) fermentation. *Scientific Reports*, *6*(January), 1–13. https://doi.org/10.1038/srep28307

Zheng, X.-J., & Yu, H.-Q. (2005). Inhibitory effects of butyrate on biological hydrogen production with mixed anaerobic cultures. *Journal of Environmental Management*, *74*(1), 65–70. https://doi.org/10.1016/j.jenvman.2004.08.015

Zheng, Y., Kahnt, J., Kwon, I. H., Mackie, R. I., & Thauer, R. K. (2014). Hydrogen formation and its regulation in *Ruminococcus albus*: involvement of an electron-bifurcating [FeFe]-hydrogenase, of a non-electron-bifurcating [FeFe]-hydrogenase, and of a putative hydrogen-sensing [FeFe]-hydrogenase. *Journal of Bacteriology*, *196*(22), 3840–3852. https://doi.org/10.1128/JB.02070-14

Zuroff, T. R., Xiques, S. B., & Curtis, W. R. (2013). Consortia-mediated bioprocessing of cellulose to ethanol with a symbiotic *Clostridium phytofermentans*/yeast co-culture. *Biotechnol Biofuels* 6:59. http://dx.doi.org/10.1186 /1754-6834-6-59.

Supplementary Materials

Supplementary Tables

Table S3.1 Regression analysis between GC and TOGA measurements for carbonate species.

Analyte	Regressed slope	Standard error slope	95 % confidence interval	Regressed intercept	Standard error intercept	95 % confidence interval	R^2	Number of measurement
CO_2	1.058	0.258	0.397	-0.288	0.289	1.844	0.990	5
HCO_3^-	1.009	0.360	0.209	-0.018	0.018	0.116	0.999	5
CO_3^{2-}	1.059	0.068	0.011	<0.002	<0.002	<0.011	1.000	5

Table S4.1 Substrate specific yields (mol/mol of xylose) between control and perturbed experiments (20-24 h pi)

Events	N	Lactate	Formate	Acetate	EtOH	H_2	CO_2	Cell Protein
Xylose Control 2 g/L (no acetate)	1	0.11	0.98	1.10	0.41	0.86	0.46	0.061
	2	0.07	0.87	1.11	0.41	0.77	0.47	0.058
	3	0.11	0.75	0.93	0.37	0.85	0.38	0.057
	Average	0.10	0.86	1.05	0.39	0.82	0.44	0.059
	SD	0.02	0.12	0.10	0.02	0.05	0.05	0.002
Xylose Perturbed 2 g/L (acetate treated)	1	0.04	0.74	0.84	0.44	0.66	0.36	0.061
	2	0.05	0.75	0.81	0.46	0.70	0.39	0.059
Yields $^{\Psi}$ change %		(-) 47-53	(-)13-15	(-)20-23	(+)11-18	(-)15-20	(-)10-17	(+)1- 4
Statistical Analysis/ Comment		t = 2.93, p = 0.061, significant @ p<0.10	t = 1.42, p = 0.251, insignificant @ p<0.10	t = 2.91, p = 0.062, significant @ p<0.10	t = -2.84, p = 0.065, significant @ p<0.10	t = 3.70, p = 0.034, significant @ p<0.05	t = 1.60, p = 0.207, insignificant @ p<0.10	t = -0.77, p = 0.495, insignificant @ p<0.10

Ψ: negative sign (-) means decrease and positive sign (+) means increase; N = Biological replicates; t = Two tailed t-test was performed with two independent means

Table S6.1 Reliability assessment of various end-products (H_2, CO_2, EtOH) obtained from real-time on-line measurements throughout entire growth phase of *C. termitidis* with two biological replicates on 10 g/L cellobiose (regression analysis).

Analyte	Regressed slope	Standard error slope	95% Confidence intervals	Regressed intercept	Standard error intercept	95% Confidence intervals	R^2	Number of measurement
H_2	1.134	0.001	1.136	-0.642	0.032	-0.578	0.996	N = 3068
CO_2	1.364	0.004	1.371	-1.149	0.049	-1.052	0.980	N = 2900
EtOH	0.999	0.002	1.003	0.723	0.028	0.109	0.992	N = 3196

Table S6.2 Correlation between predicted and discretely measured formate and acetate concentrations of *C. termitidis* with two biological replicates (BR) on 10 g/L cellobiose (regression analysis derived from Figure 6.2).

Analytes	Biological replicates	Regressed slope	Standard error slope	95% Confidence intervals	Regressed intercept	Standard error intercept	95% Confidence intervals	R^2	Comment
Formate	BR1	0.893	0.018	0.931	1.266	0.545	2.529	0.996	$p < 0.05$; N=12
	BR2	0.892	0.050	1.003	1.167	1.331	-1.762	0.966	$p < 0.05$; N=13
Acetate	BR1	0.910	0.019	0.951	1.508	0.543	2.827	0.995	$p < 0.05$; N=12
	BR2	0.873	0.034	0.947	2.053	0.993	-0.132	0.985	$p < 0.05$; N=13

Table S6.3 Statistical analysis of unknown metabolites (H+ ion equivalent) predicted from metabolic acids and base consumption (derived from Table 6.2).

Substrate Load g/L	Biological replicates	t-test	p	R^2	Comment
10	2	3.63	0.068	0.996	Significant at $p < 0.10$
2	3	2.10	0.103	0.966	Insignificant at $p < 0.10$
1	2	0.68	0.565	0.995	Insignificant at $p < 0.10$

Supplementary Figures

Supplementary Figures: Chapter 3

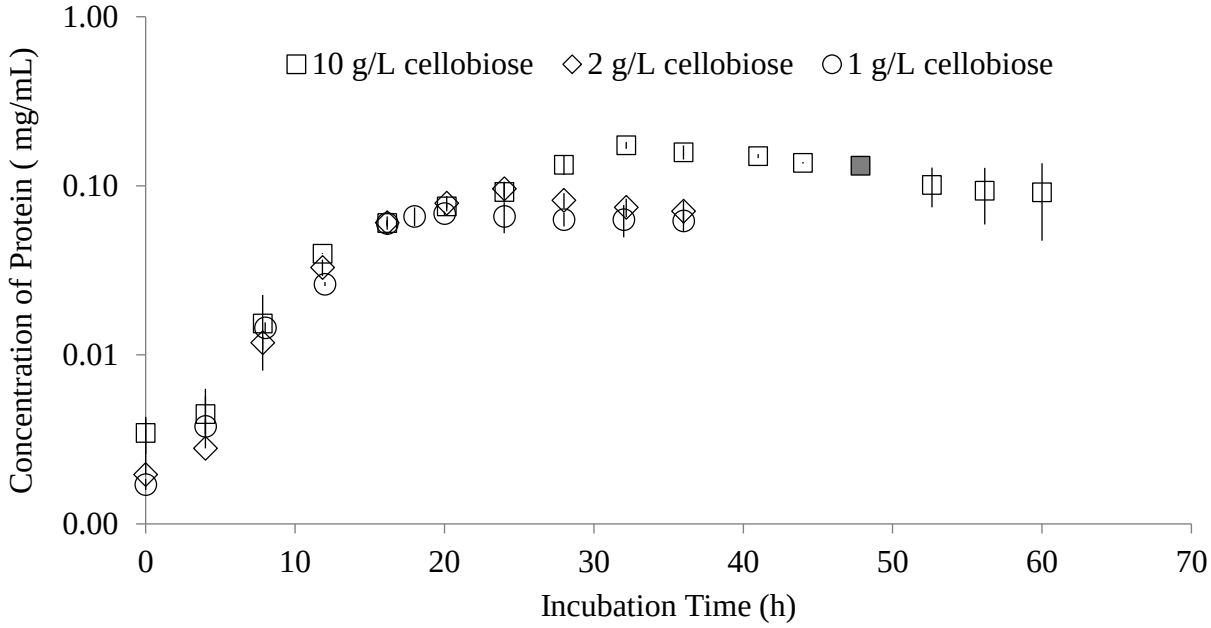

Figure S3.1 Growth kinetics of *C. termitidis* in a pH controlled (7.20 ± 0.02) bioreactor. Protein concentrations from the growth of *C. termitidis* in a 7 L reactor with 3.0 L working volume in 1191 media containing 10 g/L cellobiose: open square (□), 2 g/L cellobiose: open diamond (◊), and 1 g/L cellobiose: open circle (○).

A)

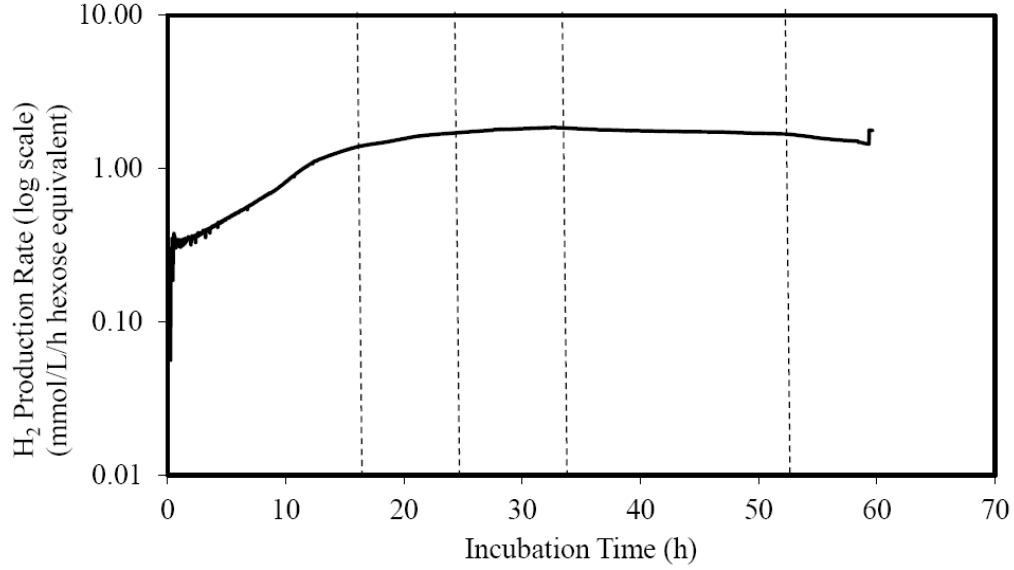

B)

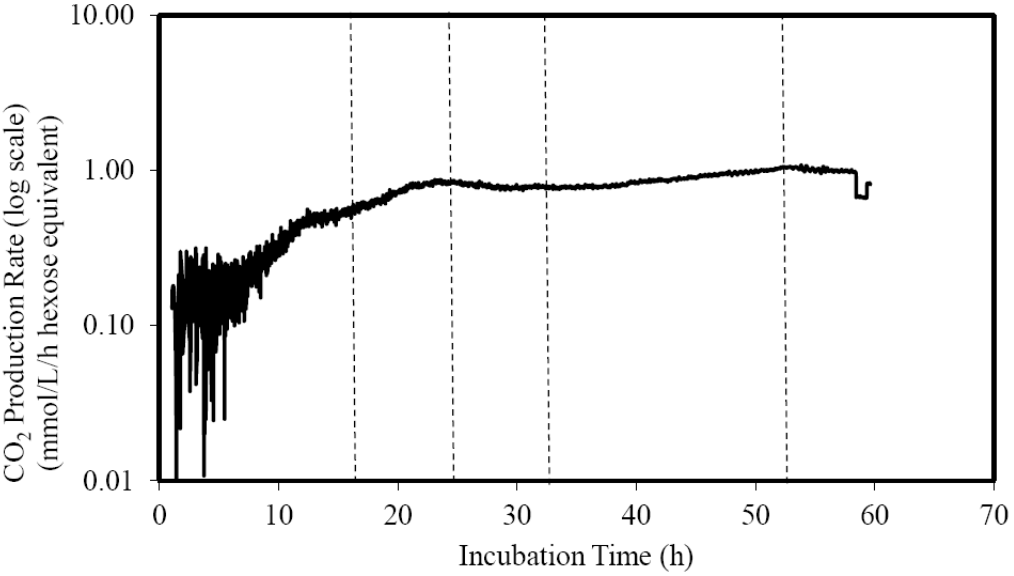

Figure S3.2 Gas production rates A) H_2 and B) CO_2 over the course of fermentation on 10 g/L cellobiose in a pH controlled bioreactor. Dotted lines indicate various growth phases as described in Figure 3.2.

Supplementary Figures: Chapter 4

A)

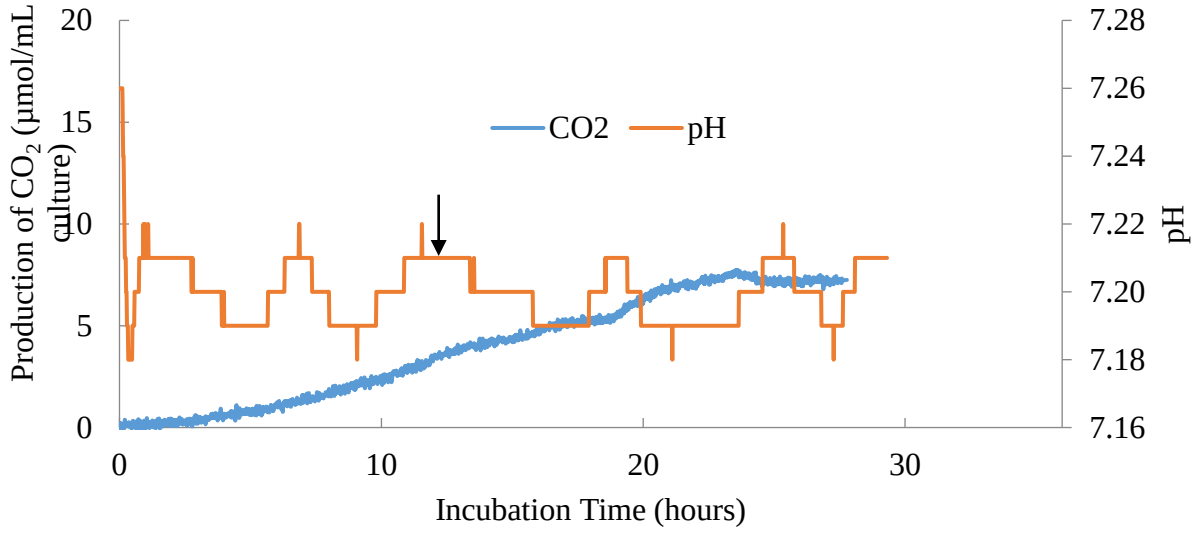

B)

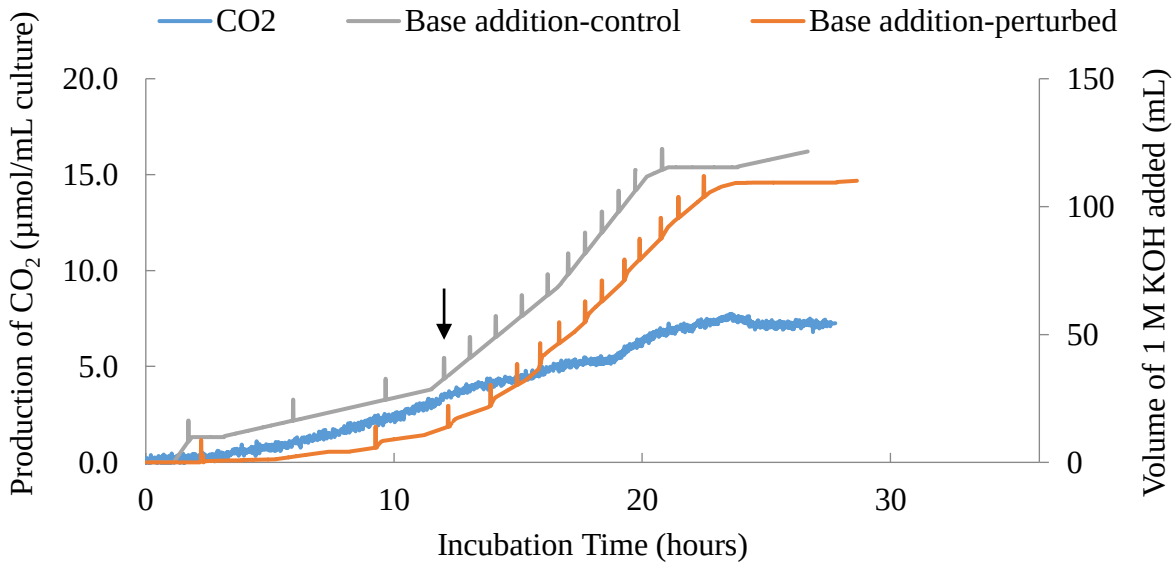

Figure S4.1 Variation of A) pH against CO_2 production and B) base consumption with CO_2 production when perturbed with exogenous Na-acetate. Vertical arrow indicates when Na-acetate added.

A)

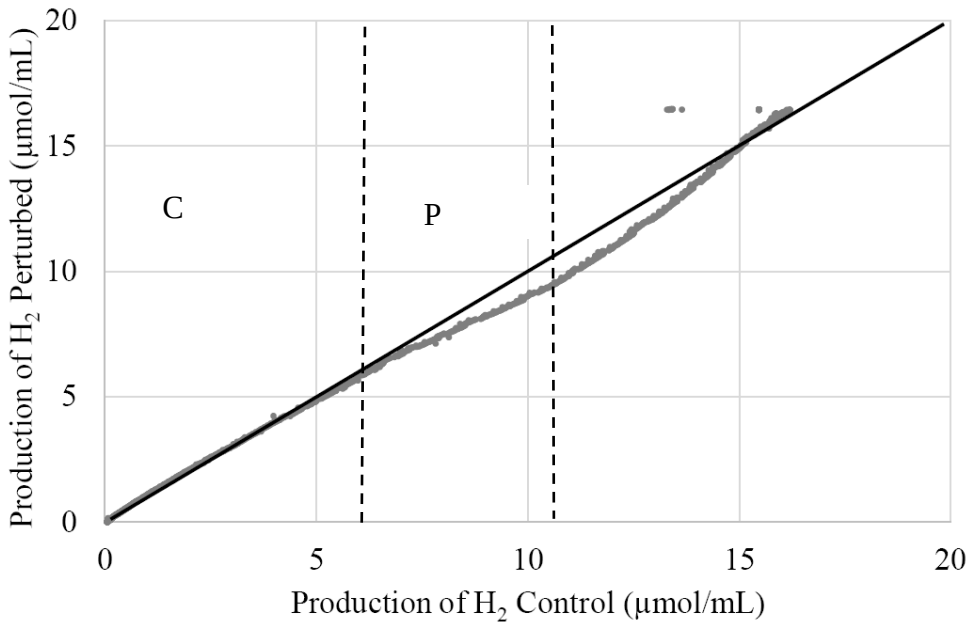

B)

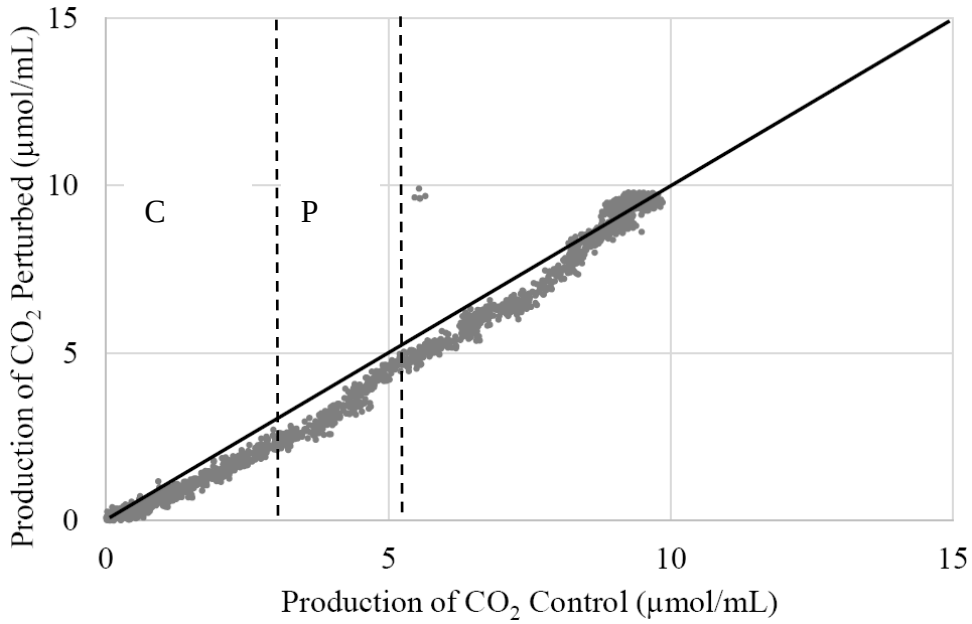

Figure S4.2 Cumulative gas production correlation between control and perturbed biological experiment set 1. Region C: strongly correlated with insignificant difference. Region P: poor correlation with significant difference.

A)

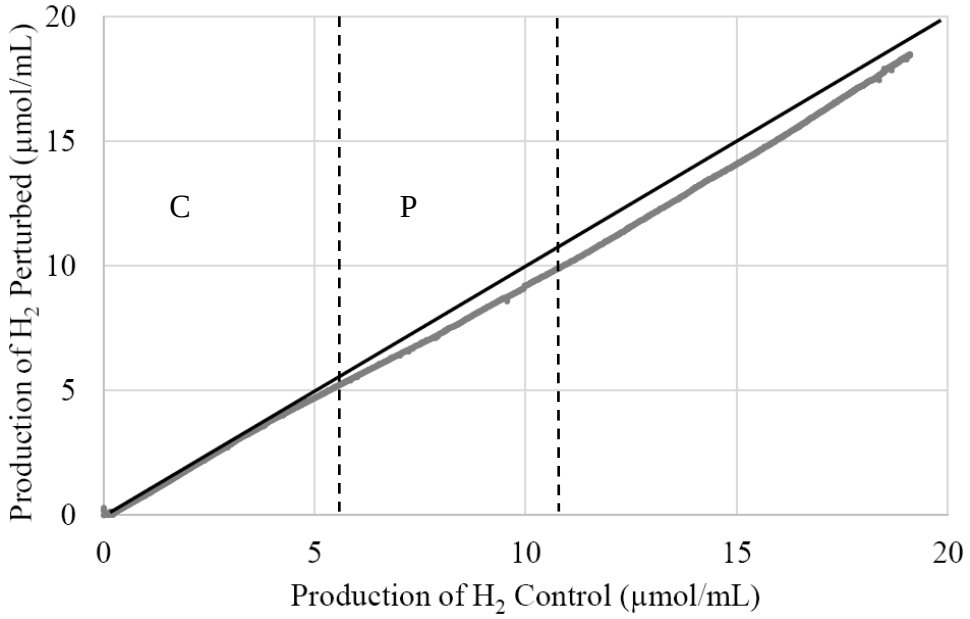

B)

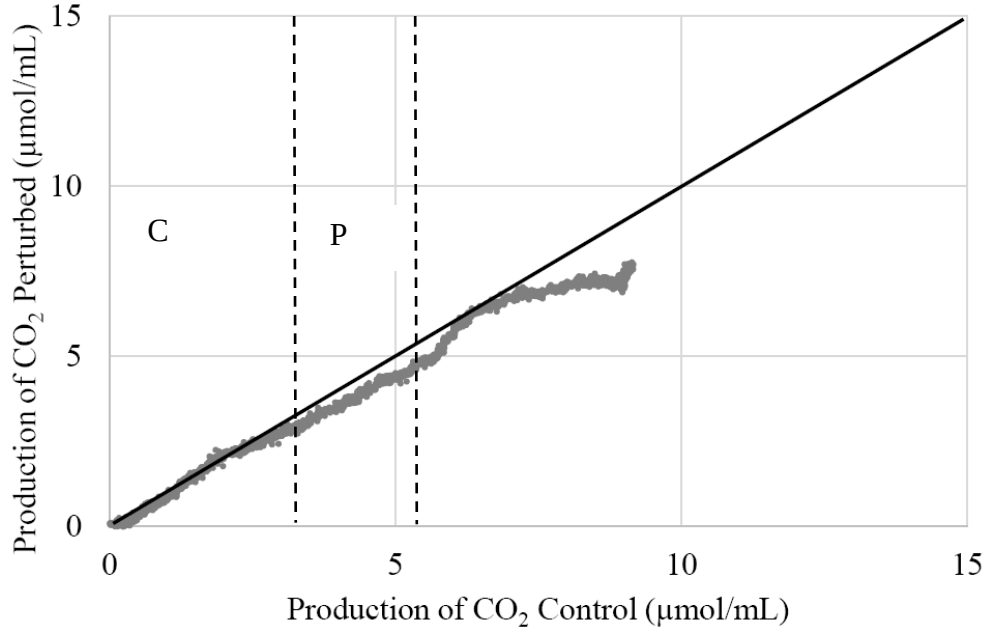

Figure S4.3 Cumulative gas production correlation between control and perturbed biological experiment set 2. Region P: poor correlation with significant difference.

A)

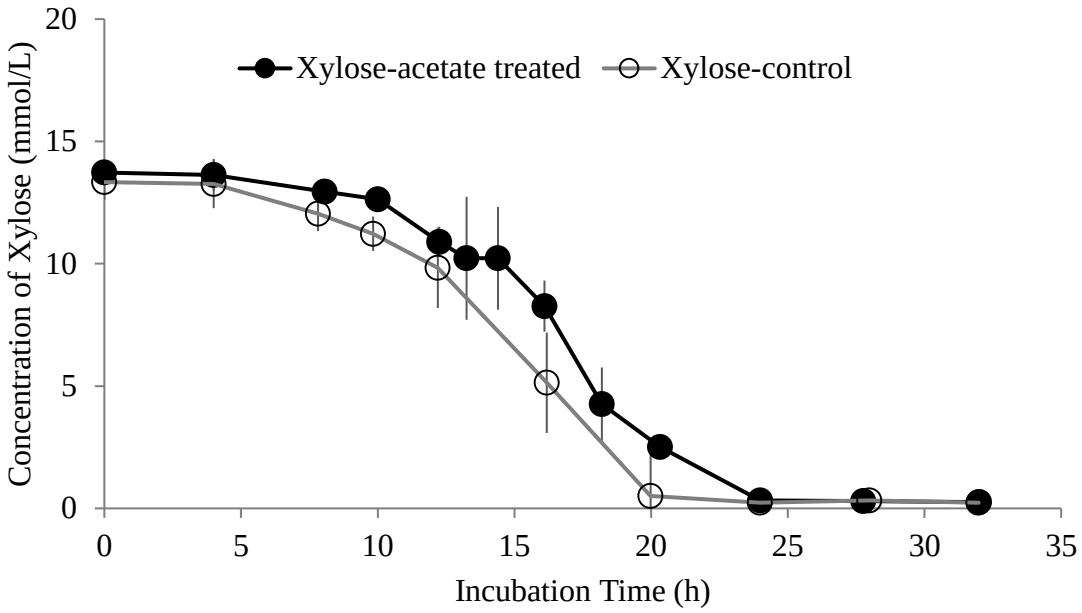
Xylose-acetate treated
Xylose-control
Concentration of Xylose (mmol/L)
Incubation Time (h)
0
5
10
15
20
25
30
35

B)

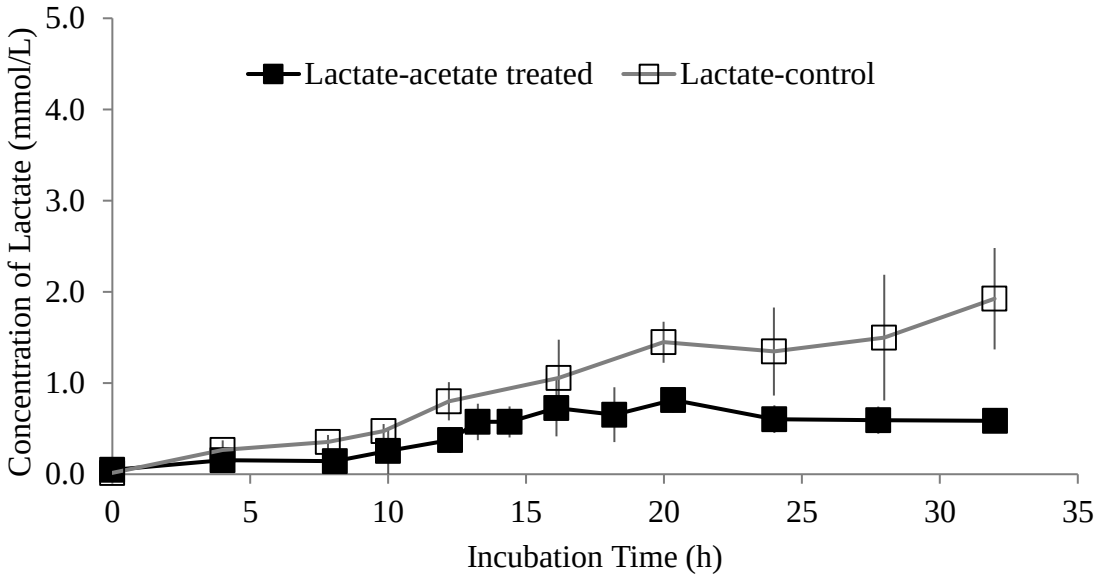
Lactate-acetate treated
Lactate-control
Concentration of Lactate (mmol/L)
Incubation Time (h)
0.0
1.0
2.0
3.0
4.0
5.0
0
5
10
15
20
25
30
35

C)

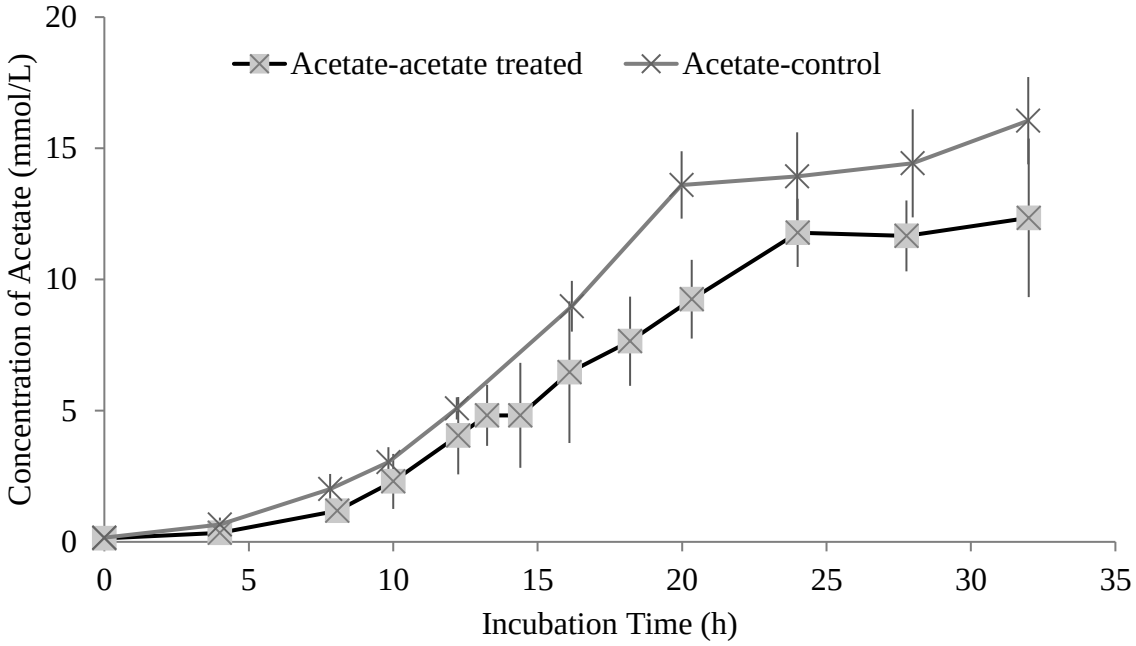
Acetate-acetate treated
Acetate-control
Concentration of Acetate (mmol/L)
Incubation Time (h)
0
5
10
15
20
25
30
35

D)

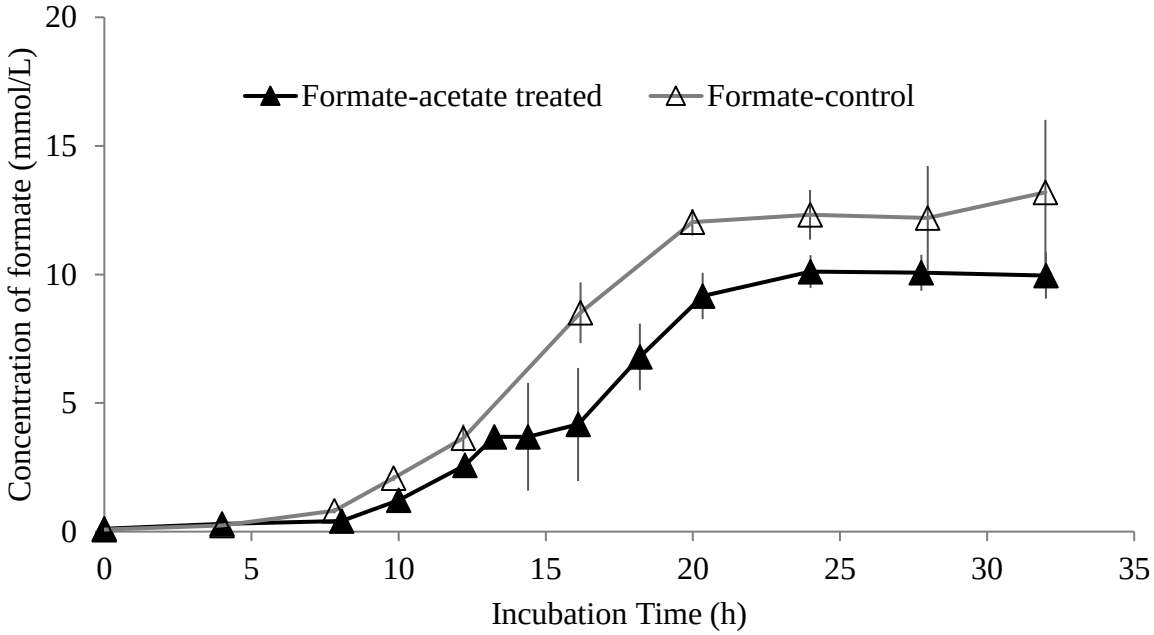
Formate-acetate treated
Formate-control
Concentration of formate (mmol/L)
Incubation Time (h)
0
5
10
15
20
25
30
35

E)

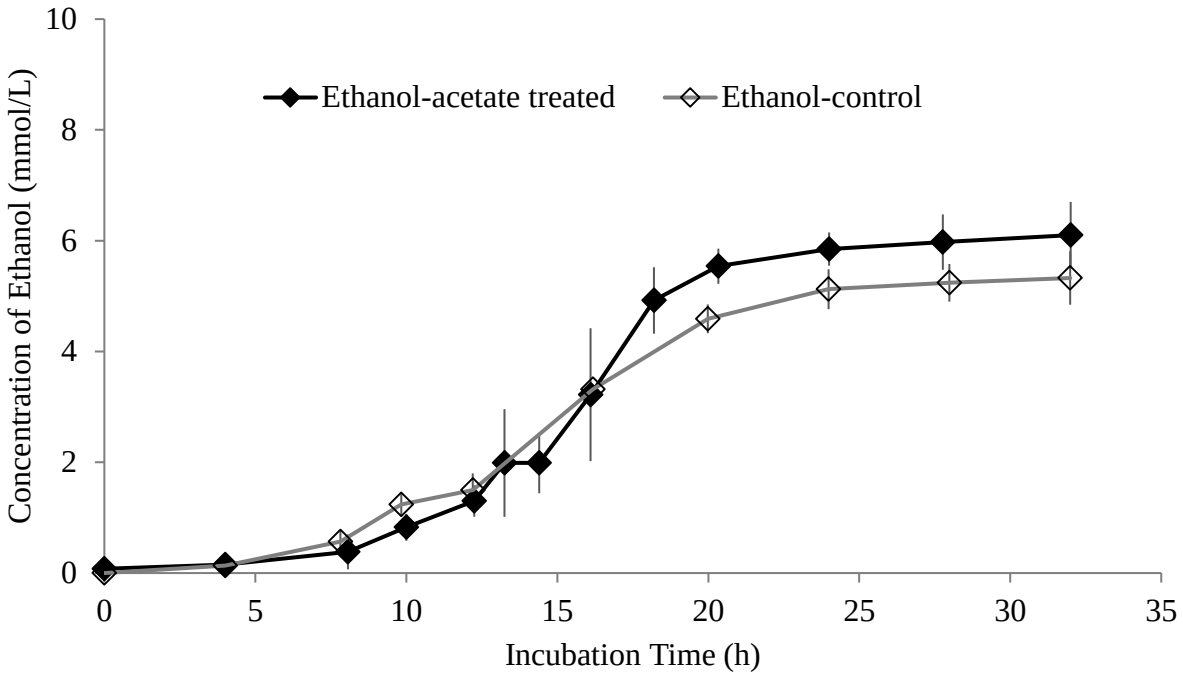

Figure S4.4 A) Xylose consumption, and synthesis of B) lactate, C) acetate, D) formate and E) ethanol in *C. termitidis* grown on 2 g/L xylose-control (open circle, square, cross, triangle, diamond) and 2g/L xylose-acetate treated (filled circle, square, cross, triangle, diamond). Error bars represent standard deviations of two biological replicates.

Supplementary Figures: Chapter 5

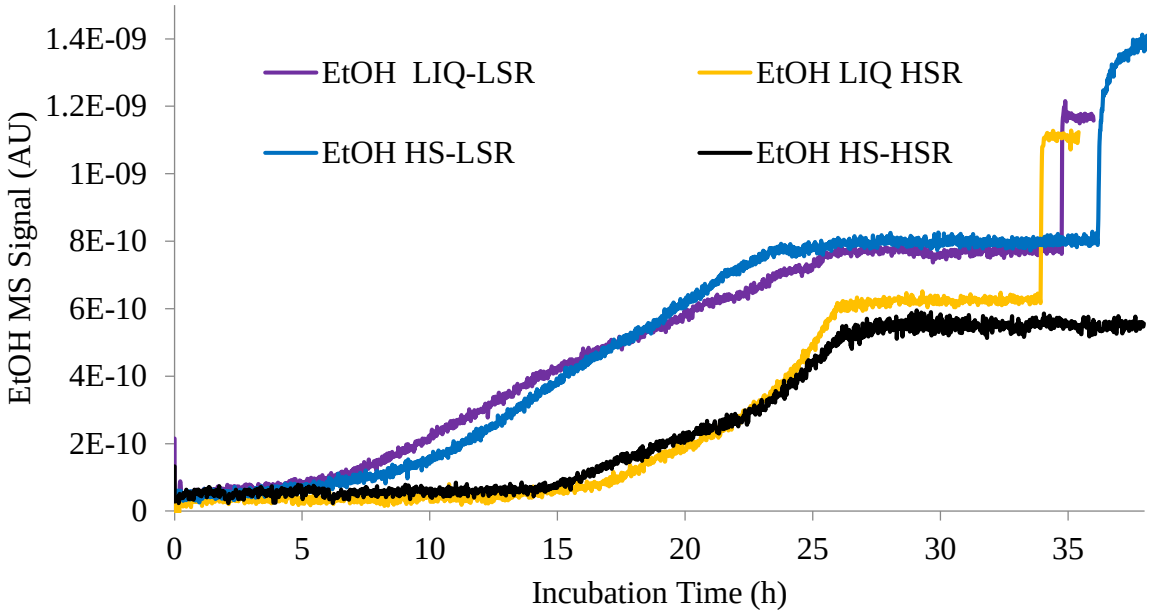

Figure S5.1 Production of ethanol by *C. termiditis* cultures under low sparging rate (LSR: 20 mL/min, 100 rpm) and high sparging rate (HSR: 400 mL/min, 200 rpm) conditions measured in the headspace and aqueous phase in real-time by the MIMS probe. Purple line, ethanol signal in aqeuous phase under LSR conditions; Yellow line, ethanol signal in the aqueous phase under HSR conditions; Blue line, ethanol signal in in headspace under LSR conditions; Black line, ethanol signal in the headspace under HSR conditions.

A)

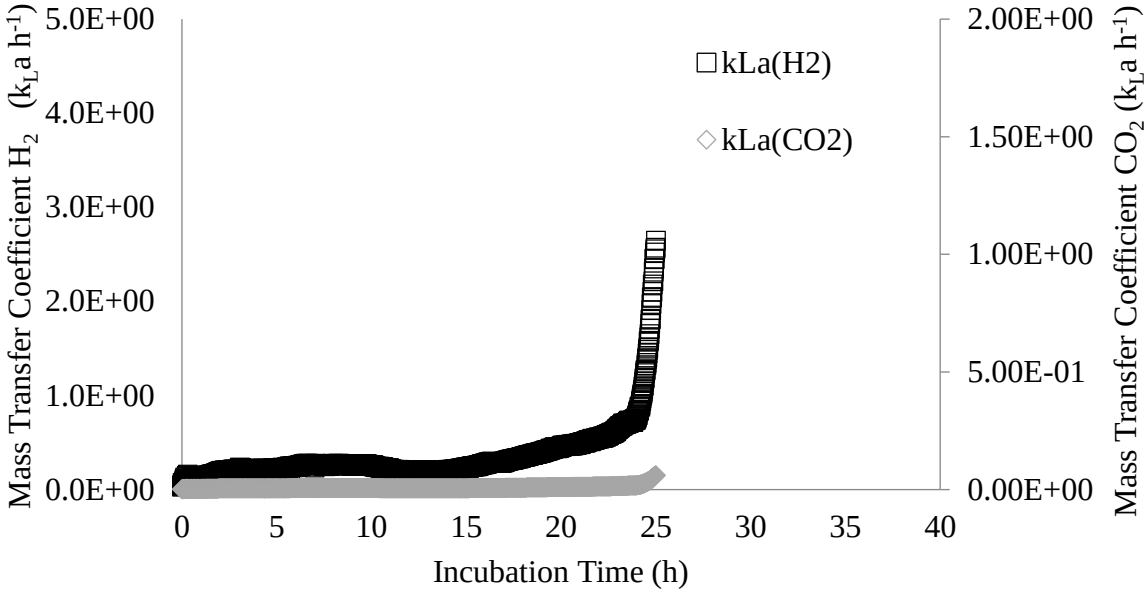

B)

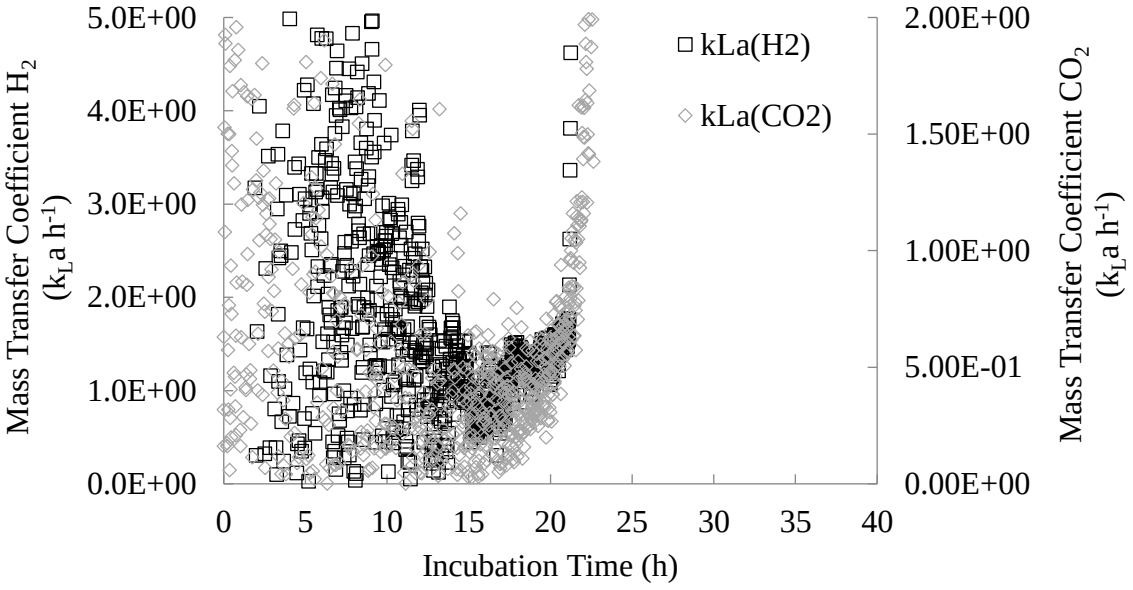

Figure S5.2 Mass transfer coefficient (k_La h^{-1}) under A) low sparging rate and B) high sparging rate conditions, using Equation 5.2.

A)

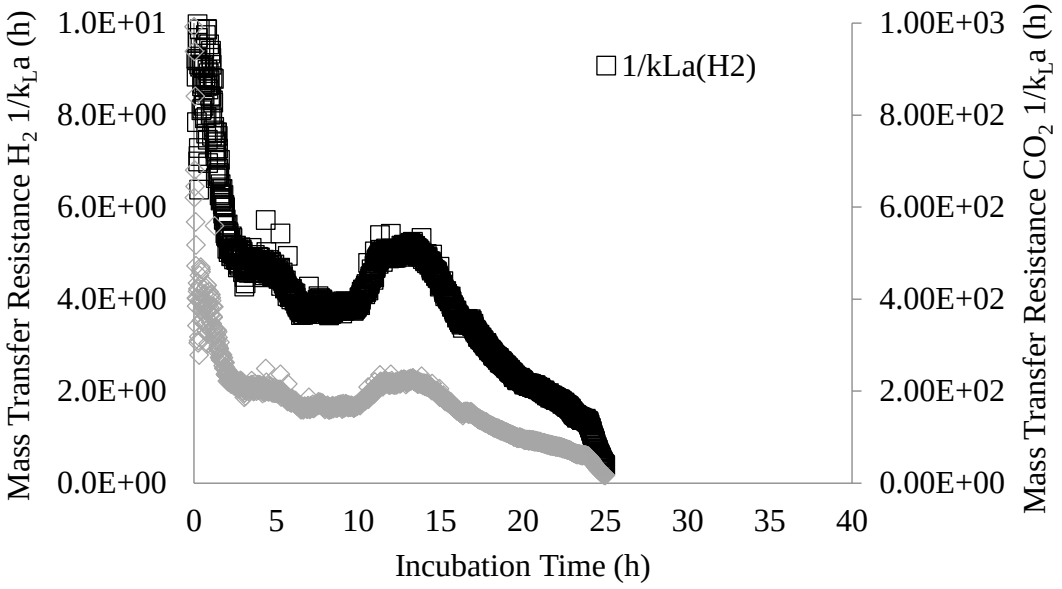

B)

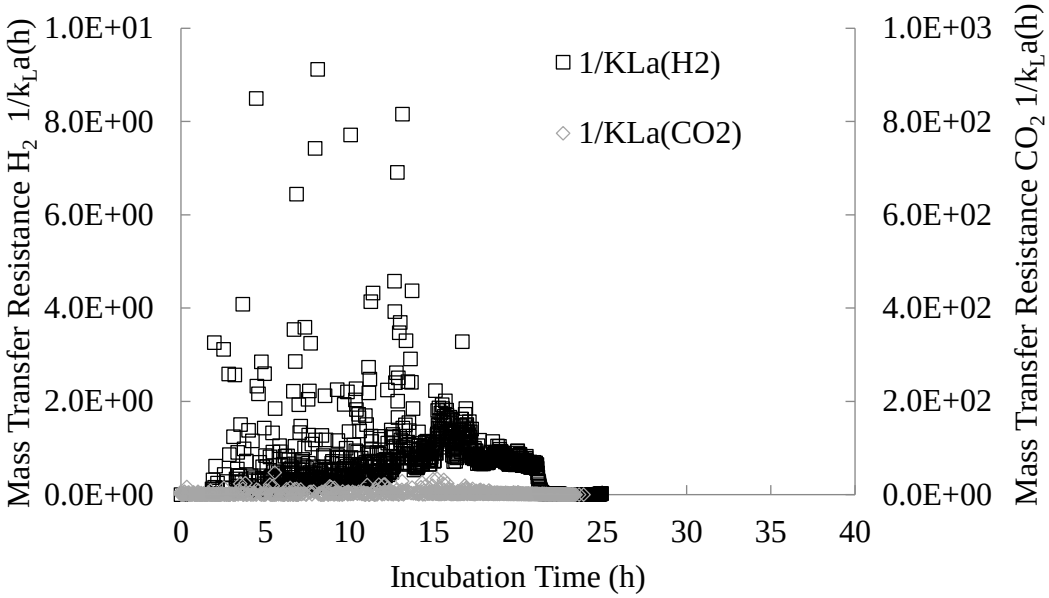

Figure S5.3 Mass transfer resistance ($1/k_La$ h) under A) low sparging rate and B) high sparging rate conditions.

A)

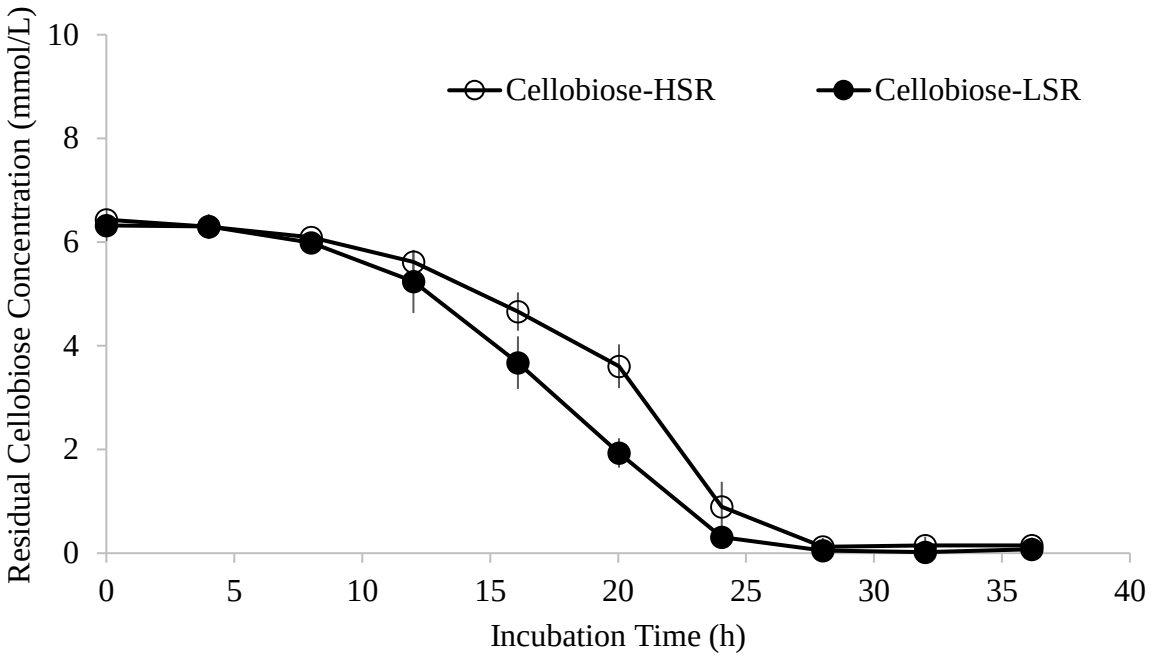
Residual Cellobiose Concentration (mmol/L)
10
8
6
4
2
0
Cellobiose-HSR
Cellobiose-LSR
0
5
10
15
20
25
30
35
40
Incubation Time (h)

B)

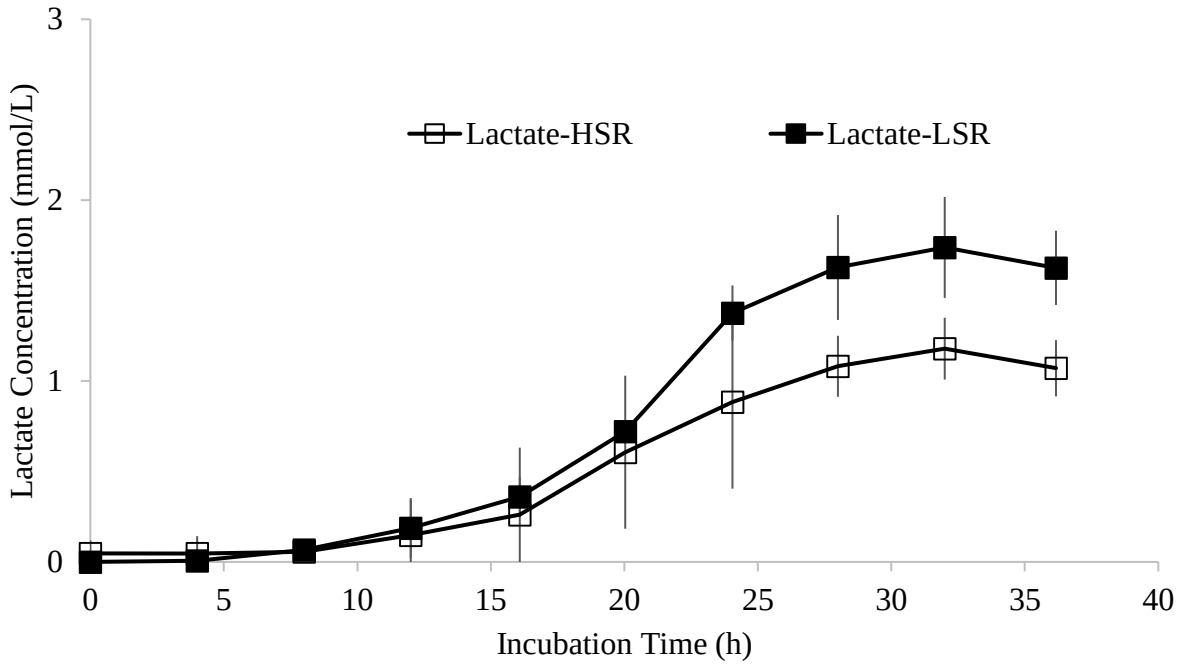
Lactate Concentration (mmol/L)
3
2
1
0
Lactate-HSR
Lactate-LSR
0
5
10
15
20
25
30
35
40
Incubation Time (h)

C)

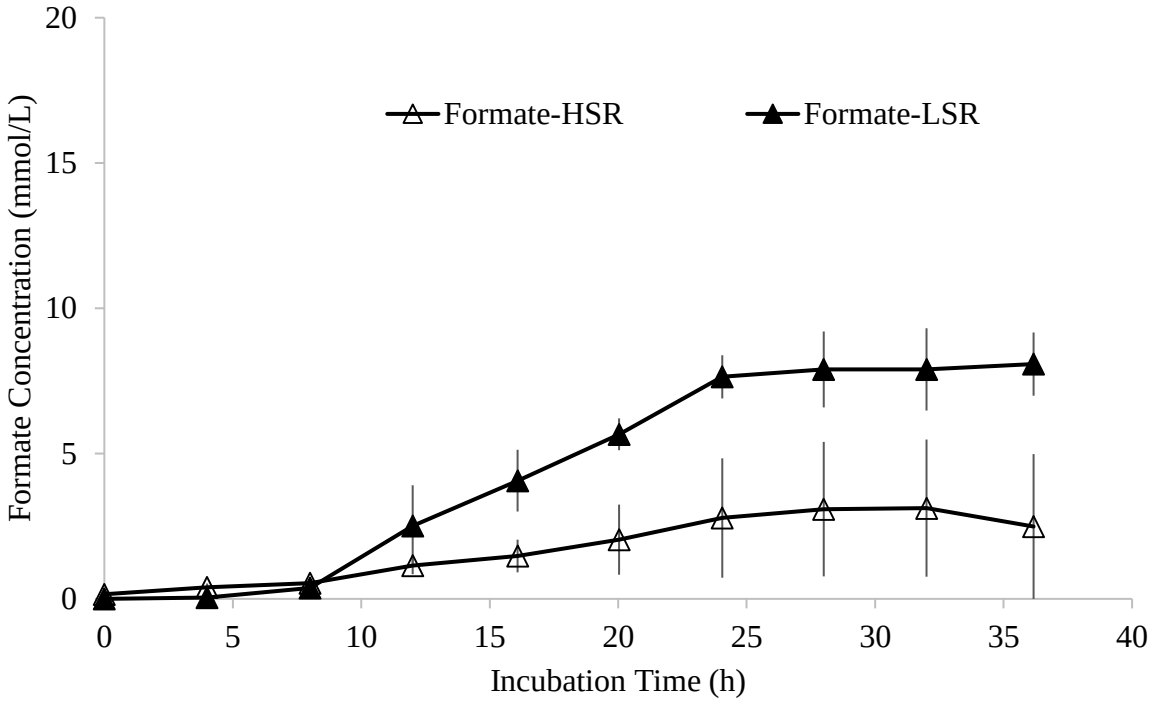
Formate-HSR
Formate-LSR
Formate Concentration (mmol/L)
Incubation Time (h)
0
5
10
15
20
25
30
35
40

D)

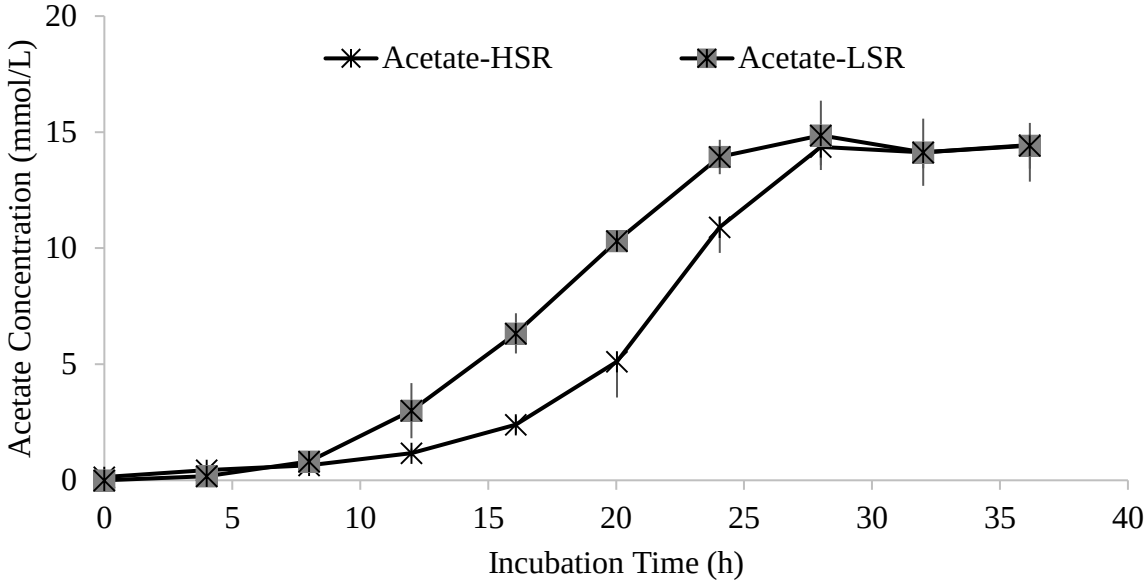
Acetate-HSR
Acetate-LSR
Acetate Concentration (mmol/L)
Incubation Time (h)
0
5
10
15
20
25
30
35
40

E)

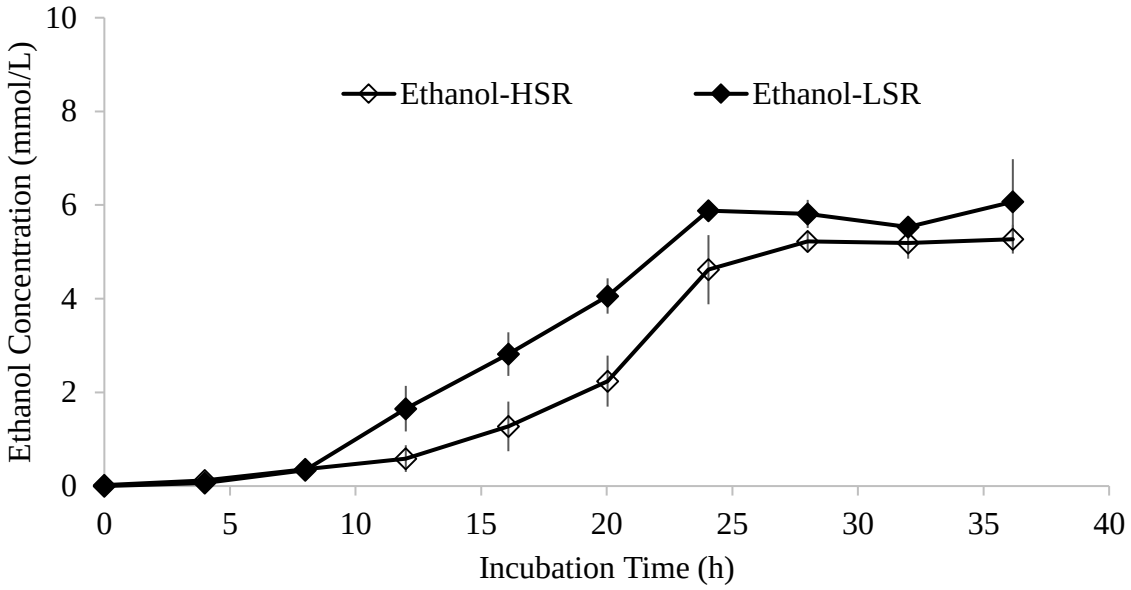

Figure S5.4 A) Residual substrate (cellobiose) concentration, and accumulation of B) lactate, C) formate, D) acetate and E) etahnol in *C. termitidis* grown on 2 g/L cellobiose under low sparging rate (LSR) conditions (solid discrete points) and high sparging rate (HSR) conditions (open discrete points). Error bar represents standard deviations of four biological replicates.

Supplementary Figures: Chapter 6

A)

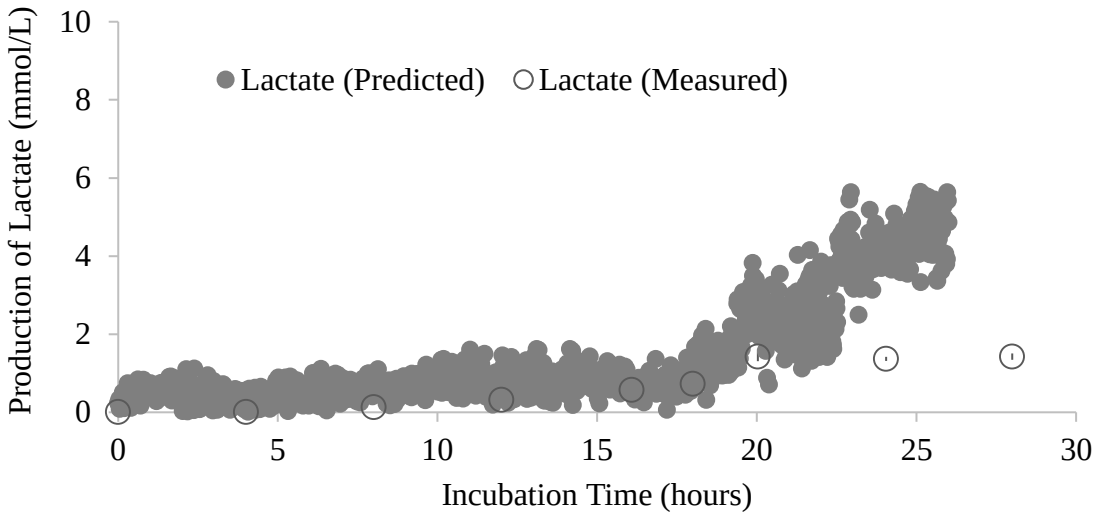

B)

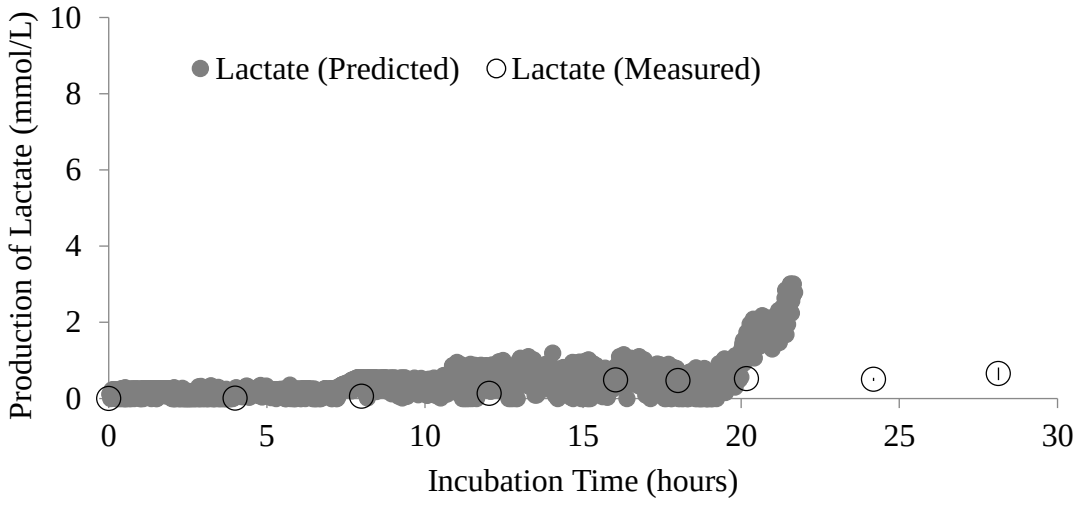

Figure S6.1 Estimation of lactate synthesis using the stoichiometric algorithm, with concentrations obtained by discrete HPLC measurement for A) 2 g/L cellobiose, and B) 1 g/L cellobiose. Grey solid circle (●) represents predicted lactate concentration, and open circle (○) discrete HPLC concentration of lactate.